# MECHANISMS FOR MODIFYING THE PHYSICOCHEMICAL AND PHYSICOMECHANICAL PROPERTIES OF POLY (LACTIC-CO-GLYCOLIC) ACID: IMPACT ON CONTROLLED DRUG DELIVERY

SIBONGILE RUTH SIBAMBO

A Dissertation Submitted to the Faculty of Health Sciences,

University of the Witwatersrand, in Fulfillment of the

Requirements for the Degree of Master of Pharmacy

**Supervisor:**

Prof Viness Pillay

Department of Pharmacy and Pharmacology, University of the Witwatersrand, South Africa

**Co-Supervisor:**

Prof Michael Paul Danckwerts

Department of Pharmacy and Pharmacology, University of the Witwatersrand, South Africa

Parktown, Johannesburg, 2007

## DECLARATION

I, Sibongile Ruth Sibambo declare this dissertation as my own work. It is being submitted for the degree of Master of Pharmacy in the Faculty of Health Sciences in the University of the Witwatersrand, Johannesburg. It has not been submitted before for any degree or examination at this or any other University.

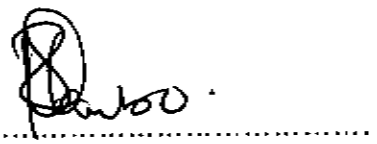

This 16th day of July 2007

## ACKNOWLEDGEMENTS

I would like to express my gratitude to Prof Viness Pillay for his counsel, inspiration and enthusiasm in my work and for granting me the opportunity to work under his supervision. This study would not have been attainable were it not for his vast knowledge and willingness to share. My sincere appreciation is extended to Prof Michael P. Danckwerts for co-supervising this study with all his experience and pertinent direction throughout the study; and to Yahya E. Choonara for the contribution of his academic and technical expertise in this work.

A special thanks is extended to Prof Clem Penny and to Dr Jeanette Lotter for lending a helping hand and offering their academic expertise, with patience and diligence. To Mr David N. Bayever and Dr Robyn L. Van Zyl, I am sincerely grateful for always being there to support, counsel and heal. I especially thank Mmapule A. Mongalo, Mr and Mrs Muzi J. Maseko, and Jeanette Tilana for your care in sickness and in health throughout my student life at Wits University. My cousin and friend Nomagugu J. Nxumalo, you are appreciated for your understanding and willingness to lend a hand at all times. To João Carapinha and Shirona Naidoo, thank you for persuading me into pursuing postgraduate studies in pharmacy.

My dear friends, Ayanda S. Mabaso, Mohlamme J. Mathabathe, Themba R. Mnguni, Rupal Patel, Angela K. Mamiane, Lebogang Makale, Mapule Kholong, Neha Singh, Lisa Du Toit, Busi Damane, Sheri-Lee Harilall, Ntiyiso Shingwenyane, Oluwatoyin Kolawole, Maria P. Paraskeva Samantha Pillay, Gladys M. Madidimalo, Dale and Deshree Janneker, Mandlakhe O. Mashabane and Lungelo L. Ncede, thank you for inspiring me into pursuing this study and for the constant technical and emotional support throughout my life. I also wish to thank Tebogo Chandu, Sello Ramarumo, Mama Florence Makeketa, Elizabeth Sibutha, Olga Kunene and all my colleagues in the department of Pharmacy and Pharmacology for the support throughout my studies.

I would like to express my gratitude to my whole family, Sibambo and Nxumalo for their support over the years. In particular, my uncle Mr Moses M. Nxumalo who continues to be an inspiration and a role model in our family. Lastly, my deepest gratitude belongs to my mother Mrs Msesi Elizabeth Sibambo; my brothers Bhekifa and Sipho; my sisters Foggy, Goodness and Veronica; my brother and sisters in law Bhekithemba B Mnisi, Solani and Phumzile Sibambo; my niece and nephew Sibusisiwe and Vernon for their steadfast love, patience and support. I will always be indebted to this family, without whom a degree would have been just a dream.

This research was made possible through the financial assistance of the National Research Foundation (NRF), Department of Labour (DoL), South Africa.

To God be the Glory, for His Mercy and Loving-kindness endure forever!

## SUMMARY

*Neurodegenerative disorders are debilitating brain diseases. A number of these diverse genetic and sporadic neurological disorders lead to dementia and/or abnormal motor symptoms. Among them are those characterized by neuronal or microglia-initiated accumulation of tau (τ) proteins. These tauopathies form a diverse group of diseases that have several commonalities, since most are characterized by accumulations of misfolded proteins that aggregate into fibrillar deposits that lead to the atrophy of the nervous system structures. The major ones include Alzheimer's Disease, Parkinson's Disease, Amyotrophic Lateral Sclerosis and Huntington's Disease and affect a distinct section/s of the brain, causing motor and/or cognitive deficits.*

*Frequent dosing is a major limitation of the current approaches. Ideal therapy could provide long-term controlled drug delivery. This may be achieved through the modification of polymeric materials forming matrices with drugs. Biodegradable thermoplastics, such as, poly (lactic-co-glycolic acid (PLGA) have been verified as excellent bioactive carriers, owing to their biodegradability, biocompatibility, and hence approved by the Food and Drug Administration (FDA). Exploring the mechanisms for the modifying the physicochemical and the physicomechanical properties of polymers can lead to novel production techniques for polymers with desirable properties for drug delivery and other biomedical uses.*

*In this regard, this study established the mechanisms associated with the salting-out and cross-linking of PLGA in the presence of organic solvents. Using the foundation of these physicochemical and physicomechanical transitions, a polymeric scaffold and a compressed monolithic matrix system with both viscoelasticity and mechanical strength were designed. A combination of salting-out and cross-linking reagents such as N,N dimethyl formamide (DMF), acetone and salts were utilized based on statistical Design of Experiments, namely, Central Composite design (CCD) and Response Surface Method (RSM).*

*The principles of salting-out and cross-linking mechanisms were established with respect to the influence of salting-out chemical inducers on the physicochemical and physicomechanical transitions of PLGA. The extent of PLGA chain transitions and the applicability of the scaffold for controlled drug delivery were elucidated by scanning electron microscopy, calorimetric scans, Fourier Transform Infrared, textural profiling, quantum energy computation, in vitro polymer degradation and in vitro drug release studies.*

*Salting-out and cross-linking demonstrated the capacity to modulate the properties of PLGA through the incorporated salts that produce stochastic fluctuations and non-collapsible diffusion channels within polymeric structures thereby altering their physicochemical and physicomechanical properties. Novel polymeric attributes, such as the increase in matrix resilience and strength were distinguished. The vast quantum energy transitions determined at a molecular level interaction in a congealed energy state signified the ability of the composite system to contribute to the stabilization of the physicochemical and the physicomechanical properties of the newly formed PLGA scaffolds. Furthermore, the findings indicated the flexibility and the potential for the PLGA scaffolds and it's suitability for use in rate-modulated drug delivery.*

*Subsequent to elucidating its structural integrity, the scaffold was adapted into a 3-dimensional compressed monolithic matrix system. Factors such as the compressibility and the Brinell Hardness Number of PLGA Resomer® grade employed in the formulation of the scaffold and the monolithic matrix system were determined. The two model drugs, melatonin and amitriptyline HCl were incorporated into the PLGA scaffold and monolithic matrix system respectively, in order to demonstrate the applicability of these devices in the treatment of neurodegenerative disorders and the associated depression. The devices were then subjected to in vitro erosion, degradation and drug release studies in Phosphate Buffer Saline pH 7.4.*

*The novel PLGA devices displayed an ideal zero-order melatonin and amitriptyline HCl release with potential for use as implantable drug delivery devices. Kinetic modeling of swelling and erosion on WinNonlin® Version 5.1 confirmed the mechanisms of drug release of these matrices. The present mechanisms of polymer modification have demonstrated the ability to produce viscoelastic PLGA scaffold and compressed monolithic matrix system capable to house and control the release of both hydrophobic such as melatonin, and hydrophilic drugs such as amitriptyline HCl.*

*In memory of my father Ezekiel 'Macabula' S. Sibambo, I confer this dissertation to all the Sibambo's, the true warriors, who will stop at nothing to get to the crown. May this dissertation be a declaration, that all things are possible with God. Sibambo, Ngazini, Mafuyeka!*

# PUBLICATIONS, PRESENTATIONS AND PATENTS

## PUBLICATIONS:

I. Elucidation of the Physicomechanical and *Ab Initio* Quantum Energy Transitions of a Novel Crosslinked PLGA Scaffold during *In Vitro* Degradation. Sibongile R. Sibambo, Viness Pillay, Yahya E. Choonara, Riaz A Khan and Joe L. Sweet. Biomaterial, 28, 2007, 3714-3723.

II. Blister Packaging: The Way of the Future. Sibongile Sibambo, Neha Singh, Viness Pillay, Michael P. Danckwerts and David Bayever. Pharmaceutical and Cosmetic Review, 2005, 41-45.

III. A Novel Salted-Out and Subsequently Crosslinked Poly (Lactic Co-Glycolic) Acid (PLGA) Scaffold Applied to Monolithic Drug Delivery. Sibongile R. Sibambo, Viness Pillay, Yahya E. Choonara and Clem Penny. Submitted, Journal of Bioactive and Compatible Polymers, 2007.

IV. Current Trends and Challenges of Pathological and Physiologically Common Neurodegenerative Disorders. Sibongile R. Sibambo, Viness Pillay and Yahya E. Choonara. Submitted, Brain Research Bulletin, 2007.

**PRESENTATIONS:**

I. A poster entitled "Optimization of the Physicomechanical Properties of Modified Hydrophobic α-OH Polyester". Sibongile R. Sibambo, Viness Pillay, Michael P. Danckwerts Academy of Pharmaceutical Sciences 26th Annual Conference, Nelson Mandela Metropolitan university, 2005.

II. A poster entitled "Microscopic Characterization of Biodegradable Lactide-Glycolide Blocks". Sibongile R. Sibambo, Viness Pillay, Michael P. Danckwerts and Clem Penny. Academy of Pharmaceutical Sciences 26th Annual Conference, Nelson Mandela Metropolitan University, 2005.

III. A poster entitled "Analysis of Thermal Transitions and Bond Dynamics within a Hydrophobic α-Polyester". Sibongile R. Sibambo, Viness Pillay, Michael P. Danckwerts. Academy of Pharmaceutical Sciences 26th Annual Conference, Nelson Mandela Metropolitan University, 2005.

IV. A podium presentation entitled "Elucidating the Transformations and Quantum Mechanical Energy Calculations of an alpha-OH Polyester". Sibongile R. Sibambo, Viness Pillay, Michael P. Danckwerts. Academy of Pharmaceutical Sciences 26th Annual Conference, Nelson Mandela Metropolitan University, 2005.

V. A podium presentation entitled "The Effects of Polymeric Cross-Linking on the *In Vitro* Dissolution of Amitriptyline HCl from a PLGA-Based Monolithic System". Sibongile R. Sibambo, Viness Pillay, Yahya E. Choonara and

Michael P. Danckwerts. 4th International Conference on Pharmaceutical and Pharmacological Sciences, VanderBijl Park, 2006.

VI. A poster entitled "*In Vitro* Dissolution and Optimization of Melatonin-Loaded PLGA Implants for Use in Neurodegenerative Disorders". Sibongile R. Sibambo, Viness Pillay, Yahya E. Choonara and Michael P. Danckwerts. 4th International Conference on Pharmaceutical and Pharmacological Sciences, VanderBijl Park, 2006.

VII. A podium presentation entitled "Modeling of mechanistic predictors for drug transport from salted-out and crosslinked PLGA scaffolds". Sibongile R. Sibambo, Viness Pillay and Yahya E. Choonara. Academy of Pharmaceutical Sciences 27th Annual Conference, Western Cape University, 2007, (Abstract accepted).

**PATENT:**

I. Title: Improved Monolithic Drug Delivery Systems.

Inventors: Sibongile R. Sibambo, Viness Pillay, Yahya E Choonara and Michael P. Danckwerts.

Applicant: University of the Witwatersrand.

South African Provisional Patent Application Number: SA 2006/09747.

Filed: 23/11/2006.

# TABLE OF CONTENT


| | | |
|---|---|---|
| Declaration | | ii |
| Acknowledgements | | iii |
| Summary | | iv |
| Dedications | | v |
| Publications | | vi |
| Presentations | | vii |
| Patent | | viii |
| Table of Content | | ix |
| List of Tables | | xvii |
| List of Figures | | xix |


## CHAPTER ONE

### INTRODUCTION AND MOTIVATION FOR THIS STUDY


| | | |
|---|---|---|
| 1.1 | **Background** | 1 |
| 1.2 | **Modification of Biodegradable Polymers for Drug Delivery** | 2 |
| 1.3 | **Current Trends and Challenges of Neurodegenerative Disorders** | 4 |
| 1.4 | **Statement of the Problem** | 6 |
| 1.4.1 | Limitations in the Current Therapeutic Approaches for Neurodegenerative Disorders | 6 |
| 1.4.2 | The Constraint of the Blood Brain Barrier (BBB) | 8 |
| 1.4.3 | Drug Targeting to the CNS | 9 |
| 1.5 | **Proposed Solution to the Problem** | 11 |

1.5.1 Designing a PLGA-Based Implantable Device for Localized Drug delivery 11

1.6 **Rationale and Motivation for this Study** 14

1.7 **Aim and Objectives of this Study** 16

1.8 **Overview of Dissertation** 17

## CHAPTER TWO

### DEVELOPMENT OF A SALTED-OUT AND CROSS-LINKED PLGA SCAFFOLD

2.1 **Introduction** 22

2.2 **The Properties of Native PLGA** 25

2.3 **Establishing Suitable Independent Formulation Variables** 29

2.3.1 Solvent Selection for Salting-Out and Cross-Linking 29

2.3.2 Salt Selection for Salting-Out and Cross-Linking 31

2.4 **Mechanisms of PLGA Modification: Salting-Out and Subsequent Cross-Linking** 35

2.5 **Materials and Methods** 37

2.5.1 Materials 37

2.5.2 Synthesis of the PLGA Scaffold 38

2.5.3 The Effect of the Independent Variables on the Salting-Out of Various PLGA Grades 38

2.6 **Results and Discussion** 39

2.7 **Concluding Remarks** 45

## CHAPTER 3

## ELUCIDATION OF THE *IN VITRO* PHYSICOMECHANICAL AND *AB INITIO* QUANTUM ENERGY TRANSITIONS OF THE PLGA SCAFFOLD


| | | |
|---|---|---|
| 3.1 | **Introduction** | 46 |
| 3.2 | **The Degradation of PLGA** | 49 |
| 3.2.1 | Chemical Degradation of PLGA | 49 |
| 3.2.2 | Physical Degradation of PLGA | 50 |
| 3.3 | **Effects of PLGA Modification on the Stability and Degradation of PLGA** | 51 |
| 3.4 | ***Ab Initio* Quantum Mechanical Energy Calculations** | 53 |
| 3.5 | **Statistical Design of Experiments** | 57 |
| 3.6 | **Materials and Methods** | 61 |
| 3.6.1 | Materials | 61 |
| 3.6.2 | Formulation of the PLGA Scaffolds | 61 |
| 3.6.3 | Construction of the Experimental Design | 62 |
| 3.6.4 | Physicomechanical Profiling of the PLGA Scaffolds | 63 |
| 3.6.4.1 | Determination of the Matrix resilience, Matrix Tolerance and Energy absorbed | 63 |
| 3.6.4.2 | Gravimetric Analysis of Salted-out PLGA Scaffolds | 66 |
| 3.6.5 | *Ab Initio* Quantum Mechanical Energy Computations | 66 |
| 3.7 | **Results and Discussion** | 67 |
| 3.7.1 | Stereomicroscopic Image of a Salted-Out PLGA Scaffold | 67 |
| 3.7.2 | Simulation of PLGA Monomeric Interactions during Solubilization, Salting-Out and Subsequent Cross-Linking into the PLGA Scaffold | 68 |
| 3.7.3 | Physicomechanical Analysis of the PLGA Scaffolds Employing Textural Profile Analysis | 72 |
| 3.7.4 | Response Surface Optimization of Scaffold Formulations | 75 |

3.7.5 Comparison of the Experimental Vs. (Predicted) Fitted Response Values for Matrix Resilience, Energy Absorbed, and Mass Deflection Properties 82

3.7.6 Elucidation of the Quantum Mechanical Energy Transitions at a Molecular Interaction Level 83

3.8 **Concluding Remarks** 84

## CHAPTER FOUR

## THE EFFECTS OF SALTS ON THE PHYSICOCHEMICAL AND PHYSICOMECHANICAL PROPERTIES OF THE PLGA SCAFFOLD

4.1 **Introduction** 88

4. 2 **Polymer Modification with Salts and Ions** 89

4.3 **Materials and Methods** 92

4.3.1 Materials 92

4.3.2 Building the Experimental Design 92

4.3.3 Preparation of PLGA Scaffolds 93

4.3.4 Morphological Characterization of the PLGA Scaffolds 94

4.3.5 Determination of the Physicomechanical Properties of the PLGA Scaffolds 95

4.3.6 Elucidation of the Molecular Structural Transformations within PLGA Scaffolds 98

4.3.7 Thermal Transition Analysis of the PLGA Scaffolds 98

4.4 **Results and Discussion** 99

4.4.1 Proposed Interactions between PLGA Chains and Cross-linking Ions 99

4.4.2 Scanning Electron Microscopic Image Analysis of the PLGA Scaffold Morphology 100

| | | |
|---|---|---|
| 4.4.3 | Textural Profile Analysis to Quantify the Physicomechanical Properties of PLGA Scaffolds | 104 |
| 4.4.4 | Response Surface Performance | 107 |
| 4.4.5 | Determination of the Main and Interactions Effects on the Various Responses | 109 |
| 4.4.6 | Correlation between the Experimental and Predicted (Fitted) Responses Employing a Quadratic Model | 111 |
| 4.4.7 | Assessment of the Polymer-Salt Interactions and Polymeric Structural Transitions | 113 |
| 4.4.8 | Thermal Transitions within the PLGA scaffolds | 114 |
| 4.5 | **Concluding Remarks** | 117 |


## CHAPTER 5

### MODEL DRUG: MELATONIN (WATER INSOLUBLE)

### THE *IN VITRO* DRUG RELEASE STUDIES MELATONIN-LOADED PLGA SCAFFOLDS


| | | |
|---|---|---|
| 5.1 | **Introduction** | 119 |
| 5.2 | **The Use of Melatonin in Neurodegenerative Disorders** | 125 |
| 5.2.1 | Structure-Function Relationship of Melatonin as a Free Radical Scavenger in the Treatment of Neurodegenerative Disorders | 126 |
| 5.3 | **Developing the Experimental Design** | 128 |
| 5. 4 | **Determination of the Drug Entrapment Efficiency (DEE) of the PLGA Scaffold** | 128 |
| 5.5 | **Optimization of the Drug Entrapment Efficiency, Mean Dissolution Time and Drug Release Kinetics of the PLGA Scaffold** | 129 |
| 5.6 | **Kinetic Modeling of the Drug Release Data to Determine the Drug Release Mechanism from the PLGA Scaffold** | 130 |
| 5.7 | **Materials and Methods** | 131 |

| | | |
|---|---|---|
| 5.7.1 | Materials | 131 |
| 5.7.2 | Building the experimental design | 131 |
| 5.7.3 | Preparation of the Scaffolds | 132 |
| 5.7.4 | Preparation of a Calibration Curve for the Spectrophotometric Determination of Melatonin Release from the PLGA Scaffold | 132 |
| 5.7.5 | Drug Entrapment Efficiency of the Scaffolds | 133 |
| 5.7.6 | *In vitro* Drug Release from the PLGA scaffolds | 134 |
| 5.7.7 | Statistical Optimization | 134 |
| 5.7.8 | Kinetic Models Employed to Elucidate the Drug Release Mechanism from the PLGA scaffolds | 134 |
| 5.8 | **Results and Discussion** | 140 |
| 5.8.1 | Drug Entrapment Efficiency of the PLGA Scaffolds | 141 |
| 5.8.2 | Characterization of the In Vitro Drug Release from the PLGA Scaffolds | 143 |
| 5.8.3 | Response Surface Plots Indicating the Effects of Salts on the Dependent Formulation Variables | 147 |
| 5.8.4 | Statistical Analysis for Optimization of the Drug Entrapment Efficiency, Mean Dissolution Time and Drug Release Kinetics of the PLGA Scaffold | 152 |
| 5.8.5 | *In Vitro* Drug Release studies from the Optimized PLGA Scaffold | 154 |
| 5.8.6 | Kinetic Analysis of the Drug Release Mechanisms from the PLGA scaffold | 155 |
| 5.4 | **Concluding Remarks** | 162 |

## CHAPTER 6

### MODEL DRUG: AMITRIPTYLINE HCl (WATER SOLUBLE)

### *IN VITRO* AMITRIPTYLINE HCl RELEASE FROM A PLGA COMPRESSED MONOLITHIC MATRIX SYSTEM


| | | |
|---|---|---|
| 6.1 | **Introduction** | 164 |
| 6.2 | **Basic Characteristics and Release Mechanisms of Monolithic Systems** | 165 |
| 6.3 | **Hydrophilic Drugs in Monolithic Systems** | 167 |
| 6.4 | **Hardness and Compression of Polymers** | 169 |
| 6.5 | **The Use of Amitriptyline HCl in the Treatment of Depression caused by Neurodegenerative Disorders** | 171 |
| 6.5.1 | Structure-Function Relationship of Amitriptyline HCl | 173 |
| 6.6 | **Materials and Methods** | 174 |
| 6.6.1 | Materials | 174 |
| 6.6.2 | Preparation of the PLGA Compressed Monolithic Matrix System | 175 |
| 6.6.3 | Measurement of Compressibility | 176 |
| 6.6.3.1 | Calculating the Brinell Hardness Number | 177 |
| 6.6.4 | Preparation of a Calibration Curve for Spectrophotometric Determination of Amitriptyline HCl Release from the Compressed Monolithic Matrix System | 178 |
| 6.6.5 | In Vitro Drug release from the Compressed Monolithic Matrix system | 178 |
| 6.7 | **Results and Discussion** | 179 |
| 6.7.1 | The Compressibility and the Hardness Number of the Compressed Monolithic Matrix System | 179 |
| 6.7.2 | The Calibration Curve for Amitriptyline HCl | 181 |
| 6.7.3 | Drug Release Studies from the Compressed Monolithic Matrices | 182 |
| 6.8 | **Concluding Remarks** | 187 |

## CHAPTER 7

### CONCLUSIONS AND RECOMMENDATIONS


7.1 **Conclusions** 189

7.2 **Recommendations** 191

8 **REFERENCES** 194

## LIST OF TABLES


| | | |
|---|---|---|
| *Table 1.1* | *The benefits and the limitations of the current and explored strategies of drug delivery to the brain* | *10* |
| *Table 2.1* | *General physicochemical and the physicomechanical properties of native PLGA grades* | *27* |
| *Table 2.2* | *The physicochemical properties of solvents used in salting-out PLGA* | *30* |
| *Table 2.3* | *Series illustrating the ability of ions to cause water stabilization, a predictor of the degree to which the ion can salt-out the polymer* | *32* |
| *Table 2.4* | *Classification of ions used in terms of molar aqueous ionic volume, entropy of hydration and the viscosity Jones-Dole B-coefficient* | *34* |
| *Table 2.5* | *The reaction of random input variables on the salting-out of various PLGA grades (RG 502, RG 503 and RG 504)* | *40* |
| *Table 2.6* | *Scaffold yield after salting-out and cross-linking with various salts* | *42* |
| *Table 3.1* | *Normalized factor levels of the independent variables for the FCCD* | *62* |
| *Table 3.2* | *Randomized experimental runs generated from the FCCD* | *63* |
| *Table 3.3* | *Textural parameters and settings* | *64* |
| *Table 4.1.* | *Factor levels of the independent variables for the Box-Behnken Design* | *93* |
| *Table 4.2* | *Box-Behnken template with randomly generated PLGA formulations* | *94* |
| *Table 4.3* | *Textural parameter settings* | *95* |
| *Table 4.4* | *Physicochemical properties of the salts employed during cross-linking of PLGA* | *100* |
| *Table 4.5* | *Thermal parameters of native and salted-out PLGA employing DSC* | *116* |

| | | |
|---|---|---|
| *Table 5.1* | *The Physicochemical and the Physicomechanical Properties of the Neurohormone Melatonin* | *125* |
| *Table 5.2* | *Factor Levels of the Independent Formulation Variables* | *132* |
| *Table 5.3* | *The drug release at 30 days (%), Mean Dissolution Time $(MDT)_{30}$ and the release constant (K) of the PLGA scaffolds* | *144* |
| *Table 5.4* | *Settings for Response Optimisation* | *152* |
| *Table 5.5* | *Desired and Experimental responses for the optimised PLGA scaffold formulations* | *154* |
| *Table 5.6* | *Drug release kinetics obtained from the various diffusion, relaxation and erosion models for the optimized PLGA scaffold formulation* | *156* |
| *Table 5.7* | *Mechanistic predictors for melatonin release from the PLGA scaffolds* | *158* |
| *Table 5.8* | *Swelling studies of the PLGA scaffolds loaded with melatonin* | *161* |
| *Table 6.1* | *The Physicochemical and the Physicomechanical Properties of the TCA Amitriptyline* | *172* |
| *Table 6.2* | *Normalized factor levels of the independent variables* | *175* |
| *Table 6.3* | *Textural settings employed for BHN value calculations* | *176* |
| *Table 6.4* | *BHN values obtained from the fourteen samples of compressed monolithic matrix systems Formulations.* | *180* |

## LIST OF FIGURES


| | | |
|---|---|---|
| *Figure 2.1* | *Schematic diagram of the metabolic degradation of PLGA.* | *28* |
| *Figure 3.1* | *Typical textural force-distance and force-time profiles of salted-out PLGA scaffolds for the determination of (energy absorbed and matrix resilience.* | *65* |
| *Figure 3.2* | *A stereomicroscopic image of a salted-out PLGA scaffold depicting the exterior surface morphology.* | *67* |
| *Figure 3.3* | *PLGA-interactions illustrating PLGA, interaction after DMF, water and acid addition addition. In the last structure, DMF and protonated water interaction showing temporary proton and charge transfer from water molecule to DMF molecule.* | *70* |
| *Figure 3.4* | *Profiles depicting the physicomechanical transitions of the salted-out PLGA scaffolds immersed in PBS (pH 7.4, 37°C) matrix resilience, energy absorbed and mass deflection, over a 30-day period.* | *73* |
| *Figure 3.5* | *Response surface plots depicting resilience vs water volume and polymer mass; water volume and salting-out time; water volume and polymer concentration; polymer molecular weight and salting-out reaction time; polymer molecular weight and polymer concentration; polymer concentration and salting-out time.* | *76* |
| *Figure 3.6* | *Response surface plots depicting energy of absorption vs water volume and polymer mass; water volume and salting-out time; water volume and polymer concentration; polymer molecular weight and salting-out reaction time; polymer molecular weight and polymer concentration; polymer concentration and salting-out time.* | *78* |
| *Figure 3.7* | *Response surface plots depicting weight deflection vs water volume and polymer mass; water volume and salting-out time; water volume and polymer concentration; polymer molecular weight and salting-out reaction time; polymer molecular weight and polymer concentration; polymer concentration and salting-out time.* | *80* |
| *Figure 3.8* | *Profiles demonstrating the correlation between experimental and fitted values for the responses. R=Matrix resilience; E=Energy absorbed; WD= Mass deflection.* | *82* |
| *Figure 4.1* | *Typical Force-Distance and Force-Time profiles of PLGA scaffolds for determining energy absorbed, deformability modulus and matrix resilience.* | *97* |

| | | |
|---|---|---|
| *Figure 4.2* | *Scanning Electron Micrographs of Salted-out PLGA. These micrographs demonstrate the surface morphology of PLGA: salted-out with NaCl [Figure 4.2(a) and 4.2(b)] at 2000X Mag (a nd b), WD of 23mm and 37mm; $CaCl_2$, [Figure 4.2(c) and 4.2(d)] at 2000X Mag (c) and 20X Mag (d), WD of 22mm (c and d) as well as $AlCl_3$ [Figure 4.2(e) and 4.2(f)] at 2000X Mag (e) and 1000x Mag (f), WD of 20mm (e and f). Mag= Magnification, WD=Weight distribution.* | *102* |
| *Figure 4.3* | *Profiles depicting differences in the physicomechanical properties of PLGA scaffolds. Plot (a) Resilience (R), (b) Energy absorbed (E) and (c) Deformability modulus (DM).* | *105* |
| *Figure 4.4* | *Typical surface response plots depicting the effects of the independent formulation variables on the physicomechanical properties of the salted-out PLGA scaffolds, namely (a) Resilience (R) (%); (b) Energy absorbed (E) (J); and (c) Deformability modulus (DM) (N/mm). AC= $AlCl_3$, CC= $CaCl_2$, SC= NaCl. -1=0%$^{w}/_{v}$ 0=5%$^{w}/_{v}$ 1=10%$^{w}/_{v}$.* | *108* |
| *Figure 4.5* | *Typical profiles used to construe the main and interactions effects of NaCl (a) and (d); $CaCl_2$ (b) and (e); $AlCl_3$ (c) and (f) for resilience in the presence of a combination of parameters.* | *110* |
| *Figure 4.6* | *Profiles demonstrating the correlation between experimental and fitted response values. R=Resilience; E=Energy absorbed; DM= Deformability modulus.* | *112* |
| *Figure 4.7* | *Five superimposed FTIR profiles depicting transitions from native PLGA to salted-out PLGA scaffolds. (a) = Native PLGA, (b)-(e) = PLGA salted-out with NaCl, $CaCl_2$, $AlCl_3$ and a combination of NaCl + $CaCl_2$ + $AlCl_3$ respectively.* | *114* |
| *Figure 4.8* | *Differential Scanning Calorimetry (DSC) profiles of native and salted-out PLGA scaffolds demonstrating thermal transitions of (a) native PLGA, (b) PLGA salted-out with NaCl, (c) $CaCl_2$, (d) $AlCl_3$, and (e) a combination of NaCl, $CaCl_2$, and $AlCl_3$.* | *115* |
| *Figure 5.1* | *Flow diagram displaying three main types of controlled drug release systems.* | *120* |
| *Figure 5.2* | *Chemical structure of melatonin: (5-methoxy-N-acetyltryptamine)* | *127* |
| *Figure 5.3* | *Melatonin calibration curve at 278.2nm in PBS (pH 7.4) (S.D. within ±0.049)* | *140* |
| *Figure 5.4* | *Plot depicting the differences in the DEE of the salted-out* | *142* |

*and cross-linked PLGA scaffolds.*

*Figure 5.5* *Release profiles of melatonin from the PLGA scaffolds (a) Formulations 1-7 and (b) Formulations 8-14.* *146*

*Figure 5.6* *Surface response plots depicting the effects of the independent formulation variables on the Drug Entrapment Efficiency (DEE) (%) in salted-out PLGA scaffolds. AC= $AlCl_3$, CC= $CaCl_2$, SC= NaCl. -1=0%$^w/_v$ 0=5%$^w/_v$ 1=10%$^w/_v$.* *149*

*Figure 5.7* *Surface response plots depicting the effects of the independent formulation variables on the Release Constant (k) of the salted-out PLGA scaffolds. AC= $AlCl_3$, CC= $CaCl_2$, SC= NaCl. -1=0%$^w/_v$ 0=5%$^w/_v$ 1=10%$^w/_v$.* *150*

*Figure 5.8* *Surface response plots depicting the effects of the independent formulation variables on the Mean Dissolution Time (MDT) of the salted-out PLGA scaffolds AC= $AlCl_3$, CC= $CaCl_2$, SC= NaCl. -1=0%$^w/_v$ 0=5%$^w/_v$ 1=10%$^w/_v$.* *151*

*Figure 5.9* *Optimization and Desirability plots illustrating the type and concentration of salt required to produce a desired response that will give an optimal PLGA scaffold* *153*

*Figure 5.10* *Melatonin release profile of melatonin from an optimized PLGA scaffold.* *154*

*Figure 6.1* *Chemical structure of amitriptyline: (3-(10,11-dihydro-5H dibenzo[a,d]cyclohepten-5-ylidene)-propyldimethylamine).* *173*

*Figure 6.2* *Typical force-displacement profiles for PLGA monolithic matrices in the determination of matrix indentation hardness.* *177*

*Figure 6.3* *Typical compressibility profile depicting the effects of compression force on the compressed monolithic matrix system* *179*

*Figure 6.4* *Amitriptyline HCl calibration curve at 240.1 nm in PBS* *182*

*Figure 6.5* *Fractional drug release profiles of amitriptyline from 14 PLGA scaffolds of monolithic matrix systems prepared by either (a) cross-linking PLGA with amitriptyline followed by compression or (b) cross-linking PLGA without amitriptyline followed by compression of PLGA and amitriptyline.* *185*

# CHAPTER ONE

## INTRODUCTION AND MOTIVATION FOR THIS STUDY

### 1.1 Background

Biodegradable polymers have presented new approaches to clinical medicine by improving drug delivery technology (Burkoth et al., 2000; Kakinoki et al., 2003; Kushibiki and Tabata, 2004; Chowdhury and Akaike, 2005). The use of these polymers in the formulation of implantable devices has particularly allowed for localized treatment and the controlled release of bioactives transported by the device, such as, drugs, vaccines, hormones and cells for tissue engineering (Kim et al., 2006; Li et al., 2006; Piotrowicz and Shoichet, 2006; Xue et al., 2006).

By virtue of its biodegradability, such a device is able to function for a predetermined period of time, and subsequently degrade hydrolytically or enzymatically and be completely eliminated from the body. Thus, biodegradable polymers not only eliminate the need for subsequent surgery for the removal of the device, but also enhance drug efficacy. Recently, there has been a significant advance in the science of the behaviour of polymeric materials, which has permitted a more systematic approach to their modification for drug delivery and tissue engineering (Dhanikula and Panchagnula, 2004; Kimura et al., 2006; Li et al., 2006; Virto et al., 2006; Cheng et al., 2007; Kumar et al., 2007; Yang et al., 2007).

There is a huge demand for novel biodegradable polymers with unique properties to match their specific applications. The challenge is to accelerate research in the development and modification of these materials in order to address the wide range

of biomedical applications. Such materials must have the ability to degrade controllably with non-toxic degradation products without posing any immune reaction *in vivo*. Hydrophobic aliphatic α-hydroxy (-OH) polyesters such as poly-lactic acid (PLA), poly-glycolic acid (PGA), and particularly the co-polymer poly(lactic-co-glycolic) acid (PLGA) have been verified as excellent bioactive carriers owing to their desirable properties, namely, biodegradability, biocompatibility, non-immunogenicity, superb mechanical strength and hence has approval by the US Food and Drug Administration (FDA) as 'Generally Regarded as Safe' (GRAS) materials. Furthermore, the ability of PLGA to dissolve in both organic and inorganic solvents as well as their potential to be designed into various drug delivery and tissue-engineering devices has been instrumental in their use for medical applications (Sander et al., 2004; Garvin and Feschuk, 2005).

### 1.2 Modification of Biodegradable Polymers for Drug Delivery

Biodegradable polymers can be natural or synthetic. Natural polymers are obtained from numerous sources. With the aid of enzymes, some of the natural polymers can degrade, however, the variability of polymer quality, the lack of stability and the intricate processing mechanisms have made them unpopular in biomedicine. Alternatively, synthetic biodegradable polymers are more favourable, since most can be produced with modifiable properties (Blomeier et al., 2006).

The majority of synthetic biodegradable polymers are linear thermoplastics such as PLA, PGA and PLGA. Their physicochemical and physicomechanical properties are mainly tailored by altering the molecular mass during polymerization or alternatively, by altering the chemical backbone or side chain of the existing polymer (Kranz et al.,

1999; Helminen et al., 2000; Middleton, and Tipton, 2000; Masahiko, 2002; Jayakumar et al., 2007).

The correlation between the physicochemical, physicomechanical and release properties of drug delivery devices is key to the functioning of biodegradable polymers in physiological media. The dynamics of these processes are primarily dependent on hydrolytic degradation, and the influence of pH on disentanglement. The performance of drug delivery devices *in vitro* and *in vivo* depends on the mechanisms of engineering and transformation of the polymer in terms of such parameters.

The significance of modified biodegradable polymers in controlled and sustained drug release, especially in illnesses that require chronic suppressive maintenance therapy, cannot be sufficiently accentuated. The advantages of such a system include maintenance of drug levels within the desired therapeutic range, fewer drug administrations and optimal use of central nervous system (CNS) drugs. Consequently, there is selectivity of the pharmacological activity at receptor site, owing to the regulated pharmacokinetics and pharmacodynamics of drug effects (Takatori et al., 2005; Ennett et al., 2006).

A future concept, namely, patient independence is extremely important. In diseases that traditionally demand high care, it is vital to reduce nursing care, establish patient's autonomy and to reduce the psychological and fiscal burdens of nursing care. In such cases a localized controlled drug release implant may be beneficial.

This in turn, will eliminate the need for monitored and nurse-regulated drug therapy (Jamzad and Fassihi, 2006).

### 1.3 Current Trends and Challenges of Neurodegenerative Disorders

The term neurodegenerative disorders, encompasses a variety of underlying conditions, sporadic and/or familial. A number of diverse genetic and sporadic neurological disorders lead to dementia and/or abnormal motor symptoms. Among them are those characterized by neuronal or microglia-initiated accumulation of tau proteins (Matsuo, 1994; Lee et al., 2001; Shahani and Brandt, 2002; Rissman et al., 2004; King, 2005).

These tauopathies form a diverse group of diseases that have several commonalities at the molecular level, since many of them are characterized by accumulations of misfolded proteins that aggregate into fibrillar deposits with amyloid. Such disorders are associated with atrophy of the central or peripheral nervous system structures. The major disorders include Alzheimer's Disease, Parkinson's Disease, Amyotrophic Lateral Sclerosis and Huntington's Disease.

Each of these disorders affects a distinct section/s of the brain, causing motor and/or cognitive deficits such as aphasia, apraxia and agnosia, consequently disrupting the personality, intellectual, social and occupational functions in the patient (Broom et al., 2004; Lefaucheur, 2004; Ahmed et al., 2005; Ivanoiu et al., 2005; Veldink et al., 2005). Postmortem investigations have enlightened researchers on the microglia-produced inflammatory and neurotoxic factors such as cytokines and tumor necrosis factor-α (TNFα) with free radicals that are deleterious to neurons (Gao et al., 2002).

These disorders usually begin after the age of 60, and risk goes up with age. For example, the number of South Africans suffering from Alzheimer's Disease has grown from 80,788 in the year 2000 to 95,869 in 2005. The prevalence is approximately 13% for age group 60-69 years and 35% for age group above 80 years (Potonick, 2005). Statistics by a United Nations (UN) project predicts a prevalence of 9 billion people by the year 2070 and 34% of that population to be over the age of 60 (Potonick, 2005).

The world prevalence of Parkinson's Disease is 150 per 100,000 and increasing rapidly in those over 70 years of age. Risk factors include age, sex, race and geographical location. The incidence for Amyotrophic Lateral Sclerosis is approximately 5,000 people per year and 5 in a 100,000 people suffer from Huntington's Disease world-wide. These are some of the most persistent and devastating dementing disorders of old age, since they eventually lead to complete loss of memory and the loss of ability to function independently (Julien et al., 2006).

The burden of neurodegerative disorders on individuals, families and our health care system makes it one of South Africa's country's greatest medical, social and fiscal challenges (Hayden et al., 1980; Nahin, 2005). Alzheimer's Disease, Parkinson's Disease, Amyotrophic Lateral Sclerosis and Huntington's Disease are extremely complex neurodegenerative disorders. Their etiology is mostly unknown; however severe genetic mutations that lead to misfolding and aggregation in extracellular protein depositions have been observed. Currently, there are no completely effective therapies that have been developed (Stuss and Levine, 1996; Ying 1996; Salmon and Filotoe, 2007).

Research findings that implicate the commonalities in protein aggregations and molecular pathogenic mechanisms could insinuate that neurodegenerative disorders may share a common or overlapping pathogenic mechanism(s) which could be targeted by synchronized therapeutic strategies (Huang, 2006; Limviphuvadh et al., 2007).

## 1.4 Statement of the Problem

### *1.4.1 Limitations in the Current Therapeutic Approaches for Neurodegenerative Disorders*

The major limitations of current therapies for neurodegenerative disorders is that they are either formulated as orally administered tablets, capsules or liquids which require frequent dosing and hence leading to continuous nursing, numerous deleterious side effects and incompliance. An ideal form of therapy could provide long-term controlled drug delivery, which would reduce nursing care, and in the absence of nursing care, eradicate the need for patients to remember to take their daily dose.

In addition, the formulation could be implanted into the central nervous system (CNS) to provide localized drug delivery that improves drug efficacy. For example, current limitations in Alzheimer's Disease include oral administration of cholinesterase inhibitors (ChE-I) such as donepezil (Aricept®), that is administered daily, depending on the therapeutic goal. This results in greater frequency of side effects at higher doses due to dose accumulation.

Galantamine (Reminyl®) is also available in the form of tablets and requires twice daily administration (Masterman, 2004). In their study, Olin and Schneider (2001) reported that galantamine consistently failed to display statistically significant treatment effects at doses of 8mg/day and produced adverse gastrointestinal symptoms similar to other ChE-Is with higher doses. Clinical trials demonstrated no statistical benefit on increasing the regular dose of 8-12mg twice daily (Ritchie et al., 2004).

The same shortcomings are experienced with other neurodegenerative disorders, such as, Parkinson's Disease and Huntington's Disease. In the treatment of Parkinson's Disease, levodopa is combined with an aromatic amino acid decarboxylase inhibitor, carbidopa (Carbilev®), to reduce peripheral conversion of levodopa to dopamine in an effort to reduce peripheral side effects. These oral dosage forms, however, lead to increased peripheral levodopa and the toxicity causes dyskinesia, rigidity and tremor because of the uncontrolled rate of drug delivery. For Huntington's Disease, olanzapine 2.5mg daily, a dopaminergic-serotonergic antagonist, has been recommended (Squitieri et al., 2001; Laks et al., 2004).

Alternatively, olanzapine 5mg per day is given with lofepramide 140mg per day for psychiatric improvement, however, these formulations also lead to side effects such as dizziness, akathisia, asthenia and tremor due to peripheral toxicity. Few of these side effects are due to peak-trough changes of the drug plasma concentration and could be reduced by controlled drug delivery.

The above mentioned conventional drugs and their respective delivery systems have been found to have numerous side effects, such as, higher doses required, lower therapeutic efficacy, drug toxicity and high nursing care. To date, there has been no successful conventional tablet that has the ability for localized and controlled drug delivery in the treatment of these disorders (Martin-Garcia et a., 2007; Voisine et al., 2007).

### *1.4.2 The Constraint of the Blood Brain Barrier (BBB)*

Another sobering fact in the treatment of neurodegenerative disorders is the constraint of the BBB on the passage of drugs to the brain, and the drug release kinetics that cause side effects. The BBB controls the passage of substances into the brain, permitting only molecules that have a molecular mass smaller than 500 Da. Of all known central nervous system drugs, 98% have a molecular mass larger than 500 Da and therefore cannot cross the BBB.

Consequently, the development of bioactives to manipulate central acetylcholine systems has lagged behind due to the poor CNS penetration along with the significant peripheral nervous system side effects. Therapeutic failure of some bioactive agents in the diagnosis and therapy of neurodegenerative disorders may not be due to a lack of drug potency, but rather attributed to the limitations in the methods of drug delivery.

In view of these facts, local delivery of drugs to the brain may produce a solution to these limitations. This will ensure a controlled increase in drug concentrations over extended periods at the affected neurons as well as a reduction in side effects. Novel

mechanisms of polymer modification are being explored in order to design therapeutic strategies that will deliver drugs to the CNS in a safe and effective manner (Killian et al., 2000; Bartzatt, 2004).

### *1.4.3 Drug Targeting to the CNS*

The BBB has major repercussions for the passage of bioactives into the brain. The passage of compounds across the endothelial cells of the BBB depends on the physicochemical and the physicomechanical properties of the compound, such as, lipid solubility, molecular mass and the extent of ionization, (Rapoport et al. 1979). Considerable efforts have gone into developing novel delivery techniques to the brain, such as, prodrugs. While these options are available for drug delivery to the CNS, few have serious limitations. Table 1.1 displays some of the current strategies employed in the delivery of bioactives to the CNS.

**Table 1.1.** *The benefits and the limitations of the current and explored strategies of drug delivery to the brain*

| Brain Delivery Mechanisms | Benefits | Limitations |
|---|---|---|
| ❖ Passive diffusion | ❖ Highly selective.<br>❖ Lipid soluble compounds can pass without difficulty. | ❖ Diffusion is dependent on a concentration gradient and the properties of molecules including size.<br>❖ Non-homogenous distribution of drugs and toxicity.<br>❖ Subject to an active efflux barrier. |
| ❖ Drug Lipidization via conjugation of lipid soluble functional groups or carrier | ❖ Increase of the permeability surface area for non-lipophilic drugs.<br>❖ Drugs larger than 500Da can pass the BBB. | ❖ Increase uptake of lipidized drug by systemic organs.<br>❖ Loss of drug to the brain due to conjugation.<br>❖ Decreased therapeutic efficacy due to loss of drug. |
| ❖ Catalyzed transport via carrier-mediated Transport or receptor-mediated transport | ❖ Can recognise and select substrate.<br>❖ No need for energy. | ❖ Only for small drug molecules.<br>❖ Drug molecular structure must be similar to endogenous molecules.<br>❖ Overlap of substrate specificity leads to mistransportation. |
| ❖ Prodrugs | ❖ High residence time in the brain.<br>❖ Good for drug distribution. | ❖ Requires modification of therapeutic agent to be delivered.<br>❖ Drug may be deactivated by enzymes of the BBB. |
| ❖ Hyper-osmolar BBB disruption | ❖ Non selective.<br>❖ Can allow several types of drug molecules including cancer and neurodegenerative drugs. | ❖ BBB disruption.<br>❖ General increase in brain uptake of plasma constituents.<br>❖ Causes neuropathological problems. |
| ❖ Intracerebro ventricular Injection | ❖ This method is a targeted, localized delivery of a drug | ❖ Limited drug entry into brain parenchyma and very costly.<br>❖ Diffusion dependent, does not work if the drug must reach other parts of brain in effective concentrations. |
| ❖ Intracerebral implantation of devices | ❖ Easily implantable by stereotaxy in discrete, precise and functional parts of the brain tissues | ❖ Size dependent, if the molecule is very small, it may be taken up by macrophages<br>❖ Need for subsequent surgery if not biodegradable<br>❖ Causes neuro-inflammation if the device is immunogenic. |
| ❖ Intranasal passage | ❖ Non-invasive and rapid.<br>❖ Bypasses the BBB.<br>❖ Good for proteins. | ❖ Drug concentration is variable.<br>❖ Intranasal drug degradation may cause mucosal irritation. |

The need for improvement of drug delivery systems to the brain cannot be disputed. Controlled drug release in the brain through implantable biodegradable polymeric devices is an option that this research is proposing.

## 1.5 Proposed Solution to the Problem

### *1.5.1 Designing a PLGA-Based Implantable Device for Localized Drug Delivery*

Novel biodegradable materials are increasingly receiving attention to address the growing need for controlled drug therapy (Eerikainen et al., 2004; Feng et al., 2004; Jackson et al., 2004; Li and Liu, 2004; Parojcic et al., 2004; Puoci et al., 2004; Satturwar et al., 2004; Vogt et al., 2004; Yang et al., 2004; Yue et al., 2004). In neurodegenerative disorders such delivery devices based on polymer matrices include in particular, the thermoplastic polymer, PLGA. These polymers have been used in various applications, some of which include the fabrication of tissue scaffolds (Katz, 2001; Vozzi et al., 2003), surgical sutures (Benicewicz, 1991), and the formulation of drug delivery devices (Jain, 2000).

Most recently Sweet (2005) conducted both *in vitro* and *in vivo* studies to investigate the use of a PLGA-alginate polyspheric drug delivery device as a potential subcutaneous implant for the delivery of diclofenac sodium in the treatment of Alzheimer's Disease. It was demonstrated that drug delivery could be achieved over a period of more than three months. This subcutaneous implant could be further upgraded into a CNS implant, incorporated with anti-oxidants and anti-inflammatory drugs for the localized treatment of neurodegenerative disorders.

Despite the overall attractiveness of most thermoplastic polymers, they degrade through bulk hydrolysis of the ester bonds (Ramchandani and Robinson, 1997). When a native PLGA device is in contact with an aqueous environment, water penetrates into the implant and hydrolytic cleavage of ester bonds begin. Each ester bond cleavage generates a new carboxyl end group that, in principle, can catalyze the hydrolytic reaction of other ester bonds. Transiently, partially degraded macromolecules remain insoluble in the surrounding medium and sequential degradation proceeds homogeneously.

As soon as the molecular mass of the partially degraded macromolecules is low enough to allow dissolution in the aqueous medium, diffusion begins within the bulk polymer, with soluble compounds moving slowly towards the diffusion front as polymeric degradation simultaneously continues. This process combines diffusion, chemical reaction(s) and dissolution principles, results in a differentiation between the rates of degradation at the surface and the interior of the matrix. In general, oligomers can escape from the polymeric surface before total degradation, resulting in a smaller autocatalytic effect (Göpferich and Langer, 1995; Fu et al., 2000).

Considering the interdependence of polymeric degradation and polymeric properties, the release rate of the bioactive agent may be significantly regulated. In addition to diffusion and erosion, the processes of polymeric relaxation and disentanglement are key to controlling the release of the bioactive agent. Other shortcomings of existing microparticulate PLGA formulations include the uptake by macrophages, which is vastly dependent on the microparticle size, variability of drug loading and encapsulation efficiency (average of 5-35%), as well as inadequacy and non-

reproducibility of formulation processes. This can therefore be a very costly process especially when expensive materials such as proteins, vaccines and genes are encapsulated (Gomez-Gaete et al., 2007; Haddadi et al., 2006; Lee et a l., 2007).

In consideration for the development of a drug delivery device for the treatment of neurodegenerative disorders, the polymers should display enhanced adhesion (Kang et al., 1999), superior physicomechanical strength and restricted swelling (Atta, 2002). The chemical nature, processing variables and morphologic characteristics affect the mechanical, electric and thermal properties of the polymer. Mechanical properties are also profoundly affected by the increase in temperature. In general, temperature reduces Young's modulus as well as tensile strength and hence the overall chain flexibility of the polymer. Changing the molecular mass and functionality of the polymer can also control characteristics such as rigidity and permeability. Stress-strain curves may provide information on the brittleness and ductility of the polymer.

Salting-out and salting-in have been used in polymer modification. Zhang et al. (1995) described the use of insoluble electrolytes to modulate the release and swelling of biodegradable polyesters. The addition of salts to an aqueous phase causes an increase in the distribution ratio of that particular solute, reduces the mutual partial miscibility of the two liquids, thereby, causing phase separation (Izutsu and Aoyagi et al., 2005; Cilurzo et al., 2005; Huang et al., 2005).

Furthermore, polyesters can be rendered stiffer by introducing chemical bonds between their monomers (cross-linking). The number of cross-links is proportional to

the rigidity of the material. The extent of cross-linking attained depends on the relative concentrations of the polymer as well as the bi-functional molecule. Such cross-linked polymers are extremely large, multi-dimensional molecules with distinctly diverse physicochemical and physicomechanical properties. This study, therefore sought to establish the mechanisms associated with the salting-out and subsequent cross-linking of PLGA with ionic salts in the presence of organic and inorganic solvents, in order to design a polymeric scaffold to be used in the treatment of neurodegenerative disorders (Cadee et al., 2001; Liu et al., 2004; Porjazoska et al., 2006).

### 1.6 Rationale and Motivation for this Study

Development of novel biodegradable materials with both high initial strength and controlled moduli is of great demand for new biomedical applications. Numerous studies conducted on biodegradable polymers generally focus on biocompatibility, physicomechanical properties, morphological behaviour and thermal characterization (Sato et al., 2000; Deng, 2002; Mc Cullagh et al., 2004; Tapia et al., 2004).

One of the limitations associated with current thermoplastic polymers is that there is a significant lack of research directed towards the mechanisms associated with the manipulation of the actual methods for modifying the physicochemical and the physicomechanical properties such as salting-out and the subsequent cross-linking of polymers. Exploring the processes for the modification of the polymeric physicochemical and physicomechanical properties may lead to the design of novel materials with desirable properties for controlled drug delivery.

Various polymeric materials need to be synthesized to appropriately match a number of biomedical applications. An ideal biodegradable polymer should possess physicochemical and physicomechanical properties that will allow it to match its application. In order to achieve this, the flexibility in the synthesis of native polymers may be enhanced. However for each application, the polymer has to be re-synthesized from its initiator steps. This process can be exhaustive, time-consuming and costly. Therefore, an alternative approach could be to apply a series of chemical modifications to the existing backbone of the polymer.

The latter approach poses a challenge to most polymer scientists. If attainable for all biodegradable materials, this approach would allow for the design of tailor-made polymers with physicochemical and physicomechanical properties that are consistent with its application. In this study, we are recommending the modification of the PLGA backbone. Thus specific physicochemical and physicomechanical properties of PLGA can be precisely altered to achieve superior degradation and drug release kinetics during its application as a drug delivery scaffold.

To date, no research has fully explored the mechanisms of modifying the properties of PLGA through salting-out. In this regard, the application of salts and other solvent systems may be used as salting-out and cross-linking agents to alter the properties of PLGA. In this study, modification of PLGA was based on the principle of salting-out and subsequent cross-linking of this hydrophobic polymer using the interaction between a water-miscible organic solvent and an aqueous-salt environment. The drug-loaded modified PLGA scaffold is envisaged to serve as an alternative device

that could be implanted into the subarachnoid cavity of the brain by means of a stereotaxic procedure in order to provide prolonged drug release.

### 1.7 Aim and Objectives of this Study

The overall aim of this study is therefore, to establish the mechanisms associated with the salting-out and subsequent cross-linking of PLGA in the presence of organic and inorganic solvents. Based on the foundation of these physicochemical and the physicomechanical transitions, a polymeric slab with a balance between viscoelasticity and brittleness will be designed as a potential scaffold for the controlled delivery of bioactive agents, such as, melatonin, and amitriptyline HCl which may be useful in the treatment of common neurodegenerative disorders and depression.

In order to accomplish this aim, the following objectives are outlined:

1. To synthesize variants of PLGA using salting-out and subsequent cross-linking technology and a combination of chemical inducers such as N,N dimethyl formamide (DMF) and acetone based on statistical Design of Experiments, namely, Face-Centered Central Composite Design (FCCD) and Response Surface Methodology (RSM);
2. To elucidate the physicomechanical and *ab initio* quantum energy transitions of the novel cross-linked PLGA scaffold during *in vitro* degradation ;
3. To elucidate the physicochemical and physicomechanical properties, particularly the fibre morphology and stress-strain behaviour of PLGA through textural profiling and the correlation between the reactivity of the chemical inducers and the extent of polymeric cross-linking;

4. To formulate novel drug delivery systems such as a scaffold and a compressed monolithic matrix system incorporating bioactives for the treatment of neurodegenerative disorders, the model drugs being melatonin and amitriptyline HCl;
5. To assess the *in vitro* dissolution and drug release characteristics of the novel PLGA scaffold and compressed monolithic matrix system; and
6. To predict and simulate responses such as polymer swelling and erosion kinetics based on Design of Experiments (DoE) such as Response Surface Methodology (RSM) and kinetic modelling of drug release data using WinNonlin® software V5.1 (Pharsight®, U.S.A.).

### 1.8 Overview of Dissertation

Chapter One of this dissertation introduces the study by presenting the fundamental aspects of modifying biodegradable polymers for drug delivery. It also outlines the current trends and challenges of neurodegenerative disorders and the delivery of drugs to the brain. The limitations of the present therapeutic approaches for neurodegenerative disorders, the constraint of the BBB are specified. This section then outlines the solution to these challenges using novel biodegradable polymers and a proposed plan of action to be performed throughout the study. A flow diagram is provided for the reader not to lose focus of the fundamental issues of this study.

Chapter Two of this dissertation describes the development of the PLGA scaffold through the process of salting-out and subsequent cross-linking. It attempts to explicate the mechanisms associated with salting-out and the subsequent cross-linking of PLGA in the presence of organic solvents and ionic salts. In this Chapter,

the author also discusses the selection process of the materials used and the independent formulation variables.

In Chapter Three, the study elucidates the physicomechanical transitions and the *ab initio* quantum energy transitions of the novel cross-linked PLGA scaffold during *in vitro* degradation. Variants of PLGA scaffolds were synthesized using salting-out and cross-linking technology in accordance with a statistical screening design, namely, FCCCD, in order to select the optimal number of experiments needed for process optimisation. The physicomechanical transitions in matrix resilience, energy absorbed and mass deflection during degradation of the novel PLGA scaffolds in phosphate buffered saline (PBS) are used as assessment tools for elucidating the scaffold degradation dynamics.

In addition these transitions are used to establish if it can be tailored to suit its application as a device to be implanted into the subarachnoid space in the brain. Quantum energy transitions in the congealed energy state of the scaffold and the interacting molecules are used to indicate the ability of the composite system to contribute to the stabilization of the physicomechanical properties of the PLGA scaffolds.

Subsequent to establishing the stability of the novel modified PLGA in Chapter Three, the Fourth Chapter of this dissertation demonstrates the effect of various reagents on the degree of salting-out and cross-linking of PLGA. In this regard, the correlation between the types of salts employed and the extent of PLGA chain transitions are established.

Variants of PLGA scaffolds were prepared using salting-out and cross-linking technology in accordance with a Box-Behnken statistical design to select the optimal number of experiments for optimisation. Geometric, physicochemical, physicomechanical and thermal transitions were then analysed by Scanning Electron Microscopy (SEM), Fourier Transform Infrared (FTIR), Differential Scanning Calorimetry (DSC) and textural profiling analysis. The principles by which the physicochemical and the physicomechanical transitions of the polymer occur are identified in this Chapter.

The applicability of the scaffold for controlled drug delivery is determined in Chapter Five. *In vitro* dissolution and drug release studies were conducted, in order to optimize the formulation for application in the delivery of melatonin to the brain. In this Chapter, *in vitro* release studies are performed in phosphate buffered saline (PBS; pH 7.4; 37°C), and the release media is sampled at pre-determined intervals and analyzed by UV-spectroscopy (278 nm) to establish if the scaffold is capable of achieving an ideal zero-order melatonin release.

Chapter Six of this dissertation focuses on adapting the PLGA scaffold into a compressed monolithic matrix system. In this section of study, two approaches were adopted. The first approach incorporates the salting-out and subsequent cross-linking of PLGA at various salt concentrations in the presence of the drug, which was followed by direct compression of the samples into compressed monolithic matrix systems. In the second approach, PLGA was salted-out and subsequently cross-linked in the absence of the drug, which was followed by direct compression of the drug and the modified PLGA. Amitriptyline HCl was used as the model drug. The

drug release characteristics of the compressed monolithic matrix systems were categorized. This section of the study also considered the compressibility of PLGA.

Finally in Chapter Seven, the author outlines the concluding summary of the study. Supplementary to that are the recommendations for future research in this area.

The work plan is designed in a form of a flow diagram that guided the study in a step-by-step manner through the entire project. The following flow diagram verifies the objectives of the study and also delineates the practical work that is to be undertaken in fulfilment of each objective.

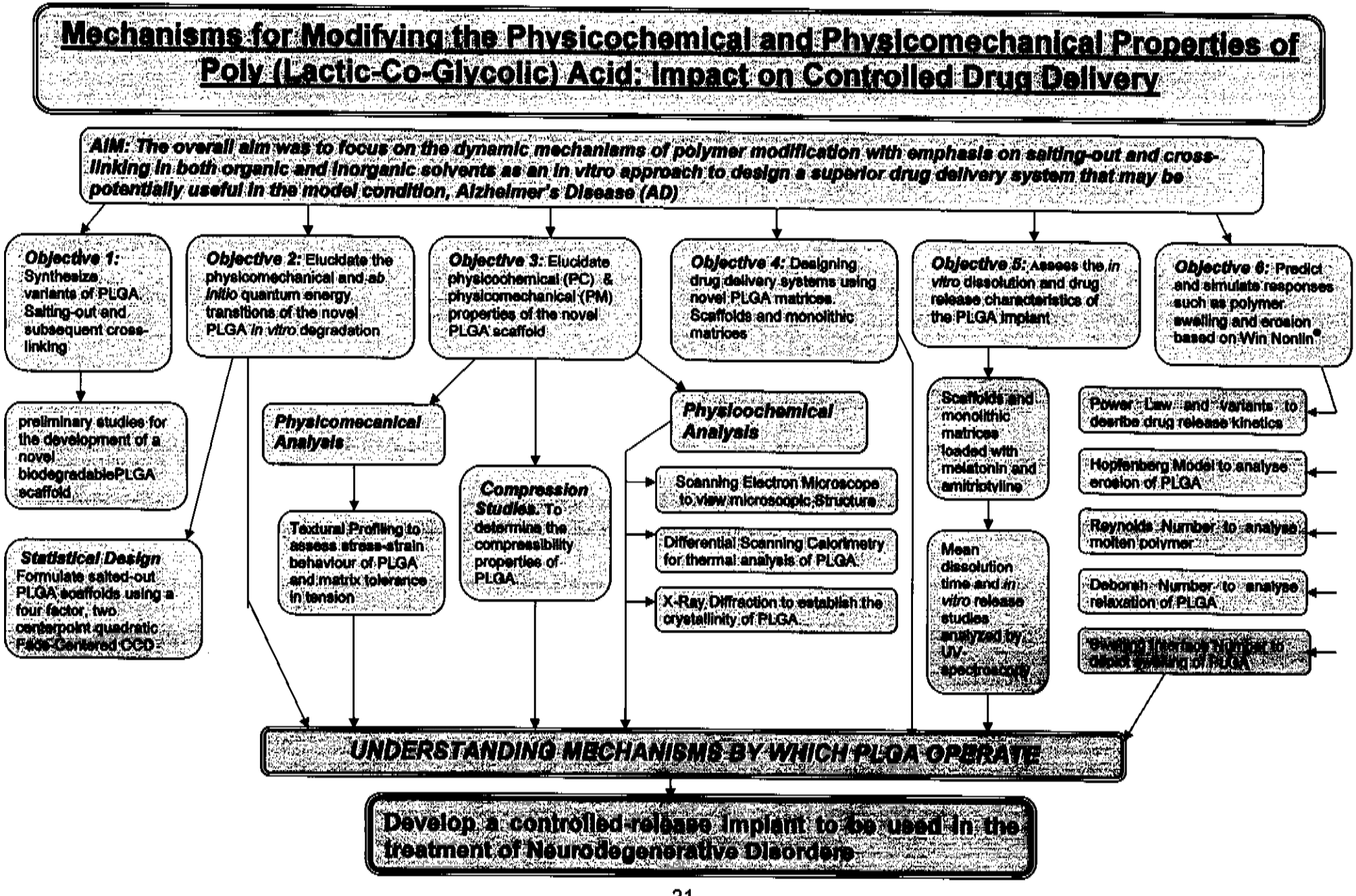
Mechanisms for Modifying the Physicochemical and Physicomechanical Properties of Poly (Lactic-Co-Glycolic) Acid: Impact on Controlled Drug Delivery
AIM: The overall aim was to focus on the dynamic mechanisms of polymer modification with emphasis on salting-out and cross-linking in both organic and inorganic solvents as an in vitro approach to design a superior drug delivery system that may be potentially useful in the model condition, Alzheimer's Disease (AD)
Objective 1: Synthesize variants of PLGA. Salting-out and subsequent cross-linking
Objective 2: Elucidate the physicomechanical and ab initio quantum energy transitions of the novel PLGA in vitro degradation
Objective 3: Elucidate physicochemical (PC) & physicomechanical (PM) properties of the novel PLGA scaffold
Objective 4: Designing drug delivery systems using novel PLGA matrices. Scaffolds and monolithic matrices
Objective 5: Assess the in vitro dissolution and drug release characteristics of the PLGA implant
Objective 6: Predict and simulate responses such as polymer swelling and erosion based on Win Nonlin®
preliminary studies for the development of a novel biodegradablePLGA scaffold
Statistical Design Formulate salted-out PLGA scaffolds using a four factor, two centerpoint quadratic Face-Centered CCD
Physicomecanical Analysis
Textural Profiling to assess stress-strain behaviour of PLGA and matrix tolerance in tension
Compression Studies. To determine the compressibility properties of PLGA
Physicochemical Analysis
Scanning Electron Microscope to view microscopic structure
Differential Scanning Calorimetry for thermal analysis of PLGA
X-Ray Diffraction to establish the crystallinity of PLGA
Scaffolds and monolithic matrices loaded with melatonin and amitriptyline
Mean dissolution time and in vitro release studies analyzed by UV-spectroscopy
Power Law and variants to describe drug release kinetics
Hopfenberg Model to analyse erosion of PLGA
Reynolds Number to analyse molten polymer
Deborah Number to analyse relaxation of PLGA
UNDERSTANDING MECHANISMS BY WHICH PLGA OPERATE
Develop a controlled release implant to be used in the treatment of Neurodegenerative Disorders

# CHAPTER TWO

## DEVELOPMENT OF A SALTED-OUT AND CROSS-LINKED PLGA SCAFFOLD

### 2.1 Introduction

A device for drug delivery must not fail or be rejected by the body after implantation because of cell immunity responses or unregulated drug delivery (Lallemand et al., 2003; Laeschke, 2004). This means that the material must neither elicit an unresolved inflammatory response nor demonstrate extreme immunogenicity or cytotoxicity. It is therefore, imperative to select materials that exhibit good biocompatibility. In addition, biocompatible and biodegradable polymers need to be modified in accordance with their specific applications, to develop materials that are non-immunogenic and capable of controlling the rate of drug release (Mokry et al., 2000).

This section of this study focused on the establishment of the mechanisms for modifying the polymer, PLGA, in order to develop a novel biodegradable scaffold with specifically designed physicochemical and physicomechanical features to suit its application as a scaffold for implantation into the subarachnoid cavity in the brain. In addition, the -device should have minimal undesired harmful degradation, and must be readily processable (Shi et al., 2005; Savalani and Harris, 2006).

In this study, the modification of PLGA was based on the principles of rapidly salting-out and subsequent cross-linking, where the polymer interacts with a water-miscible organic solvent and an aqueous environment at a particular pH and ionic strength. Due to the hydrophobicity of PLGA, it instantaneously coagulates upon contact with

an aqueous phase, thus resulting in a solid 'ceramic-like' material. The effects of salting-out and cross-linking encompass a large variety of phenomena induced by salts in polymer matrices that lead to the transformation of the physicochemical and physicomechanical properties of the polymer.

Furthermore, this phenomenon is able moderate the swelling and erosion kinetics of an ionic and non-ionic polymeric matrix (Czimerova et al., 2004; Mei and Ballauff, 2005; Coughlan and Corrigan, 2006). Accordingly, preliminary studies were conducted to establish the lower and upper limits for the dependent and independent formulation variables to be employed in the process. In addition, factors such as, the chemical composition, distribution of repeating units in multi-mers, the presence of polar groups such as –OH and –COOH, configuration of structure, molecular mass, molecular mass distribution and morphology of the polymer were determined. According to Okamoto and co-workers (2004) as well as Okamoto and Fukuzumi (2005), these factors may impact the formulation process of a superior scaffold.

Thus, a polymer with desirable functional groups that can form complexation networks through hydrogen and ionic bonding was selected. The processing conditions such as the temperature and the pressure were also considered. For the purposes of salting-out and cross-linking, the chemical inducers, namely, solvents and salts were examined for features such as the ability to dissolve PLGA, adsorb onto PLGA, ion exchange ability, ionic strength, ionic volume, pH in aqueous solutions, density and the ability to stabilize water. For the final product, the site of implantation of the device was also considered, as it would determine the parameters of the implant that include size of the scaffold.

An ideal device for implantation into the subarachnoid cavity of the brain should possess characteristics such as:

i. Biodegradability, thus eliminating the need for a second surgery to remove the implant;
ii. Provide a depot effect of the drug and prolong its release over time;
iii. Stabilise the drug in the physiological environment against rapid degradation;
iv. Be readily reproducible, cost-effective with a stable shelf-life;
v. Be free from toxic degradation products and neuro-compatible;
vi. Possess an optimum level of resilience, modulus and endurance in order to retain its physicochemical and physicomechanical properties during its use *in vivo* (McCormick and Stoessl, 2003; Kulbatski et al., 2005; Georges et al., 2006).

The consistency of a device's performance strongly depends on the properties of the polymer used, the mechanism used for polymer modification, chemical inducers employed and the final physicochemical and physicomechanical properties. Thus, the polymer, the chemical inducers used to transform the polymer and the mechanisms of modification were selected in accordance with the above-mentioned specifications. In addition, the product yield had to be considered, as it impacts on the manufacturing costs and the feasibility.

## 2.2 The Properties of Native PLGA

The type of polymer employed will have an influence on the degradation rate, degradation type, degradation products and subsequently, the rate of drug release and the success of the device's functioning *in vivo*. Thus, the material selected ought to be easily bulk-producible and its properties readily tailored for specific applications. This includes creating degradable polymers that allow room for programmable degradation while eliminating the need for a second surgery to remove the implant. The selection of a suitable polymer was therefore, a major concern for this study (Basu et al., 2007).

PLGA is a copolymer of two aliphatic polyesters, polylactic acid (PLA) and polyglycolic acid (PGA). PLA is a poly-α-OH acid that posseses an asymmetrically substituted −C≡ atom. It is found in two enantiomeric forms, namely, L(+)-lactide and D(-)-lactide stereoisomers and a racemic mixture of D,L-lactide. The presence of a pendant $-CH_3$ on the α-carbon of PLA offers the chirality (Jain et al., 2000). In contrast, PGA is one of the simplest linear aliphatic polyesters with no chiral centre or enantiomer. It is a highly crystalline polymer as compared to the amorphous Poly(D,L-lactide) (PDLL) (Middleton and Tipton, 2000).

The degradation rates of the two enantiomeric forms of PLA differ considerably, which implies that during the polymerization process of PLGA, the relative amounts of the L(+) or D(-) will affect the physicomechanical properties and degradation rate of PLGA *in vitro* and *in vivo* (Therin et al., 1992; Li, 1999). In addition, the ratios of PLA:PGA tend to affect the degree of crystallinity of the co-polymer, which in turn affects the functioning of the polymer in drug delivery. Thus, during the selection

process of various PLGA grades, the ratios of PLA:PGA need to be verified in order to achieve the required degree of crystallinity of the native PLGA (Park, 1994; Chung et al., 2006).

The majority of synthetic biodegradable polymers, including PLGA have a wide range of molecular masses and inherent viscosities. As the polymeric dimensions, such as, molecular mass are increased, its viscosity tends to increase; however, its solubility decreases (Rwei et al., 2005; Basu et al., 2006; Neuzillet et al., 2006). In polyesters, such as PLGA, molecular mass increases in direct proportion with the ester functional groups (Ranucci et al., 2006; Nadeau et al., 2005).

The difference in molecular mass is attributed to various stochiometric quantities of catalysts, temperature, as well as the position of equilibrium involving water during esterification reactions in the process of polymerization. Viscosity is, in such a case, a direct result of molecular mass (Korhonen et al., 2006). As a result, PLGA grades with higher molecular masses tend to have higher inherent viscosities (Table 2.1).

**Table 2.1.** *General physicochemical and the physicomechanical properties of native PLGA grades*

| Property | *RG 502 | *RG 503 | *RG 504 |
|---|---|---|---|
| Type of Polymer | A –OH polyester | A-OH polyester | α-OH polyester |
| Molecular formula | $[(C_3H_4O_2).(C_2H_2O_2)]_n$ | $[(C_3H_4O_2).(C_2H_2O_2)]_n$ | $[(C_3H_4O_2).(C_2H_2O_2)]_n$ |
| Molecular Mass (g/mol) | 15000 | 41000 | 55000 |
| Morphology | Orthorombic | Orthorombic | Orthorombic |
| Inherent Viscosity (dl/g) | 0.16-0.24 | 0.32-0.44 | 0.45-0.60 |
| Glass Transition Temperature (°C) | 40-55 | 40-55 | 40-55 |

**RG= Resomer® Grade (Trade name)*

Some of the properties of PLGA that has made this polymer a favourable candidate for biomedical uses are as follows:

i. Biocompatibility, non-thrombogenicity and non-toxicity (Langer and Folkman, 1976; Visscher et al., 1985; Yamaguchi and Anderson, 1993; Shive and Anderson, 1997; Johansen et al., 2000).

ii. Hydrophobicity, chemical stability, excellent thermo-reversible properties and the modifiable intrinsic structure (Dong et al., 2006; Jeong et al., 2006).

iii. Non-toxic degradation products and modifiable degradation rate (Massey et al., 2004; Fahmy et al., 2005).

The choice of PLGA as a polymer for the formulation of the scaffold originated from its use in the medical device industry to make bioabsorbable sutures (Langer and

Vacanti, 1993). This co-polymer's unique properties that include the established safety, biocompatibility and biodegradability made it an ideal material for this research. The degradation products of PLGA, namely, PLA and PGA and further to lactic and glycolic acids respectively, enter into the tricarboxylic acid cycle (also known as the kreb's cycle), to be broken down into $CO_2$ and water and are eliminated through the kidneys and the reticular endothelial system (RES) from the body as illustrated in Figure 2.1 (Nam et al., 2000; Hsu et al., 2006).

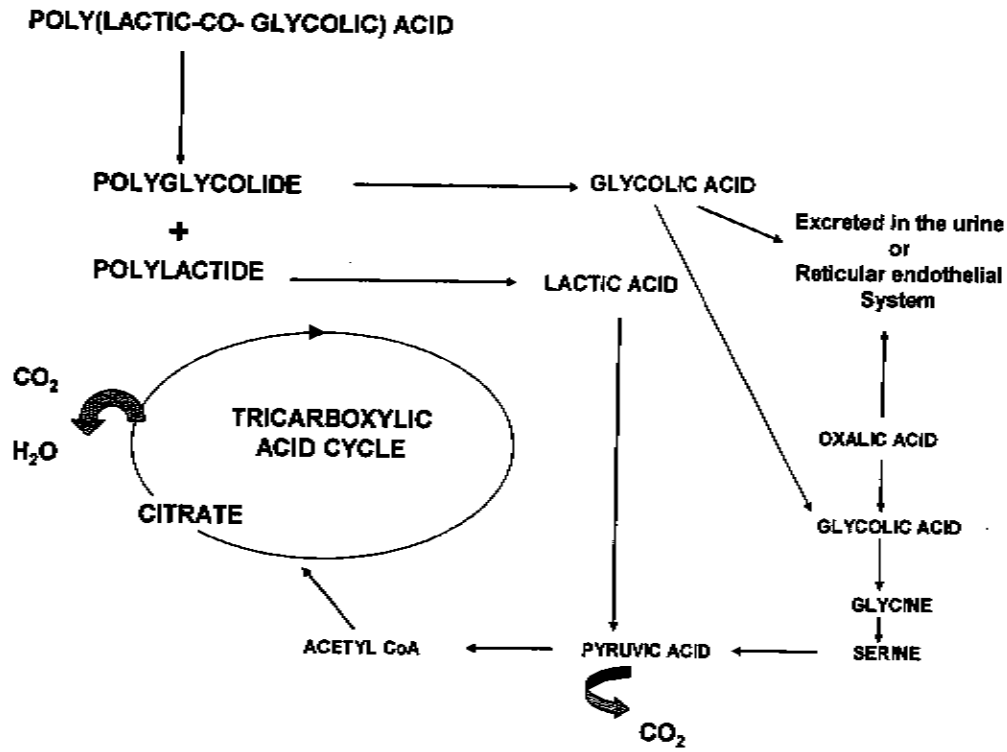


**Figure 2.1.** Schematic diagram of the metabolic degradation of PLGA (Source: adapted from Böstman et al., 1977; Garvin and Feschuk, 2005).

The PLGA device is intended for use *in vivo* and fast degradation would create setbacks such as the decrease in pH and affecting the surrounding tissues. Furthermore, the non-toxic elimination confers cost-effectiveness to the system, as there will be no local inflammation in the area (Hsu et al., 2006).

## 2.3 Establishing Suitable Independent Formulation Variables

During salting-out, an organic phase (containing the polymer) is separated from the aqueous phase with subsequent cross-linking, where molecules are covalently or ionically bonded. The reagents, namely, the solvents and ionic salts are incorporated into the polymer in order to induce salting-out and cross-linking as well as enhance the physicochemical and the physicomechanical properties of the polymeric matrix. In addition, these reagents are incorporated to create and maintain the desired solubility and stability of the scaffold.

There can be a synergistic interaction between the solvent, the salt and the polymer that produces enhanced stability, improved viscoelasticity and strength of the polymer. In contrast, the interaction between the chemical inducers may result in an antagonistic effect such as decrease in reactivity, stability or solubility (Zangi and Berne, 2006). During preliminary studies we set out to establish chemical inducers that would salt-out PLGA into a polymeric scaffold with balanced viscoelastic and brittle properties that are tailor-made to match its intended application.

### *2.3.1 Solvent Selection for Salting-Out and Cross-Linking*

The solubility of polymers depends on the chemical and the physical properties of both the polymer and the solvent employed (Basu et al., 2006). Most procedures of polymer modification and/or drug incorporation are performed in solution. Thus, the solvent plays a key role in the chemical reactions that take place during the processing and curing of the polymer, such as facilitating collisions between the reactants and the polymer.

Furthermore, the solvent offers a means of temperature control as a catalyst, by either increasing the energy of colliding particles or absorbing generated heat in the case of exorthemic reactions. For polymer synthesis and modification, the selection of a suitable solvent is guided by theory and experience. An appropriate solvent for salting-out and cross-linking should be inert to reaction conditions, water soluble, with less solvent residual volume in the scaffold. Table 2.2 below lists some of the properties of solvents selected to dissolve and salt-out PLGA.

***Table 2.2.*** *The physicochemical properties of solvents used in salting-out PLGA*

| **Solvent**[a] | **Density ($g/cm^3$)** | **Chemical Formula** | **DM**[b] | **DC**[c] | **BP**[d] **(°C)** | **Polarity** | **Protic/ Aprotic** |
|---|---|---|---|---|---|---|---|
| Water | 0.9980 | $H_2O$ | 1.85 | 80.0 | 100 | Polar | Protic |
| Chlorobenzene | 1.1075 | $C_6H_5Cl$ | 1.60 | 2.71 | 131 | Polar | Protic |
| Dimethyl acetate | 0.8820 | $CH_3COOC_4H_9$ | N/A* | N/A* | 97 | Polar | Protic |
| Methanol | 0.7910 | $CH_3OH$ | 1.70 | 33.0 | 68 | Polar | Protic |
| Acetone | 0.7860 | $(CH_3)_2C=O$ | 2.88 | 20.7 | 56 | Polar | Aprotic |
| Acetonitrile | 0.8000 | $CH_3CN$ | 3.92 | 36.6 | 81 | Polar | Aprotic |
| Chloroform | 1.4800 | $CHCl_3$ | 1.80 | 4.81 | 62 | Polar | Aprotic |
| N,N Dimethyl Formamide (DMF) | 0.9940 | $HCON(CH_3)_2$ | 3.82 | 38.3 | 153 | Polar | Aprotic |
| Dimethyl Sulfoxide (DMSO) | 1.0920 | $(CH_3)_2SO$ | 3.96 | 47.2 | 189 | Polar | Aprotic |
| Dimethyl Sulfoxide (DMSO) | 1.0920 | $(CH_3)_2SO$ | 3.96 | 47.2 | 189 | Polar | Aprotic |

[a] *All of these solvents are clear, colourless liquids;*
[b] *DM= Dipole Moment*
[c] *DC=Dielectric Constant*
[d] *BP= Boiling Point*
* *Not available*

The advances in the studies of solvation dynamics have allowed better understanding of the solvents effect on electron transfer reactions. During a chemical reaction, the solvent offers an ion or free radical to the system, which acts as a catalyst in the reaction. Protic solvents have a hydrogen atom attached to an electronegative atom such as $O^{2-}$ or $N^{3-}$ and can exchange protons. As a result, water, a typical protic solvent can donate an H+ from its –OH group to form H–bonds during a chemical reaction, while aprotic solvents such as acetone and DMF cannot donate a proton, since they only have a =C=O group. Polar solvation will differ from non-polar solvation, because the dielectric constant of polar solvents is unequally distributed, leading to different charges at each end. Thus, in polar solvation, van der Waal forces, dipole-dipole and electrostatic forces are the key to the chemical reaction (Gnanakaran, 1998; Chandra, A. and Bagchi, 2000; Bagchi, 2001).

Dipolar solvents such as acetone, DMF, and DMSO contain a C=O bond without a –OH bond and because they are protic, they will accept a proton from the aqueous solution during the salting-out and cross-linking processes, thereby enhancing the phase separation process. Solvent induced interactions during salting-out and cross-linking are greatly influenced by the type of salt in the aqueous solution (Gul et al., 1999; Moelbert et al., 2004; Zangi and Berne, 2006).

### *2.3.2 Salt Selection for Salting-Out and Cross-Linking*

Salts were selected in terms of their capability to salt-out and cross-link polymers. The effect of salts on the interaction between polymeric particles in aqueous solution is a function of the salt's ionic charge density. Salts with ions that have higher charge densities tend to increase the propensity of polymers to aggregate and salt-out

(Zangi and Berne, 2006). Work done by Melander & Horvath (1977) deduced that in aqueous-salt solutions, the salt increases the surface tension of water, there by changing the solubility and stability of the polymer that will be introduced to that solution. The principle of Hofmeister's precipitation of polymers such as, proteins facilitated the discerning of the ideal ions for salting-out and subsequent cross-linking of PLGA.

The Hofmeister series of precipitation can be given in terms of the ability of saltsand their ions to stabilize the structure of polymers, similar to the series displayed in Table 2.3. Thus, salting-out can be elucidated in terms of the degree of binding of ions to water. As the ions bind to water, the polymer concentration in the remaining unbound water will increase, aggregate and salt-out (Izutsu and Aoyagi, 2005; Maccarini et al., 2007; Renoncourt et al., 2007).

***Table 2.3.*** *Series illustrating the ability of ions to cause water stabilization, a predictor of the degree to which the ion can salt-out the polymer*

| ***Most stabilizing*** ➡ | ***Most destabilizing*** |
|---|---|
| $Citrate^{3-} > Sulphate^{2-} > Phosphate^{2-} > F^- > Cl^- > Br^- > I^- > NO_3^- > ClO_4^-$ | |
| $N(CH_3)_4 > NH_4 > Cs > Rb > K^+ > Na^+ > H^+ > Ca^{2+} > Mg^{2+} > Al^{3+}$ | |
| ***Weakly hydrated ions*** ➡ | ***Strongly hydrated anions*** |

*(Source: adapted from Hofmeister series, Para et al., 2006).*

In aqueous solution, the hydration of ions tends to influence the breakdown of the tetrahedral network of water by interrupting the hydrogen bonding capacity. The stronger the hydration of ions, the weaker the hydrogen bonding between the water

molecules will be. This will cleave the dodecahedral structure of water and free the polymer in order to salt-out (Sobott et al., 1999).

Moreover, salts may have preferential action on polymers. The subsequent preferential exclusion of both salts from the solvation shell and from the polymer particles leads to stabilisation of polymeric aggregates during salting-out. Kosmotropic salts such as $Li^+$, $Na^+$ and $F^-$ promote the aggregation of hydrophobic solute particles (salting-out), while chaotropic salts such as $K^+$, $Cs^+$ and $I^-$ act to destabilise such aggregates and cause them to solubilize (salting-in) (Vlachy, et al., 2004). Table 2.4, presents various properties of the typical salting-out cations and anions, which include molar aqueous ionic volume, entropy of hydration, and the viscosity Jones-Dole ß-coefficient.

***Table 2.4.*** *Classification of ions used in terms of molar aqueous ionic volume, entropy of hydration and the viscosity Jones-Dole* B-coefficient

| Cations | Ionic volume[a] | $\Delta S^b$ | Jones-Dole[c] | Anions | Ionic volume[a] | $\Delta S^b$ | Jones-Dole[c] |
|---|---|---|---|---|---|---|---|
| $Al^{3+}$ | -58.7 | -396 | +0.670 | Citrate$^{3-}$ | +77.0 | N/A[d] | +0.270 |
| $Mg^{2+}$ | -32.2 | -174 | +0.385 | $SO_4^{2-}$ | +25.0 | -126 | +0.206 |
| $Ca^{2+}$ | -28.9 | -132 | +0.298 | $PO_4^{2-}$ | N/A[d] | N/A[d] | +0.382 |
| $H^+$ | -5.5 | N/A[d] | +0.068 | $F^-$ | +4.3 | -70 | +0.127 |
| $Na^+$ | -6.7 | -5 | +0.085 | $Cl^-$ | +23.3 | +6 | -0.005 |
| $K^+$ | +3.5 | +34 | -0.009 | $Br^-$ | +30.2 | +28 | -0.033 |
| $Rb^+$ | +8.6 | +52 | -0.033 | $I^-$ | +41.7 | +55 | -0.073 |
| $Cs^+$ | +15.8 | +59 | -0.047 | $NO_3^-$ | +34.5 | +9 | -0.045 |
| $NH_4^+$ | +12.4 | +5 | -0.008 | $ClO_4^-$ | +49.6 | +30 | -0.061 |
| $N(CH_3)_4^+$ | +84.1 | N/A[d] | +0.123 | - | - | - | - |

*(Source: adapted from Marcus, 1997)*
[a]*Molar aqueous ionic volume, $cm^3\ mol^{-1}$, 298.15 K, the negative values indicate contraction in volume;*
[b]*Entropy of hydration, kJ $mol^{-1}$, 298.15 K, standard molar entropy minus the entropy of the primary*
[c]*Viscosity Jones-Dole ß-coefficient,($dm^3\ mol^{-1}$)298.15 K*
[d]*Not available*

Small ions are strongly hydrated, leading to negative entropies of hydration. This creates a higher local density of water, while larger ions have positive entropies of hydration and may reside comfortably within the dodecahedral structure of water chlathrate shells, thus, decreasing the local density of water. When used for salting-out and cross-linking the above-mentioned properties of the salts will influence the physicochemical and the physicomechanical properties as well as the configurational structure of the newly synthesized polymer. In addition, the hydration of the polymer during dissolution and drug release in physiological media is attributed to the type of salt employed (Sobott et al., 1999).

## 2.4 Mechanisms of PLGA Modification: Salting-Out and Subsequent Cross-Linking

Salting-out occurs when solvated ions precipitate polymers in the presence of aqueous solutions and cause them to dissolubilize, as opposed to solubilizing (salting-in). Salting-out employs thermodynamic principles to create polymer-rich and polymer-poor phases within a water-salt-polymer solution. The 3-dimensional polymer network is then removed from the solution, leaving a polymer-deprived phase. Salting-out, a colloidal phenomenon, also has the capacity to modulate the physicochemical and the physicomechanical properties of a polymer by incorporating ions that produce stochastic fluctuations. This can be explained as a transition of the polymeric 'hydrophobic effect', which is attributed to the reactivity of the salts (Lo et al., 1996; Schugens et al., 1996; Nam and park, 1999).

In water-salt-polymer solutions, the salts tend to transform the molecular structure of water permitting the polymer to aggregate, subsequently cross-link and form a 3-dimensional scaffold. This phenomenon is termed the 'hydrophobic effect'. It has been postulated that the 'hydrophobic effect' is directly proportional to the concentration of the ion or salt species as illustrated in the following equation known as Setchenow's Equation (Equation 2.1) (Friedman, 1972).

$$\ln[c_i/c_i(0)]=-ks*c_s \qquad \textit{Equation 2.1}$$

where,

$c_i$ is the molar solubilities of the hydrophobe (polymer) in salt solution;

$c_i(0)$ is the molar solubilities of the hydrophobe (polymer) in water;

$c_s$ is the molar concentration of the salt and

Ks is the Setchenow's salting-out coefficient of the salt

The range of parameters that influence the salting-out system, and thus the resulting physicochemical and physicomechanical properties, include molar solubilities of the polymer in water and in salt solution, the salt concentration, and the Setchenow's salting-out coefficient of the salt which can direct the interfacial tension between phases and increase pore size and interconnectivity of the scaffold. Ions that possess higher charge densities tend to bind covalently to water, such that the polymer is excluded from the first hydration shell of the solution. The polymer is thus free from hydration, increases in concentration, coalesce and salt-out, hence it is called the 'hydrophobic effect'. Polymers that have polar groups such as –OH and –COOH tend to adsorb water molecules in a configuration that depends on the properties of the polar group (Stephenson et al., 2007; Tareste et al., 2007; Zainuddin et al., 2007).

Berthold and co-workers (1996) revealed that the quantity of adsorbed water molecules around a polar group also depends on the physicochemical properties of the ions. Thus, the ion-pairs present in charged polymers are responsible for their swelling and gellation in aqueous media (Rinaudo, 1976). Hydrophilic sites of a polymer are also an area of target for water to adsorb, such as, in Nylon-6 where the $-NH_3$ groups are the specific sites of adsorption for water molecules (Reimschuessel, 1978). Although PLGA used in this study is a hydrophobic polymer, it possesses polar groups such as OH- and COOH- and therefore interacts with the salt and water molecules in a similar manner.

Cross-linking can bond the polymer and the salts both covalently and ionically. Cross-linking ions are employed to generate flexible polymers and to augment polymeric structural integrity. Cations that have been utilized in cross-linking of polymers comprise sodium, a monovalent cation, as well as divalent, trivalent and multivalent cations such as copper, calcium, aluminum, magnesium, strontium, barium, tin, and di-, *tri-* or tetra-functional organic cations such as alkylammonium salts. In this study, the inter-cross-linking between the monomers of PLGA strands and the salts as well as the intra-cross-linking among PLGA strands is subsequent to the salting-out of the polymer, due to ion interactions between the salts and the polar groups of the polymer.

## 2.5 Materials and Methods

The following experiments were conducted to establish the lower and upper limits for the independent formulation variables, synthesize the PLGA scaffold and to determine the ability of the independent formulation variables to salt-out various PLGA grades.

### *2.5.1 Materials*

PLGA was purchased from Boehringer Ingelheim Pharma (Ingelheim, Germany) (Resomer® RG502, RG503 and RG504) with 50:50 PLA:PGA ratios (The various molecular masses and inherent viscosities of these grades are listed in Table 2.1). Distilled water, acetone, acetonitrile, chlorobenzene, chloroform, DMF, DMSO and methanol (Ultrafine Limited, Finchley, UK) were used as solvents. HCl, KCl, NaCl, $CaCl_2$, $CaCO_3$, $Na_2SO_4$, $AlCl_3$, $Al_2(SO4)_3$, $CaOH_2$, Zinc Gluconate and $NaHCO_3$ (Rochelle Chemicals, South Africa) were used as salts. An analytical mass balance

(Denver Instruments Co., USA, ± 0.5 mg) was used to determine the mass of each substance and the scaffolds.

### *2.5.2 Synthesis of the PLGA Scaffold*

PLGA grades were salted-out and subsequently cross-linked with various quantities of solvents and salts to form scaffolds. Approximately 0.2g and 0.4g of each native PLGA grade was dissolved in 15mL of solvent, in separate glass vials. To salt-out using HCl, a 100mL of hydrochloric acid (0.1M) was added to the solution to decrease the pH to a pH range of 1,5 – 3. Salting-out and cross-linking solutions were prepared as 5%$^{w}/_{v}$ salt aqueous solutions and added to the polymer-solvent solution to induce salting-out of the polymer. The resulting scaffolds were removed from the cross-linking solution, washed with deionized water to remove any excess solvent or salt and allowed to dry over a period of 48 hours.

### *2.5.3 The Effect of the Independent Formulation Variables on the Salting-Out of Various PLGA Grades*

The salts used were evaluated quantitatively in terms of the scaffold yield and qualitatively in terms of their ability to induce salting-out PLGA. The efficiencies of the solvents were evaluated with respect to the ability and the time taken to dissolve the polymer as well as facilitating salting-out of PLGA. With regards to the salts, indicators of success in salting-out were the ability of the salt to cause coagulation and precipitation of the polymer as well as obtaining a desirable yield.

## 2.6 Results and Discussion

The numerous interactions between variables during salting-out need to be considered and has to be monitored individually as well as collectively. This will be explicated in Chapters Three and Four of this study using a statistical design of experiments approach.

This section will however, focus on elucidating the solvents and salts that were successful in salting-out and subsequently cross-linking of PLGA in pharmaceutically acceptable quantities (yield). PLGA is insoluble in water due to the hydrophobic nature of this polymer. Numerous solvents, namely, acetone, DMF and DMSO were able to dissolve PLGA; however, there was a variation in the amount of time taken to dissolve the polymer as outlined in Table 2.5.

In any solvent that dissolved PLGA, the time taken to dissolve the Resomer® grade was as follows: RG 502 > RG 503 > RG 504. This occurrence could be explained in terms of the inherent viscosity of each PLGA grade as listed in Table 2.1. This suggests that the inherent viscosity of each grade was inversely proportional to the time taken to dissolve, given that the inherent viscosity of RG 502= 0.16-0.24 dl/g < RG 503= 0.32-0.44 dl/g < RG504 = 0.45-0.60 dl/g.

Solvents, namely, acetonitrile, chlorobenzene, chloroform and methanol succeded to dissolved PLGA, but were not able to salt-out and subsequently cross-link the polymer when a salt solution was added; Even though the salt solution was successful in salting-out PLGA with other solvents. Solvents that could not salt-out PLGA were mainly the protic solvents, including methanol. The chloride and sulphate

salts including NaCl, $CaCl_2$, $AlCl_3$, $Na_2SO_4$ and $Al_2(SO4)_3$ successfully salted-out PLGA in pharmaceutically acceptable quantities (Table 2.5). Salts that did not succeed to salt-out and subsequently cross-link PLGA include, $CaOH_2$ and $NaHCO_3^-$ and Zn Gluc.

**Table 2.5.** *The reaction of random input variables on the salting-out of various PLGA grades (RG 502, RG 503 and RG 504)***

| **Solvent Employed and Interaction with Polymer** | **Salts Employed for Salting-out** | **Outcomes** |
|---|---|---|
| • Water<br>D=N; t= 0 min S/O=N<br>• Acetonitrile<br>D=Y; t= 1.0 min S/O=N<br>• Chlorobenzene<br>D=Y; t= 10 min S/O=N<br>• Chloroform<br>D=Y; t= 3.0 min S/O=N<br>• DMF<br>D=Y; t= 2.0 min S/O=Y<br>• DMSO<br>D=Y; t= 2.0 min S/O=Y<br>• Methanol<br>D=Y; t= 3.0 min S/O=N<br>• Acetone<br>D=Y; t= 1.0 min S/O=Y<br>• Acetone + DMF<br>D=Y; t= 1.5 min S/O=Y<br>• Acetone + DMSO<br>D=Y; t= 1.5 min S/O=Y<br>• Acetone + DMF + DMSO<br>D=Y; t= 1.5 min S/O=Y | • HCl<br>• KCl<br>• NaCl<br>• $NaHCO_3^-$<br>• $BaCl_2$<br>• $CaCl_2$<br>• $CaOH_2$<br>• Zn Gluc<br>• $AlCl_3$<br>• $Na_2SO_4$<br>• $Al_2(SO4)_3$ | **Ions that salted-out PLGA successfully**<br>• HCl<br>• KCl<br>• NaCl<br>• $CaCl_2$<br>• $AlCl_3$<br>• $BaSO_4$<br>• $Na_2SO_4$<br>• $Al_2(SO4)_3$<br>**Ions that did not salt-out PLGA**<br>• $CaOH_2$<br>• Zinc Gluconate<br>• $NaHCO_3^-$ |

***The polymer was varied between 0.8% to 4% $^{w}/_{v}$ in each solvent, (concentration gradients suitable for practical applicability).*
*The experiment was conducted at T= 25$^0$C and Pressure= Atmospheric;*
*D=Dissolved; S/O = Salting-out; Y=Yes, N=Not salted-out; t=Time taken to dissolve polymer (min/hr)*
*Salt solution ranged between 0 and 10% $^{w}/_{v}$ in distilled water and PH 1.0 to 3.0 for Protonated water.*

During salting-out reactions, there is an interaction between the salt solution and the solvent, whereby a proton may be momentarily transferred from the salt solution to the polymer solvent. A solvent that is unable to accept the proton from the salt solution may not be able to salt-out PLGA. This study earlier mentioned that in a chemical reaction, a protic solvent, such as, methanol donates a proton. This could be the reason most protic solvents failed to salt-out PLGA.

Further illustrations on this phenomenon are found in Figure 3.3 (Chapter Three), where DMF and protonated water undergo temporary charge transfer between water and DMF molecules, and subsequently causes coagulation and salting-out of PLGA from the solution. The effectiveness of the salts to salt-out PLGA was further measured with respect to the scaffold yield as listed in Table 2.6. The scaffold measured was the cohesive ceramic-like structure.

**Table 2.6.** *Scaffold yield (g) after salting-out and cross-linking with various salts*

| Salt[a] | Resomer 502 (F1)[b] | Resomer 502 (F2)[c] | Resomer 503 (F1)[b] | Resomer 503 (F2)[c] | Resomer 504 (F1)[b] | Resomer 504 (F2)[c] |
|---|---|---|---|---|---|---|
| HCl | 0.162 | 0.260 | 0.195 | 0.348 | 0.218 | 0.433 |
| KCl | 0.100 | 0.165 | 0.110 | 0.219 | 0.135 | 0.274 |
| NaCl | 0.158 | 0.269 | 0.185 | 0.359 | 0.213 | 0.448 |
| $BaCl_2$ | 0.139 | 0.225 | 0.164 | 0.296 | 0.187 | 0.374 |
| $CaCl_2$ | 0.148 | 0.243 | 0.174 | 0.323 | 0.199 | 0.404 |
| $AlCl_3$ | 0.167 | 0.272 | 0.199 | 0.362 | 0.225 | 0.452 |
| $Na_2SO_4$ | 0.073 | 0.178 | 0.086 | 0.238 | 0.098 | 0.297 |
| $Al_2(SO_4)_3$ | 0.093 | 0.242 | 0.154 | 0.334 | 0.204 | 0.428 |

*(Yield may be greater than polymer mass, due to incorporated salts)*
[a]*Aqueous salt solution 5%w/v.*
[b]*(F1) input mass of polymer=0.2g*
[c]*(F2) input mass of polymer=0.4g*

The results displayed in Table 2.6 reveal that the scaffold yield was influenced by the salt and the polymer grade employed in salting-out the PLGA. In general, the chloride salts produced higher quantities of scaffold yield in comparison with the sulphate salts with the exception of $Al_2(SO_4)_3$. This implies that chloride ions could be involved in salting-out by enhancing the formation of bonds, thus augmenting the coalescence of the PLGA strands.

The rapid solvation of PLGA in any biocompatible organic solvent is fundamental for employing PLGA in the formulation of devices for *in vivo* application. This study has revealed that the time taken by PLGA to dissolve depends on both the type of solvent and the viscosity of the polymer. In dissolving PLGA in the various solvents, two distinct stages were observed,

i. PLGA absorbed the solvent to form a gel and;

ii. The solution turned into a yellowish sticky gel, which then slowly dispersed into a less viscous yellow solution.

The time taken to change the viscosity of the solution from a gel to a less viscous solution was influenced by the solvent and PLGA grade used. The Gibbs free energy (G) change of mixing a polymer and a solvent depends on the temperature, pressure, volume and the number of moles present in the system. This can be explained thermodynamically using Sperling's solution thermodynamic nomenclature as presented in Equation 2.2.

$$\Delta G_M = kT\,(N_1 \ln V_1 + N_2 \ln V_2 + X_1 N_1 V_2) \qquad \textit{Equation 2.2}$$

Where,

$\Delta G_M$ is the Gibbs free energy change of mixing;

$k$ is the Boltzman's constant (1.38066 x $10^{23}$ Joules per Kelvin, relates energy to temperature);

$T$ is the temperature;

$N_1$ is the number of solvent molecules;

$V_1$ is the volume fraction of the solvent;

$N_2$ is the number of polymer molecules;

$V_2$ is the number of solvent molecules and

$X_1$ is the Flory Huggins interaction parameter.

The temperature and pressure of the system are influenced by the interaction between the polymer and solvent. The factors delineated in the above Equation 2.2 reveal that the quantities of solvent and polymer molecules will influence the pressure and temperature of the reaction. This in turn will affect the rate of polymeric salting-out and cross-linking on addition of a salt solution.

Furthermore, in solution, the polymeric chains adopt a configuration such that the attractive and repulsive forces on each polymeric segment (owing to other monomers as well as solvent molecules) are exactly counter-balanced. The coupled effect of these forces leads the polymer to assume a configuration that permits a free rotation about the bonds between segments, with no interaction between the segments, resulting in an intact configuration.

Polymers that have their chemical backbone based on C-C such as PLGA have the C-C-C bond-angle fixed at $109^0$, and the C-C molecular distance at 1.54 Å. However when a salt solution is added, the solvent interacts with water molecules whilst the salts interact with the polymeric chains causing them to salt-out and form a 3-dimensional structure. Thus the polymer is activated by the solvent to interact with ions during salting out and subsequent cross-linking. The monomeric units of PLGA are multi-functional, and have sites that can react with several adjacent molecules including salts.

## 2.7 Concluding Remarks

The yields were found to vary, depending on the various factors such as salting-out and cross-linking species as well as the viscosity, molecular mass and concentration of PLGA. The chloride salts such as NaCl and $AlCl_3$ demonstrated a higher yield when compared to other salts. Thus, the ability of the polymer and the salt to coagulate into a thick gel appeared to be influenced by both the salt and the molecular mass of the polymer.

Chapter Two of this study focussed on establishing the type and the quantities of independent formulation variables that may be used in synthesizing the PLGA scaffolds. Chapters Three and Four that follow evaluates the physicochemical, physicomechanical and the *ab initio* quantum mechanical energy transitions of the novel PLGA scaffolds produced.

# CHAPTER THREE

## ELUCIDATION OF THE *IN VITRO* PHYSICOMECHANICAL AND *AB INITIO* QUANTUM ENERGY TRANSITIONS OF THE PLGA SCAFFOLD

### 3.1 Introduction

In this section, the study elucidated the *in vitro* physicomechanical transitions of the PLGA scaffold, utilizing quantum mechanics to compute the *ab initio* energy requirements of the salted-out and subsequently crosslinked PLGA scaffold interacting with simulated physiological fluid, phosphate buffered saline (PBS) at a molecular level. These studies were conducted to understand the degradation characteristics and the stability of the potential scaffold from a molecular viewpoint in an attempt to predict its suitability for use in rate-modulated drug delivery.

Conventional drug delivery systems are characterized by vigorous polymeric degradation, with uncontrolled release kinetics of the delivered bioactive, due to lack of toughness and viscoelasticity (Blagoeva and Nedev, 2006). In physiological media, these devices undergo rapid degradation and instantaneous drug release causing a sharp rise of the drug plasma concentration. This is often followed by an analogous decrease in the concentration, which leads to toxicity and a 'peak-trough' effect. In addition, the accumulation of degradation products *in vivo* tends to cause an immune and an inflammatory tissue response.

Amid the array of polymeric biomaterials that have been explored for drug delivery and tissue engineering devices, thermoplastic aliphatic polyesters such as PLA, PGA and PLGA are renowned for their biocompatibility and biodegradability (DeLuca et al., 1993; Mehta et al., 1994; Sisay et al., 2000; Dorta et al., 2002). PLGA is

increasingly being utilized for fabricating drug delivery devices and scaffolds for cell seeding in tissue engineering.

Structural stability studies on PLGA regarding solvent addition, physicochemical and physicomechanical transitions, and molecular dynamics during *in vitro/in vivo* degradation still require further exploration (Li and Vert, 1995; Shive and Anderson, 1997; Wu, 2004). The influence of these factors on application and adaptation to the microenvironment of the tissue/organ is pertinent to the performance of the device (Oldham et al., 2000; Garg and Kokkoli, 2005).

A limitation of employing PLGA in fabricating drug delivery devices is that bulk erosion occurs when exposed to physiological media. Devices made of native alpha-OH polyesters, PGA, PLA and PLGA usually undergo bulk degradation with simultaneous loss of mass (Spain et al., 1998; Yoon and Park, 2001). Fluid infiltration instigates hydrolytic cleavage of the ester bonds. Each ester bond cleavage generates a new carboxyl end group that catalyzes the hydrolytic reaction of the other ester bonds. Partially degraded macromolecules remain insoluble in the surrounding medium and sequential erosion proceeds homogeneously (Witt and Kissel, 2001; Von Burkrrsroda et al., 2002). Once the molecular mass of the partially degraded macromolecules is sufficiently low, diffusion begins within the matrix, leading to bulk erosion.

Some of the factors that influence PLGA degradation include:

i. Polymer intrinsic properties, such as, Hydrophobicity, chemical structure, the ratio of lactic:glycolic acid in PLGA, crystallinity, and molecular weight (Shin et al., 2006);
ii. Physiological fluid or release medium properties such as, temperature, ionic strength, pH, solvent, presence of biocatalysts (Tomoda et al., 2005);
iii. Formulation properties, such as, shape, size, presence of salts in the device, particle size, presence of plasticizer or coating (Ishihara et al., 2005; Dong et al., 2006) and
iv. Incorporated bioactive, such as, acidic drugs, salt based drugs and tertiary amine-based drugs (Siegel et al., 2006).

Thus the morphology of the device, the amount of biological molecules incorporated into the device, the pH of the system, the environmental temperature, as well as the solvents and ions that are present in the system will determine the type and the rate of degradation of the device (Blanco and Alonso, 1998; Barakat and Radwan, 2006; De Jong et al., 2005). In a study by Dong and co-workers (2006) the degradation of PLGA in *in-situ* forming systems was found to increase with the increase in storage temperature and water content in the biocompatible solvents used.

In addition, Dong and co-workers (2006) revealed that degradation of PLGA may be accelerated by polar protic solvents, such as 2-pyrrolidone as compared to polar aprotic solvents, namely, DMF, DMSO and acetone. Curing and sterilization of the PLGA devices has also been found to considerably affect the degradation rate of the OH-polyesters. This tendency to physical and chemical degradation during storage

and during application presents a limitation in the use of this thermoplastic polymer (Siepmann, 2006).

### 3.2 The Degradation of PLGA

#### *3.2.1 Chemical Degradation of PLGA*

Biodegradable polymeric devices can degrade either by enzymatic or non-enzymatic hydrolysis of the labile bond. This is termed chemical degradation. Polymers can be classified according to the type of hydrolysis they undergo. Several mechanisms of chemical degradation have been reported, which include, Type I, where cleavage of the labile bond in the polymer backbone result in low molecular weight degradation products that undergo solubilization. Göpferich (1996) detailed that PLGA degrades predominantly via chemical hydrolysis of the hydrolytically unstable ester bonds into lactic acid and glycolic acid. These non-toxic products are bioerodible, and are eliminated from the body by normal metabolic pathways.

The next mechanism, Type II, is where the hydrophobic side groups of a polymer are ionized and hydrolyzed, leading to the solubilization of the entire structure. Type III mechanism involves the cleavage of unstable linkages of a cross-linked network that cause the liberation and the solubilization of the polymer fragments. Type IV mechanism is a combination of the three mechanisms. Zhang and co-workers (1993) revealed that native PLGA, being an α-OH polyester undergoes the Type I degradation mechanism. This is one of the challenges of this polymer, as mentioned in section one.

### *3.2.2 Physical Degradation of PLGA*

Polymeric devices synthesized from polyanhydrides and poly(ortho)esters usually undergo surface erosion, (Dickers et al., 2002). The rate of degradation of these polymers occurs in such a way that the mass loss is more rapid than the ingress of water into the bulk polymer. The device undergoes surface erosion that is predictable such that drug release may be easily controlled.

On the other hand, devices made from PLGA display bulk erosion, where the ingress of water into the bulk polymer is faster than the degradation of the polymer. This implies that the degradation of the polymer will occur simultaneously throughout the polymeric device and proceed until the critical molecular weight of the polymer has been reached, where chemical degradation takes place. At this point, the degraded polymeric particles start to solubilize (Välimaa and Laaksovirta, 2004)

The limitation of this type of degradation is that the entire polymeric device degrades concurrently at an unpredictable rate. In terms of PLGA, there is a decrease in the pH of the surrounding area tissues caused by the increase in the degradation products, namely, lactic and glycolic acids. Although PLGA has been used in many health care devices, the challenge of uncontrollable degradation still exists.

In order to solve this problem, one needs to revise the factors that influence the rate and type of degradation of the polymer. PLGA undergoes two degradation stages, where water diffuses into the amorphous regions quickly and then cleavage of the ester bond occurs. During this stage the physicomechanical properties, such as resilience and work preformed are compromised. The second stage is the hydrolysis

of the crystalline regions, which causes a decrease in the weight of the PLGA device.

### 3.3 Effects of PLGA Modification on the Stability and Degradation of PLGA

In Chapter Two of this dissertation, we investigated the logical development of the scaffold through the process of salting-out and cross-linking PLGA. Modification of PLGA matrices by a salting-out and subsequent cross-linking technique to form a 3-dimensional biodegradable polymeric scaffold under conditions of altering monomeric ratios, molecular mass, cross-linking reagents and salting-out reaction times may result in a polymeric material with improved degradation rates, physicochemical and physicomechanical properties.

Salting-out confers partial covalent bonding leading to cross-linking between PLGA polymeric chains and increased viscosity of the evolving structure. Polymeric voids resulting from cross-linked interactions have a stereochemical orientation that is able to constantly engulf clusters of fluid molecules in the presence of physiological media. These voids are a result of interactions between short and long distance chains and cross-linking ions, due to the presence of electronegative sites within inter-atomic reactions. Salting-out and cross-linking techniques can be used to modify the physicomechanical properties of the device to restrict the transport of water inside the polymer matrix (Grassi and Grassi, 2005). The presence of cross-links between the polymeric chains obstructs the free movement of water molecules and impedes dissolution of the polymeric network.

The overall textural properties and energy transitions occurring at a molecular level within the scaffold will depend on the extent of cross-linking ions located within the matrix that could be either cross-linked within the polymeric voids or salted-out externally and thus will elucidate the overall design of the scaffold. If ionic or covalent bonding is restricted, the contours of the scaffold may be attributed to hydrogen bonding. Otherwise, the polymeric chain dimensions may outline the nature, stability and performance of the intermediate sol-gel matrix as well as its energy status.

A polymeric scaffold whereby the stereochemical configuration provides a void area for hydrated and unhydrated ions to bind without obscuring other atoms is assumed to be moderately stable. Restriction of these voids and subsequently fewer hydrated ion clusters within the matrix will result in further stability to the polymeric backbone. When hydrated and unhydrated ions are bound externally to voids it may result in increased swelling of the micro-environmental structure with a decrease in quantum energy. Studies by Paulaitis and Pratt (2002) have yielded evidence on the dependence of polymeric hydration free energy on the solute size and shape (Sweet, 2002).

The physicomechanical properties such as the energy absorbed and matrix resilience are projected to be augmented by salting-out and subsequent cross-linking of native PLGA, through the formation a scaffold that links the PLGA structural backbone with solvation ions. However, the degree of these physicomechanical enhancements may decrease during incubation in PBS that is attributable to cleavage of the cross-links resulting in PLGA chain disentanglement.

However, it is assumed that PLGA scaffolds may react slower than hydrogels, depending on the stereochemical configuration of the polar groups. In general, the degree of PLGA chemical-backbone hydrophobicity combined with hydrolytically degradable anhydride cross-linking may result in a controllable surface erosion mechanism, with degradation timescales ranging from 48 hours to 1 year (Cochran and Cox, 1992; Alvarez-Lorenzo et al., 2002; Fries W and Schlapp, 2002; Sweet, 2002; Manjubala et al., 2005).

The resultant molecular dynamics of a salted-out PLGA scaffold and stereochemical configuration of molecules may also lead to pertinent energy transitions within the matrix of the newly formed scaffold at a molecular level. The energy flux of molecular interactions during salting-out may further elucidate the scaffolds final energy of stability. The emerging field of molecular modeling with *ab initio* quantum energy computations can aid in elucidating these energy transitions.

### 3.4 *Ab Initio* Quantum Mechanical Energy Calculations

An additional aspect of equal importance, when a polymeric device is introduced into physiological fluids, is the transitions in the quantum mechanical energy of the system, that result from molecular interactions between the polymer, incorporated bioactive and the aqueous environment. The transition in energy is used a significant indication of the stability of the device in buffer solutions, in storage and at variable conditions, as well as to predict the polymeric interactions between PLGA chains and various biological molecules of lower and higher molecular weights.

To our knowledge, the effects of molecular interactions between PLGA and various substances, such as DMF, water, hydrochloric acid and phosphate buffer ions on the stability of PLGA scaffolds have not been reported. Moreover, the structural stability studies on PLGA regarding solvent addition, incorporation of biological fragments, physicochemical and physicomechanical advancement, and the molecular dynamics during *in vitro/in vivo* degradation still require further exploration (Li and Vert, 1995; Shive and Anderson, 1997; Wu, 2004). The influence of these properties on application and adaptation to the microenvironment of the tissue/organ is pertinent to the performance of the device during drug delivery or tissue engineering (Oldham et al., 2002; Garg and Kokkoli, 2005).

The primary objective of quantum chemical and mechanical studies is to be able to verify geometries and force constants for regions of a molecule's potential energy surface near local minima or transition states. The advancement in computational chemistry and numerical analysis in the last few decades has made possible the fulfilment of the enduring promise that quantum mechanics has held for biochemistry (Pedersen et al., 1985).

The theory and the mathematics of interference postulate that if two processes or particles interfere with one another, they both contribute to the net energies of the system, which is smaller than it would be if either of the particles was on its own. The study of quantum mechanical energy is concerned with the motion of such particles and the forces that act upon them, as well as the kinetic energy or the potential energy stored in their physical arrangement. These parameters can be employed to determine the stability of molecules (Qiu et al., 2007).

The change in the average kinetic energy of the particles is reflected in the corresponding change in temperature of the molecules, and the potential energy is stored within the bonds of that molecule. In bonded atoms, the energy components results from the vibrational motions, angular motions and electrical charge on the nuclei. Further energy transitions of bonded atoms may be attributable to secondary electromagnetic considerations such as Van der Waals forces and the quantum mechanical contributions derived from the energy state of the electron shells.

The most common ways to predict the energy for a molecular system were defined by Schaefer (1972). Firstly to formulate the Born-Oppenheimer approximation and secondly, to assume the Hartree-Fock theory wherein the simplest useful wave function, λ, for an n-electron system, is the single determinant of the occupied molecular orbitals. In addition to energies, equilibrium and transition-state geometries plus frequencies, the effects of solvation on the conformation energies of polymers can be studied by *ab initio* calculations up to MP2/cc-pVTZ//MP2/6-31G, utilizing the polarizable continuum model (PCM) to mimic these effects. The changes in potential energy change throughout the interactions between the solvent, ions, water and polymer molecules, can be estimated by *ab initio* quantum mechanical calculations following molecular dynamics (MD) simulations (Nielsen et al., 2007).

This method is able to determine the proton-transfer processes that occur when a polymeric molecule is placed in a solvent or a buffer system by molecular dynamics and quantum chemical calculations. In their study, Yoshiharu and co-workers (2006) revealed that potential energy change during the proton transfer is tightly regulated

by the composition and the geometry of the surrounding molecules of the polymer and the incorporated ions from the buffer and the solvent.

In this work we set to use both the textural analysis and the *ab initio* computational chemistry data in order to elucidate the physicomechanical and energy transitions of the PLGA scaffolds obtained by salting-out and subsequent cross-linking of the native PLGA. The salted-out PLGA scaffolds can be analyzed using textural analysis for their physicomechanical properties but the data generated from such experiments do not provide further insight into the occurring at a molecular level which may related to the physicomechanical transitions occurring on formation of the novel PLGA scaffold. Understanding the chemistry at a molecular level is crucial in elucidating the effect of salting-out and cross-linking reactions on the transitioned physicomechanical properties of the novel salted-out PLGA scaffold produced.

Computational chemistry will permit us to study the chemical and the physical phenomena by running calculations on computers rather than by examining reactions and compounds experimentally. This is of prime interest if we want to establish a reaction mechanism since computational chemistry can be used to model transition states which may provide information about molecules or reactions and how they are able to impact on the overall physicomechanical transitions of the PLGA scaffold which are difficult and even impossible, to render evident through laboratory experiments. These programs are able to predict a realistic description of the interactions between the molecules and the transitions that result.

Computational chemistry is therefore both an independent research tool that uses the power of molecular mechanics and quantum chemical calculations which allows us to confirm experimental results, and a crucial adjunct to experimental studies which allows us to obtain additional information such as the chemistry related to the physicomechanical transitions occurring during salting-out of native PLGA to form PLGA scaffolds through.

### 3.5 Statistical Design of Experiments

In the preliminary studies of the scaffold development, the experiments employed were screening designs that comprise the trial and error runs at the extreme lower and upper levels of the combinations of the variable study ranges. This type of information, however, only provides information on the direct additive effects of the study variables on a pair-wise interaction effects. The preliminary studies in Chapter Two, accordingly, enabled us to single out the best materials and equipments for the study, as well as also to focus on the significant variables for the development and optimization of the study.

In this part of the experimental work, the goal is shifted from screening to scaffold optimization. Most of the tests conducted on the scaffold involved several factors and were conducted in order to optimize certain processes, such as the *in vitro* chemical and physical degradation of the scaffold and to investigate and understand the relationships between the physicomechanical factors such as the resilience and the characteristics of the responses of interest.

In order to design experiments efficiently and be able to monitor each formulation process, and to achieve the desired characteristics of a drug delivery device, it is necessary that we can identify factors that are influential to the properties of the formulation. Design of Experiments (DOE) is therefore an efficient statistical procedure for setting up experiments with the intention that the data obtained can be analysed to yield applicable and objective conclusions. DOE can be used to perform a planned sequence of tests, called a design, the influence of the random input variables and their interactions on response variations can be established.

The experimental design strategy is selected in accordance with the particular objectives of the study, and it may be successfully employed in order to find the best variables and experimental conditions for achieving the optimized process. The most widely used statistical experiment designs for the optimization of experiments are known as the response surface methods (RSMs). RSMs are based on the fundamental hypothesis that low-order polynomial models can be used to approximate the relationship between a set of controllable random input variables and a simulated response within restricted regions of the operability space (Donohue et al., 1990).

RSM allows one to define empirical models, such as quadratic polynomials, that illustrate precisely how responses behave at all values of the variables in the experimental region (Myers and Montgomery, 1995). In general, the first-order experimental designs are applied when locating the region containing the optimal response. Second-order experimental designs are then, employed to fit a quadratic response function in order to predict the system optimum more accurately.

The RSM include trials in which one or more of the independent variables are set at the midpoint of the study range, while the other levels in the interior of the range may also be represented. Moreover, the RSM is able to provide information on the direct effects, pair-wise interaction effects and curvilinear variable effects on the response of interest. The basic dilemma of experimental designs is deciding what pattern of design points will best reveal aspects of the process of interest (Box et al., 1978).

One of the most preferred RSM to solve this dilemma is the central composite design (CCD). CCD is one of the RSM designs that can fit a full quadratic model. A Box-Wilson CCD, commonly known as CCD contains an imbedded factorial or fractional factorial design with center points, augmented with a group of star points that permit the estimation of curvature. To determine quadratic regression model coefficients, each design variable has to be studied at three distinct levels at least and, therefore, the CCD is often used to provide estimation of a second-order equation.

Each CCD consists of cube points at the corners of a unit cube that is the product of the intervals [-1,1], star points along the axes at or outside the cube, and center points at the origin. A CCD for $k$ factors consists of $2^k$ factorial points, $2k$ axial or 'star' points and $n_0 \geq 2$ center points. The axial points are located at a distance $\alpha$, from the design center.

$$\alpha = (N_F)^{1/4} \qquad \textit{Equation 3.1}$$

Where,

$N_F$ represents the number of factorial runs used to study the variables at not more than three levels (−1; 0; +1) (Lewis et al., 1999). The CCDs have gained popularity, owing to their following advantages:

i. CCDs are very efficient with respect to the number of runs required, and are able to provide much information on experiment variable effects and overall experimental error in the least number of required runs (Donato et al., 2006).
ii. A CCD can be conducted sequentially, that is, it can be partitioned into two subset estimates linear and two-factor interaction effects while the second subset estimates curvature effects. The second subset need not be run when analysis of the data from the first subset points indicates the absence of significant curvature effects.
iii. The CCDs are extremely flexible and can be used under different experimental regions of interest and operability due to their variability.

Furthermore, a face-centered CCD can be used when the region of operability includes the region of interest as defined by the variable bounds. There are three types of CCDs, namely, Circumscribed (CCC), Inscribed (CCI) and Faced-centred (CCF) designs. CCFs have three levels per factor, in contrast with the other types, which have five levels per factor. A face-centred CCD (FCCD) was chosen for this study, with $\alpha = \pm 1$ (Pinzauti et al., 1996).

This study therefore, proposes to explicate the *in vitro* physicomechanical property transitions of novel salted-out and subsequently crosslinked PLGA scaffold employing Design of Experiments. Furthermore, the *ab initio* quantum mechanical

energy transitions employing PLGA monomeric units and interacting molecules in PBS, (pH 7.4, 37°C) was explored to deduce the *in vitro* stability of the novel PLGA scaffold at a molecular interaction level.

## 3.6 Materials and Methods

### *3.6.1 Materials*

Resomer® grades comprising poly(lactide-co-glycolide) (PLGA) with a 50% lactide content and inherent viscosities ranging from 0.16-8.2dl/g were utilized (Boehringer Ingelheim, Ingelheim, Germany). N, N dimethyl formamide (DMF) was used as a solvent (Rochelle Chemical, Johannesburg, South Africa) and disodium hydrogen orthophosphate, sodium chloride and potassium dihydrogen phosphate were used to prepare the phosphate buffered saline (PBS), (Saarchem (Pty) Ltd., Brakpan, South Africa). All other reagents were of analytical grade and used as supplied.

### *3.6.2 Formulation of the PLGA Scaffolds*

PLGA of various molecular masses designated as 1, 2 and 3 in Table 1 were weighed, dissolved in DMF, and placed in 200mL glass beakers. Varying quantities of protonated water (pH 1.5), ($H_3O^+$) was added to the polymeric solution and induced salting-out into scaffolds that were vacuum dried to remove excess solvent. The dehydrated scaffold samples were then immersed in 100mL PBS (pH 7.4, 37°C) and oscillated at 100rpm in a shakerbath (Labex, Stuart SBS40®, Gauteng, South Africa). At 0, 7, 10, 26 and 30 days post-incubation the scaffolds were assessed for their physicomechanical properties.

### *3.6.3 Construction of the Experimental Design*

**Table 3.1.** *Normalized factor levels of the independent variables for the FCCD*

| Independent Variables | Factor Level | | | Units |
|---|---|---|---|---|
| | Low | Middle | Upper | |
| Water volume | 10 | 55 | 100 | mL |
| PLGA molecular Mass[a] | 1 | 2 | 3 | Daltons |
| PLGA concentration | 1 | 5.5 | 10 | $\%\ ^{w}/_{v}$ |
| Salting-out time | 2 | 13 | 24 | Hours |

[a] *1= 55,000 Daltons; 2=100,000 Daltons; 3=160,000 Daltons*

A four factor, two centerpoint quadratic Face-Centered Central Composite Design (FCCD) was selected for optimization of the PLGA scaffolds. The statistical model allows for simultaneously studying the effect of several independent formulation variables influencing the desired responses, by altering the variables in a limited number of experiments. FCCD was employed in this study to determine coefficients of a second order. This is more superior to conventional methods of optimization which involves varying one factor at a time, while keeping constant all other parameters, thus not screening the main interactions and effects of all the involved factors simultaneously (Cochran and Cox, 1992).

**Table 3.2.** *Randomized experimental runs generated from the FCCD*

| Formulation No. | Water Volume | PLGA *Mw*[a] | [PLGA][b] | Salting-out Reaction Time |
|---|---|---|---|---|
| 1 | 10 | 1 | 10 | 2 |
| 2 | 100 | 2 | 5.5 | 13 |
| 3 | 100 | 1 | 1 | 24 |
| 4 | 10 | 3 | 1 | 24 |
| 5 | 10 | 1 | 1 | 2 |
| 6 | 55 | 2 | 1 | 13 |
| 7 | 100 | 1 | 1 | 2 |
| 8 | 55 | 2 | 10 | 13 |
| 9 | 10 | 2 | 5.5 | 13 |
| 10 | 10 | 3 | 10 | 24 |
| 11 | 55 | 2 | 5.5 | 13 |
| 12 | 100 | 3 | 10 | 24 |
| 13 | 55 | 2 | 5.5 | 13 |
| 14 | 100 | 1 | 10 | 2 |
| 15 | 55 | 3 | 5.5 | 13 |
| 16 | 55 | 1 | 5.5 | 13 |
| 17 | 55 | 2 | 5.5 | 2 |
| 18 | 100 | 3 | 1 | 2 |
| 19 | 10 | 3 | 10 | 2 |
| 20 | 10 | 1 | 10 | 24 |
| 21 | 10 | 1 | 1 | 24 |
| 22 | 100 | 1 | 10 | 24 |
| 23 | 100 | 3 | 10 | 2 |
| 24 | 55 | 2 | 5.5 | 24 |
| 25 | 10 | 3 | 1 | 2 |
| 26 | 100 | 3 | 1 | 24 |

[a]*PLGA Molecular weight: 1=55,000 Daltons; 2=100,000 Daltons; 3=116,000 Daltons*
[b]*Concentration*

### 3.6.4 Physicomechanical Profiling of the PLGA Scaffolds

#### *3.6.4.1 Determination of the Matrix Resilience, Matrix Tolerance and Energy Absorbed*

The physicomechanical transitions of the salted-out PLGA scaffolds in PBS were analyzed using a Textural Analyzer (*TA.XTplus* Texture Analyzer, Stable MicroSystems, Surrey, England) which captured stress-strain profiles with a high

degree of accuracy and reproducibility. Textural parameters calibrated for the analysis is shown in Table 3.

**Table 3.3.** *Textural parameters and settings*

| **Parameters** | **Energy absorbed** | **Matrix resilience** |
|---|---|---|
| Pre-test speed | 1mm/sec | 1mm/sec |
| Test speed | 0.5mm/sec | 0.5mm/sec |
| Post-test speed | 1mm/sec | 1mm/sec |
| Compression force / strain | 40N | 50% |
| Trigger type | Auto | Auto |
| Trigger force | 0.5N | 0.5N |
| Load cell | 50kg | 50kg |

Matrix resilience and energy absorbed were the two physicomechanical properties that were determined by Force-Distance and Force-Time profiles generated (Figure 3.1).

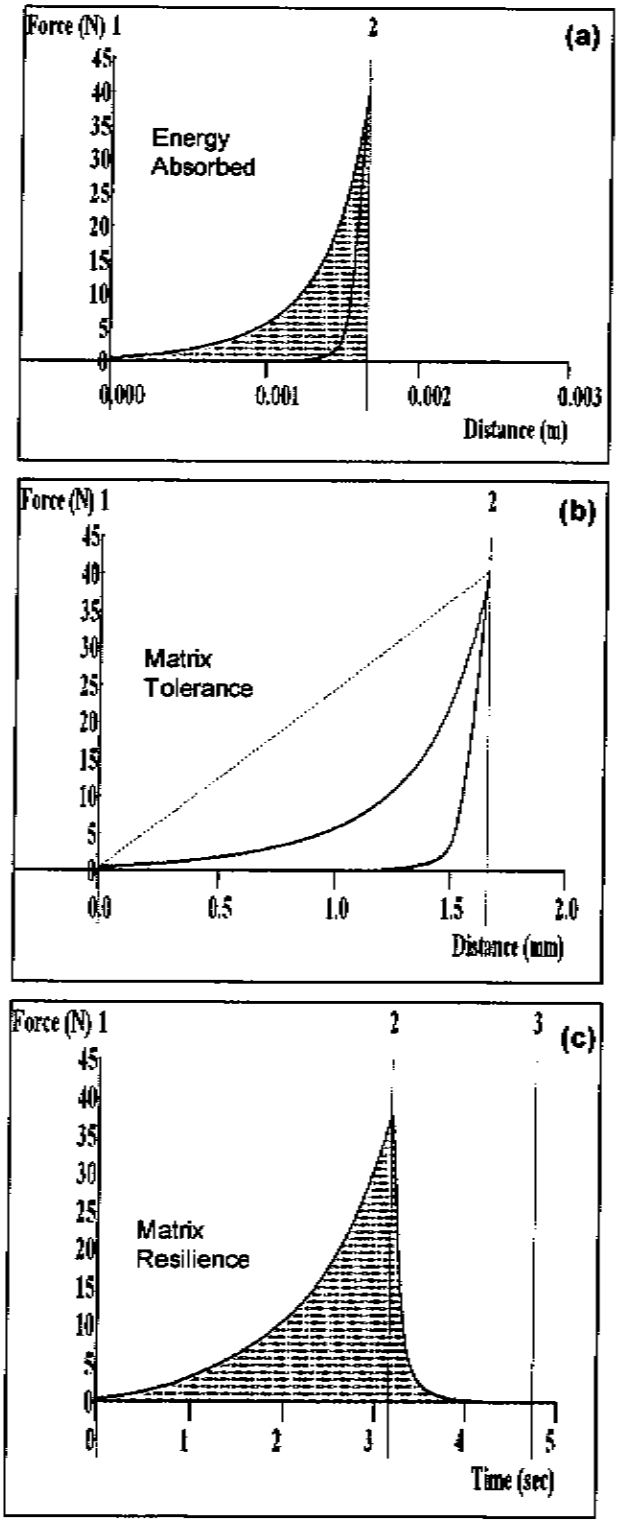


**Figure 3.1.** Typical textural force-distance and force-time profiles of salted-out PLGA scaffolds for the determination of (a) and (b) energy absorbed and (c) matrix resilience (N=10).

Figure 3.1*a* depicts the profile anchors used in calculating the energy absorbed i.e. area under the curve (AUC) [Nm=Joules]. Figure 3.1*b* depicts the anchors used for computing the matrix tolerance to assess the tendency of the PLGA scaffolds to change shape on application of stress. Figure 3.1*c* depicts a Force-Time profile used for calculating matrix resilience, which is represented by the ratio of the AUC between anchors 2 and 3 and 1 and 2 ($AUC_{32}/AUC_{12}$).

### *3.6.4.2 Gravimetric Analysis of Salted-Out PLGA Scaffolds*

Scaffold samples were pre-weighed, immersed in 100mL PBS and oscillated at 100rpm in a shakerbath (Labex, Stuart SBS40®, Gauteng, South Africa) at 250rpm. At 7, 10, 14, 26 and 30 days post-incubation scaffolds were removed, dried and gravimetrically analyzed utilizing a calibrated analytical mass balance. The mass of the scaffolds recovered at 7, 10, 14, 26 and 30 days after incubation were compared to their initial mass that was pre-weighed at time zero. The mass deflection from time zero was computed and recorded.

### *3.6.5 Ab Initio Quantum Mechanical Energy Computations*

Energy transitions were calculated using Spartan 04, M 001 (HF/3-21G Wavefunction, Inc., Minato-ku, Tokyo, Japan) software which predicted a hypothetical template of PLGA monomeric interactions with various quantities of dimethyl formamide (DMF) molecules, water ($H_2O$), hydrochloric acid (HCl) and PBS buffer ions ($PO_4^-$, NaCl, KCl). Templates were built by the atomic fragments, molecules, and ligands provided in the software.

The simulated minimization energy levels were obtained for the optimized stable conformations at the global minimum energy levels for interacting molecules in a template framework of singular and collective interactions. The values obtained were for PLGA at room temperature and pressure (excluding moisture, radiation, effects of other physical variants like magnetic field, gravitation and electric current).

## 3.7 Results and Discussion

### *3.7.1 Stereomicroscopic Image of a Salted-Out PLGA Scaffold*

The external morphological features of the salted-out PLGA scaffolds are indicative of the physicomechanical transitions that occurred during salting-out and subsequent cross-linking. Such transitions may directly impact the percentage of drug entrapment, degree of cell and tissue regeneration as well as the rate of drug delivery upon application of the scaffold for intended purpose.

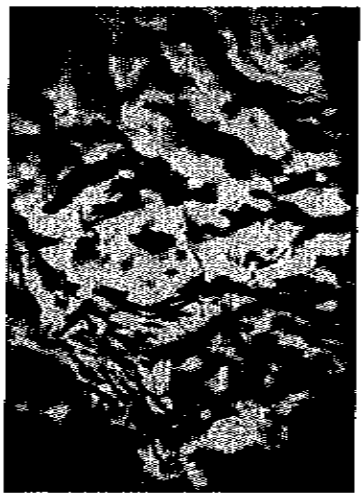

**Figure 3.2.** A stereomicroscopic image of a salted-out PLGA scaffold depicting the exterior surface morphology.

Figure 3.2 depicts the surface morphology of a woven composite flat-shaped salted-out PLGA scaffold (thickness=1mm) obtained. Surface folds and inter-connectivity, resembling the body's extra-cellular matrix were present. The exterior roughness and interconnected folds may be ascribed to cross-linked fibers within the PLGA matrix to form a scaffold. These folds provide an increased surface area for further drug entrapment as well as cell-seeding in drug delivery and tissue engineering.

### *3.7.2 Simulation of PLGA Monomeric Interactions during Solubilization, Salting-Out and Subsequent Cross-Linking into the PLGA Scaffold*

Solvation was conducted via mixed quantum/molecular mechanics. This allowed for computing the solvation energy and the solvent effects at a molecular interaction level. The interactions between PLGA, DMF, $H_2O$ and HCl are depicted in Figure 3.3. The model predicted experimentally observed trends such that by increasing the pH of the system resulted in increased partitioning of PLGA that led to immediate salting-out by phase separation of the organic and aqueous phases and subsequent cross-linking of native PLGA. Cross-linking of the matrix occurred mainly by covalent bonding of reactive molecules to form a 3-dimensional scaffold.

During solubilization of PLGA in DMF, two distinct stages were observed. Initially PLGA adsorbs DMF to form a gel-like stage that slowly dispersed into solution. During the second stage PLGA chains assumed a configuration such that the attractive and repulsive forces on each chain were precisely counter-balanced. The coupled effect of these forces induced the PLGA chain to adopt a meticulous stereochemical configuration, with a free rotation about the chiral carbons that resulted in the unperturbed formation of the C-C-C bond-angle fixed at 109° and the

C-C molecular distance of 1.54 Å, as depicted in Figure 3.3. Accordingly, this model allowed us to speculate the relative importance of polymer-solvent (PLGA-DMF) and ion-solvent ($H^+$-DMF) interactions on phase separation during salting-out of native PLGA to form the novel scaffold.

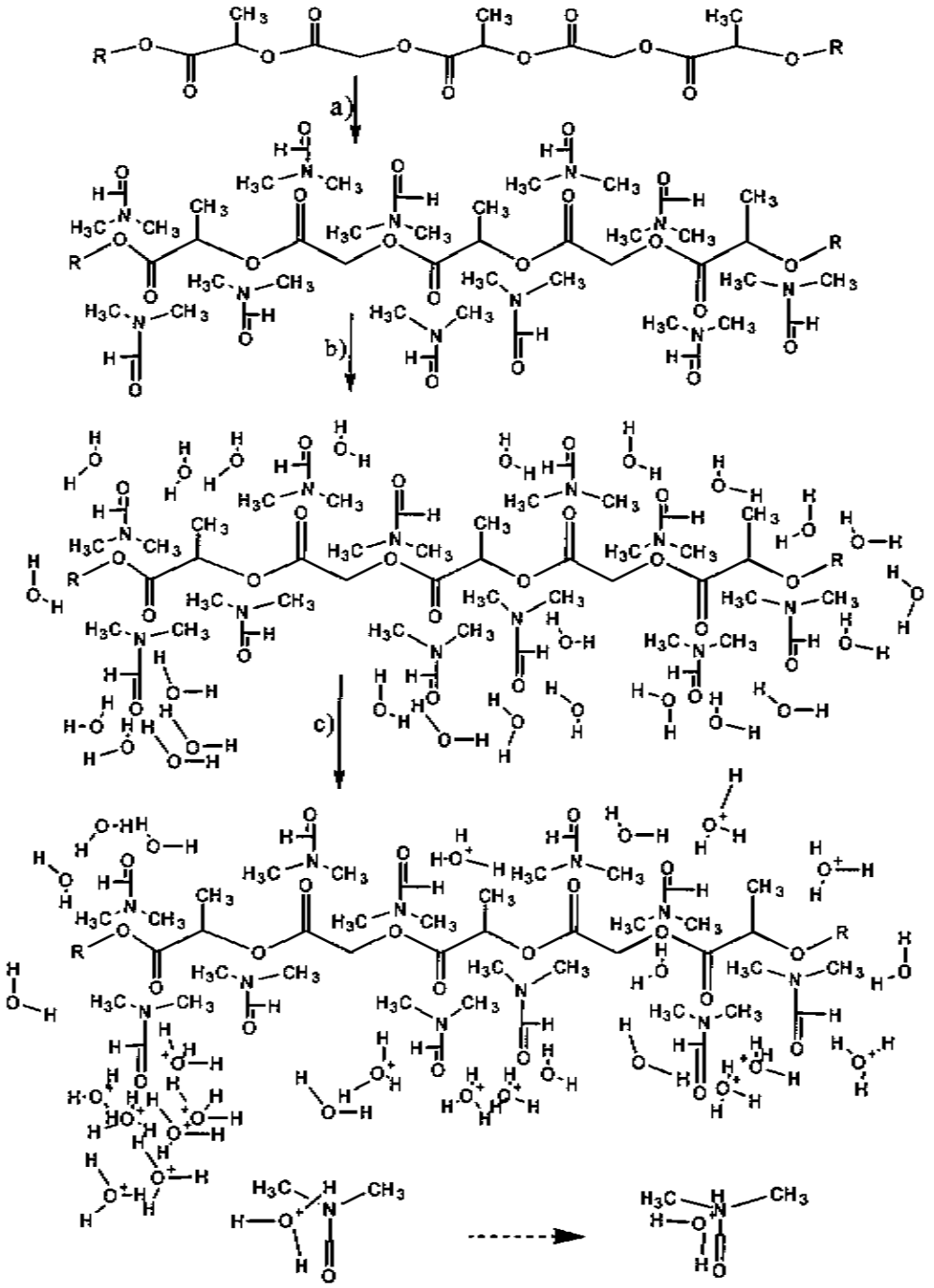

**Figure 3.3.** PLGA- interactions. Figures 2(a)-(c) illustrating PLGA, an α-OH polyester and a) interaction after DMF addition, b) interaction after water addition to the solubilized polymer, note outer solvation shell depicting water molecules and c) interaction after acid addition or addition of protonated water. In the last structure, DMF and protonated water interaction showing temporary proton and charge transfer from water molecule to DMF molecule.

Figure 3.3*a* depicts the ionic bond interactions between the N-O atoms of DMF and PLGA respectively. In Figure 3.3*b*, the hydrophobicity of PLGA networks drives water molecules to the periphery, thereby causing water clathrates to form at the surfaces, forming of an outer solvation shell. In Figure 3.3*c*, as the reaction proceeds, ionic interactions involving $H_2O$ and DMF occurred. The charge transfer from $H_2O$ molecules to DMF allowed PLGA to salt-out. It is presumed that the salting-out effect increased due to acidity of the system and thus the polar aprotic solvent was key during the reaction.

Furthermore, the 'Hydrophobic Effect' may have also enhanced the salting-out of PLGA into scaffolds. Owing to the hydrophobic nature of PLGA, junction zones were formed around the PLGA, which affected the configuration and solvation shells of $H_2O$, directing them away from the immediate surface of the PLGA. This phenomenon is proposed to have exerted a preferential partitioning of the hydrophobic PLGA chains. In addition, the salting-out and subsequent cross-linking of PLGA may have resulted in an increase in steric strain and internal energy of the scaffold, which is caused by a gain of electron energy introduced by the ions in the salts.

The summation of energies of the system during molecular interactions, determined the final quantum energy of the newly formed PLGA scaffold, which in turn influences its stability. The enthalpy changes during salting-out and cross-linking of PLGA resulted from bond formation, resonance, and steric strain. Bond stretching, bond-angle deformation, as well as interactions between atoms augmented the internal energy of the system.

Formation of a 3-dimensional PLGA scaffold decreased chain delocalization and resulted in resonance stabilization that also caused an increase in the enthalpy of the system. Bond formation and configurational changes of the structure during salting-out brought about transitions in the physicochemical and physicomechanical properties of native PLGA. However, these properties are anticipated to transform as the scaffolds erode in PBS over time. In order to assess the integrity of the salted-out PLGA scaffold during residence in PBS the physicomechanical transitions of PLGA scaffolds were assessed.

### *3.7.3 Physicomechanical Analysis of the PLGA Scaffolds Employing Textural Profile Analysis*

The physicomechanical transitions of the PLGA scaffolds interacting with the PBS environment were analyzed. The extent of physicomechanical modification was quantified in order to predict the dynamic transitions for flexibility and reproducibility of each scaffold variant. The PLGA scaffolds degraded at varying rates when immersed in PBS. Scaffolds may have interacted with the PBS by means of polar-hydrophobic interactions and hydrogen bonding.

The physicomechanical properties of the scaffolds were governed by the PLGA molecular mass, PLGA concentration, volume of water and salting-out reaction time. These variables may have also affected the cross-linking density. As the cross-linking density is reduced, the matrices will have increased resilience and a decreased degradation rate in PBS.

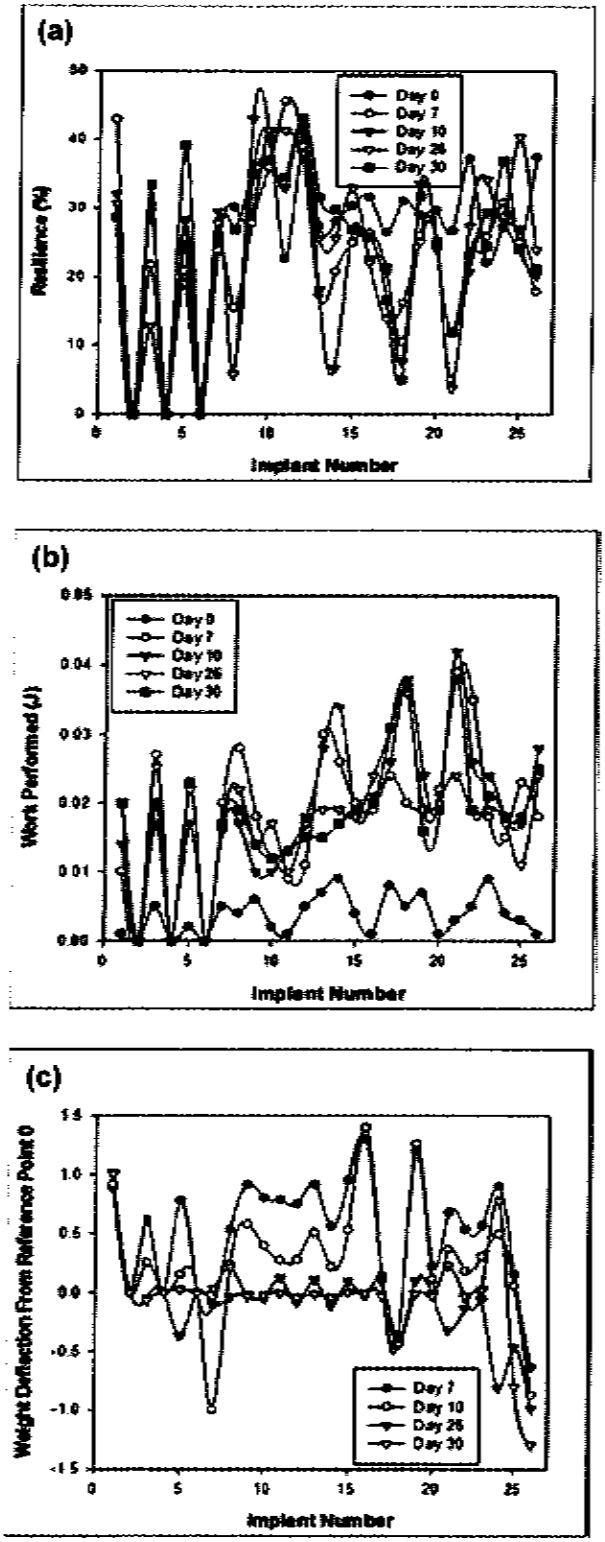


**Figure 3.4.** Profiles depicting the physicomechanical transitions of the salted-out PLGA scaffolds immersed in PBS (pH 7.4, 37°C). Plot (a) Matrix resilience, (b) Energy absorbed and (c) Mass deflection, over a 30-day period.

Figure 3.4*a* depicts the transitions in matrix resilience of the twenty six PLGA scaffold formulations immersed in PBS for 7, 10, 14, 26, and 30 days. Matrix resilience decreased with an increase in the incubation period (Figure 3.4*a*) and depended on the PLGA scaffold formulation. For instance, the matrix resilience of scaffold formulation numbers 1, 8, 10, 12, 14, 19, 20, 22, and 23 indicated a transition in matrix resilience between 35-45% during the 30-day incubation. Scaffolds that were salted-out utilizing higher PLGA concentrations exhibited minimal transition in matrix resilience whereas higher salting-out water volumes decreased the matrix resilience.

The ability of the scaffold to absorb energy was found to correlate with the residence time in PBS. Higher water volumes caused a decreased quantity of energy to be absorbed by the scaffolds during textural probe penetration (Figure 3.4*b*, formulations 2, 3, 7, 26). On the contrary, higher PLGA molecular masses caused an increased resistance to textural probe penetration. This indicated that excess energy was absorbed by the scaffolds when higher molecular masses of PLGA were used. The peak energy absorbed by the scaffolds occurred at day 10. The mass variation of scaffolds was also observed to decrease with an increase in scaffold residence in PBS which signified erosion.

Several deductions could be made from these findings. The general trend revealed by the data was that the scaffolds with higher PLGA molecular masses and concentrations were less susceptible to degradation and physicomechanical transitions when immersed in PBS. The salted-out PLGA scaffolds produced were

more hydrophobic and hence less prone to hydrolysis in PBS, hence, retarding degradation and conferring further flexibility to control drug release.

### *3.7.4 Response Surface Optimization of Scaffold Formulations*

By utilizing the salting-out and subsequent cross-linking process scaffolds with novel physicomechanical properties were obtained. Surface plots were able to focus on establishing the optimal combination of independent formulation variables for the enhancement of the scaffold physicomechanical properties making them suitable for controlled drug delivery.

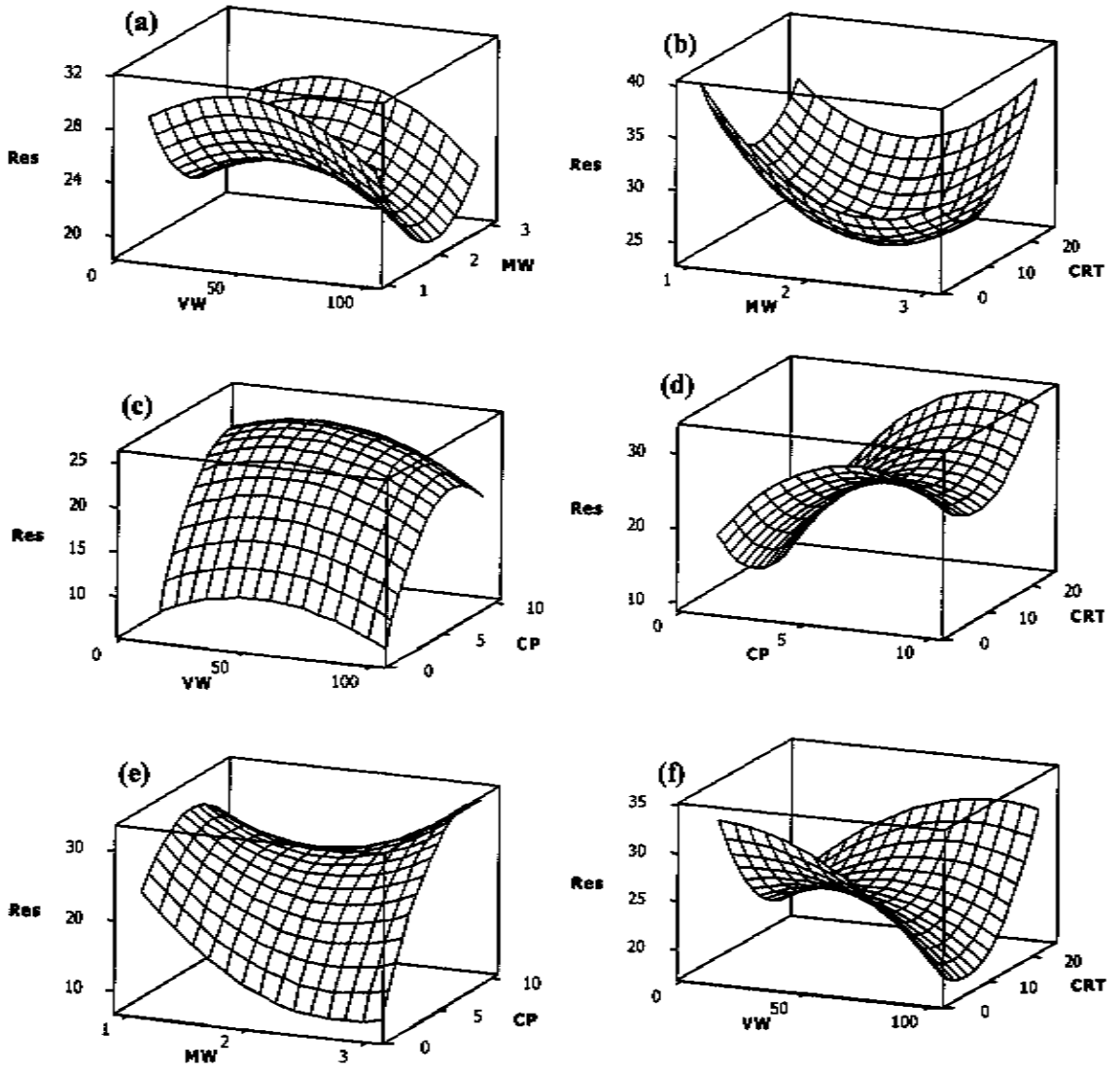


**Figure 3.5.** Response surface plots depicting resilience vs water volume and polymer molecular weight (a); water volume and salting-out time (b); water volume and polymer concentration (c); polymer molecular weight and salting-out reaction time (d); polymer molecular mass and polymer concentration (e); polymer concentration and salting-out time (f).

Response surface plots indicated that the PLGA molecular mass increased matrix resilience up to an optimal level of 100, 000 Daltons. As the PLGA molecular mass increased further matrix resilience decreased linearly (Figure 3.5*a*, *b* and *e*).

Increasing the PLGA concentration increased matrix resilience in spite of changes in water volume or salting-out reaction time (Figure 3.5*c*, *d* and *f*). Thus the PLGA concentration and molecular mass were significant in determining the matrix resilience. Also an increased water volume generally led to decreased matrix resilience values, especially when the salting-out reaction time is decreased (Figure 4.5*f*). These observations also highlighted that higher PLGA molecular masses increased matrix resilience only when the salting-out reaction time was longer. The salting-out reaction time proved to be effective in augmenting the PLGA concentration in increasing matrix resilience.

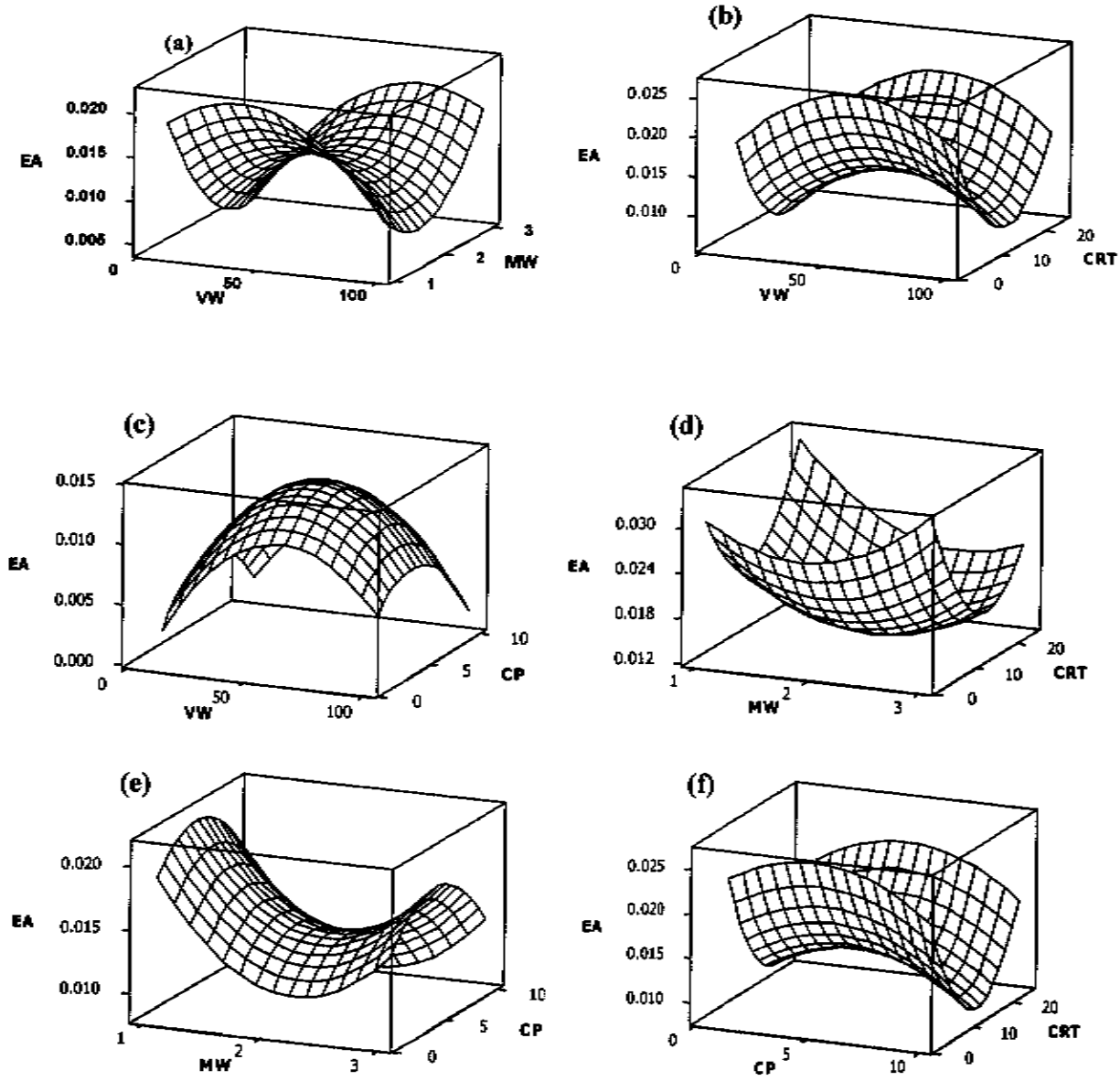


**Figure 3.6.** Response surface plots depicting energy of absorption vs water volume and polymer molecular weight (a); water volume and salting-out time (b); water volume and polymer concentration (c); polymer molecular weight and salting-out time (d); polymer molecular weight and polymer concentration (e); polymer concentration and salting-out time (f).

Figure 3.6*a*, *b* and *c* demonstrated that water volume was found to influence the quantity of energy absorbed during textural probe penetration of the scaffolds. Higher water volumes caused lower quantities of energy to be absorbed. The

increased volume of water during salting-out may have resulted in the entrapment of excess water molecules within the polymeric voids coupled with ion hydration, thereby decreasing the absorption of hydration-free energy. Higher PLGA concentration and molecular mass resulted in increased energy absorption (Figure 5*d*). However the PLGA concentrations reached a threshold level of 5% $^{w}/_{v}$, whereby the absorption of energy started to decrease.

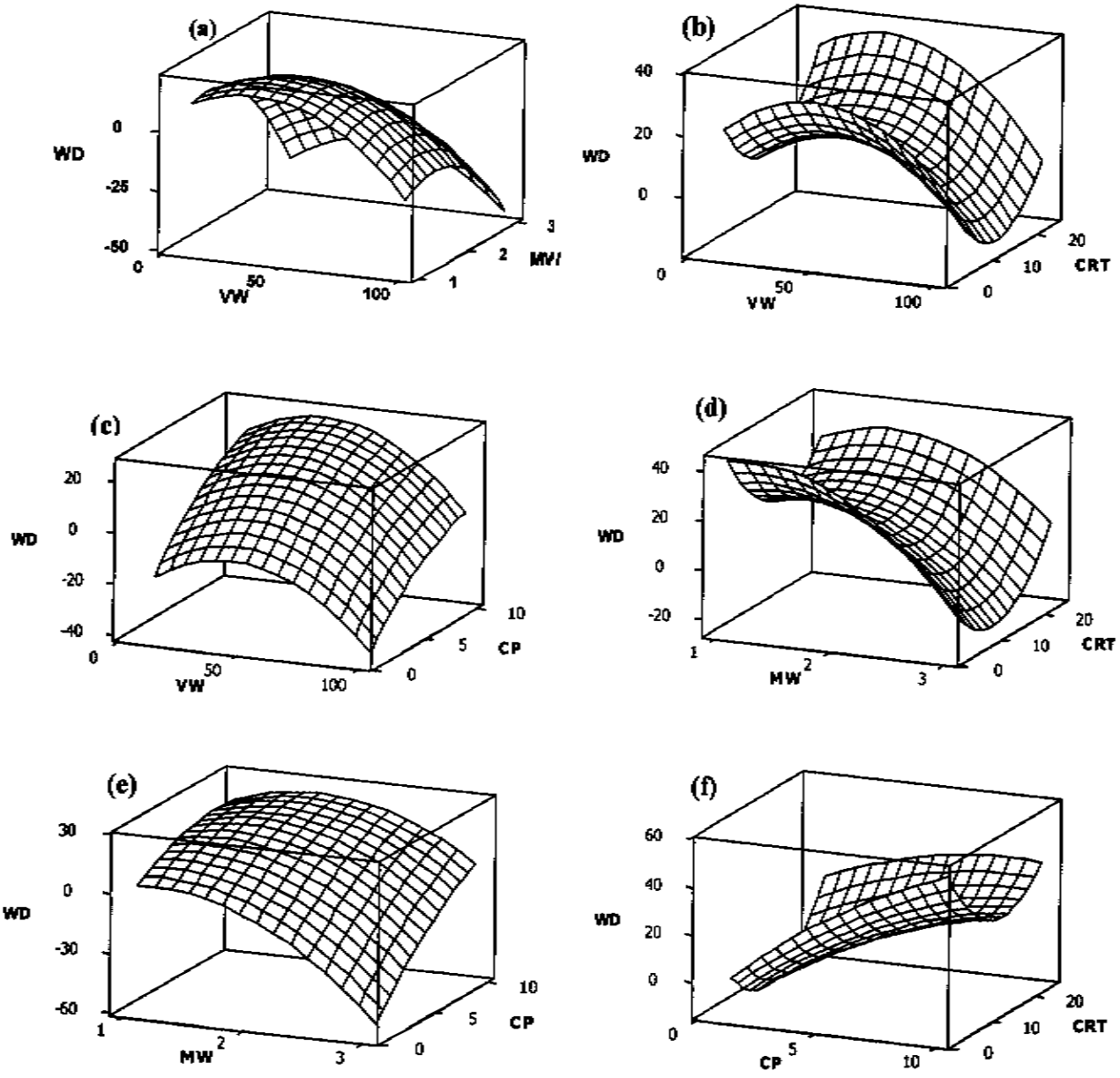


**Figure 3.7.** Response surface plots depicting weight deflection vs water volume and polymer molecular weight (a); water volume and salting-out time (b); water volume and polymer concentration (c); polymer molecular weight and salting-out time (d); polymer molecular weight and polymer concentration (e); polymer concentration and salting-out time (f).

Figure 3.7 demonstrates similar trends for mass deflection as shown by Figures 3.5 and 3.6 and concluded a fairly close correlation between all three physicomechanical properties of the novel PLGA scaffolds formed.

### *3.7.5 Comparison of the Experimental Vs. Predicted (Fitted) Response Values for Matrix Resilience, Energy Absorbed, and Mass Deflection Properties*

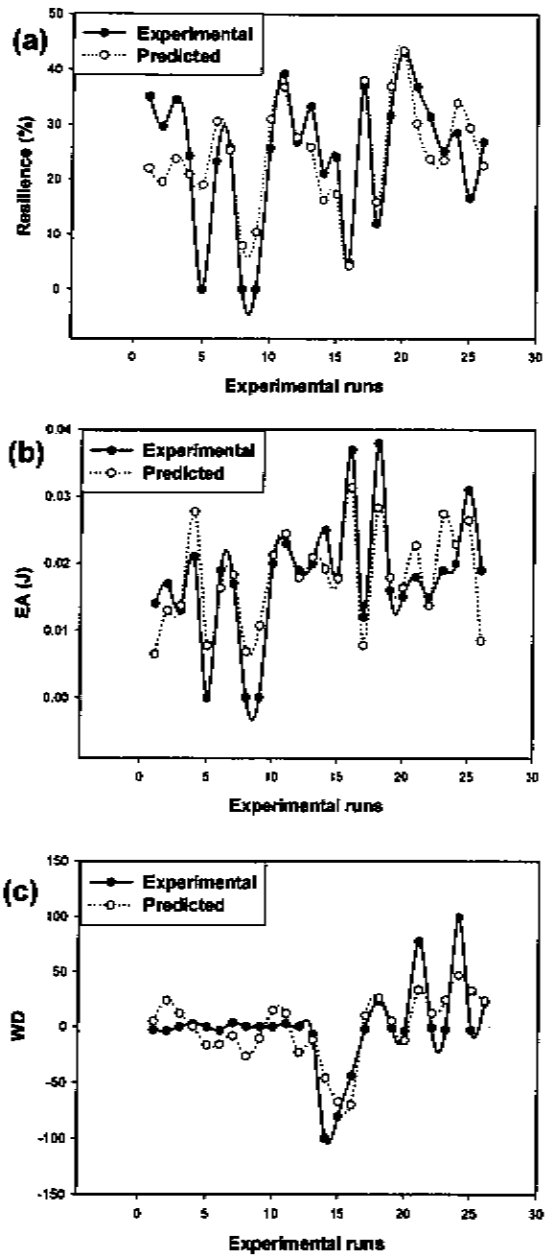


**Figure 3.8.** Profiles demonstrating the correlation between experimental and predicted (fitted) values for the responses. R=Matrix resilience; E=Energy absorbed; WD= Mass deflection.

Figure 3.8a, *b* and *c* depicts the close correlation between the model experimental and fitted values for the dependent formulation variables. No statistically significant differences were noted between the fitted and experimental values ($p>0.05$), indicating a good fit to the model chosen.

### *3.7.6 Elucidation of the Quantum Mechanical Energy Transitions at a Molecular Interaction Level*

A single PLGA monomeric unit was found to be stabilized at a minimum energy level of 38.03Kcal/mol utilizing Spartan 04, M 001 software.

The addition of 1 DMF molecule for solitary interaction with 1 PLGA monomeric unit produced an energy level of 5.35Kcal/mol, with the H-bond of DMF unbroken in the primary molecular interaction after repeated energy computations for a global minimum. The lower energy level value of 5.35Kcal/mol indicated the stability and scope for further molecular interactions to occur. This observation prompted the addition of more than 1 DMF molecule versus 1 PLGA monomeric unit during analysis.

The addition of a second DMF molecule, yielded an energy value of -19.25Kcal/mol followed by a third molecule of DMF to confer a minimum energy constraint for the most stable conformation to co-exist at -44.95Kcal/mol. This indicated an endothermic nature of the interaction comprising of 3 DMF molecules and 1 PLGA monomeric unit.

The decreasing energy values revealed a trend of energy conservation that accounted for the lower solubility of PLGA when DMF was used as a solvent. The energy requirement for this stable conformation of all 4 molecules (3 DMF molecules and 1 PLGA monomeric unit) formed a PLGA-DMF interaction template at a unit level which was a theoretical requirement for the primary solvation shell of DMF molecules versus the entire PLGA backbone. The energy levels were lower for the interactions resulting in minimal interaction and slower solvation of PLGA in DMF. The solvation of PLGA in DMF was achieved mainly over longer periods of time (>12 hours) and under the constant supply of external mechanical energy in the form of uniform magnetic agitation with minimal distortion of molecules.

The addition of $H_2O$ to this composite system (1 PLGA unit; 3 DMF molecules) raised the energy requirements. Energy values of -28.95Kcal/mol and -37.14Kcal/mol were obtained at this level with 1 PLGA monomeric unit, 2 molecules of DMF, and the presence of 1 and 2 $H_2O$ molecules respectively. The difference between the $H_2O$-borne energy requirements for a stable energy system was -10.00Kcal/mol which indicated a superior endothermic energy domain capable of imparting further stability to the system.

The composite system having an energy requirement of -44.95Kcal/mol indicated a stronger interaction between DMF and $H_2O$ molecules. The system consisting of 1 and 2 $H_2O$ molecules at -28.95Kcal/mol and -37.14Kcal/mol respectively required the presence of 1 PLGA monomeric unit for its energy dynamics. Significantly, all energy requirements at this level of interaction indicated subtle positive energy contributions of approximately 8.00Kcal/mol [-44.94-(-37.14)Kcal/mol] and 15 Kcal/mol [-44.95-(-

28.95)Kcal/mol] to the system to raise the energy profile from an endothermic to exothermic interaction phase between DMF and $H_2O$ molecules. This exothermic phenomenon was short-lived but significantly contributed to the primary solvation shell formation between PLGA and DMF which was important during solubilization.

The strong molecular interaction between DMF and $H_2O$ molecules predictably formed the secondary solvation shells around electronegative moieties of the PLGA molecule. The displacement of DMF molecules by $H_2O$ from the primary solvation shells at the electronegative moieties around the PLGA backbone was anticipated. However, this reaction was measured and possessed a weak energy profile thus not instantly favored.

Addition of 1 molecule of HCl to the solvation template comprising of 1 PLGA monomeric unit, 2 molecules of DMF, and 2 molecules of $H_2O$ further lowered the energy requirements to -42.32Kcal/mol. This indicated an endothermic energy requirement and hence the ability to absorb more energy. The energy profile changed further with the addition of a further HCl molecule (-45.45Kcal/mol). The energy level of the composite system at -44.95Kcal/mol and a 2 HCl molecule system with an energy value of -45.45Kcal/mol stood out in terms of similar energy requirements and revealed the complexity of the systems energy profile.

The fact that the composite and the 2 HCl molecule systems had similar energy values at -44.95Kcal/mol and -45.45Kcal/mol, respectively, indicated a significant fact regarding the solvation and thermodynamic stability of the reaction. In terms of energy the system remained stable at this level by a percentage of 99% per

100.00Kcal/mol. This indicated the overall stable energy required in the system to afford transient stability from DMF solvation to $H_2O$ interactions and ultimately to the HCl stage of the composite system. The higher energy requirements when $H_2O$ molecules were added displayed an exothermic phenomenon in comparison to when DMF molecules were added. The presence of HCl in the system neutralized the effects of $H_2O$ molecules and restored the system to the primary solvation levels with an energy level of -45.45Kcal/mol. More significantly, an energy exchange of equal values at this level may lead to biphasic phases, with a few DMF, $H_2O$ and HCl molecules in the gel phase while others might tend to remain in a solution phase.

Upon addition of PBS to the template it significantly changed the energy profile of the system. A difference of approximate -290Kcal/mol occurred with the addition of 1 phosphate ion ($PO_4^-$) in the presence of DMF, $H_2O$, HCl, and 1 PLGA monomeric unit constituting the computation domain. The addition of 1 molecule of sodium chloride (NaCl) affected the system further to yield an energy value of -6Kcal/mol with the minimum energy level arising at -338.16Kcal/mol.

Further addition of 1 molecule of potassium chloride (KCl) decreased the energy requirements by 5Kcal/mol to -343.89Kcal/mol. Addition of 1 and 2 $H_2O$ molecules changed this energy requirement to -353.56Kcal/mol and -361.44Kcal/mol respectively (1 molecule of $H_2O$, effective change ~ 10Kcal/mol) thus contributed to the predominant endothermic energy trend which was relatively more stable. A further leap in energy occurred with the addition of 1 more $PO_4^-$ that resulted in an almost twofold change in energy to a value of -663.72Kcal/mol. This value was

# CHAPTER FOUR

## THE EFFECTS OF SALTS ON THE PHYSICOCHEMICAL AND PHYSICOMECHANICAL PROPERTIES OF THE PLGA SCAFFOLD

### 4.1 Introduction

Based on the findings of the preceding Chapter Three, on the effects of polymer concentration and Mw on the *in vitro* degradation of PLGA, grade RG 504, with molecular mass of 55,000 Daltons was selected for further investigation towards attaining an optimized scaffold with modified physicochemical and physicomechanical properties. Numerous laboratory findings have shown that the modification of aliphatic thermoplastic polyesters, such as, PLGA can be achieved by manipulating of the chemical backbone using salts (Gao et al., 1998; Ju et al., 2000; Hasirci et al., 2001; Smith et al., 2001; Kuo and Leou, 2006).

Furthermore, evidence has shown the influence of salts on the stability and release of bioactives from PLGA delivery devices (Zhu and Schwendeman, 1999). The alteration of the 3-dimensional polymeric network that results from changes in bond vibrations, morphology, resilience and glass-transition temperature can be attained through ionic interactions between polymer-salt and polymer-polymer during salting-out and cross-linking (Smith et al., 2001; Di Noto and Zago, 2004). Therefore, this work evaluates the pivotal role of salts in the transformation of the chemical backbone of PLGA.

### 4.2 Polymer Modification with Salts and Ions

Several other studies have explored the use of salts in to enhance the properties of polymers. The incorporated salts are capable of changing the polymeric network from a homogenous to a heterogeneous matrix which leads to the transition in the physicochemical and the physicomechanical properties of the polymer (Muhiddinov et al., 2004). Nam and co-workers (2000) reported on the use of ammonium bicarbonate salts as gas foaming agent and porogen additives and further immersing the semi-solidified polymer-salt mixture into an aqueous solution of citric acid for the gas-foaming process at room temperature in order to produce macroporous biodegradable scaffolds.

In polymer modification, the mineral salt is primary selected based on its cation as the modifying effect is a function of this cation's capacity to react with the polymer. The anion selected should not be not be an electron pair donor or a strong oxidant as it would induce reduction-oxidation reactions and initiate the degradation process of the polymer. In addition, the anion should not form strong complexes with the metal cation. The anion also determines the solubility of the salt.

In accordance with the key findings from the preliminary studies in Chapter Two and in conjunction with the above-mentioned conditions, this study considered metal chlorides as suitable salts for the use in the salting-out and subsequent cross-linking of PLGA. This study adopted the use of monovalent, divalent and trivalent chloride salts in order to enhance the properties of the PLGA scaffold.

Salting-out, a colloidal phenomenon, has the capacity to change the morphology, resilience and glass-transition temperature of polymers, by means of salts that cause stochastic fluctuations of the free energy proportional to the salt concentration (Horvath, 1985; Tanaka and Takahashi, 2000). Zhang et al. (1995) showed that the salts can also modulate the release and swelling kinetics of bioerodible polyesters. Pillay and Fassihi (1999) reported on how electrolyte inclusions can alter the configuration and the micro-environment within hydrating matrices to control their swelling kinetics as well as physical rigidity. Furthermore, the complexation of ions such as calcium and magnesium to polyesters by ion-dipole bonds was illustrated by various researchers (Judas et al., 1986; Weihe et al., 2002; Mariette et al., 2005). These ionizable salts allows for non-collapsible diffusion channels to form within the polymeric structure. The salts function as both a pore forming reagent and cross-linker for the formation of PLGA networks; the process combines creating pores and cross-linking polymers in one step.

The presence of salts in polymeric matrices can control the rate of polymeric hydration and subsequent degradation. As the matrix hydrates, the salts and polymer compete for water of hydration, resulting in a programmed degradation and drug release rate (Pillay and Fassihi, 2001; Swenson, 2001). Thus the salts will attract water molecules in an effort to solvate themselves, thereby dehydrating the polymer and retarding dissolution and degradation.

One of the principal mechanisms of salting-out is the salt-induced surface tension increase of the water molecules (Izutsu et al., 1998; Melander and Horváth, 1977). Electron donor/acceptor interactions are a significant part of the salting-out

Salting-out, a colloidal phenomenon, has the capacity to change the morphology, resilience and glass-transition temperature of polymers, by means of salts that cause stochastic fluctuations of the free energy proportional to the salt concentration (Horvath, 1985; Tanaka and Takahashi, 2000). Zhang et al. (1995) showed that the salts can also modulate the release and swelling kinetics of bioerodible polyesters. Pillay and Fassihi (1999) reported on how electrolyte inclusions can alter the configuration and the micro-environment within hydrating matrices to control their swelling kinetics as well as physical rigidity. Furthermore, the complexation of ions such as calcium and magnesium to polyesters by ion-dipole bonds was illustrated by various researchers (Judas et al., 1986; Weihe et al., 2002; Mariette et al., 2005). These ionizable salts allows for non-collapsible diffusion channels to form within the polymeric structure. The salts function as both a pore forming reagent and cross-linker for the formation of PLGA networks; the process combines creating pores and cross-linking polymers in one step.

The presence of salts in polymeric matrices can control the rate of polymeric hydration and subsequent degradation. As the matrix hydrates, the salts and polymer compete for water of hydration, resulting in a programmed degradation and drug release rate (Pillay and Fassihi, 2001; Swenson, 2001). Thus the salts will attract water molecules in an effort to solvate themselves, thereby dehydrating the polymer and retarding dissolution and degradation.

One of the principal mechanisms of salting-out is the salt-induced surface tension increase of the water molecules (Izutsu et al., 1998; Melander and Horváth, 1977). Electron donor/acceptor interactions are a significant part of the salting-out

technique, since the various anionic and cationic species in aqueous solution order certain extents of changes according to their efficacies in salting-out thermoplastic polymers such as OH-polyester (Smith et al., 2000).

Thermodynamic studies by Arakawa and Timashef (1983) demonstrated that the salts that decrease dissolution of hydrophobic polymers are preferentially excluded from the vicinity, strongly bind to the polymers and are called kosmotropes, whereas salts that increase the polymer solubility display weak preferential binding with the polymer and tend to settle at the polymeric surfaces (Arakawa and Timasheff, 1985; Galinski et al., 1997; Moelbert et al., 2004).

Although there is a large variety of forces present, including electrostatic and Lifshitz-Van der Waals, the interactions responsible for the salting-out phenomena seem to be dominated by the hydration forces ruled by electron donor/acceptor. Kosmotropes tend to tighten the inter- and intra-molecular structure allowing polymeric interactions, thus enhancing the polymeric properties that include resilience, energy of absorption and the deformability modulus of the polymer.

In aqueous polymeric solutions, salting-out creates stabilization of the water structure, thereby decreasing the hydrogen-bonding between water molecules and the polymeric chain. This is an alternate mode that enhances the hydrophobic interaction between polymeric chains (Bolen and Baskakov, 2001). These chains are rendered stiff by the introduction of chemical bonds between their monomers (cross-linking), and between the polymeric chains and the salts, which further transform the properties of the polymer (Nyström et al., 1995).

The resulting cross-linked polymeric networks are dimensionally stable, with minimal hydrolysis of the polymer bonds, and exhibit superior structural integrity, making them suitable for sustained drug delivery applications. While polymeric strengths are controlled by the degree of cross-linking, the degradation rate of these networks can be controlled independently by the chemical composition.

In this work, we evaluate the physicochemical and physicomechanical transitions occurring within salted-out poly lactic-co-glycolic acid (PLGA), an α-OH polyester, using a statistical approach to develop a mechanistic understanding. These salted-out complexes are termed "scaffolds". In order to achieve this various techniques were employed namely, textural analysis, SEM, FTIR and DSC.

## 4.3 Materials and Methods

### *4.3.1 Materials*

PLGA was obtained from Boehringer Ingelheim Pharma (Ingelheim, Germany) (Resomer® RG504 50:50; $M_w$ 48,000; i.v. 0.48-0.60dl/g). Acetone was used as a solvent, and analytical grades of sodium chloride (NaCl), calcium chloride ($CaCl_2$), (Rochelle Chemicals, South Africa) and aluminium chloride ($AlCl_3$) (Merck, Darmstadt, Germany) were used as the ionic salts.

### *4.3.2 Building the Experimental Design*

A 3 factor, 3 level Box-Behnken statistical design was built in order to model the number of experiments needed for formulation optimisation and to establish the main and interaction effects of the independent formulation variables on the

physicochemical and physicomechanical properties of the PLGA scaffolds using Minitab V14 (Minitab, USA).

### *4.3.3 Preparation of PLGA Scaffolds*

PLGA scaffolds were prepared by salting-out and subsequent cross-linking using a combination of acetone and ionic salts in accordance with a Box-Behnken design template outlined in Table 1. Fourteen polymeric solutions comprising 0.4g of PLGA dissolved in 15mL of acetone were prepared. The cross-linking solutions comprising 75mL of $0^{w}/_{v}$, $5^{w}/_{v}$ or $10\%^{w}/_{v}$ of NaCl, $CaCl_2$ or $AlCl_3$ was added to the polymeric solution and agitated for a period of 30 minutes.

The resultant PLGA scaffolds were removed from the cross-linking solution washed thrice with 500mL deionised water and dried to constant mass at room temperature. Each PLGA scaffold was stored for a maximum of 48 hours prior to physicochemical and physicomechanical evaluation. Table 4.1 below designates the independent variables and the factor levels used in the Box-Behnken Design, with generated PLGA formulations that are shown in Table 4.2 below.

**Table 4.1.** *Factor levels of the independent variables for the Box-Behnken Design*

| Variables | Factor Level | | | Units |
|---|---|---|---|---|
| | Low | Middle | Upper | |
| NaCl | 0 | 5 | 10 | $\%\ ^{w}/_{v}$ |
| $CaCl_2$ | 0 | 5 | 10 | $\%\ ^{w}/_{v}$ |
| $AlCl_3$ | 0 | 5 | 10 | $\%\ ^{w}/_{v}$ |

**Table 4.2.** *Box-Behnken template with randomly generated PLGA formulations*

| Scaffold Formulations | Randomized Run Order | [NaCl] ($\%^{w}/_{v}$) | [$CaCl_2$] ($\%^{w}/_{v}$) | [$AlCl_3$] ($\%^{w}/_{v}$) |
|---|---|---|---|---|
| 1 | 6 | 10 | 5 | 5 |
| 2 | 11 | 5 | 10 | 0 |
| 3 | 7 | 5 | 5 | 5 |
| 4 | 4 | 5 | 0 | 10 |
| 5 | 2 | 10 | 5 | 10 |
| 6 | 3 | 5 | 10 | 0 |
| 7 | 5 | 5 | 5 | 5 |
| 8 | 12 | 10 | 5 | 10 |
| 9 | 8 | 5 | 10 | 0 |
| 10 | 13 | 5 | 5 | 5 |
| 11 | 9 | 5 | 0 | 10 |
| 12 | 14 | 10 | 5 | 10 |
| 13 | 1 | 5 | 10 | 0 |
| 14 | 10 | 5 | 5 | 5 |

The quadratic model for the responses is shown in Equation 4.1:

$$Response = b_0 + b_1[NaCl] + b_2[CaCl_2] + b_3[AlCl_3] + b_4[NaCl]^2 + b_5[NaCl][CaCl_2] + b_6[NaCl][AlCl_3] + b_7[CaCl_2][AlCl_3] + b_8[CaCl_2]^2 + b_9[AlCl_3]^2 \quad \textit{Equation 4.1}$$

where, the *Response* is associated with each factor level, $b_0 ... b_9$ are the regression coefficients, and [NaCl], [$CaCl_2$] and [$AlCl_3$] are the independent formulation variables.

### *4.3.4 Morphological Characterization of the PLGA Scaffolds*

The surface morphology of the PLGA scaffolds was assessed from Scanning Electronic Microscopic (SEM) images employing a thermal emission JEOL JSM-

(Japanese Electronic Optical Laboratories, Tokyo, Japan) electron micrograph. Samples of PLGA scaffolds were sectioned and mounted on aluminium stubs prior to sputter-coating with a layer of carbon. Each sample was viewed under varying magnifications at an accelerating voltage of 20 kv.

### *4.3.5 Determination of the Physicomechanical Properties of the PLGA Scaffolds*

The physicomechanical properties of the PLGA scaffolds were evaluated using a Texture Analyzer (TA.*XTplus* Texture Analyzer, Stable Microsystems, UK). Stress-strain profiles with a high degree of accuracy and reproducibility were capture at a rate of 200 points per second employing Texture Exponent software V3.2 and subsequently analyzed. A 3.5cm flat-tipped circular steel probe was attached to the force transducer. The parameter settings employed to obtain the energy absorbed, deformability modulus and matrix resilience are shown in Table 4.3.

***Table 4.3.*** *Textural parameter settings*

| **Settings** | **Energy Absorbed and Deformability Modulus** | **Matrix Resilience** |
|---|---|---|
| Pre-test speed | 1mm/sec | 1mm/sec |
| Test speed | 0.5mm/sec | 0.5mm/sec |
| Post-test speed | 1mm/sec | 1mm/sec |
| Compression force / strain | 40N | 50% |
| Trigger type | Auto | Auto |
| Trigger force | 0.5N | 0.5N |
| Load cell | 50kg | 50kg |
| Distance | 20mm | 20mm |

To elucidate the energy absorbed, matrix resilience and deformability modulus, Force-Distance and Force-Time profiles for each PLGA scaffold was generated. Typical textural profiles used for quantifying the physicomechanical properties are depicted in Figure 4.1.

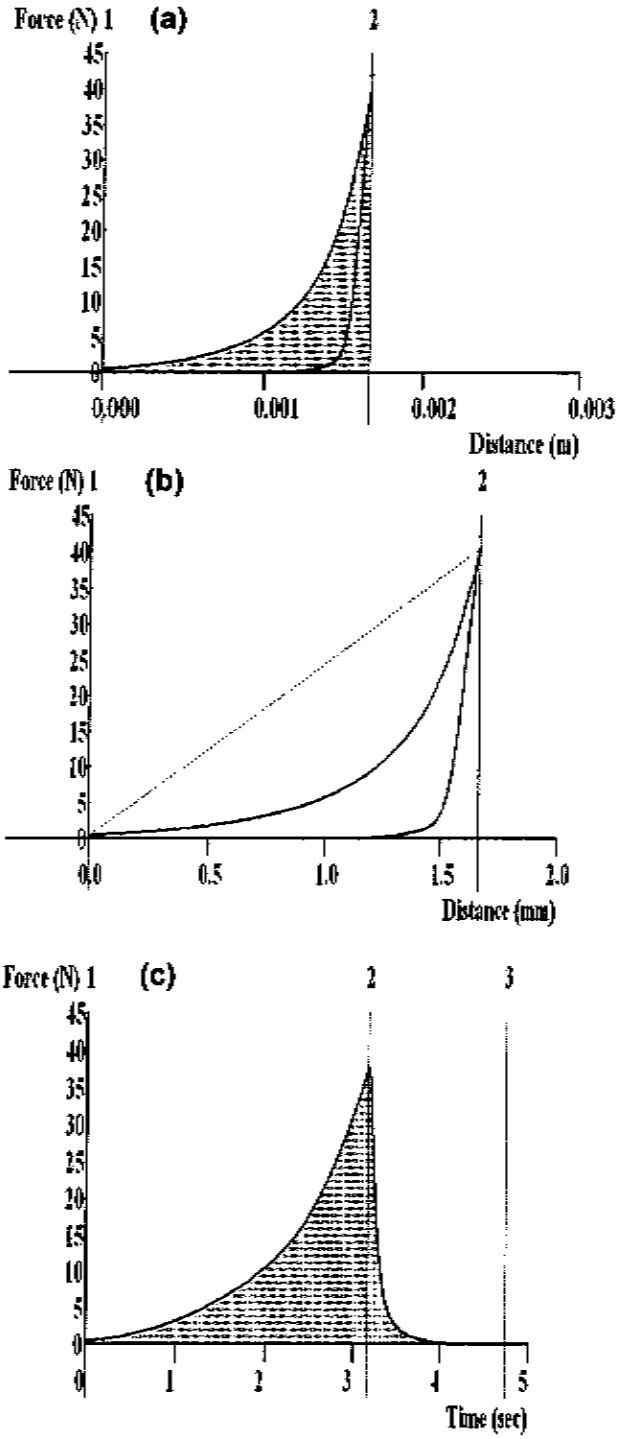


**Figure 4.1.** Typical Force-Distance and Force-Time profiles of PLGA scaffolds for determining (a) energy absorbed (b) deformability modulus and (c) matrix resilience (N=10).

Figure 4.1*a* depicts the anchors used in a Force-Distance profile for calculating the energy absorbed i.e. the total area under the curve (AUC) [Nm=Joules] between anchors 1 and 2. Figure 4.1*b* depicts the anchors employed for determining the deformability modulus (the tendency of the PLGA scaffolds to change shape upon the application of stress) i.e. the gradient between anchor 1 and the maximum force attained during sample analysis. Figure 4.1*c* depicts the anchors employed for calculating the matrix resilience, i.e. the ratio of the AUC between anchors 2 and 3 and 1 and 2 ($AUC_{32}/AUC_{12}$) for a Force-Time profile.

### *4.3.6 Elucidation of the Molecular Structural Transformations within PLGA Scaffolds*

Fourier Transform Infra-Red (FTIR) spectroscopy was performed on native PLGA and on the novel PLGA scaffolds to determine chemical transformations potentially occurring within the polymeric backbone due to salting-out and subsequent cross-linking using a Nicolet Impact 400D (Nicolet Instrument Corporation, Pennsylvania, USA) instrument. The potassium bromide (KBr) disc approach was employed, whereby 7.5mg samples of each PLGA scaffold was triturated with 200mg of KBr and compressed in a transparent circular disc using a Beckman Hydraulic Press (WIKA Instruments (Pty) Ltd, Johannesburg, South Africa). Background scans were obtained for all samples and the % transmittance was recorded between 4000 – 400$cm^{-1}$ at an intermediate resolution.

### *4.3.7 Thermal Transition Analysis of the PLGA Scaffolds*

Differential Scanning Calorimetry (DSC) was used to record transitions in specific heat capacity and latent heat, which indicated changes in the amorphous or

crystalline structure as a result of scaffold formation from cross-linking native PLGA. Thermal transitions were recorded on a Perkin-Elmer Pyris-1 connected to a controller model TAC1/DX (Perkin-Elmer, Inc. USA). Samples were heated in increments from 25°C to 400°C at a rate of 10°C/min. Samples of 5-10mg of each PLGA scaffold was placed within a crimped aluminium pan and subjected to the heat gradient. Thermograms were obtained and subsequently analyzed.

## 4.4 Results and Discussion

### *4.4.1 Proposed Interactions between PLGA Chains and Cross-linking Ions*

The solvated ion pairs of $Na^{+}$, $Ca^{2+}$, and $Al^{3+}$ develop into electron nodes that facilitate ionic reactions. These solvated ion pairs are able to attract the adjacent cations of $Cl^{-}$ and $O^{2-}$ within the polymeric matrix thus contributing to cross-linking of lactide and glycolide chains within the PLGA molecular structure. The sodium, calcium and aluminium salts function as pore forming reagents and as cross-linkers for the formation of PLGA networks; the method combines creating pores and cross-linking polymers in one step (Liu et al., 2003). This cross-linking reaction depends primarily on the ionization energies of the salting-out ion, hydration enthalpies in solution and the thermodynamic stability of the monomeric PLGA units.

Furthermore, the coordination number of each salt (8, 6 and 4 for $Al^{3+}$, $Na^{+}$ and $Ca^{2+}$ respectively) along with the atomic radii of the metals of the salts, (Table 4.4) manipulated the attraction of adjacent cations during cross-linking. The salt and/or ion that possesed the highest coordination number and atomic radius exerted the most influence on the cross-linking reaction and subsequently becoming a central

factor in modifying the native PLGA polymeric structure to produce a robust PLGA scaffold.

***Table 4.4.*** *Physicochemical properties of the salts employed during cross-linking of PLGA*

| **Salt Type** | **Atomic radius of Metals (pm)** | **Metal Coordination Number** | **Cation Coordination Number** |
|---|---|---|---|
| NaCl | 186 | 6 | 6 |
| $CaCl_2$ | 197 | 4.2+/-0.5 | 5.4+/- 0.3 |
| $AlCl_3$ | 125 | 8 | 6 |

The salts used in this study, namely NaCl, $CaCl_2$ and $AlCl_3$ differ with regard to the physicochemical, physicomechanical and morphological structure of the resultant PLGA scaffolds. Furthermore, the shape and stereo-orientation within the PLGA structure differs and therefore, the ability of water molecules to be imbibed within the matrix depends on the rate of polymer-salt interactions, the reactivity, atomic size and coordination number of the concerned ions, the nature of the crystal-lattice packing of ions and the polymeric substrate present during salting-out and subsequent cross-linking.

### *4.4.2 Scanning Electron Microscopic Image Analysis of the PLGA Scaffold Morphology*

3-dimensional architecture comprising various fiber volume and diameters, interconnections and pore sizes were obtained from polymer-salt interactions as a result of cross-linking during PLGA scaffold formation. The presence of salts

generated areas of high entropy at the solid-liquid interfaces resulting in altered fibrous structures with distinct morphologies (Figure 4.2). The ionic interactions between the salts and PLGA molecules were dependent on the ionization energies of cross-linking ions, hydration enthalpy of the salt in solution as well as the thermodynamic stability and molecular accumulation of salts and water at the lactide-glycolide strands of native PLGA. As a result several morphological conformations of each PLGA scaffold were obtained (Figure 4.2). Furthermore, the coordination number of each salt influenced the number of covalent bonds formed. Hence, H-bonding and other intra and inter-ionic forces located on the PLGA molecule (oxygen residues) cluster-packed with water molecules influenced the nature and size of pores and fibers of the newly formed PLGA scaffolds.

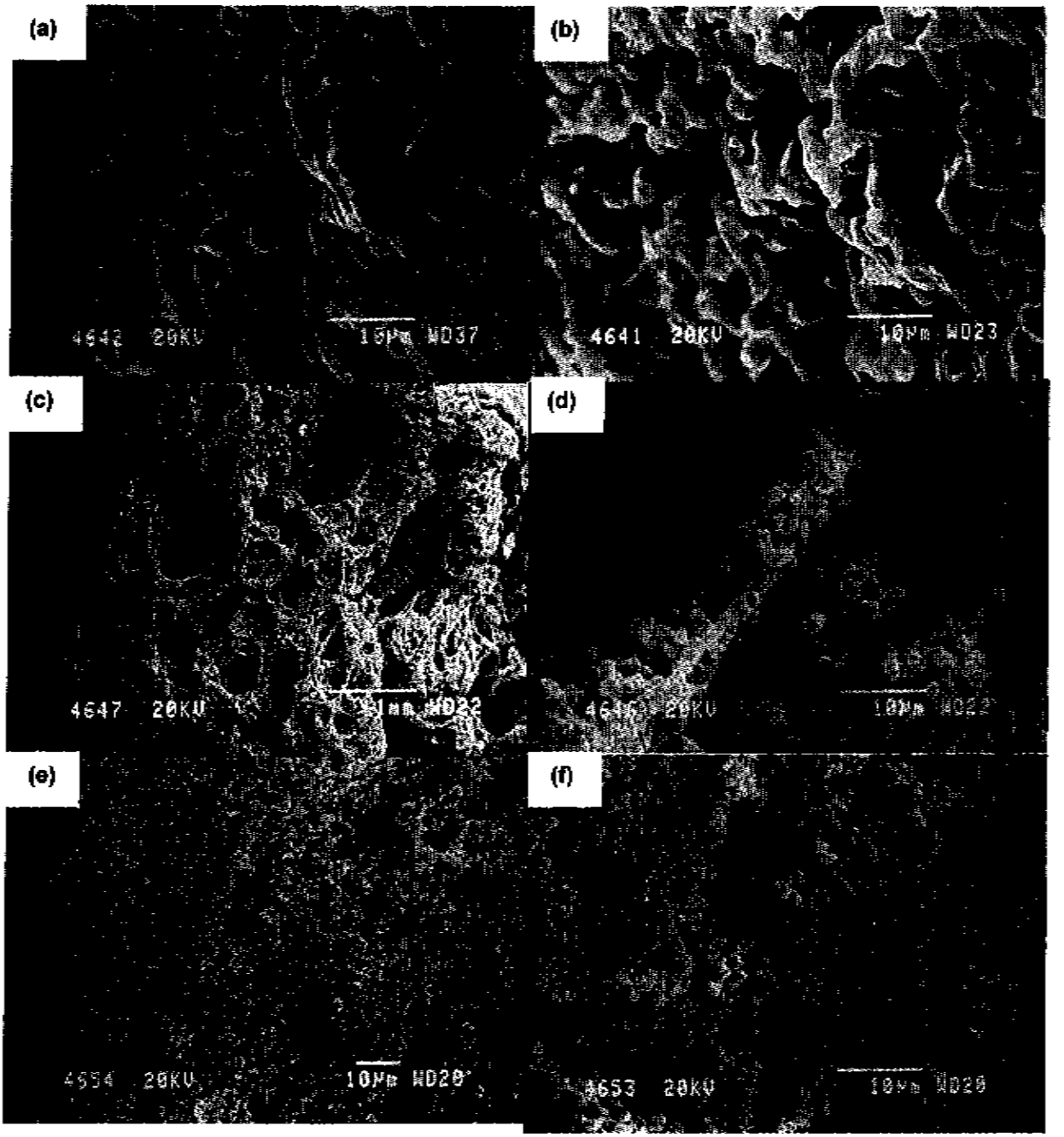


**Figure 4.2.** Scanning Electron Micrographs of Salted-out PLGA. These micrographs demonstrate the surface morphology of PLGA: salted-out with NaCl [Figure 4.2(a) and 4.2(b)] at 2000X Mag (a nd b), WD of 23mm and 37mm; $CaCl_2$, [Figure 4.2(c) and 4.2(d)] at 2000X Mag (c) and 20X Mag (d), WD of 22mm (c and d) as well as $AlCl_3$ [Figure 4.2(e) and 4.2(f)] at 2000X Mag (e) and 1000x Mag (f), WD of 20mm (e and f).
*Mag= Magnification, WD=Weight distribution.*

SEM images of PLGA scaffolds salted-out with NaCl revealed a uniform distribution of interconnected pores, divided by struts of microporous structures that maintained homogeneity of cross-linked fibers in a neuronal meshwork archetype (Figure 4.2*a* and *b*). These fibers possessed pores and fiber diameters ranging between 0.1-1.4μm, and fiber volumes ranging from 0.01-0.03μm$^3$. In Figure 4.2*c* and *d*, the divalent salt $CaCl_2$ produced a fibrillar composite PLGA scaffold with interconnecting channels in a distinct voluminous trabecular formation with scales of pore sizes and diameters ranging between 7.5-15μm and fiber volumes of 800-14000μm$^3$.

In Figure 4.2*e* and *f*, PLGA scaffolds salted-out with a trivalent salt namely $AlCl_3$ revealed fine fibrous morphologies with distinct cross-links that resulted in a ramified interconnection of the PLGA scaffold design with pore sizes and diameters ranging from 0.03-0.10μm and fiber volumes between 0.09-0.17μm$^3$.

In general, introduction of salting-out ions to the polymeric solution facilitated the native PLGA polymeric structure to assume a fixed 3-dimensional configuration into cross-linked lactide-glycolide chains. The configuration depended significantly on the nature of the salt, which is explained by different degrees of structuring of the polymeric matrices caused by the ions of the salts. Furthermore, the adjacent voids resulting from such a configuration were able to accommodate water molecules in accordance to the dimensions of voids created due to short and long distance interactions between native PLGA chains. These voids significantly provided the space for binding water molecules which was dependent on the size and the rate of the ion in salting-out and subsequently cross-linking PLGA.

An increase in the fibrillar nature of the PLGA scaffolds augmented the physicomechanical properties such as matrix resilience. The distinct differences in morphology revealed in each micrograph of the PLGA scaffolds suggest the versatility of the scaffold and hence may be suitable for tailored manufacturing that match specific applications.

### *4.4.3 Textural Profile Analysis to Quantify the Physicomechanical Properties of PLGA Scaffolds*

Analysis of the textural profiles provided an insight on the Stress-Strain relationships for the PLGA scaffolds. Results demonstrated that native PLGA could be modified into a highly resilient polymeric material by rapid ionic salting-out and subsequent cross-linking in order to achieve elasticity that depended mainly on the type and the concentration of salt employed. The matrix resilience values of PLGA scaffolds salted-out with NaCl and $AlCl_3$ were superior to that of PLGA scaffolds salted-out with $CaCl_2$ (Figure 4.3).

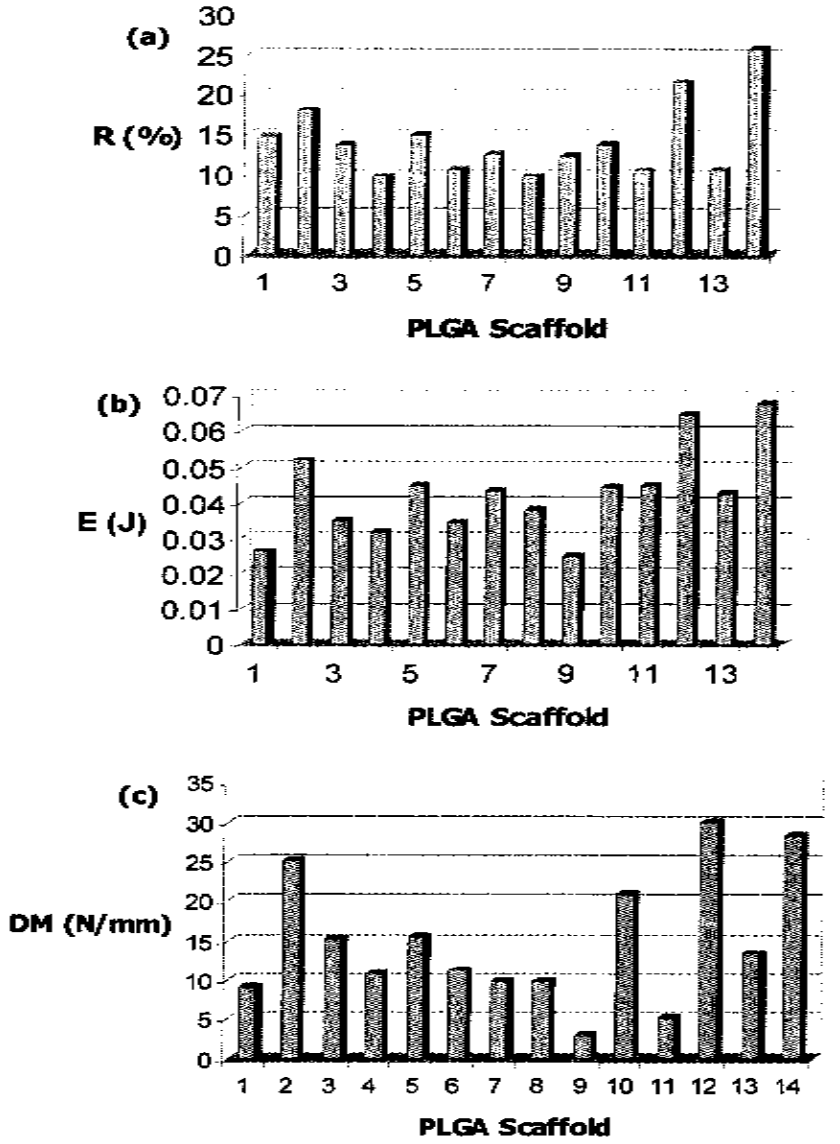


**Figure 4.3.** Profiles depicting differences in the physicomechanical properties of PLGA scaffolds. Plot (a) Resilience (R), (b) Energy absorbed (E) and (c) Deformability modulus (DM).

The physicochemical nature of the salt employed during salting-out created a micro-environment which accentuated the viscoelastic behaviour of the PLGA scaffold. The viscoelasticity caused densification of the PLGA scaffolds, which resulted in resistance of the scaffold to deform under stress during textural analysis. Figure 4.3a

and *b* revealed significant increases in the resilience and energy absorbed when concentrations of NaCl and $AlCl_3$ were increased, for instance in formulations 2, 12 and 14. The concentration of $CaCl_2$ was found to be inversely proportional to the energy absorbed as demonstrated in formulations 6, 9 and 13. The increase in resilience and deformability moduli was linearly correlated to the quantity of energy absorbed by the PLGA scaffolds per unit volume shown in Figure 4.3*b* and *c*.

The modification of the physicomechanical properties revealed by these profiles is consistent with the dense surface morphology of the PLGA scaffolds depicted in Figure 4.2. In general, salts that produced more compact polymeric structures with smaller and more uniform pores, such as NaCl and $AlCl_3$ accentuated the physicomechanical properties of the PLGA scaffolds, whereas salts that produced larger pores decreased the resilience.

Furthermore, the resultant accumulation of additional water molecules within the polymeric chains conferred more dipoles to the matrix, which causes them to be less responsive to the resilience activity within the PLGA backbone. Ferry (1980) reported that the presence of water molecules which are dipole and contributors of interfacial tension decreases matrix resilience. The proximity of the polarising dipoles to the PLGA backbone and the extent to which they are influenced by the configurational activity of the PLGA chain directly influenced the total resilience, energy absorbed, and deformability modulus of the PLGA scaffold.

### *4.4.4 Response surface Performance*

Surface plots (Figure 4.4) were constructed to visually demonstrate the individual and synergistic effects of the salts on modifying the physicomechanical properties of native PLGA by scaffold formation. Figure 4.4a revealed that at lower concentrations (between 0 and 5%$^{w}/_{v}$), NaCl significantly increased resilience of PLGA scaffolds up to a limit of 15% at which any further increase of NaCl (above 5%$^{w}/_{v}$) resulted in a decreased resilience. At low concentrations (between 0 and 5%$^{w}/_{v}$) of $AlCl_3$ a resilience of 10% was maintained and a further increase in $AlCl_3$ beyond 5%$^{w}/_{v}$ resulted in a linear increase of resilience.

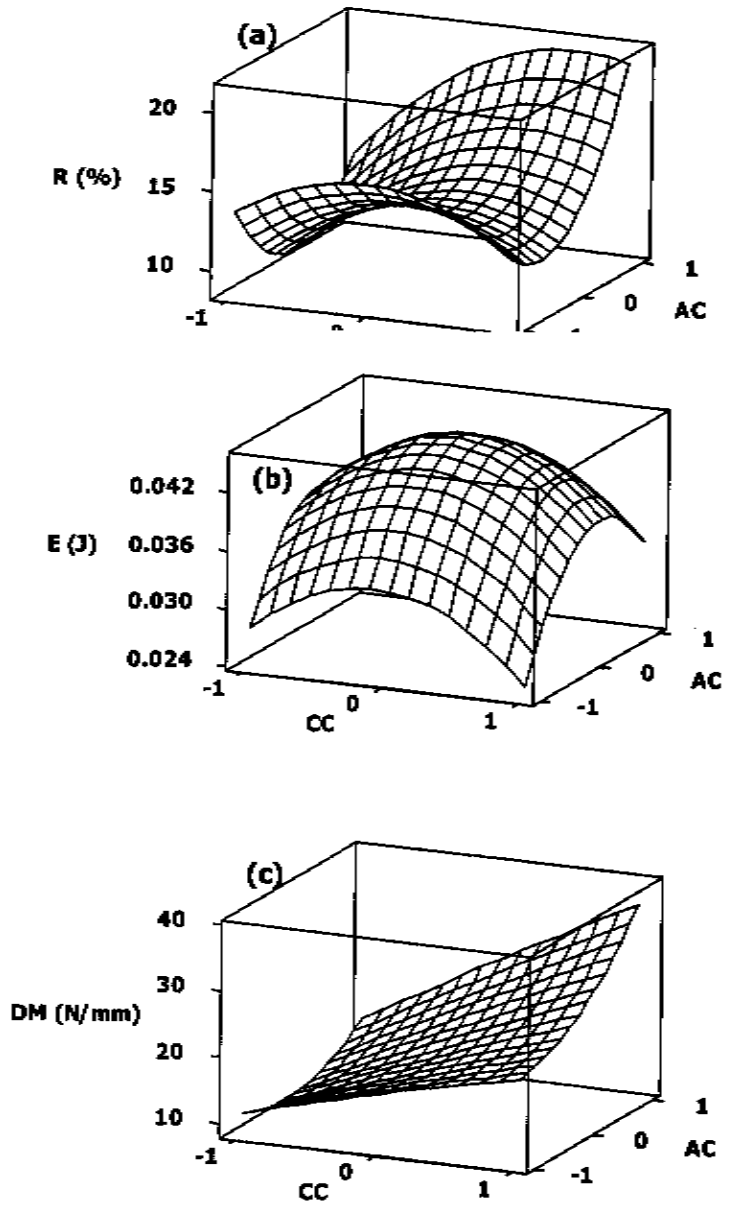


**Figure 4.4.** Typical surface response plots depicting the effects of the independent formulation variables on the physicomechanical properties of the salted-out PLGA scaffolds, namely (a) Resilience (R) (%); (b) Energy absorbed (E) (J); and (c) Deformability modulus (DM) (N/mm). *AC= $AlCl_3$, CC= $CaCl_2$, SC= NaCl. -1=0%$^w/_v$ 0=5%$^w/_v$ 1=10%$^w/_v$.*

Figure 4.4*b* demonstrated that a concentration of $CaCl_2$ above 5%$^w/_v$ lowered the energy absorbed and that a 10%$^w/_v$ $CaCl_2$ significantly diminished the ability of the PLGA scaffolds to absorb energy. Furthermore, Figure 4.4c depicts that the

concentration of $CaCl_2$ had a minor effect on the deformability modulus of the PLGA scaffolds, whereas an increase in $AlCl_3$ concentrations largely increased the deformability modulus of the PLGA scaffolds. The following 3-dimensional surface plots depict each of the responses (physicomechanical properties) resulting from changes in the independent formulation variables.

### *4.4.5 Determination of the Main and Interactions Effects on the Various Responses*

The main and interaction effects of the salt type and concentration and their influence on the physicomechanical properties of PLGA are demonstrated in Figure 4.5. The plots of main and interaction effects were run to provide a visual authentication of the significant variables on the resilience, energy absorbed, and deformability modulus model terms. The effects on the responses were found to be attributable to the main effects (i.e. the salts) as well as other interactions such as the polymeric substrate, solvent, water volume, and salting-out reaction time up to the last variable interactions.

The degree of interactions was observed to rise exponentially with the number of factors. Digression from the centre-point designated a change in response over the tested range. Visually, the discrepancies in the mean values of the plot are the least squares estimate for the effect. Huge discrepancies indicated by higher gradients as in Figure 4.5*a*, *c*, *d*, and *f* signified important variables while diminutive discrepancies indicated by lower gradients signified trivial variables in a given plot. Parallel plots as in Figure 4.5*b* and *e* implied minimal or no interaction of the independent formulation variable.

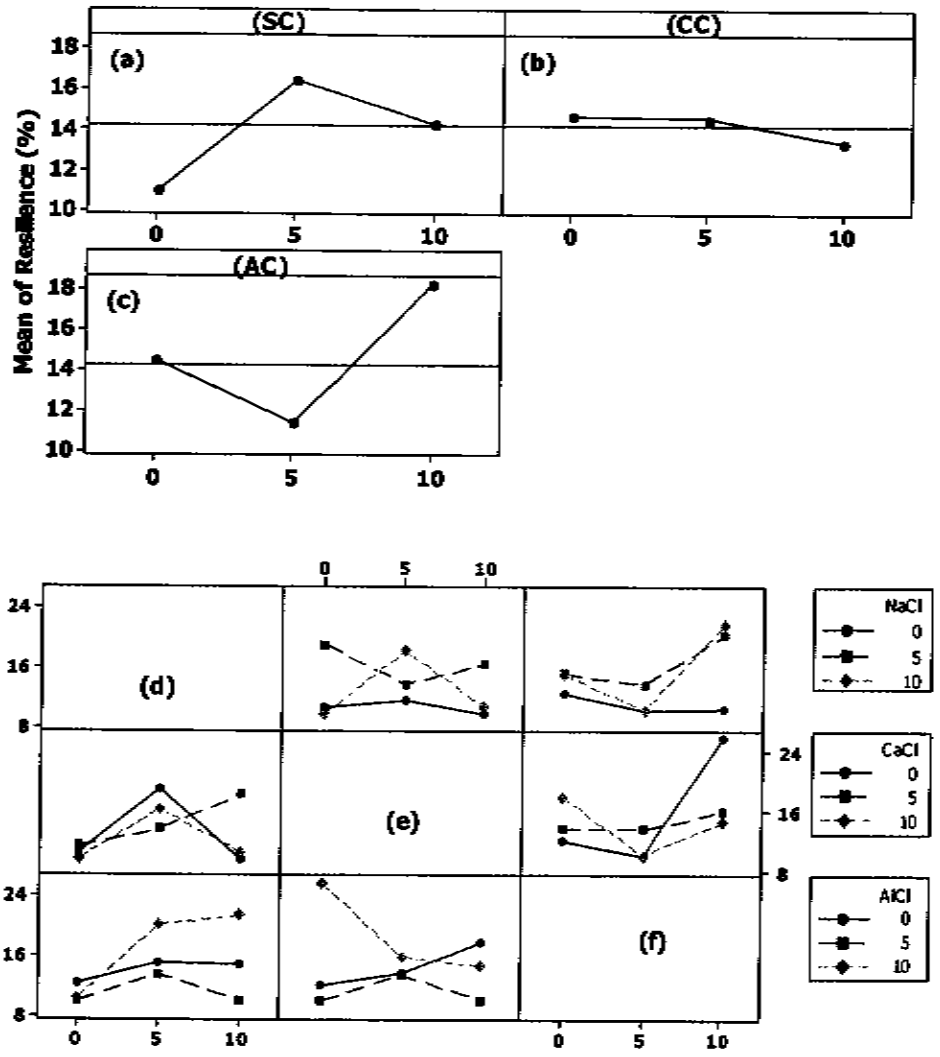


**Figure 4.5.** Typical profiles used to construe the main and interactions effects of NaCl (a) and (d); $CaCl_2$ (b) and (e); $AlCl_3$ (c) and (f) for resilience in the presence of a combination of parameters.

As demonstrated in Figure 4.5, the type and concentration of salt played a vital role in the nature and extent of PLGA modification. In Figure 4.5*c* NaCl, a monovalent salt had the greatest effect on resilience with optimal resilience experienced at 5%$^{w}/_{v}$. The divalent salt $CaCl_2$ had a minor effect on resilience, regardless of the change in concentrations. It was also observed that the resilience increased with the

increase in concentration of the trivalent salt $AlCl_3$ from 5%$^{w}/_{v}$. A similar correlation could be seen from Figure 4.3 and Figure 4.4.

These observed transitions in resilience can be explained as a contribution from a combination of several effects such as variations of the water molecule structure present in the matrix hydration sheath as well as the adjustments of the interactions between the PLGA and solvent due to the presence of various salts.

### *4.4.6 Correlation between the Experimental and Predicted (Fitted) Responses Employing a Quadratic Model*

Figure 4.6 depicts the close correlation between the experimental and fitted values for the dependent formulation variables, namely, resilience, energy absorbed, and deformability modulus. No significant differences were noted between the experimental and fitted values ($p>0.05$). This therefore, indicated that the Box-Behnken design provided a suitable statistical approach to evaluate the effects of various salts on modifying native PLGA into salted-out PLGA scaffolds.

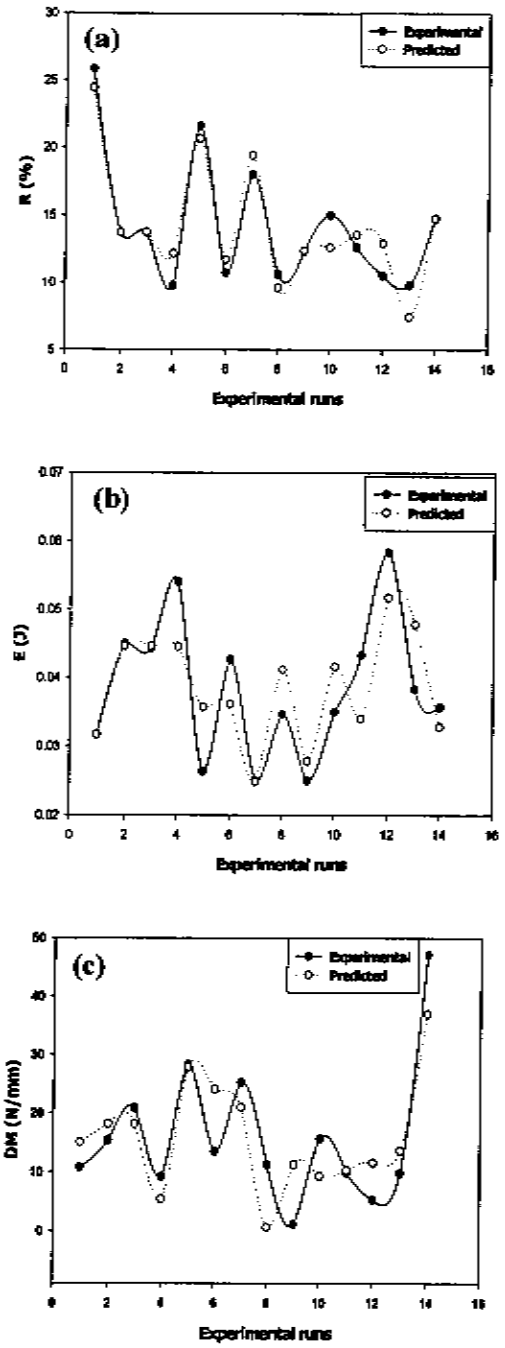


**Figure 4.6.** Profiles demonstrating the correlation between experimental and predicted (fitted) response values. *R=Resilience; E=Energy absorbed; DM= Deformability modulus.*

### 4.4.7 Assessment of the Polymer-Salt Interactions and Polymeric Structural Transitions

As observed in the FTIR profiles depicted in Figure 4.7, the functional groups of PLGA involved in interactions with the salts were similar. However, the degree and extent of these bond vibrations at finger-print regions varied. This implied that the polymer-salt interaction in solution was clearly influenced by the molecular structure of the salt as well as the chemical backbone of PLGA that resulted in the diverse morphological, physicochemical, and physicomechanical transitions demonstrated by the PLGA scaffolds.

During salting-out and subsequent cross-linking the salts ionized in water and reacted with the δ, π, σ, C-O and H-groups, to form hydrogen, ether bonds and salt-oxygen bonds between the PLGA chains. This resulted in cross-linking of the lactide-glycolide units within the PLGA molecular structure. Hydrogen, ether and ion-oxygen bonds were formed by the salts between free pendant carbonyl groups of PLGA into resonance stabilized bonds. This was demonstrated by the prominent vibrational increase in the frequency ranges of 1180-1300 $cm^{-1}$ (COC), 3200-3700 $cm^{-1}$ (OH stretching), 1600-1900 $cm^{-1}$ (CO) and the synchronous decrease in the C=O groups (bending) vibration intensities in the range of 1530-2500 $cm^{-1}$.

The intensities of transmittance of aliphatic ester bonds present in PLGA were also decreased. Furthermore, cross-links formed by the non-uniform length of polymeric chains resulted in a 3-dimensional dense network that caused further vibrational intensities (Figure 4.7).

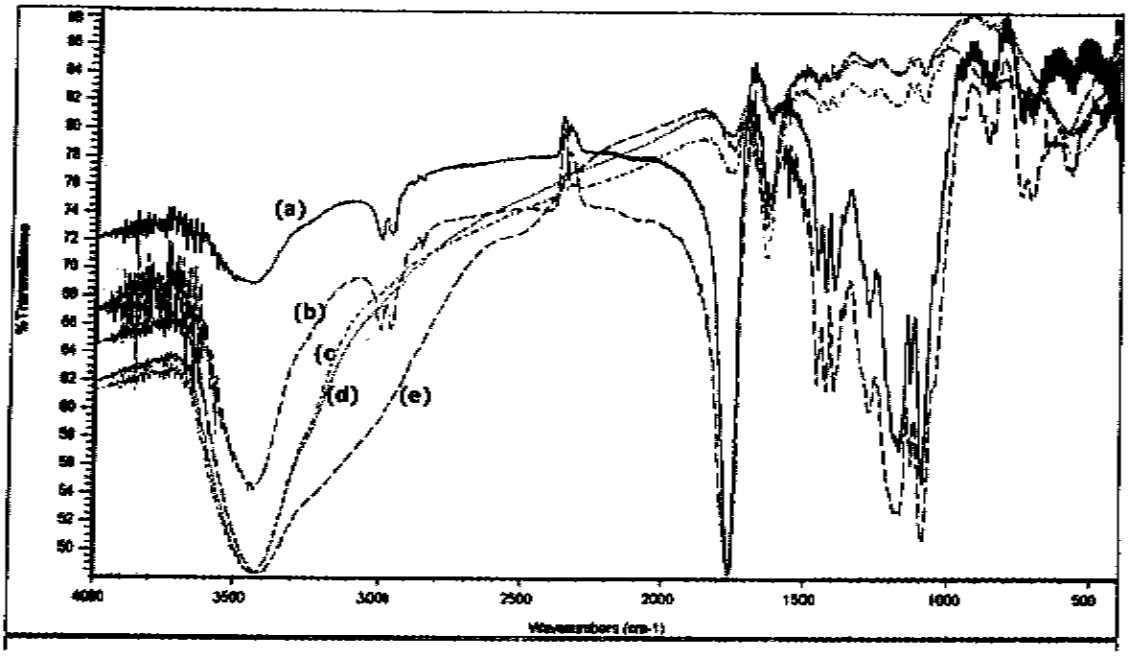


**Figure 4.7** Five superimposed FTIR profiles depicting transitions from native PLGA to salted-out PLGA scaffolds. (a) = Native PLGA, (b)-(e) = PLGA salted-out with NaCl, $CaCl_2$, $AlCl_3$ and a combination of NaCl + $CaCl_2$ + $AlCl_3$ respectively.

### *4.4.8 Thermal Transitions within the PLGA Scaffolds*

Figure 4.8 demonstrates the enthalpy changes due to various polymer-salt interactions. During salting-out of PLGA, the enthalpy of the PLGA scaffolds was enhanced by the increase in steric strain attributable to a gain of electron energy. Furthermore, enthalpy changes also occurred as a result of bond formation that increased the bond-energy of the system and resonance stabilization thereby increasing the internal energy and enthalpy of the PLGA scaffolds. Furthermore, the steric strain caused by bond stretching, bond-angle deformation, and polymer-salt interactions increased the internal energy and enthalpy of the system. As molecules gained sufficient mobility to initiate the cross-linking reaction exothermic changes

occurred in the temperature range of 40-47°C which essentially described the glass transition point.

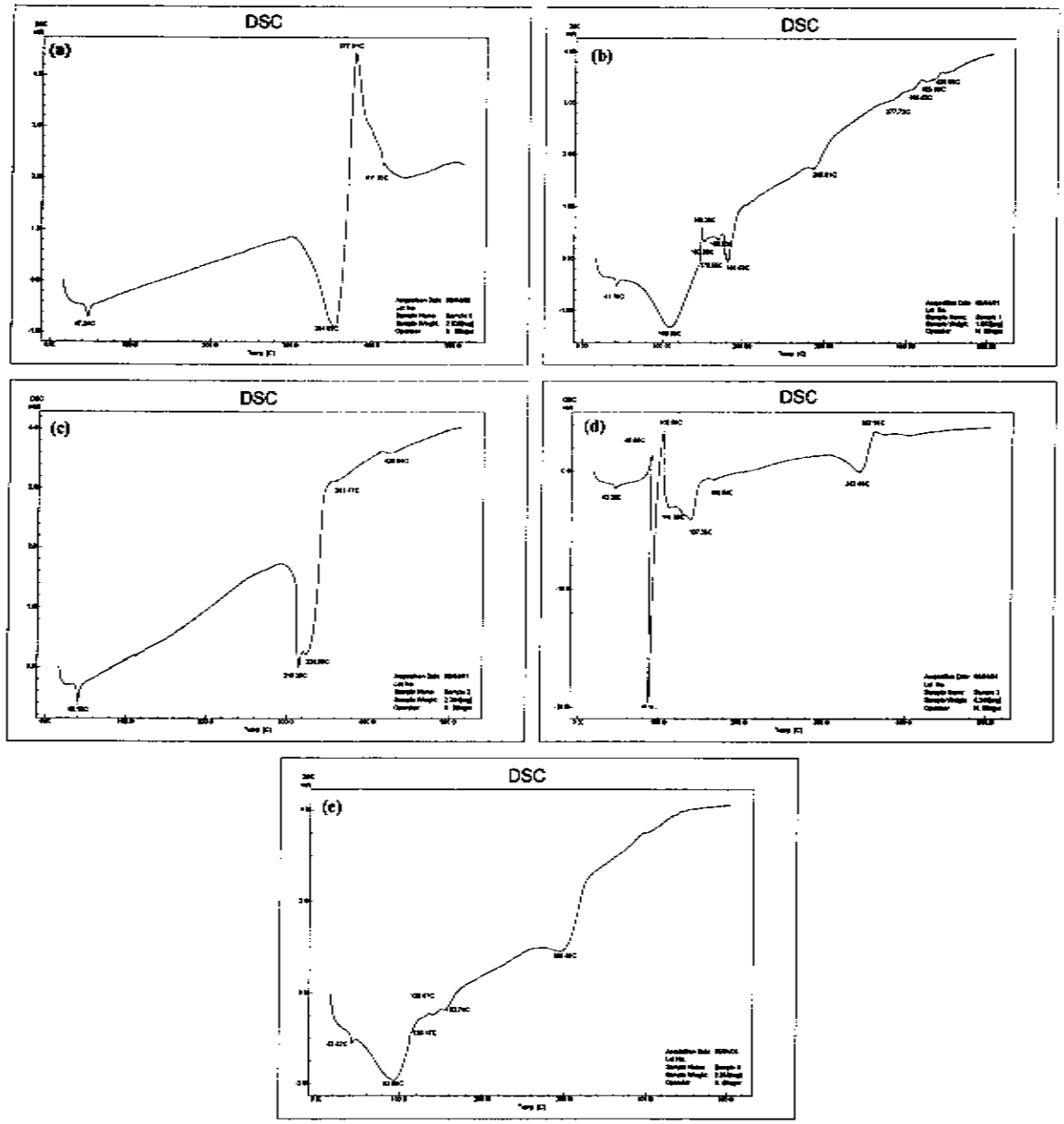


**Figure 4.8.** Differential Scanning Calorimetry (DSC) profiles of native and salted-out PLGA scaffolds demonstrating thermal transitions of (a) native PLGA, (b) PLGA salted-out with NaCl, (c) $CaCl_2$, (d) $AlCl_3$, and (e) a combination of NaCl, $CaCl_2$, and $AlCl_3$.

Table 4.3 lists the significant parameters obtained from analysis of the DSC profiles. In Figure 4.8*a-e* a step transition from glass to rubbery state on the heating cycle was clearly observed as sharp peaks at 47.24, 41.79, 40.19, 43.35 and 42.82°C respectively. The melting point range of PLGA scaffolds was 140-160$^0$C which was a significant reduction from native PLGA that has a melting point range of 280-300$^0$C. Re-crystallization and further decomposition of the polymeric-salt complex took place between 410-430°C.

***Table 4.5.*** *Thermal parameters of native and salted-out PLGA employing DSC*

| Formulation | Tg$^0$C | mp$^0$C | Tc$^0$C | Td$^0$C |
|---|---|---|---|---|
| Native PLGA | 47.24 | 280-300 | 354.85 | 411.65 |
| B | 41.79 | 148.30 | 285.61 | 428.05 |
| C | 40.19 | 280.00 | 315.30 | 426.94 |
| D | 43.35 | 166.54 | 343.04 | 420.06 |
| E | 42.82 | 270.10 | 293.85 | 420.00 |

*Tg =Glass transition temperature; mp =Melting point; Tc =Re-crystallization temperature; Td =Degradation temperature*

Depending on the type of salt employed, water can be trapped within the polymeric matrix and thus depress the $T_g$. The size of ions ($Al^{3+} < Na^+ < Ca^{2+}$) determined the degree of $T_g$ depression. Kelly and co-workers (1987) reported that a significant change in $T_g$ is observed with a 10% increase or decrease in the water content within the polymeric matrix. Thus the dynamic activity of PLGA chains may be restricted by confines of water molecules within the matrix. The large ionic radius of $Ca^{2+}$ led to an increase in the number of voids within the scaffold utilized by water molecules.

Conversely, $Na^+$ and $Al^{3+}$ ions decreased the number of voids. Hence PLGA scaffolds salted-out with $CaCl_2$ had a lower $T_g$ of 40.19°C. Studies by Paulaitis and co-workers (2004) have yielded verification on the dependence of polymeric hydration free energy on the solute size and shape. Moreover, work done by Bernazzani and co-workers (2003) demonstrated that precipitation of polymers from dilute solutions would depress the $T_g$ which may be attributed to the cross-link induced shorter and free chain ends that disarray the crystallinity of the matrix. This was consistent in the findings of this study as well.

### 4.5. Concluding Remarks

The salting-out and subsequent cross-linking approaches applied in the study in order to modify the physicochemical and the physicomechanical properties of native PLGA displayed significant potential. The resulting cross-linked PLGA scaffolds exhibited superior structural integrity as determined by parameters such as resilience, energy of absorption and deformability moduli which contributed to the overall robustness and level of porosity of the PLGA scaffolds making it a favourable candidate for controlled drug delivery.

The close correlation between the experimental and predicted (fitted) response values demonstrated the reliability of the selected statistical design for experimental optimisation. The monovalant, divalent and trivalent ionic salts employed in the study proved to be suitable in transforming the structure of native PLGA into a modified PLGA scaffold with superior physicomechanical properties. These superior properties were confirmed by textural profile analysis, SEM, DSC and FTIR studies. In general, the degree of bond formation in the PLGA backbone demonstrated by

vibrational intensity transitions from FTIR studies, in combination with the newly formed hydrolytically degradable PLGA cross-links present a possible application of the PLGA scaffolds in rate-modulated drug delivery.

This study has also demonstrated that salting-out and subsequent cross-linking of PLGA can significantly modify the physicochemical and the physicomechanical properties of native PLGA into a novel scaffold with superior structural integrity that show potential to be used ton control the rate of drug release as a result of strong bonds formed between the drug and PLGA during cross-linking ultimately leading to zero-order release kinetics. The following study in Chapter Five, is to identify the *in vitro* dissolution and drug release characteristics of the novel PLGA.

# CHAPTER FIVE

## MODEL DRUG: MELATONIN (WATER INSOLUBLE)

## *IN VITRO* DRUG RELEASE STUDIES OF MELATONIN-LOADED PLGA SCAFFOLDS

### 5.1 Introduction

Melatonin is a potent model drug that would benefit from a localized drug depot system prior to being released at its site of action, as it has a short half-life ($t_{1/2}$), 32-40 minutes, and a high first pass metabolism (Challa et al., 2005). One successful approach to control the release of such drugs is to synthesize a polymer with more desirable properties through cross-linking the polymer with a biocompatible salt.

Hence, the thermoplastic biodegradable PLGA scaffold was prepared and characterized in Chapters Two, Three and Four, in order to explore the *in vitro* release of melatonin from the cross-linked PLGA scaffold in this section of the study. The objective of the present and the subsequent studies is therefore, to assess the PLGA scaffolds employing *in vitro* drug release studies in order to optimize the formulation for application in the delivery of melatonin to the brain.

Controlled drug delivery technology signifies one of the frontier areas of pharmaceutical science that engage multidisciplinary contributions to clinical medicine. These novel drug delivery systems are of key significance to the implementation of present-day therapeutic treatment, which accentuates drug effectiveness and patient compliance. The desirable features of controlled release systems are the ability to sustain the bioactive concentration in the physiological

medium, at a desired quantity, warrant control of the release rate and prolong the duration of action of the bioactive agent (Langer and Wise, 1984; Siepmann and Peppas, 2001). Substantial surveys by Kydonieus (1992) and Park (1997) identified three main types of drug release systems, namely passive pre-programmed, active pre-programmed and active self-programmed systems illustrated in Figure 5.1. However, some controlled release systems may behave slightly different from the norm. The PLGA scaffold formulated in the study is envisaged to behave in a manner that is mostly passive pre-programmed system.

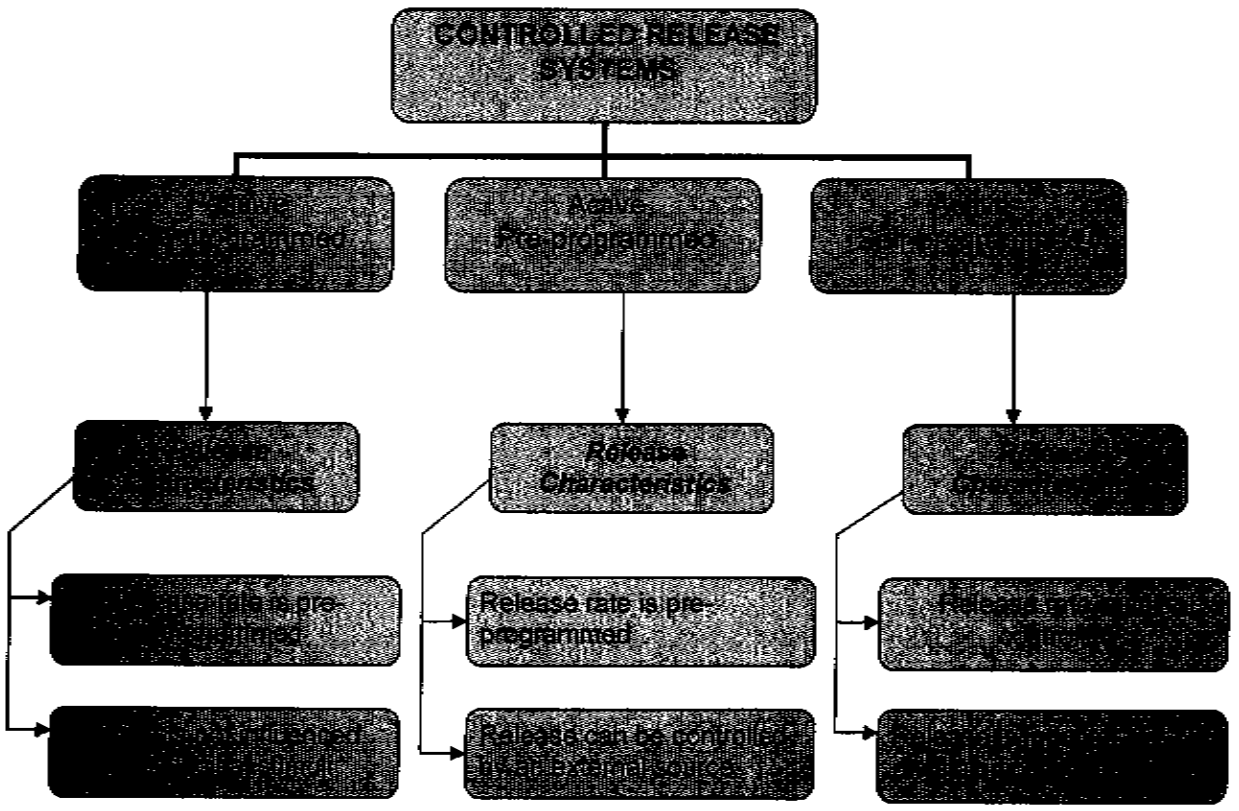


**Figure 5.1.** Flow diagram displaying three main types of controlled drug release systems (Source: adapted from Kydonieus (1992) and Park (1997).

In order to understand the effect of polymer modification on dissolution and controlled drug release, the theory of dissolution needs to be considered. Dissolution studies remain the most frequently used tool in the development and characterization processes of controlled release devices. During the formulation of pharmaceutical devices, *in vitro* dissolution testing becomes the major tool of evaluating the best formulation and the bioavailability of the drug (Dave et al., 2004).

Dissolution is defined by Amiji and Sandman, 2003, as the process by which a solid solute with relatively low solubility enters into a solution in the presence of a solvent. Whereas the dissolution rate is defined as the quantity of active ingredient in a solid dosage form dissolved per unit time, under standardized conditions of liquid/solid interface, temperature and media composition.

The role of dissolution studies in pharmaceutical science include:

i. Screening formulations during development;
ii. The assessment of batch to batch quality, where the performance specifications of the device depends on its dissolution;
iii. To provide process control and quality assurance;
iv. To control bioavailability and avoid the possible risk of toxicity that result from *in vivo* dose dumping;
v. To characterize or compare different batches of drug substances using the dissolution rate;
vi. To assess the need for further bioequivalence (BE) studies relative to minor post-approval changes (Almeida et al., 2006; Cho et al., 2006; Kalantzi et al.,

2006; Khan et al., 2006; Panchagnula et al., 2006; Wei and Lobenberg, 2006; Yu et al., 2006).

Dissolution and drug release studies are therefore, the key predictors of a drug delivery device's performance *in vitro* and *in vivo*. The efficient development of *in vitro* models of the physiological media is fundamental to the applications of the device *in vivo*, as this is able to mimic specific parameters that include the temperature and pH of physiological fluids, as well as the drug release rate. In addition, *in vitro* dissolution studies should be able to detect the least variations in formulations that may affect *in vivo* performance of the device.

In this section, salted-out and subsequently cross-linked melatonin-loaded PLGA scaffolds were evaluated with respect to their ability to release melatonin in an active pre-programmed manner as illustrated in Figure 5.1, and the influence of the salt employed in the modification process was also explored. In addition, the drug entrapment efficiency (DEE) into the PLGA scaffold, the mean dissolution time (MDT) and the drug release kinetics ($k$) were determined and optimized. During dissolution of PLGA, degradation can be varied between weeks and months depending on the design of the polymer to match its application.

In physiological media, PLGA undergoes chain cleavage, the initial step in its degradation process followed by a decrease in molecular mass and matrix erosion, as outlined in Chapter Three. In salted-out and cross-linked OH-polyesters, the ability to predictively control the process of dissolution and drug release lies in the full understanding of the drug, the incorporated salt and the polymeric properties

(Hite et al., 2003). Thus, one may envisage the interactio ns between these variables, and how each of them affects the rate of drug release.

During dissolution, the principal mechanisms by which bioactives are released from a device include diffusion, swelling, erosion and degradation. The drug may be released from drug delivery devices by diffusion through fluid-filled pores within the polymeric matrix. In the case of drugs with higher molecular masses, polymer erosion becomes a key causal factor to drug release (Kiortsis et al., 2005).

Diffusion is when a drug passes through the pores of a polymeric matrix or/and between the polymer chain. Drugs with lower molecular masses such as melatonin can easily escape from the device by diffusion. Amid the basic features required for dissolution, a polymer should have inherent physicochemical and physicomechanical properties that promote the attainment of retarded swelling and erosion as well as complete dissolution of the polymer at the end of drug release.

Alternatively, a programmed release system is sought, for which swelling and erosion remain the prime factors in controlling drug release. The ideal polymer would permit these processes to operate synchronously, thereby allowing a balance between the key processes of swelling, erosion and dissolution.

Furthermore, dissolution and drug release from a salted-out/cross-linked device will be affected by the physicochemical and the physicomechanical properties of the modified polymer, the salts incorporated, the fluid within which it is immersed, as well as upon environmental factors such as, temperature, pressure, and the pH of the

solution. Studies by several researchers have revealed that even though salts may retard polymeric disentanglement and slow the degradation of polymers, they can however, accelerate the release of drugs and increase the initial burst effect, depending on the drug solubility (Abbrent et al., 2000; Pillay and Fassihi, 2000; Pillay and Fassihi, 2001). Salts achieve this through their contribution by creating a contractible micro-environment within the matrix, whereby pH is then mediated by the pKa of the salt, thus either enhancing or suppressing the solubility of the polymer. As the matrix hydrates, the salts and the polymer compete for the water of hydration, which slows the dissolution of the polymer and retards drug release. Thus, in such systems, degradation of the PLGA device and the drug release will vary according to the type of salts loaded in the polymeric matrix and the drug itself (Bae, 2003).

In PLGA devices, the release of a drug may take place by:

i. Diffusion of the drug through aqueous pores that are generated during degradation of the polymer.
ii. Another mechanism involves the leaching of drug from bioactive domains at or near the surface of the device.
iii. In addition, the degradation of the polyester may decrease the rigidity of polymeric chains, which could compromise the pore structure of the matrix and facilitate the release of drug. The hydrolytic chain scission of PLGA which is auto-catalyzed by its carboxylic acid end-groups could cause the commencement of drug release by increasing the degree of polymeric hydration and decreasing the glass transition temperature (Shah et al., 1992; Park, 1995).

### 5.2 The Use of Melatonin in Neurodegenerative Disorders

Melatonin is a pineal neurohormone with decrease levels during aging, especially in neurodegenerative patients. It is the principal hormone produced by pinealocytes of the pineal gland. It is a derivative of the amino acid tryptophan and also produced by the retina of the eye and the gastro-intestinal-tract cells, on a smaller scale.

***Table 5.1*** *The Physicochemical and the Physicomechanical Properties of the Neurohormone Melatonin*

| **PHYSICOCHEMICAL AND THE PHYSICOMECHANICAL PROPERTIES OF MELATONIN** | |
|---|---|
| Trade Name | Melatonin® |
| Chemical Name | 5-methoxy-N- acetyltryptamine |
| Empirical formula | $C_{13}H_{16}N_2O_2$ |
| Molecular mass | 232.28 g/mol |
| Bioavailability | 30-50% |
| Melting Range | 116-118°C |
| Solubility at 25°C | Low solubility in water |
| Stability in light | Photolabile |
| Atmospheric and chemical stability | Interacts with reactive oxygen and nitrogen |
| Storage | Below 20°C, air tight<br>amber container, away from light |

Melatonin is metabolized in the liver and its elimination half-life ($t_{1/2}$) is 32–40 minutes with a high first pass metabolism (Challa et al., 2005). A dosage of 3mg melatonin one hour before bedtime is usually effective for insomnia, although doses as low as 0.1 to 0.3mg daily may improve sleep. In addition, this bioactive has strong

antioxidant properties and there is evidence that it may help strengthen the immune system.

Scientists have uncovered that melatonin has the capacity to scavenge numerous free radicals that include $O^{\cdot}$,-OH, $H_2O_2^{\cdot}$ and NO, attributable to its configuration and chemical structure. Furthermore, studies have demonstrated that this neurohormone has protective effects against Aß-induced apoptosis of microglial cells in neurodegenerative diseases. These microglia-produced inflammatory and neurotoxic factors, including the cytokines and tumor necrosis factor-α (TNFα) produce free radicals that are deleterious to neurons, as mentioned in Chapter One.

### *5.2.1 Structure-Function Relationship of Melatonin as a Free Radical Scavenger in the Treatment of Neurodegenerative Disorders*

The amide and methanol side chains are significantly active scavenging chemical groups in the melatonin molecule. However, the major scavenging action can be attributable to the indole moiety due to its higher resonance stability and very low activation energy barrier towards free radical reactions. The N-C=O structure in the $C_3$ amide side chain is the main functional group. The carbonyl in the N-C=O is the key group for melatonin to scavenge the second reactive free radical species. The nitrogen in the N-C=O structure is necessary for melatonin to form the new five membered ring after the drug's interaction with a reactive species. The methoxy group in $C_5$ prevents melatonin from exhibiting pro-oxidative activity (Kato et al., 2007; Yasuo et al., 2007).

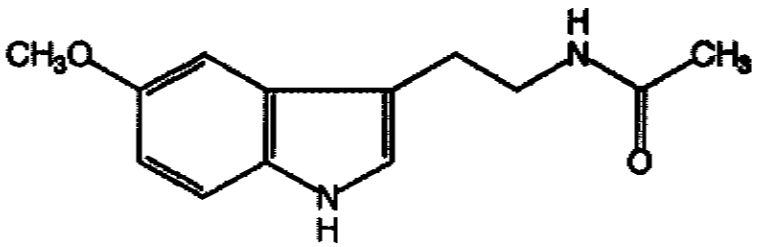


**Figure 5.2.** Chemical structure of melatonin: *(5-methoxy-N-acetyltryptamine)* (*Source: adapted from* Lehnig and Kirsch, 2007).

Unlike classical antioxidants, melatonin is devoid of pro-oxidative activity and all known intermediates generated by the interaction of melatonin with reactive species are also free radical scavengers. This phenomenon is defined as the free radical scavenging cascade reaction of the melatonin class. Due to this cascade, one melatonin molecule has the potential to scavenge up to 4 or more free radicals. This makes the drug very efficient as an antioxidant in neurodegenerative disorders. Melatonin is a good candidate for use in neurodegenerative disorders due to its anti-oxidative and anti-inflammatory properties (D'Agostino et al., 2007; Gulati et al., 2007 Liu et al., 2007; Paredes et al., 2007)

However, it has a very short half-life and is promptly metabolized to 6-sulphatoxy melatonin (6-STMT) after oral administration. Due to the first pass metabolism of melatonin, it is not available in therapeutic amounts to cross the blood-brain barrier (Kikwai et al., 2002). Therefore, the objective of this study was to develop a novel implant employing the PLGA scaffolds loaded with melatonin in the treatment of neurodegenerative disorders. The *in vitro* drug release studies and optimization of

melatonin-loaded PLGA scaffold was performed in order to pursue its use as a drug delivery implant for treatment of neurodegenerative diseases.

### 5.3 Developing the Experimental Design

The independent formulation variables may affect DEE, MDT and k expression profiles. It is therefore recommended that an experimental design be applied. In the study, a 3 factor, 3 level randomized Box-Behnken statistical design was constructed in order to model the number of experiments needed for formulation optimisation and to establish the main and interaction effects of the independent formulation variables on the of the DEE, MDT and k of the PLGA scaffolds, using MINITAB®, (V14, Minitab, USA).

### 5.4 Determination of the Drug Entrapment Efficiency (DEE) of the PLGA Scaffold

Several parameters, such as, the type and quantity of model drug, the type and concentration of salt, along with the method by which the drug is loaded into the device, may influence the DEE of a polymeric device (Peltonen et al., 2004). By evaluating the effects of formulation parameters on the DEE of the hydrophobic PLGA scaffold, one can improve the percentage of drug particles that can be entrapped by the device during synthesis, thus affording more higher and consistent drug-loading.

Although PLGA has been investigated for the controlled release of drugs, most studies have involved nano- and microparticle formulations and the efficiency of the

methods in encapsulating drug within these particles. The entrapment of drug particles in a porous PLGA scaffold has not been adequately ventured. DEE of hydrophobic drugs in PLGA nano- and micro-particles has been found to be less challenging than that of hydrophilic drugs, due to the lack of affinity between the hydrophilic drug substances and the hydrophobic polymer (Barichello et al., 1999; Govender et al., 1999).

Furthermore, during salting-out, if the interactions between the drug and polymer are weak, the drug tends to migrate from the polymeric organic phase to the aqueous phase thus becoming excluded from the polymeric device. In this study, the model drug, melatonin has low water solubility (3.17+/- 0.06 mg/mL) and easily dissolves in the solvent used to dissolve PLGA (Kikwai et al., 2002). This, therefore, facilitated blending of the polymer and the drug solutions before and during salting-out. One of the aims of this study was also to increase the melatonin entrapment efficiency into the PLGA scaffold. The DEE was explored by changing the salt type and concentration used in the salting-out and subsequent cross-linking of PLGA.

### 5.5 Optimization of the Drug Entrapment Efficiency, Mean Dissolution Time and Drug Release Kinetics of the PLGA Scaffold

Optimization techniques allow for the investigation of the effects of process parameters concurrently, without having to examine all possible combinations of the factors involved. The application of a statistically designed experiment for optimization techniques allows one to investigate associations between the interacting formulation variables. Statistical software is employed to perform

extensive analysis of the observed outputs and their rates of change as the inputs are varied to guide the selection of new trial values (Aslan et al., 2006).The most common technique used for solving constrained optimization problems, is the ANOVA, employing the Taguchi approach (Jadoun et al., 2006). In this study, the drug entrapment efficiency (DEE), the mean dissolution time (MDT) and the quantity of drug released as a function of time were validated utilising the Analysis of variance (ANOVA) (Minitab® Statistical Software, v14, Minitab, USA).

### 5.6 Kinetic Modeling to Determine the Drug Release Mechanism from the PLGA Scaffold

Several mechanisms have been elucidated to describe drug release from polymeric systems including diffusion, swelling, and erosion- controlled release. In order to characterize the drug release mode from the PLGA scaffold, the experimental data was fitted to the Peppas (Korsemeyer et al., 1985; Peppas, 1985; Harland et al., 1988), Higuchi (Higuchi, 1961; Higuchi, 1963), Fickian diffusion and matrix relaxation (Peppas, 1985) and the Hopfenberg equations, by the application of WinNonlin® software V5.1 (Pharsight®, U.S.A.). Kinetics of drug release, namely, swelling and erosion were analyzed with relevant mathematical and statistical models in order to confirm the mechanistic operation of the PLGA scaffolds. The development of suitable kinetic and mathematical models to predict drug delivery is a significant and fundamental activity during the design of controlled drug delivery systems (De et al., 2002).

## 5.7 Materials and Methods

### *5.7.1 Materials*

PLGA was purchased from Boehringer Ingelheim Pharma (Ingelheim, Germany) (Resomer® RG504 50:50; $M_w$ 48,000; i.v. 0.48-0.60dl/g). Acetone was used as a solvent, and analytical grades of sodium chloride (NaCl), calcium chloride ($CaCl_2$), (Rochelle Chemicals, South Africa) and aluminium chloride ($AlCl_3$) (Merck, Darmstadt, Germany) were used as the ionic salts. Disodium hydrogen orthophosphate, ($Na_2HPO_4$), and potassium dihydrogen phosphate ($KH_2PO_4$) were purchased from Saarchem (Pty) Ltd., South Africa. Model drug, melatonin was obtained from Sigma-Aldrich Co., Germany. The apparatus used for the *in vitro* drug release studies was a closed compartment system. A thermostated rotating shakerbath (Labex, Stuart SBS40®, Gauteng, South Africa) was set at 37.0 ± 0.5°C.

### *5.7.2 Building the experimental design*

A 3 factor, 3 level randomized Box-Behnken statistical design was employed in order to model the number of experiments needed for formulation optimisation and to establish the main and interaction effects of the independent formulation variables on the physicochemical and physicomechanical properties of the PLGA scaffolds using MINITAB®, (V14, Minitab, USA). In this design 3 factors were evaluated, each at 3 levels, and experimental trials were performed at all 14 possible combinations. The amounts of NaCl, $CaCl_2$ and $AlCl_3$ were selected as independent formulation variables. The DEE, MDT and *k*, were selected as dependent formulation variables. A statistical model incorporating interactive and polynomial terms was utilized to evaluate the response as conducted in Chapter Four of the study.

***Table 5.2.*** *Factor Levels of the Independent Formulation Variables*

| Variables | Factor Level | | | Units |
|---|---|---|---|---|
| | Low | Middle | Upper | |
| NaCl | 0 | 5 | 10 | $\%\ ^{w}/_{v}$ |
| $CaCl_2$ | 0 | 5 | 10 | $\%\ ^{w}/_{v}$ |
| $AlCl_3$ | 0 | 5 | 10 | $\%\ ^{w}/_{v}$ |
| Melatonin* | 10 | 10 | 10 | mg |

**Melatonin levels were kept constant at 10mg*

### *5.7.3 Preparation of the PLGA Scaffolds*

PLGA scaffolds were prepared by salting-out and subsequent cross-linking using a combination of acetone and ionic salts in accordance with a Box-Behnken design template outlined in Table 4.1 Chapter Four. Fourteen polymeric solutions comprising 0.4g of PLGA and 10 mg melatonin dissolved in 15mL of acetone were prepared. The cross-linking solutions comprising 75mL of either $0\ ^{w}/_{v}$, $5\ ^{w}/_{v}$ or $10\%\ ^{w}/_{v}$ of either NaCl, $CaCl_2$ or $AlCl_3$ was added to the polymeric solution and agitated for a period of 30 minutes. The resultant PLGA scaffolds were removed from the cross-linking solution washed thrice with 500mL deionised water and dried to constant mass at room temperature. Each PLGA scaffold was stored for 48 hours for equilibration prior to physicochemical and physicomechanical evaluation.

### *5.7.4 Preparation of a Calibration Curve for the Spectrophotometric Determination of Melatonin Release from the PLGA Scaffold*

Both the accuracy and precision of spectrophotometric measurements is dependent, in part, upon the calibration technique used. A calibration curve of the analytical signal (the instrument or detector response) as a function of analyte concentration

was plotted in order to determine the concentration of melatonin released from each PLGA scaffold at each time interval. It was obtained by measuring the signal from a series of standards of known concentrations.

The Lambert Beer law describes a relationship between concentration and absorption, the law states that the the absorbance (*A*) of an absorbing species in solution is directly proportional to the pathlength (*b*) through the solution and the concentration (*c*) of the absorbing species. Thus, the higher the concentration of the absorbing substance is, the higher is the absorbance. In accordance with Lambert Beer law, the concentration of a melatonin in solution was determined from its measured absorbance. A calibration curve of absorbance, measured spectrophotometrically, versus concentration was constructed for melatonin in PBS pH 7.4 at the 278.2nm absorption peak. In order to determine the best-fit straight line, linear regression analysis was used. From the equation y = mx + b we substituted in the y value (response) and we solved for x.

### *5.7.5 Drug Entrapment Efficiency of the PLGA Scaffolds*

DEE studies were performed by immersing each scaffold in 100mL acetone to effect complete dissolution of the scaffold. Thereafter, melatonin content was determined in triplicate using UV-spectroscopy at 278nm. The DEE percentage was then calculated utilizing Equation 5.8.

$$DEE\% = \frac{Mass\ of\ drug\ in\ scaffold}{Mass\ of\ drug\ loaded\ in\ formulation} \times 100 \qquad \textit{Equation 5.8}$$

### *5.7.6 In Vitro Drug Release from the PLGA Scaffolds*

Drug release studies were conducted in 100mL phosphate buffered saline (PBS) (pH 7.4; 37$^0$C) at 50 rpm. Melatonin assays were performed with UV-spectroscopy (278 nm) (SPECORD 40, Jena, Germany). The dissolution data was subjected to a model-independent analysis known as the time-point approach. Briefly, the mean dissolution time set at 30 days ($MDT_{30}$) for each formulation was calculated. The application of the mean dissolution time provided a more precise analysis of the drug release performance and a more accurate comparison of several dissolution data sets. Equation 5.9 was employed in this regard.

### *5.7.7 Statistical Optimization*

Analysis of variance (ANOVA) (Minitab® Statistical Software, v14, Minitab, USA) was performed on the data presented in Table 5.2 utilising Institution of a model-independent approach to optimize the PLGA scaffold formulation. The independent formulation variables were the type and concentration of salts employed in the salting-out and cross-linking of the polymer. The dependant formulation variables were the DEE, MDT and the release constant ($k$). Statistical optimization was therefore employed to ascertain the ideal PLGA scaffold with the desired physicochemical and physicomechanical properties capable of attaining optimum DEE, MDT and $k$.

### *5.7.8 Kinetic Models Employed to Elucidate the Drug Release Mechanism from the PLGA scaffolds*

Drug diffusion, erosion and polymer chain relaxation are the core parameters in determining drug delivery from the PLGA scaffold matrices. Models such as the

Power Law and its variants, Hopfenberg, Swelling Interface Number and Deborah Number may be applied to experimental data to predict such parameters. The purpose of this section of study was to explicate the principal drug release mechanisms from the melatonin-loaded PLGA scaffolds and to predict the time-dependence of fluid infiltration and drug release. *In vitro* drug release data of the PLGA scaffold formulations were fitted into the following phenomenological mathematical expressions.

(a) The Power Law Equation

Drug release mechanisms are complex phenomena. In order to characterize the drug release mode from the PLGA scaffold, the experimental data was fitted to the kinetic models. The mathematical expressions employed to describe the drug release kinetics from the scaffold include the Power Law equation, also known as the Peppas equation (Equation 5.1):

$M_t / M_\infty = kt^n$ *Equation 5.1*

Where:

-$M_t$ is the quantity of drug released at time $t$;

-$M_\infty$ is the drug loading;

$M_t / M_\infty$ is the fraction of drug released up to time $t$;

-$k$ is an experimentally determined kinetic constant and

-$n$ is an exponent that depends on the geometry of the polymeric device boundary and indicates the release mechanism (Ritger and Peppas, 1987; Karatas and Baykara, 2001).

In the case of a delay in release or lag time ($t_L$), as in a highly cross-linked polymer, the Higuchi equation (Equation 5.2) may be used.

$$M_t / M_\infty = k(t - t_L)^n \qquad \textit{Equation 5.2}$$

The Higuchi equation expresses a diffuse release mechanism.

In the case of a burst effect, $b$ (Kim and Fassihi, 1996), Equation 5.3 may be used.

$$M_t / M_\infty = kt^n + b \qquad \textit{Equation 5.3}$$

For Fickian diffusion and matrix relaxation, the expanded version of Power Law equation is used, as illustrated in Equation 5.4:

$$M_t / M_\infty = k_1 t^n + k_2 t^n \qquad \textit{Equation 5.4}$$

Where:

-$k_1$ is the Fickian kinetic constant;

-$k_2$ is the relaxation/dissolution rate constant and

-$n$ is the release exponent, with $n$=1, 2, 3 for a slab, cylinder or sphere respectively.

(b) The Hopfenberg Model

The erosional behaviour of the cross-linked PLGA scaffold can be analyzed with the Hofpenberg model (Hopfenberg, 1976), which allows for the differentiation between the diffusional and relaxational contributions during solvent penetration or sorption in polymers. This model also known as Hixon-Crowell equation was developed for polymers in the form of slabs, cylinders, or spheres, which exhibit heterogeneous erosion (Equation 5.5).

$$M_t/M_\infty = 1 - (1 - k_1 t)^n \qquad \textit{Equation 5.5}$$

Where,

-$k_1 = k_0/C_0 r_0$;

-$k_0$ is the erosion rate constant;

-$C_0$ is the uniform initial concentration of drug in the polymeric matrix and

-$r_0$ is the initial radius for a sphere or cylinder or the half-thickness of a slab.

The Hopfenberg model assumes that time-dependent diffusional resistances, such as drug particle size, do not affect the release kinetics. In addition, this model indicates an erosion-depended release mechanism.

(c) The Swelling Interface Number

The Swelling Interface Number is generally computed to determine the swelling and release behaviour. Franson and Peppas, 1983, studied the physical conditions that

influence the kinetics of drug release from swellable matrices and introduced the Swelling Interface Number *Sw* (Equation 5.6).

$$Sw = v.\ \delta(t)/D \qquad \textit{Equation 5.6}$$

Where:

-*v* is the velocity of the swelling front;

-$\delta(t)$ is the time-dependent thickness of the swelling phase and

-*D* is the drug diffusion coefficient in the swollen phase.

This dimensionless number compares the mobility of the solvent front relative to drug mobility in the presence of polymer relaxation.

(d) Deborah Number (De)

Swelling of PLGA scaffolds can also be analyzed by consideration of the De value. Under normal conditions the relaxation might be 0.1 and the shear rate 100/s, and thus De = 10 (0.1 divided by 1/100). When De << 1, the polymer behaves as a purely viscous fluid while for De >> 1 the polymer behaves as an elastic solid (Rothstein and Mc Kinley, 1999; Cormier et al., 2001).

$$Deb_{release} = D/k_e(r_o - r_i) \qquad \textit{Equation 5.7}$$

Where,

*D* is the drug diffusion coefficient in a matrix;

$k_e$ is the erosion rate constant;

$r_o$ is the outer radius of the scaffold;

$r_i$ is the inner radius of the scaffold.

(e) To explore the nature of volatility of the model, the Akaike Information Criterion (AIC) and the Shwartz Bayesian Criterion (SBC) were computed. These statistics are based on the log likelihood value at the estimated vector. The AIC and SBC are functions of the log likelihood values as well as the number of free parameters in estimation. They incorporate a penalty for a large number of parameters, which gives us a bias towards more parsimonious specifications. The SBC is given by:

$$SBC = [n\text{-}2.\ ln\ L + k\ ln\ (n)/n] \qquad \textit{Equation 5.8}$$

Where,

$n$ is the number of observations, equivalently, the sample size;

$k$ is the number of free parameters to be estimated. If the estimated model is a linear regression, $k$ is the number of regreassors, including the constant; and $L$ is the maximized value of the likelihood function for the estimated model. Under the assumption that the model errors or disturbances are normally distributed, BIC becomes, Equation 5.9 is employed.

$$SBC = ln\ (RSS/n) + k\ (ln\ n/n) \qquad \textit{Equation 5.9}$$

Where, *RSS* is the residual sum of squares from the estimated model. In any given model, the one with the lower value of SBC is the one to be preferred. The SBC is a decreasing function of *RSS*, the goodness of fit, and an increasing function of *k*. The BIC penalizes free parameters more strongly than does the AIC.

### 5.8 Results and Discussion

The regression coefficient, $R^2$=0.9983 for the calibration curve generated for melatonin demonstrated linearity in phosphate buffered media (pH 7.4) at 37°C achieved over the concentration range from 0.294 to 0.932 mg/mL.

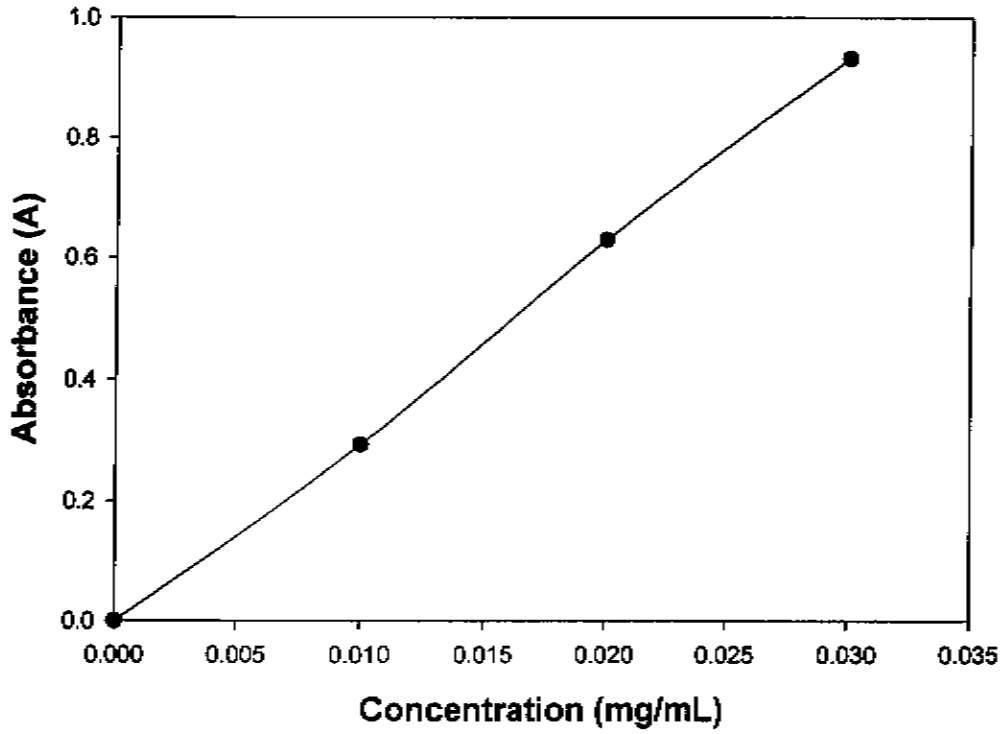


**Figure 5.3.** Melatonin calibration curve at 278.2nm in PBS (pH 7.4) (S.D. within ±0.049)

### *5.8.1 Drug Entrapment Efficiency of the PLGA Scaffold*

DEE varied between 46-90% depending on the type and concentration of the salt employed. When $CaCl_2$ was employed, an average DEE of 55% was achieved. Conversely, when NaCl and $AlCl_3$ were employed in the salting-out and cross-linking processes, an average DEE of 90% was achieved. The type of salt used during salting-out and subsequent cross-linking has been demonstrated earlier in the study to have an influence the network structure of the polymeric matrix. Chapter Four demonstrated how the physicochemical nature of the salt used in salting-out and cross-linking may influence the architecture of the PLGA scaffold matrix. This was evident in the PLGA micrographs shown in Figure 4.2. Furthermore, the nature of the micro-environment may enhance or reduce the ability of the scaffold to entrap drug particles due to the fiber structure and the pore morphology of the matrix.

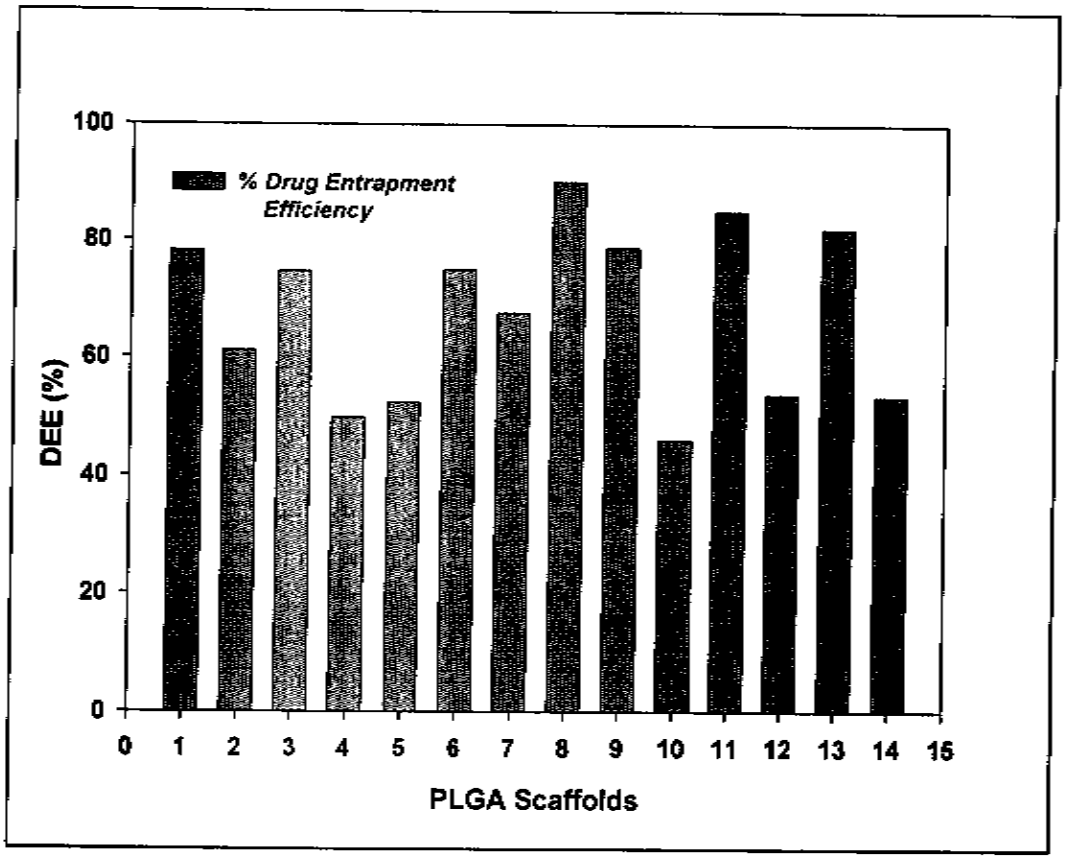


**Figure 5.4.** Plot depicting the differences in the DEE of the salted-out and cross-linked PLGA scaffolds.

The enhancement of the DEE demonstrated by these profiles in Figure 5.4 also conform to the dense surface morphology of the scaffolds as revealed in the scanning electron micrographs in Figure 4.2. NaCl and $AlCl_3$ produced fiber networks of microporous structures that maintained homogeneity of cross-linked fibers in a neuronal-like meshwork (Figure 4.2*a* to 4.2*e*), with pores and fiber diameters ranging between 0.03-1.40μm, along with fiber volumes ranging from 0.01-0.03$\mu m^3$.

The divalent salt $CaCl_2$ as demonstrated in Chapter Four produced a fibrillar composite PLGA scaffold with interconnecting channels and pores as large as 15μm and fiber volumes of 14000$\mu m^3$. In general, melatonin is a small drug molecule such that salts that tend to produce a more compact polymeric structure with minor and more uniform pores, such as NaCl and $AlCl_3$ entrapped more drug particles, whereas salts that created larger pores reduced the DEE.

### *5.8.2 Characterization of the In Vitro Drug Release from the PLGA Scaffolds*

Table 5.3 and the release profiles revealed that the scaffolds salted-out and subsequently cross-linked with NaCl and $AlCl_3$ were able to achieve up to less than 20% melatonin over a period of 30 days (Figure 5.2*c*). Whereas scaffolds salted-out and subsequently cross-linked with $CaCl_2$ had more than 75% drug released over a period of 30 days.

Scaffolds also demonstrated a mean dissolution time at 30 days ($MDT_{30}$) of 6 to 26 (Table 5.3). The lowest $MDT_{30}$ was demonstrated in scaffolds salted-out with NaCl and $AlCl_3$. Fractional drug release ($M_t/M_\infty$), and the drug release kinetics were calculated using the Power Law $M_t/M_\infty=k_0t$, where $k_0$, the kinetic constant was found to be between 0.004 and 0.038, the lower values in scaffolds salted-out with NaCl and $AlCl_3$ and higher values in scaffolds salted-out with $CaCl_2$.

**Table 5.3.** *The drug release at 30 days (%), Mean Dissolution Time $(MDT)_{30}$ and the release constant (K) of the PLGA scaffolds*

| PLGA Formulations | $DR_{30}$[a](%) | $k$[b] | $(MDT_{30})$[c] |
|---|---|---|---|
| 1 | 25.147 | 0.0356 | 8.738 |
| 2 | 54.435 | 0.0322 | 14.277 |
| 3 | 23.423 | 0.0235 | 8.246 |
| 4 | 72.857 | 0.0162 | 19.078 |
| 5 | 54.631 | 0.0266 | 15.318 |
| 6 | 29.784 | 0.0155 | 11.531 |
| 7 | 38.610 | 0.0294 | 13.821 |
| 8 | 17.982 | 0.0116 | 8.670 |
| 9 | 24.515 | 0.0125 | 10.286 |
| 10 | 75.471 | 0.0202 | 17.179 |
| 11 | 24.911 | 0.0137 | 10.487 |
| 12 | 100.000 | 0.0120 | 28.745 |
| 13 | 20.435 | 0.0299 | 6.725 |
| 14 | 53.796 | 0.0127 | 15.382 |

[a] *Drug Release at 30 Days (%)*
[b] *Release Rate Constant*
[c] *Mean Dissolution Time at 30 Days*

In general, the melatonin release profiles of all the scaffolds displayed a biphasic melatonin release model. Firstly, an initial burst was observed, followed by a slower steady diffusional phase release. The initial burst may be attributed to the rapid release of melatonin deposited on the surface of the scaffolds. The rate of melatonin

release during the diffusional phase was influenced by the type and concentration of salt employed during salting-out and subsequent cross-linking of the scaffold.

Subsequently, all the PLGA scaffolds went through a process of erosion and degradation that resulted in the release of the drug. Melatonin molecules dispersed in the PLGA matrices were released as the polymer starts eroding and degrading. Thus this system combined the advantage of long-term constant rate drug release with biodegradability. Thus, the drug delivery kinetics of these scaffolds was multifaceted and influenced by a large number of factors, such as the type and the concentration of the salts. Swelling-erosion kinetics were manipulated in order to control the mechanism and rate of drug release through the incorporation of salts.

This study demonstrated that the different types and concentrations of salts have significant rates in controlling the rate of drug release due to the strong interactions between the drug and polymeric chains. The slow diffusion of melatonin from PLGA salted-out and subsequently cross-linked with NaCl and $AlCl_3$ PLGA occurred due to shielding and coiling of polymeric reaction sites which prevented the maintenance of the same effective collision rate at which chemical reactions are obtained between the same functional groups and the aqueous environment in polymer molecules cross-linked with other salts such as $CaCl_2$.

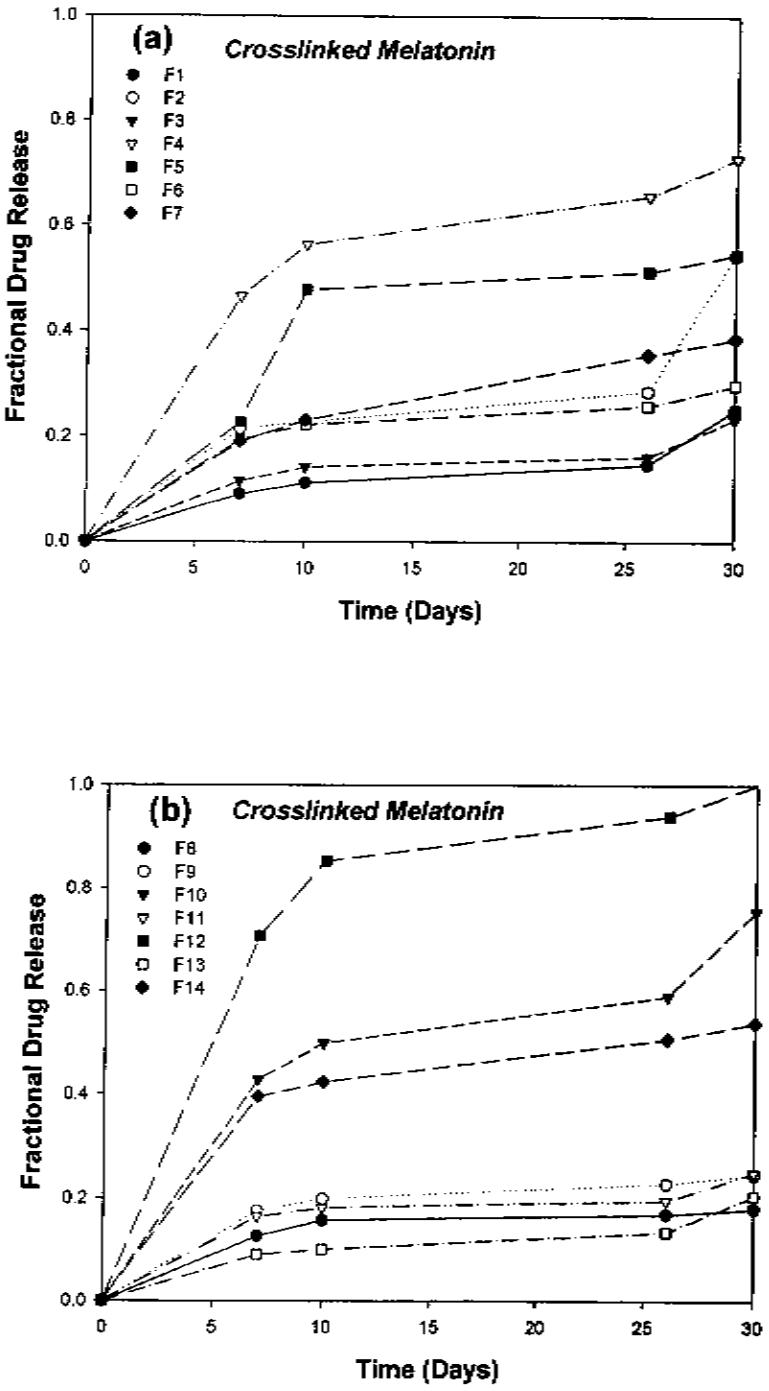


**Figure 5.5.** Release profiles of melatonin from the PLGA scaffolds (a) Formulations 1-7 and (b) Formulations 8-14.

The type of salt used in salting-out and subsequent cross-linking of PLGA was shown to have influenced the quantity of drug released. The current observations may be explicated in terms of the compactness of the scaffolds. NaCl and $AlCl_3$ tended to generate highly compact scaffolds with smaller pores, and hence were able to decrease the drug release rate. On the other hand, $CaCl_2$ generated scaffolds that were less compact with more porous polymeric matrix structures, through which the drug easily diffused from the matrix to the outer phase.

### *5.8.3 Response Surface Plots Indicating the Effects of Salts on the Dependent Formulation Variables*

Response surface plots (Figures 5.6, 5.7 and 5.8) were constructed to visually demonstrate the influence of the salts on the mean dissolution and the drug release characteristics of the PLGA scaffolds. Figure 5.6*a-c* demonstrates that DEE was higher at lower concentrations of NaCl, and was significantly decreased with the increase in NaCl concentrations as shown in Figure 5.6*a* and *b*. On the other hand, $AlCl_3$ concentrations did not significantly affect the DEE. Figure 5.6*a* demonstrates that the lower concentrations of NaCl and $CaCl_2$ had no statistically significant effect on DEE. Scaffolds salted-out with a mixture of $AlCl_3$ and $CaCl_2$ showed that $CaCl_2$ concentrations between 0 and 5% $^{w}/_{v}$ decreased DEE, whilst $CaCl_2$ concentrations between 5 and 10% $^{w}/_{v}$ increased DEE above 70% (shown in Figure 5.6*c*). However, the opposite is true for $AlCl_3$ concentrations. $AlCl_3$ concentrations between 0 and 5% $^{w}/_{v}$ increased DEE, whilst concentrations between 5 and 10% $^{w}/_{v}$ decreased DEE drastically.

Figure 5.7*d-f* revealed that in scaffolds salted-out with a mixture of $CaCl_2$ and NaCl, the increase in NaCl concentration caused an increase in the rate constant as shown in Figure 5.7*e*. In contrast, when combined with $AlCl_3$, at lower NaCl concentrations (between 0 and 5%$^{w}/_{v}$) significantly increased the value of *k* to a limit of 0.225, at which any further increase of NaCl (above 5%$^{w}/_{v}$) resulted in a decreased *k* value, demonstrated in Figure 5.6*f*. $CaCl_2$ concentrations increased linearly with *k*.

In Figure 5.8*g* and *i*, MDT was increased at lower $CaCl_2$ concentrations (between 0-5%$^{w}/_{v}$) whereas an increase of $CaCl_2$ (above 5%$^{w}/_{v}$) caused a decrease in MDT. NaCl concentration increased MDT only at lower $AlCl_3$ concentrations. These results are in close correlation with the results of the preceding studies outlined in Chapter Four, where NaCl and the $AlCl_3$ maintained an increase in resilience, energy absorbed and deformability modulus of the PLGA scaffolds as well as a matrix with fine fiber architecture and smaller pores. $CaCl_2$ produced scaffolds with a decreased resilience as well as voluminous polymer fibers with larger pore sizes and diameters. In general, these plots demonstrated that the presence of $CaCl_2$ in the scaffolds caused increased drug release. This study has demonstrated that factors such as, DEE, k and MDT may be influenced by the type of salt employed in the formulation of the PLGA scaffold.

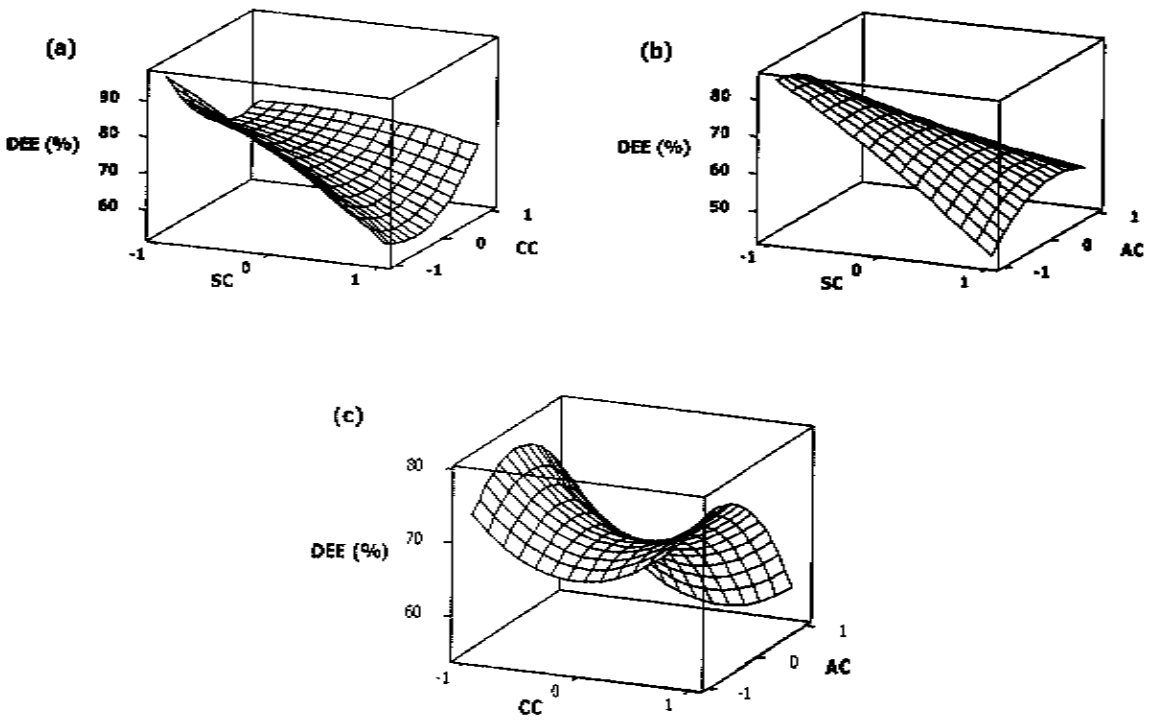


**Figure 5.6.** Surface response plots depicting the effects of the independent formulation variables on the Drug Entrapment Efficiency (DEE) (%) in salted-out PLGA scaffolds. *AC= $AlCl_3$, CC= $CaCl_2$, SC= NaCl. -1=0%$^{w}/_{v}$ 0=5%$^{w}/_{v}$ 1=10%$^{w}/_{v}$.*

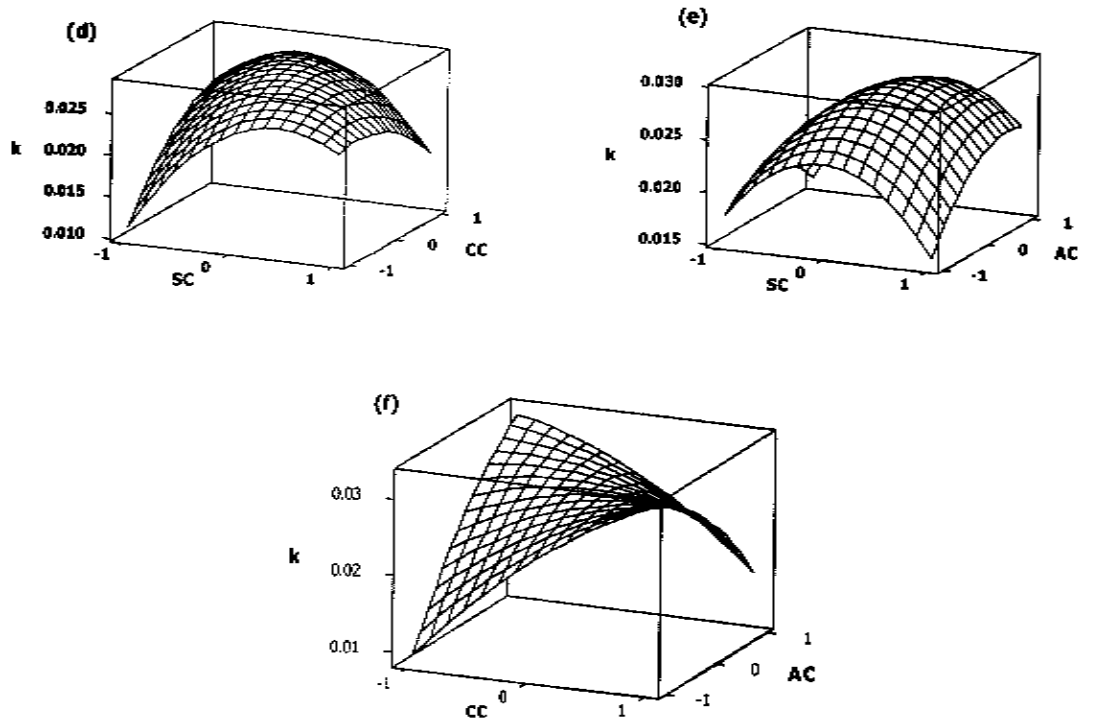


**Figure 5.7.** Surface response plots depicting the effects of the independent formulation variables on the Release Constant *(k)* of the salted-out PLGA scaffolds. *AC= $AlCl_3$, CC= $CaCl_2$, SC= NaCl. -1=0%$^{w}/_{v}$ 0=5%$^{w}/_{v}$ 1=10%$^{w}/_{v}$.*

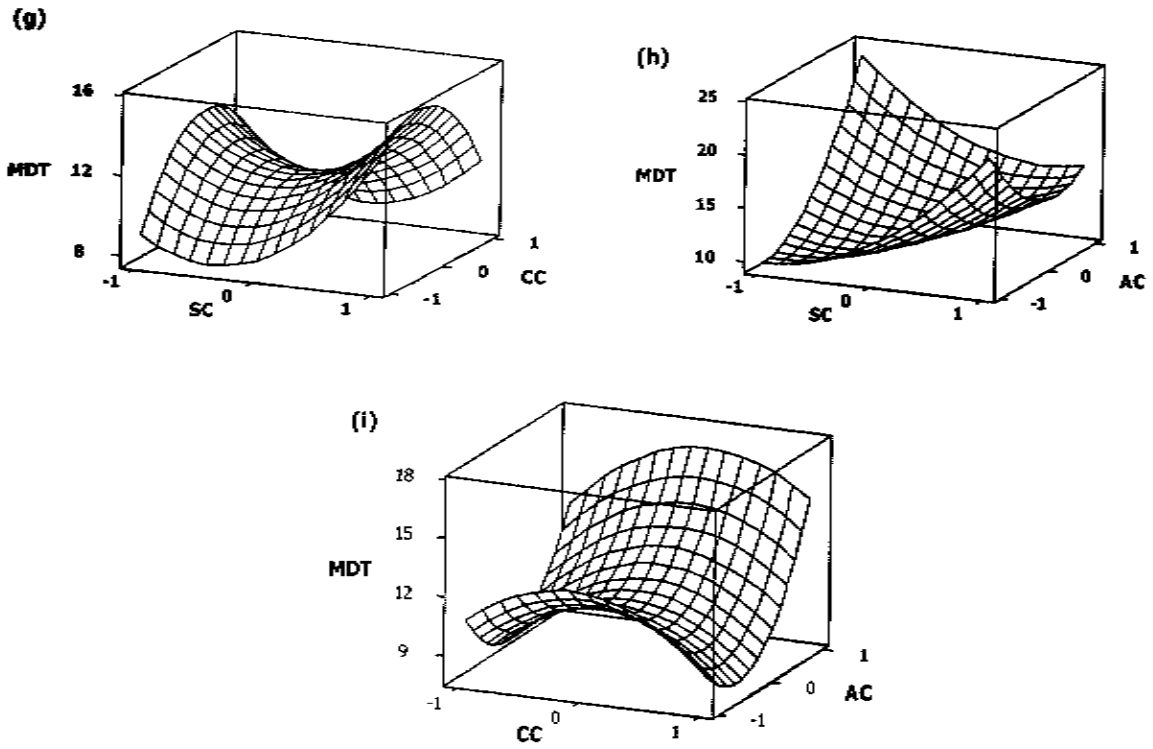


**Figure 5.8.** Surface response plots depicting the effects of the independent formulation variables on the Mean Dissolution Time (MDT) of the salted-out PLGA scaffolds *AC= $AlCl_3$, CC= $CaCl_2$, SC= NaCl. -1=0%$^{w}/_{v}$ 0=5%$^{w}/_{v}$ 1=10%$^{w}/_{v}$.*

These results suggested that NaCl and $AlCl_3$ are significant for the controlled and sustained drug delivery of melatonin by the PLGA implants.

### *5.8.4 Statistical Analysis for Optimization of the Drug Entrapment Efficiency, Mean Dissolution Time and Drug Release Kinetics of the PLGA Scaffold*

Formulation optimization by MINITAB®, (V14, Minitab, USA) was conducted to provide the significant formulation variables on the DEE, MDT and k. The effects on the responses were found to be attributable to the type of salt. Optimal responses for the desired data are depicted in Figure 5.4 DEE was calculated such that the ideal scaffold would permit a DEE of 95%. MDT and k were calculated in order that the ideal scaffold would achieve zero-order melatonin release.

***Table 5.4.*** *Settings for Response Optimisation*

| **Variables** | **Limits** |
|---|---|
| NaCl | 0-10% $^{w}/_{v}$ |
| $CaCl_2$ | 0-10% $^{w}/_{v}$ |
| $AlCl_3$ | 0-10% $^{w}/_{v}$ |
| MDT | 0.800-1.00 |
| DEE | 90%-100% |
| *K* | 0.005-1.00 |

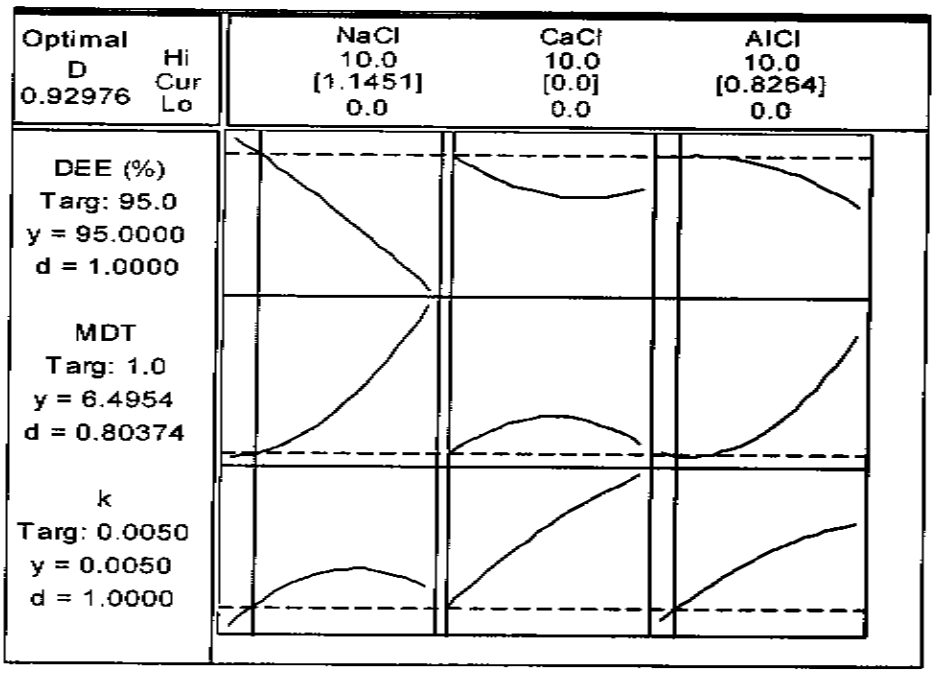


**Figure 5.9.** Optimization and Desirability plots illustrating the type and concentration of salt required to produce a desired response that will give an optimal PLGA scaffold

The settings for a desired response were illustrated in Table 5.4. According to the predictions of the statistical design, the ideal scaffold that would permit an optimal DEE of 95%, $MDT_{30}$ of 1 and a k of 0.0050 would comprise lower concentrations of NaCl and $AlCl_3$, (1.1451 $^{w}/_{v}$) and (0.8264 $^{w}/_{v}$) respectively. $CaCl_2$ would have to be excluded in the formulation in order to achieve a slow release scaffold. The responses were selected such that the optimized scaffold would be able to achieve a zero-order melatonin release rate, with no dose dumping, in order to be employed as a controlled drug delivery scaffold for the treatment of neurodegenerative disorders.

### *5.8.5 In Vitro Drug Release studies from the Optimized PLGA Scaffold*

The optimized formulation demonstrated 30-day zero-order kinetics for *in vitro* melatonin release (Figure 5.9).

***Table 5.5.*** *Desired and Experimental responses for the optimised PLGA scaffold formulations*

| Variables | Desired Response | Experimental Response |
|---|---|---|
| $MDT_{30}$ | 0.800-1.00 | 6.5 |
| DEE | 95% | 89% |
| *K* | 0.005-1.00 | 0.032 |

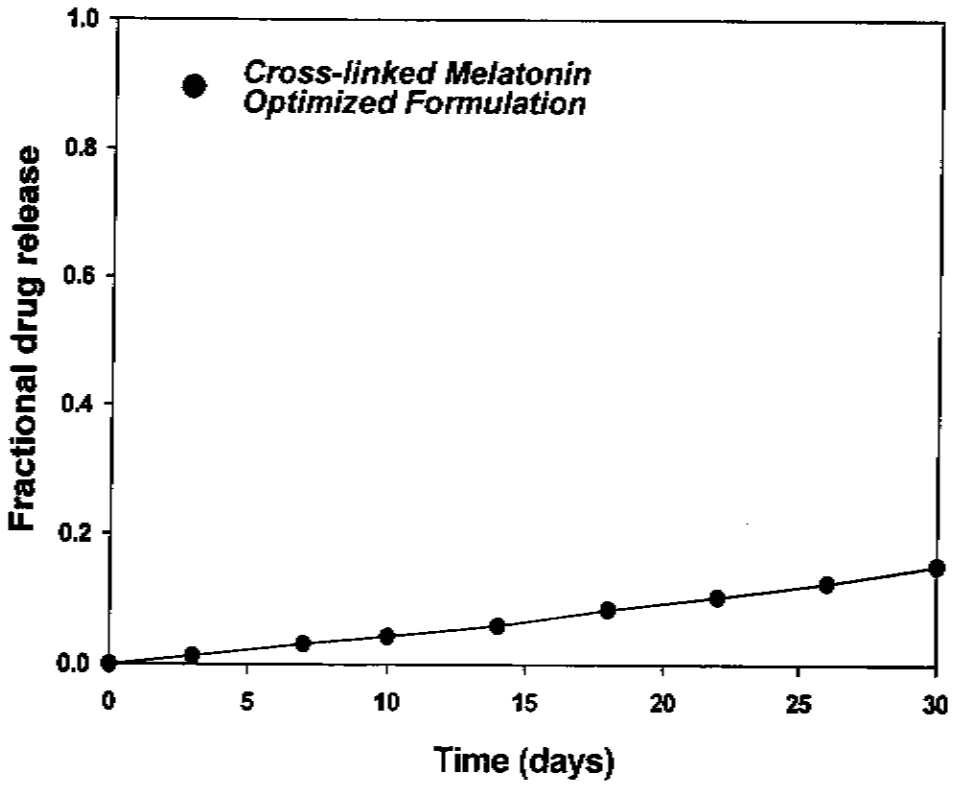


**Figure 5.10.** Melatonin release profile of melatonin from an optimized PLGA scaffold.

The salting-out and subsequent cross-linking of PLGA significantly modified the physicochemical and physicomechanical properties of native PLGA and demonstrated the ability to achieve controlled drug release. The synchronized optimisation of DEE, MDT and k for the PLGA scaffold has bestowed optimum PLGA scaffold with suitable DEE, MDT and release rate. The outcomes of the study have established that low concentrations of NaCl and $AlCl_3$ below 5%$^{w}/_{v}$ are required to formulate a controlled release PLGA scaffold with zero-order drug release rate.

In addition, this study has displayed that NaCl and $AlCl_3$ have a major influence on controlling the release of melatonin from the PLGA scaffold. This study has also demonstrated that salting-out and subsequent cross-linking of PLGA can significantly control the rate of drug release as a result of strong bonds formed between the drug and PLGA during cross-linking ultimately leading to zero-order release kinetics.

### *5.8.6 Kinetic Analysis of the Drug Release Mechanisms from the PLGA scaffold*

Theoretically, the primary drug release mechanism from PLGA scaffolds should be diffusion through the matrix layer by a Fickian release mechanism (Hutchinson and Furr, 1990). However, erosion was the significant mechanism in facilitating drug release from the scaffolds. Drug release kinetics from PLGA scaffolds shows that it was either a highly porous less compact, swelling and eroding matrix, such as those salted-out predominantly with $CaCl_2$, or the less porous more compact scaffolds erodible matrix with minimal swelling such as the ones salted-out predominantly with NaCl and $AlCl_3$. It appears that the drug diffusion process did not play a significant part in the release kinetics with the exception of highly porous matrices, such as

those salted-out predominantly with $CaCl_2$. Since melatonin is less water soluble and PLGA is a hydrophobic polymer, the rate of drug release decreased as a function of time, as it took more time for the dissolution medium front to approach the centre of the hydrophobic scaffold matrices.

Kinetic modelling elucidated the drug release mechanisms from the PLGA scaffold, that include drug diffusion, polymer erosion, polymer swelling behavior, and the subsequent drug release rate from the PLGA scaffold. Inevitably, the resultant drug release mechanism of the PLGA scaffold was dependent on the type and the molar ratio of the individual salt components (NaCl, $CaCl_2$ and $AlCl_3$) used during salting-out and subsequent cross-linking of the PLGA chain as illustrated in Chapter Four. The PLGA scaffolds salted-out with 10% $CaCl_2$ ratios disentangled faster and were hydrolyzed much more rapidly than those salted-out with 10% NaCl and $AlCl_3$.

***Table 5.6.*** *Drug release kinetics obtained from the various diffusion, relaxation and erosion models for the optimized PLGA scaffold formulation*

| **Model $M_t/M_\infty$=** | $k_1$ | $K_2$ | N | AIC[a] | SBC[b] | Correlation[c] |
|---|---|---|---|---|---|---|
| $k_1t^n$ | 0.29 | - | 0.93 | 46.32 | 43.26 | 0.89 |
| $k_1t^n+k_2t^{2n}$ | 0.12 | 0.44 | 0.95 | 38.86 | 38.77 | 0.96 |
| $1-[1- k_1t]^n$ | 0.52 | - | 3 | 42.12 | 38.16 | 0.95 |

[a] *Akaike Information Criterion*
[b] *Schwartz's Bayesian Criterion*
[c] *Correlation between experimental and predicted dissolution data*

Table 5.6 provides a summary of the important drug release kinetics obtained from the various diffusion, relaxation and erosion models for the optimized PLGA scaffold

formulation. From model fitting, it was observed that the simple exponential expression provided an n value of 0.93 for the optimized PLGA scaffold, indicating that drug release was regulated through the mechanisms of polymer erosion.

In this study, the drug release mechanism from the optimized PLGA scaffold was superlative, because it showed first order kinetics. The erosion controlled zero order release was only slightly affected by the hydrodynamic stress. Thus, it was possible to define the release mechanism, which was via the polymer particle erosion. Drug release was mostly controlled by the attrition of partially swollen polymer particles eroding from the surface of the scaffold. Furthermore, analysis using the Hopfenberg equation bestowed a release exponent values *(n)* of 0.95, also indicated an erosion-depended drug release mechanism from the optimized PLGA scaffold. Thus, the drug release kinetics was not affected by time-dependent diffusional resistances, such as the melatonin particle size.

The release rates analysis by means of the strong parametrical support from the statistical descriptors, namely, AIC, and SBC showed values that were suitably low. Therefore this indicated an excellent fitting as well as stability of the kinetic model to the release data. In addition, the value of the SBC statistic suggested that the errors are not correlated.

***Table 5.7.*** *Mechanistic predictors for melatonin release from the PLGA scaffolds*

| Scaffold Formulation | $k_e(10^{-3}$mm/min)[a] | $D(10^{-8}cm^2/sec)$[b] | $Deb_{release}$[c] |
|---|---|---|---|
| F1 | 0.11 | 0.217 | 1.312 |
| F2 | 1.42 | 0.291 | 0.020 |
| F3 | 0.41 | 0.166 | 0.082 |
| F4 | 3.78 | 0.697 | 0.016 |
| F5 | 3.08 | 0.893 | 0.024 |
| F6 | 0.19 | 0.239 | 0.824 |
| F7 | 0.34 | 0.700 | 1.091 |
| F8 | 0.15 | 0.141 | 0.517 |
| F9 | 0.23 | 0.195 | 0.427 |
| F10 | 0.74 | 0.615 | 0.333 |
| F11 | 0.13 | 0.110 | 0.667 |
| F12 | 4.69 | 0.809 | 0.017 |
| F13 | 0.24 | 0.178 | 0.215 |
| F14 | 1.79 | 0.449 | 0.035 |

[a] *Erosion Rate constant*
[b] *Drug Diffusion Coefficient*
[c] *Deborah Number for melatonin release*

Table 5.7 presents the erosion rate constant, drug diffusion coefficient and the Deborah Number values of the 14 PLGA scaffold formulations. The erosion rate constant, $k_e$, ranged from 0.11-4.69 $\times 10^{-3}$ mm/min and the diffusion coefficient $D$ ranged from 0.110-0.893 $\times 10^{-8} cm^2/sec$, thus, indicating that drug transport kinetics were not affected by time-dependent diffusional resistance, such as the drug particle

size. $De_{release}$ values ranged from 0.016-1.312 which indicated that drug transport was mainly due to erosion rather than polymeric relaxation or diffusion.

During drug release mechanisms, the loss of polymeric material from the eroding scaffold surface may have occured by a combined extrusion–forging mechanism, since PLGA is semicrystalline. Such a mechanism consists of sequential plastic deformation processes that account for each of the separate incident that result in the overall surface erosion of the scaffold. Tiny polymeric particles were initially extruded from scaffold surfaces made by the impacting fluid. Once extruded, the particles were forged into a strained condition, in which they were vulnerable to being knocked into smaller pieces. From the surface of the eroded polymeric particle, the fluid was forced to flow from in front and to the sides of the eroding particle, until the particle was sufficiently strained so as to fracture, at which time the drug loss occurred.

The erosion rate constants of the PLGA scaffolds can be rationalized via the physicochemical and physicomechanical factors that also control the degradation rates. Because all of the scaffolds are comprised of degradable ester linkages, they cannot be differentiated based on purely labile bond differences. The scaffolds salted-out and subsequently cross-linked predominantly with NaCl and $AlCl_3$ have a number of factors lowering their erosion rate. They are both more resilient than the scaffold salted-out and subsequently cross-linked predominantly with $CaCl_2$. In addition, the NaCl and $AlCl_3$ have shorter cross-linking networks that create a barrier from the approach of water to the PLGA backbone.

The erosion rate of the polymer may also have beeninfluenced by the intrinsic properties of the PLGA polymer, demonstrating that autocatalytic effects has also played a significant role, particularly in highly porous PLGA scaffolds, mainly formulated with $CaCl_2$. However, these effects were much less pronounced in scaffolds formulated with NaCl and $AlCl_3$ scaffold. Notably, the drug diffusion was suspended by the effects of the increasing diffusion pathway lengths due to porosity of the PLGA scaffold. Hence, porosity not only caused decreased drug mobility, but also adjusted the fundamental mass transport mechanisms. Thus the PLGA scaffolds' main drug release mechanism was through the process of polymer erosion.

***Table 5.8.*** *Swelling studies of the PLGA scaffolds loaded with melatonin*

| Scaffold Formulation | $\delta$(cm)[a] | v ($10^{5}$cm/sec)[b] | D($10^{5}$cm$^{2}$/sec)[c] | (Sw)[d] |
|---|---|---|---|---|
| F1 | 0.50 | 0.060 | 0.217 | 0.139 |
| F2 | 1.00 | 0.121 | 0.291 | 0.415 |
| F3 | 0.41 | 0.049 | 0.166 | 0.122 |
| F4 | 1.50 | 0.181 | 0.697 | 0.390 |
| F5 | 2.00 | 0.242 | 0.893 | 0.542 |
| F6 | 0.50 | 0.060 | 0.239 | 0.126 |
| F7 | 1.30 | 0.157 | 0.700 | 0.292 |
| F8 | 0.35 | 0.042 | 0.141 | 0.104 |
| F9 | 0.73 | 0.088 | 0.195 | 0.330 |
| F10 | 0.23 | 0.027 | 0.615 | 0.010 |
| F11 | 0.45 | 0.054 | 0.110 | 0.222 |
| F12 | 1.80 | 0.218 | 0.809 | 0.484 |
| F13 | 0.81 | 0.099 | 0.178 | 0.447 |
| F14 | 1.02 | 0.123 | 0.449 | 0.279 |

[a] *Thickness of the swelling face*
[b] *Velocity of the swelling front*
[c] *Diffusion coefficient*
[d] *Swelling Interface Number*

Table 5.8 provides a summary of the Swelling studies, essential for describing the balance between solvent penetration and drug release of the PLGA scaffold. Swelling studies of different scaffolds exhibited distinct swelling behaviors at different critical time points. The swollen matrices did not display a hydrogel-like internal structure, since they are hydrophobic matrices. Swelling studies revealed that the scaffold thickness, $\delta$ ranged from 0.23-2.00cm with a front velocity *(v)* ranging from

0.027-0.181cm/sec, and a $S_w$ between 0.010-0.542. The $v$ and the $S_w$ indicated that fluid penetration and polymeric swelling were not the major cause of drug release from the scaffolds.

Swelling was influence by the presence of salt, the porosity of the polymeric matrix and the drug properties through the solute diffusion coefficient. It was found that scaffolds salted-out with $CaCl_2$ had onsiderable water uptake into the scaffolds that induced matrix swelling, which facilitated the hydrolytic scission of PLGA chains and caused considerable drug release. However scaffolds salted-out with NaCl and $AlCl_3$ did not undergo extensive swelling and hence did not experience much of the autocatalytic effect.

Swelling of the polymeric matrix depended on the infiltration rate of the dissolution medium into the scaffold. Estimation of the rate of matrix swelling was mainly applied to approximate the extent to which the polymer-aqueous interaction affected drug release. In principle, the mode of polymeric matrix swelling only determined whether the drug is released at a steady rate or not (Roy and Rohera, 2002). Among other features of PLGA that have been attained through the use of salts are the physicochemical characteristics which provide for the attainment of slower swelling and erosion rates, thus controlling drug release.

**5.9 Concluding Remarks**

The role of salting-out and subsequent cross-linking on the physicochemical and the physicomechanical properties of PLGA as well as the influence of salt type and concentration on the *in vitro* melatonin release kinetics from the PLGA scaffold has

been elucidated in the study. In Chapter Four, electron micrographs and textural profiling for the three salt types, NaCl, $CaCl_2$ and $AlCl_3$ suggested two categories of the physicochemical and the physicomechanical behaviors of the PLGA scaffold, depending on the type and concentration of the salt employed during salting-out and subsequent cross-linking of PLGA. Drug release from all the PLGA scaffolds was mainly governed by erosion. The high porosity of the scaffold salted-out predominantly with $CaCl_2$ caused more drug particles to be released as erosion and degradation of the scaffolds were faster. On the other hand, scaffold salted-out with predominantly NaCl and $AlCl_3$ which were less porous and more resilient demonstrated less erosion, mostly steady, to a zero-order release demonstrated by the optimized formulation.

In general, scaffolds salted-out with NaCl and $AlCl_3$ had shorter crosslinked networks than $CaCl_2$, which formed a barrier to the approach of fluid into the PLGA backbone. In addition, the cross-linking voids resulted in retardation of drug release as the diffusional path length for drug release increased over time with the cross-linking networks. In conclusion, the mathematical models used in this study enabled the quantitative description of the observed *in vitro* drug release patterns from the PLGA scaffolds thus permitting the manipulation and prediction of drug release parameters that result from polymer modification.

# CHAPTER SIX

## MODEL DRUG: AMITRIPTYLINE HCl (WATER SOLUBLE)

## *IN VITRO* AMITRIPTYLINE HCl RELEASE FROM A PLGA COMPRESSED MONOLITHIC MATRIX SYSTEM

### 6.1. Introduction

Hydrophobic PLGA drug delivery devices offer an alternative means of controlled delivery of both hydrophobic and hydrophilic drugs (Kissel et al., 2002; Vogel and Mallapragada, 2005; Cheung et al., 2006; Fahmy et al., 2005; Yasukawa et al., 2006). While these devices are ideal for retarding drug release, their surface properties are not particularly suitable for the entrapment of hydrophilic drugs, (as discussed in Chapter Five).

The benefit of employing PLGA, however, is that the hydrophobic polymer exhibits the ability to be manipulated into any drug delivery device, such as, scaffolds, nanoparticles, and monolithic matrices with properties that allows it to house and control the release of both hydrophobic and hydrophilic drugs, such as melatonin and amitriptyline HCl (Meese et al., 2002; Chen et al., 2006). In preceding sections, we have confirmed the authenticity of the PLGA scaffold with regards to degradation kinetics (Chapter Three), physicochemical and physicomechanical transitions (Chapter Three and Chapter Four), drug release mechanisms of the PLGA scaffold (Chapter Five), hence, in this study the PLGA scaffold is adapted into a compressed monolithic matrix system for further pharmaceutical applications. A novel salted-out and subsequently cross-linked compressed monolithic matrix system was developed and explored for use in the delivery of hydrophilic drugs requiring pre-programmed release, such as amitriptyline HCl.

### 6.2 Basic Characteristics and Release Mechanisms of Monolithic Systems

In principle, a monolithic matrix is a simple drug delivery system comprising homogenous drug dispersed or dissolved in an inert polymer. The matrix can be hydrophilic or hydrophobic and drug release is controlled mainly by diffusion (Blagoeva and Nedev, 2006). The three major techniques for the synthesis of polymeric monolithic systems have been detailed by Grassi and Grassi, 2005.

i. The less complicated approach for preparing a monolithic matrix is by compressing the polymer, the drug and necessary excipients, in a pre-calculated ratio. The disadvantage of this method can be the lack of powder compatibilities and the lack of polymer compressibility, namely elasticity and resilience.

ii. Another approach is by polymerization of the polymer in the presence of the drug, by mixing a thin drug powder with the monomers (prepolymer) and then adding the mixture to a polymerization reactor. In this case, a solvent can be used to produce a highly concentrated drug solution, which will be added to a prepared matrix. When the drug solution comes into contact with the polymer, it generates swelling of the matrix. The solvent is then physically removed. The main disadvantage of this method is the elimination of the solvent that can be intricate and costly.

iii. The third approach is by loading the drug powder into a polymeric carrier in order to avoid the use of solvents. Alternatively the matrix can be drug-loaded using a supercritical fluid technique that easily swells the matrix. This method is based on physicochemical and physicomechanical activation.

Monolithic matrices prepared from biodegradable polymers in which the polymer is covalently bonded to the drug are chemically manageable (Blagoeva and Nedev, 2006). Dissolution of the system depends on the physicochemical and physicomechanical properties of the employed polymer. Hydrophilic polymers tend to form swellable monolithic matrices. On contact with the aqueous media, the matrix swells, allowing the dissolution medium to penetrate the matrix. The drug dispersed within the matrix is then released. On the other hand, hydrophobic polymers tend to form non-swellable monolithic matrices and drug is released through diffusion (Efentakis et al, 2000). Higuchi's analysis of drug release kinetics from monolithic matrices, demonstrated that in a monolithic slab, the drug release and the pathlength of the receding boundary is directly proportional to the square root of time (Higuchi, 1963).

Various studies have reported on the mechanisms of drug release from monolithic polymeric devices (Babay et al., 1988). Langer and Peppas (1981) proposed that during the overall release of drugs from monolithic matrices, two distinctive processes could be observed, namely, swelling and 'true' dissolution of the polymer. In case of a swellable system, the device will immediately swell as when in contact with aqueous media. Thus the release of the drug is controlled by the rate of hydration of the polymeric device. As a consequence, dissolution of the matrix depends on the relative rate of hydration and gelation of the polymer. In order to resist rapid release, the polymer employed to prepare the device must be able to form a protective gel layer prior to dissolution.

In addition, the polymer should form a more viscous gel in order to resist dilution and erosion. Viscosity of the gel is, thus, another rate-controlling factor in the dissolution of monolithic systems. Even so, if the polymeric matrix gel holds good durability virtues, soluble drugs may diffuse out of the gel before matrix erosion occurs. Thus, both diffusion and erosion contribute in controlling the release of drug from a hydrophilic matrix; although one process often plays a predominant role over the other, based on the polymer characteristics (Gohel et al., 2002; vostalova´ et al., 2003; Conti et al., 2007).

### 6.3 Hydrophilic Drugs in Monolithic Systems

Hydrophilic drugs have a tendency to diffuse out of the matrix gel before erosion occurs, such that both diffusion and erosion become the rate-controlling steps in the release of the drug (Mani and Jun, 2004; Guo et al., 2005). The physicochemical and the physicomechanical properties of the polymer, such as resilience, energy absorbed, surface morphology, porosity and glass transition temperature, will, however, affect both processes (diffusion and erosion) and influence the prevailing of one step. In addition, the drug's key properties of influence include solubility, diffusion coefficient, partition coefficient (pKa) at physiological temperatures, molecular mass and the chemical structure. Designing a controlled release compressed monolithic matrix system that can achieve zero-order drug release kinetics is often intricate, particularly for highly water-soluble agents such as, amitriptyline HCl.

Pillay and Fassihi, 2000, postulated that these drawbacks may be attributed to factors such as:

i. The increased hydrophilicity of the drug that causes a burst effect during drug release;
ii. The lack of accurate management of polymer relaxation or disentanglement over time-dependent processes in relation to drug dissolution and diffusion; and
iii. The complexity of controlling the increase in the diffusional pathlength with time is not easily attainable (Pillay and Fassihi, 2000).

The inherent inefficacies of this system can however, be manipulated through the use of salts that modulate the internal geometry of the system. Salts have been highly successful in controlling dissolution and drug release, by demonstrating differential swelling boundaries and texturally variable matrices that manifest as 'peripheral matrix stiffening', a phenomenon that retards the release of water-soluble drugs. In general, the addition of salts to hydrophobic matrices can increase or decrease the quantity of drug released due to the water-salt interaction, which depends on the salt type and concentration (Pillay and Fassihi, 2000, Pillay and Fassihi, 2001).

In order to achieve the desired release rate, therefore, the relative rate of hydration and dissolution will be directed by the salt. In view of the current facts and in line with findings from our preceding studies on the physicochemical and the physicomechanical transitions of salted-out PLGA (Chapter Four), this study employed different polymeric networks to design a compressed monolithic matrix

system for the delivery of amitriptyline HCl that is capable of achieving zero-order drug release. In this study, the compressed monolithic matrix system was developed as a novel approach for zero-order kinetics for the steady delivery of highly soluble drugs from a simple monolithic system using the PLGA scaffold with amitriptyline HCl, as the model drug.

### 6.4 Hardness and Compressibility Characteristics of PLGA

For a polymer to be exploited as a compressed monolithic drug delivery system, it should be directly compressible with or without the drug or bioactive. Secondly, the polymer should have a good compression pressure-device strength profile in order that robust devices are obtained even at lower pressures. The ability of a polymer to compress exhibits its ability to undergo a certain degree of elasticity and plastic deformation. Polymeric materials must possess some degree of elastic and plastic deformation as these properties present huge benefits for effective compression, since these materials can consolidate. Therefore, there is a need to characterize the compression behaviour of the different polymeric materials included in the formulation and to know the extent of plastic or brittle deformation of these materials at different compression intensities (Adolfsson and Nystrom, 1996). PLGA was verified for all the above-mentioned-standards.

In pursuit of a suitable technique to characterize the compressibility of PLGA, the available strategies to characterize the compression behaviour of powders were critically evaluated. These include the tablet hardness-compression force profiles (Higuchi, 1953; Fell and Newton, 1968), the ejected tablet Heckel analysis (Heckel, 1961a, b), work done calculations from force-displacement data (De Blaey et al.,

1971; Krycer et al., 1982; Kuentz et al., 2000; Antikainen et al., 2003), and force-time profile analysis (Chilamkurti et al., 1983; Hoblitzell and Rhodes, 1990; Martinez-Paracheo et al., 1990).

The hardness tests outlined above are limited in practical use since they do not provide sensitive enough data or scales in particular for modern day polymeric materials. The hardness-compression force profile approach, showed to have the necessary sensitivity, precision, reproducibility and simplicity for characterizing compressibility. The hardness is of interest for elucidating the compression process, as well as for quality control and reproducibility of compressed monolithic matrix systems. The studies of the latter technique, involved determining the indentation hardness and coverting it to the Brinell Hardness Number (BHN) employing textural analyses. In essence, the BHN value is a measure of the mean stress under a spherical indenter, which produces plastic deformation of the compact. This permanent deformation is correlated to the strength of the device (Barton et al., 1973; Izaki et al., 2002).

Compression may increase or decrease the efficacy of the polymer to retain the drug resulting in a more rapid drug release, than the anticipated retarded rate of drug release. Therefore, in order to design a monolithic device with sufficiently robust properties, compressibility and its effects must be investigated.

## 6.5 The Use of Amitriptyline HCl in the Treatment of Depression caused by Neurodegenerative Disorders

Depression has become a predominant health care problem, due to the progressive aging population, neurodegenerative sufferers and the HIV/AIDS pandemic (Clesla, and Roberts, 2001). Evidence from recent studies suggests that major depression is a common psychiatric complication of neurodegenerative disorders. There are few studies investigating the psychiatric morbidity of neurodegenerative disorders and HIV/AIDS infection, yet the potential risk factors of depression in this group remain relatively unexplored (Olley et al., 2004). While HIV/AIDS infection remains the world's major concern, particularly in the younger population, neurodegenerative disorders have also become a more pressing concern in society, especially among the people over 60 years of age. Both these conditions are complicated by major depression, thus the need for effective treatment methods of depression increases.

For the past forty years, the tricyclic antidepressants (TCA) have been one of the most widely used classes of antidepressants in psychiatric conditions such as, depression and anaesthetics (Sudoh et al., 2003). The most common TCA, amitriptyline has contributed to numerous health care products that are already on the market (Tryptanol®, Trepiline®,Etrafon® and Saroten Retard® capsules) and has a continued application in psychiatric medicine. In comparison with other TCAs or heterocyclic antidepressants (HCAs), amitriptyline HCl is more efficacious as an antidepressant used in depressive illness of psychotic or endogenous nature and in selected patients with neurotic depression (Fineberg and Craig, 2007).

***Table 6.1.*** *The Physicochemical and the Physicomechanical Properties of Amitriptyline HCl*

| PHYSICOCHEMICAL AND THE PHYSICOMECHANICAL PROPERTIES OF AMITRIPTYLINE HCL | |
|---|---|
| Trade Name | Amitriptyline ® |
| Chemical Name | 3-(10,11-dihydro-5H dibenzo[a,d]cyclohepten-5-ylidene)-propyldimethylamine |
| Empirical formulae | $C_2OH_{23}N$ |
| Molecular mass | 313.97 g/mol |
| Bioavailability | 45% |
| Melting Range | 196–197° C |
| Solubility at 25° C | Soluble |
| Stability in light | Photostable |
| Atmospheric and chemical stability | Interacts with reactive oxygen and nitrogen |
| Storage | below 20°C, air tight |

Amitriptyline HCl is passively absorbed from the gastrointestinal tract with peak plasma concentrations occurring between 2 and 12 hours after administration. Bioavailability of the drug is between 30 and 60% due to extensive first pass metabolism of the drug in the liver (Fridrich et al., 2007).

Amitriptyline HCl is over 90% protein bound. Its elimination half-life varies from 10 to 50 hours, with an average of 15 hours. Amitriptyline HCl is subsequently demethylated in the liver to its primary active metabolite, nortriptyline that has a half

life of 20-200 hours. Within 24 hours, approximately 25 to 50% of a dose of Amitriptyline HCl is excreted in the urine as inactive metabolites, and then small amounts are excreted in the bile (Oesen and Linnet, 1997; Uhr et l., 2007)

### *6.5.1 Structure-Function Relationship of Amitriptyline HCl*

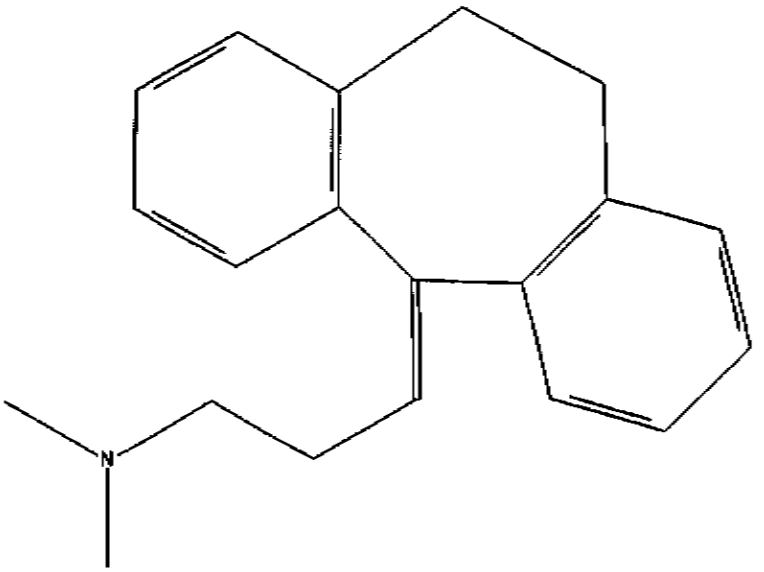


**Figure 6.1.** Chemical structure of amitriptyline: *(3-(10,11-dihydro-5H dibenzo[a,d]cyclohepten-5-ylidene)-propyldimethylamine)* (Source: adapted from Manzo et al., 2006).

Despite amitriptyline HCl's extensive applicability, pharmacokinetics studies have established that it undergoes extensive first-pass metabolism with a systemic bioavailability and an apparent volume of distribution of about 45% and 19 L/kg, respectively. Amitriptyline HCl is soluble in water 100% at $25^0$C. Drug efficacy is precluded by an increased drug absorption and hepatic metabolism. Numerous researchers are exploring novel techniques in drug delivery in order to address some of the current limitations with TCAs, especially associated with their toxicity.

The use of TCAs has to be carefully monitored due to the anticholinergic, cardiovascular, CNS and endocrine adverse effects. These occur as a result of drug sensitivity or because of increased plasma level caused by dose dumping. However, amitriptyline, nortriptyline clomipramine and desipramine seem to be the best tolerated tricyclics, particularly in older people (Rosenbaum and Kou, 2005).

## 6.6 Materials and Methods

### *6.6.1 Materials*

PLGA was purchased from Boehringer Ingelheim Pharma (Ingelheim, Germany) (Resomer® RG504 50:50; $M_w$ 48,000; i.v. 0.48-0.60dL/g). Acetone was used as a solvent, and analytical grades of sodium chloride (NaCl), calcium chloride ($CaCl_2$), (Rochelle Chemicals, South Africa) and aluminium chloride ($AlCl_3$) (Merck, Darmstadt, Germany) were used as the ionic salts. Disodium hydrogen orthophosphate, ($Na_2HPO_4$), and potassium dihydrogen phosphate ($KH_2PO_4$) were obtained from Saarchem (Pty) Ltd., South Africa. Model drug, amitriptyline HCl was purchased from Sigma-Aldrich Co., Germany. A test sieve shaker (Endcotts Octagon 200, London, UK) with a variety of sieves (Endcotts Test Sieves, Inc., London, UK) of different aperture sizes were used. An analytical mass balance (Denver Instruments Co., USA, ± 0.5 mg) was used in all mass determinations.

***Table 6.2.*** *Normalized factor levels of the independent variables*

| Variables | Factor Level | | | Units |
|---|---|---|---|---|
| | Low | Middle | Upper | |
| NaCl | 0 | 5 | 10 | % $^{w}/_{v}$ |
| $CaCl_2$ | 0 | 5 | 10 | % $^{w}/_{v}$ |
| $AlCl_3$ | 0 | 5 | 10 | % $^{w}/_{v}$ |
| Amitriptyline HCl | 50 | 50 | 50 | mg |

### *6.6.2 Preparation of the PLGA Compressed Monolithic Matrix System*

In order to ascertain the effects of salting-out and subsequent cross-linking on the release of amitriptyline from the PLGA matrix, two approaches were adopted. The first approach incorporates salting-out and subsequently cross-linking of 300mg PLGA with 50mg amitriptyline HCl at various salt concentrations in accordance with a Box-Behnken statistical design in Table 4.1, which was followed by direct compression of the samples into compressed monolithic matrix systems. In the second approach, PLGA was salted-out and subsequently cross-linked without amitriptyline HCl, which was followed by direct compression of the of a mixture comprising 300mg salted-out PLGA and 50mg amitriptyline HCl. Compression was conducted utilizing a Beckman Hydraulic Press (Beckman Instruments, Inc., Fullerton, USA), and the compression force was set at $1N/m^2$. The drug release characteristics of the compressed monolithic matrix systems were characterized.

### *6.6.3 Measurement of Compressibility*

The compressibility of PLGA was determined with a textural analyser Texture Analyzer *TA.XTplus* (Stable Micro Systems, England) using a spherical indenter of 3,175mm in diameter and a 5 kg load cell. The textural settings used to calculate the BHN values are listed in Table 6.3.

***Table 6.3.*** *Textural settings employed for BHN value calculations*

| **Test Parameters** | **BHN Settings** |
|---|---|
| Pre-test speed | 1.0mm/sec |
| Test speed | 0.5mm/sec |
| Post-test speed | 1mm/sec |
| Compression Distance | 40.0N |
| Trigger type | Auto |
| Trigger force | 0.5N |
| Load cell | 5.0kg |

Force-displacement profiles were generated for the calculation of the BHN value as shown in Figure 6.2.

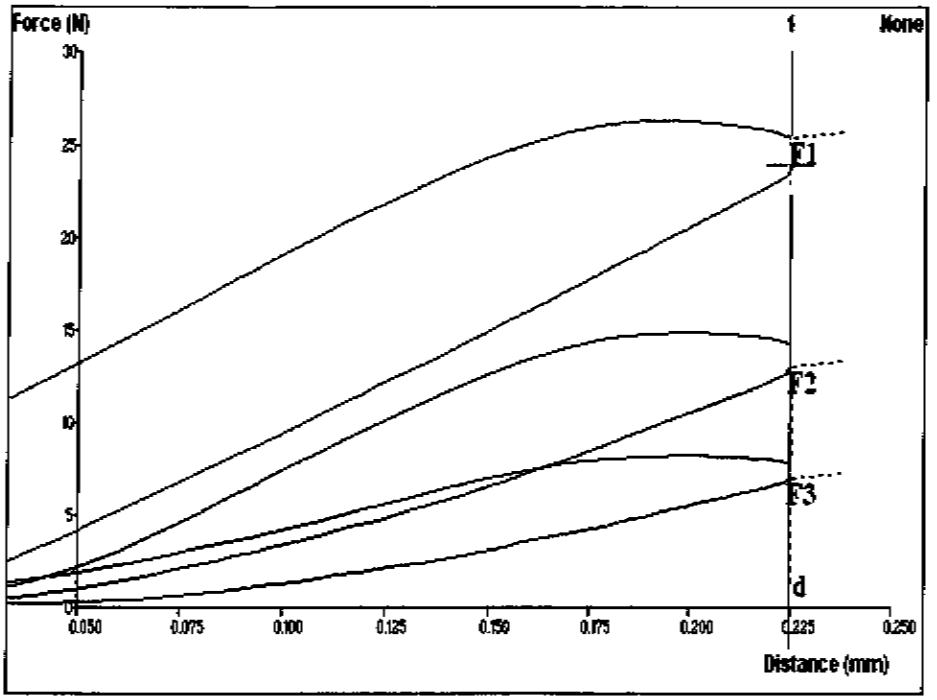


**Figure 6.2.** Typical force-displacement profiles for the PLGA compressed monolithic matrix systems in the determination of matrix indentation hardness.

### *6.6.3.1 Calculating the Brinell Hardness Number*

The Brinell hardness number is calculated by dividing the load applied by the surface area of the indentation. This technique is the best for achieving the bulk hardness of a material, particularly those materials with heterogeneous structures. The indentation hardness was calculated by a conversion to the Brinell Hardness Number (BHN) (Equation 6.1).

$BHN = 2F/\pi D[D-(D^2-d^2)^{1/2}]$ *Equation 6.1*

Where,

*F* is the force generated from indentation;

*D* is the diameter of spherical probe indenter (3.175 mm) and

*d* = the indentation depth (0.25 mm)

### *6.6.4 Preparation of a Calibration Curve for Spectrophotometric Determination of Amitriptyline HCl Release from the Compressed Monolithic Matrix System*

A calibration curve of absorbance, measured spectrophotometrically, versus concentration was constructed for amitriptyline HCl in PBS pH 7.4 at 240.1nm absorption peak. In order to determine the best-fit straight line, linear regression analysis was used. The values were calculated in accordance with the melatonin values in Chapter Five.

### *6.6.5 In Vitro Drug release from the Compressed Monolithic Matrix system*

Drug release studies were conducted in 500mL phosphate buffered saline (PBS) (pH 7.4; 37°C) using a USP39 apparatus at 50 rpm. Amitriptyline HCl assays were performed with UV-spectroscopy (240.1nm) (SPECORD 40, Jena, Germany). The dissolution data was subjected to a model-independent analysis known as the time-point approach as in Chapter Five.

## 6.7 Results and Discussion

### *6.7.1 The Compressibility and the Hardness Number of the Compressed Monolithic Matrix System*

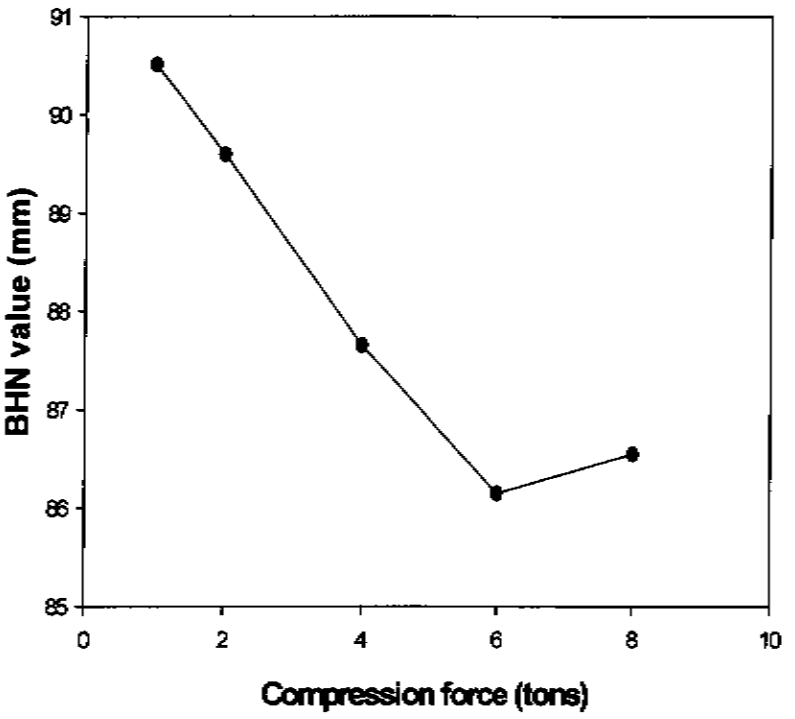


**Figure 6.3.** Typical compressibility profile depicting the effects of compression force on the compressed monolithic matrix system

The indentation hardness of the compacts indicated that as the force was being increased, the BHN of the compressed monolithic matrix system were decreased due to the amorphous properties of PLGA, until a point where the material went through a glass transition temperature and the BHN started to increase.

***Table 6.4.*** *BHN values obtained from the fourteen samples of compressed monolithic matrix systems Formulations*

| **Compressed Monolithic Matrix System** | **Indentation force (N)[a] mean ± S.D.** | **BHN ($N/mm^2$) mean ± S.D.** |
|---|---|---|
| F1 | 17.769±0.126 | 102.125±2.152 |
| F2 | 17.609±0.321 | 101.201±1.462 |
| F3 | 17.792±0.512 | 102.251±2.312 |
| F4 | 17.604±1.230 | 101.173±1.520 |
| F5 | 17.440±0.263 | 100.231±0.214 |
| F6 | 17.793±1.235 | 102.263±2.152 |
| F7 | 17.399±0.912 | 099.995±1.254 |
| F8 | 17.944±0.231 | 103.127±2.561 |
| F9 | 17.919±1.326 | 102.982±2.341 |
| F10 | 17.959±0.265 | 103.215±1.987 |
| F11 | 17.919±0.865 | 102.981±0.522 |
| F12 | 17.787±0.325 | 102.228±0.514 |
| F13 | 17.814±2.431 | 102.382±1.589 |
| F14 | 17.402±1.215 | 100.015±0.223 |

[a] *Force produced on indentation of compacts*

Table 6.4 presents force (N) generated from indentation of each of the PLGA scaffold formulations and the BHN values that were generated by converting the force values employing Equation 6.1. The indentation force of the scaffolds salted-out with higher concentrations of $CaCl_2$ such as F2, F5, F7 and F14 were comparatively smaller, as compared to the indentation force of the scaffolds salted-out with NaCl and $AlCl_3$ such as F1, F6 and F13. The indentation force and the BHN

of the scaffolds exhibited that porosity could have a significant influence on the compressibility of the scaffolds. This could be a result of the amorphous regions of the scaffold owing to the increased porosity of the scaffolds.

Hardness encompasses several properties that include resistance to deformation, resistance to friction and abrasion. The frictional resistance is influenced by the chemical affinity of materials in contact, and the hardness itself. Therefore from the Table 6.2 it is apparent that salting-out employing diverse salt types and concentration can modify material hardness and thus the behaviour of the scaffold. Furthermore, loss of particles and deformation at scaffold matrix surfaces may result in surface degradation and result in a higher initial burst effect during drug release

### *6.7.2 The Calibration Curve for Amitriptyline HCl*

The regression coefficient, $R^2$=0.9998 for the calibration curve produced for Amitriptyline HCl demonstrated a linearity in phosphate buffered media (pH 7.4) at 37°C achieved over the concentration range from 0.099 to 0.900 mg/mL. Linear regression analysis was employed to reveal the best-fit straight line. The equation was found to be y=53.00x.

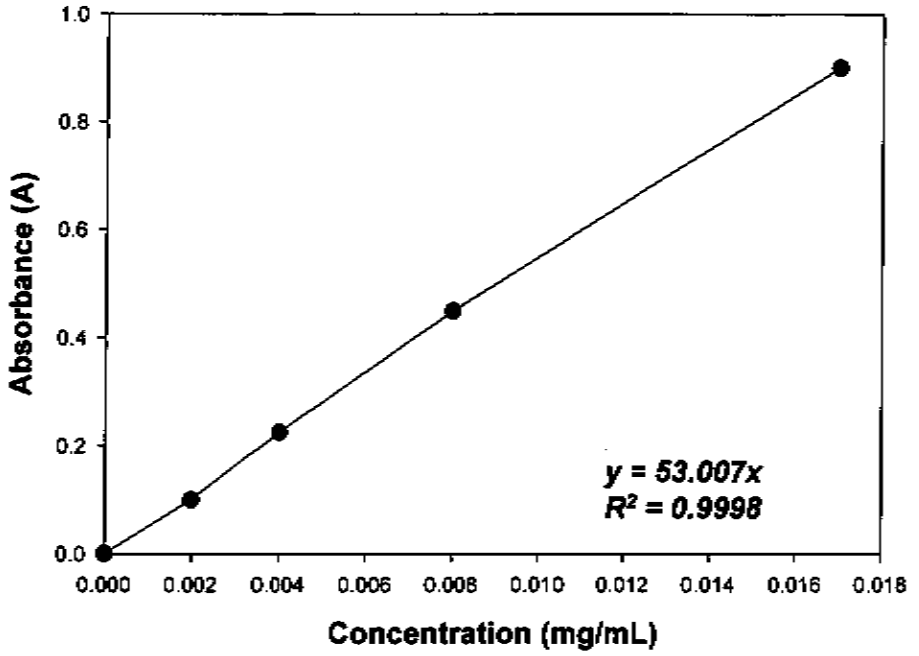


**Figure 6.4.** Amitriptyline HCl calibration curve at 240.1 nm in PBS (pH 7.4,)

### *6.7.3 Drug Release Studies from the Compressed Monolithic Matrices*

The fundamental release mechanism from the compressed monolithic matrix systems was found to be by diffusion through the matrix layer by a Fickian release. However, matrix swelling and erosion also had a significant role in the release of amitriptyline HCl. According to Higuchi (1963), drug releases in monolithic systems tend to follow the square root of time relationship.

The basic equation that may be used to describe drug release from the monolithic systems is:

$$dM_t / dt = Q_t = A\,[Dm\,(C_M - C_b k)\,(2C_T - C_M - C_b k)/4t]^{1/2} \qquad \textit{Equation 6.2}$$

For the calculation of cumulative drug release the integrated version of Equation 6.3, is:

$M_t = A\,[D_m\,(C_M - C_b k)\,(2C_T - C_M - C_b k)/t]^{1/2}$ *Equation 6.3*

The Higuchi's square root of time model for characterizing the dissolution data is given by:

$Q_t = Kt^{1/2}$ *Equation 6.4*

Where,

Mt is the quantity of drug released at time, *t*;

$Q_t$ is the drug diffusion rate;

*A* is the cross-sectional area of the matrix available for diffusion;

$C_M$ is the drug solubility in the matrix;

$C_b$ is the bulk concentration of the drug and

*k* is a kinetic constant that accounts for numerous factors such as, solubility and diffusion coefficient of the drug in permeating fluid as well as the porosity and tortuosity of the matrix.

$C_T$ is the drug loading in the matrix.

Figure 6.3*a* and *b* depicts the *in vitro* fractional drug release from each of the fourteen PLGA compressed monolithic matrix systems formulations over a period of 24hours. These profiles display that the initial burst was lower in compressed

monolithic matrix systems where PLGA was salted-out and subsequently cross-linked with amitriptyline HCl. This was followed by a steady release of the drug. On the contrary, PLGA salted-out and subsequently cross-linked without amitriptyline HCl showed a high initial burst. The fundamental release mechanism of amitriptyline from the compressed monolithic matrix systems was found to be by diffusion through the matrix layer, exhibiting a Fickian release model.

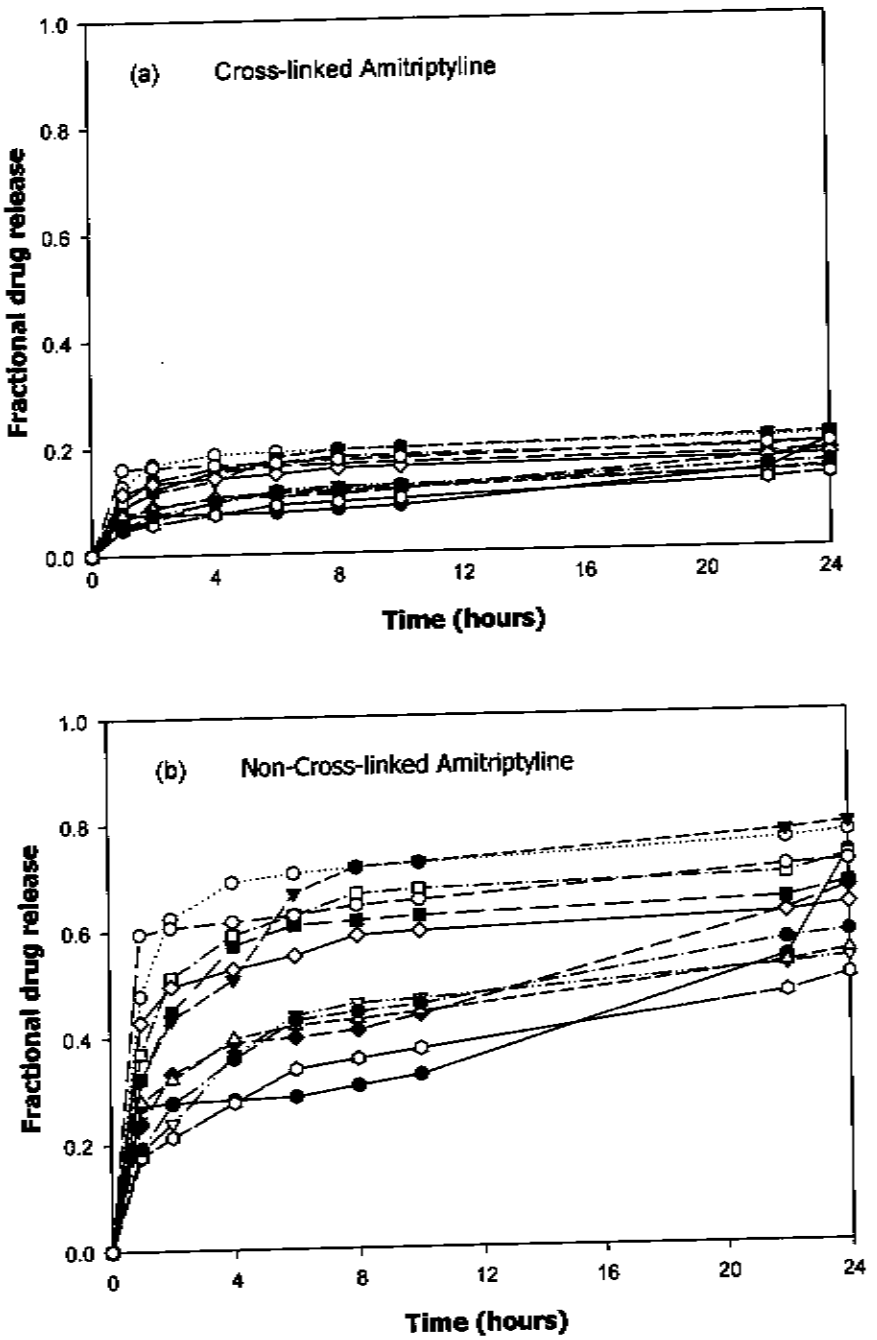


**Figure 6.5.** Fractional drug release profiles of amitriptyline HCl from the PLGA compressed monolithic matrix systems prepared by either (a) cross-linking PLGA with amitriptyline HCl followed by compression or (b) cross-linking PLGA without amitriptyline HCl followed by compression of PLGA and amitriptyline HCl.

Drug release studies demonstrated that cross-linking PLGA with amitriptyline HCl retarded the release of amitriptyline HCl from the compressed monolithic matrix systems, and was found to be less than 0.20 in 24 hours. In contrast, the compressed monolithic matrix systems prepared by cross-linking PLGA alone and adding amitriptyline HCl during compression displayed a much more rapid amitriptyline HCl release, with fractional drug release ranging from 0.50 to 7.8 within 24 hours.

Drug release kinetics were calculated by $M_t/M_\infty=k_0t$, and displayed an average release rate constant $k_0$ of 0.007 in compressed monolithic matrix system prepared by cross-linking PLGA with amitriptyline HCl and 0.03 in compressed monolithic matrix systems prepared by cross-linking PLGA alone and compressing it with amitriptyline HCl. Amitriptyline HCl is a highly water soluble drug, as mentioned earlier, and tends to diffuse rapidly out of matrices in physiological fluids. However, the current study has demonstrated that the cross-linking of amitriptyline HCl and PLGA with chemical inducers considerably reduced drug release due to the formation of strong bonds between the amitriptyline HCl, PLGA and the salts.

As mentioned earlier in the study (Chapter Three, Four and Five), cross-linking decreases the hydrodynamic volume of polymers, and increases the inherent viscosities of the matrices, thus slowing the diffusion of water soluble drugs out of the matrix. In addition, the slow diffusion of amitriptyline HCl resulted from the shielding of the polymeric reaction sites that coil and prevent the maintenance of the same effective collision rate that would be achieved in the same functional groups and the aqueous environment in non cross-linked polymer molecules.

Furthermore, the type and concentration of salt used during salting-out and subsequently cross-linking played a role, in hindered the rapid drug release and degradation of the matrices. Compressed monolithic matrix systems salted-out and subsequently cross-linked with NaCl and $AlCl_3$ displayed slower drug release than the compressed monolithic matrix systems salted-out and subsequently cross-linked with $CaCl_2$.

The compressed monolithic matrix systems salted-out with $CaCl_2$ had larger pores, and caused drug diffusion to occur faster, whereas the compressed monolithic matrix systems salted-out with NaCl and $AlCl_3$ had smaller pores that further delayed the release of amitriptyline HCl from these matrices. Thus, the intrinsic properties of PLGA, the transitions in physicochemical and physicomechanical properties that result from salting-out and subsequent cross-linking, particularly the visco-elasticity, resilience and strength have led to the sustained release of amitriptyline HCl from both the PLGA cross-linked separately and the PLGA cross-linked with the drug.

**6.4 Concluding Remarks**

The compressed monolithic matrices were capable of producing flexible yet rate-controlled drug release. The distinctiveness of the PLGA compressed monolithic matrix system lies in the claim that it may be applied for either zero-order 24-hour-drug delivery system, when PLGA is cross-linked without the drug, or a 30-day body implant when PLGA is cross-linked with the drug. This study has also demonstrated that salting-out and subsequent cross-linking can significantly reduce the release rate of water-soluble drug through salting-out and cross-linking.

All drug-release profiles yielded by the PLGA cross-linked with amitriptyline HCl demonstrated the Higuchi diffusional model of dispersed drug particles in matrices, and not the desorption kinetic model of a dissolved drug from a monolithic spherical device. The validation of the effects of salting-out and subsequent cross-linking on the release of amitriptyline HCl from PLGA matrices was achieved through this study. Furthermore, the present study has demonstrated pre-determined drug release, controlled by the rate of hydration of the polymeric device that depends on the pKa and concentration of the salt incorporated. In conclusion, the study has shown that the PLGA scaffold can be further adapted into a compressed monolithic system. Thus the novelty of the monolithic system lies with the fact that it is constructed from a 3-dimensional scaffold, as compared to the conventional systems that are formulated from native polymeric powders.

# CHAPTER SEVEN

## CONCLUSIONS AND RECOMMENDATIONS

### 7.1 Conclusions

The mechanisms of modifying the thermoplastic biodegradable polymer, PLGA were explored. This study has uniquely validated the effects of polymeric properties such as molecular mass, salting-out techniques employed on the physicochemical, physicomechanical properties and drug release properties of PLGA. Furthermore the study has ascertained that modified PLGA may be employed as a controlled and zero-order kinetic drug release system for drug the delivery of both water insoluble drugs, such as, melatonin and water soluble drugs, such as amitriptyline HCl.

In this study variants of PLGA scaffolds were formulated using a salting-out and subsequent cross-linking technique in accordance with a statistical design known as the Face-Centered Central Composite Design to select the optimal number of experiments needed to aid formulation optimization. The stability of the polymer during intermolecular interaction with the salting-out and subsequent cross-linking chemical inducers was established. This was achieved by evaluating the physicomechanical transitions of the PLGA scarffolds during *in vitro* degradation and the *ab initio* quantum energy calculations for PLGA unit interacting with PBS ions.

Transition in the physicomechanical properties and energy fluctuations during *in vitro* degradation of the polymer were significant predictors for scaffold intergrity. Geometric, physicochemical, physicomechanical and thermal transitions were then

analysed by Scanning electron microscopy, Fourier Transform Infra Red spectroscopy, Textural profiling and Differential Scanning Calorimetry. The influence of the salts on the physicochemical and the physicomechanical transitions of PLGA was determined and confirmed. The porosity and the fibre diameters of the scaffold that resulted from salting-out and the subsequent cross-linking displayed that the PLGA scaffold and compressed monolithic matrix system have potential to be used as drug delivery implants in the treatment of neurodegenerative disorders.

After substantial investigations of the physicochemical and the physicomechanical transitions of the scaffold, dissolution and drug release studies were conducted on melatonin (low water soluble), and amitriptyline HCl (highly water soluble) as model drugs. PLGA scaffolds were formulated, and loaded with either melatonin or amitriptyline HCl. The effects of polymeric cross-linking on the *in vitro* dissolution of melatonin-loaded PLGA scaffolds and on the *in vitro* dissolution of amitriptyline HCl from a PLGA-based compressed monolithic system for use in neurodegenerative disorders were established.

This unique surface-eroding PLGA scaffolds and the compressed monolithic discs were developed and explored for use in clinical applications. The scaffolds were optimized for their DEE, MDT and drug release rate. Kinetic modelling was also employed to explicate the mechanisms of drug release from the PLGA scaffold.

Other studies on hydrophobic polyesters, such as PLA, PGA and PLGA have implied that the rate of PLGA degradation is dependent on the hydrophobicity of the network

composition, and that the physicochemical and the physicomechanical properties are dependent on the thermoplastic nature of PLGA.

Through this study it was demonstrated that PLGA is versatile and can be manipulated through the incorporation of salts by salting-out and subsequent cross-linking. The formation of polymer–salt bonds has modified the physicochemical and the physicomechanical properties of PLGA composite structures. In particular, the resilience, hardness, and the rate of dissolution, depended mainly on the salt type and concentration.

### 7.2 Recommendations

The present mechanisms of polymer modification have produced a scaffold capable of achieving pre-determined drug release, controlled by the rate of hydration and erosion of the polymeric scaffold and compressed monolithic matrix system that depends on the pKa and concentration of the salt incorporated. The scaffold can be applied as a sustained drug delivery system over a period of 30 days (or more) for the treatment of neurodegenerative disorders. Meanwhile the compressed monolithic matrix system can be applied as a controlled drug delivery system, either over 24 hours when prepared by salting-out and subsequently cross-linking PLGA alone, or for 30 days (or more) when prepared by salting-out and subsequently cross-linking the PLGA and the drug.

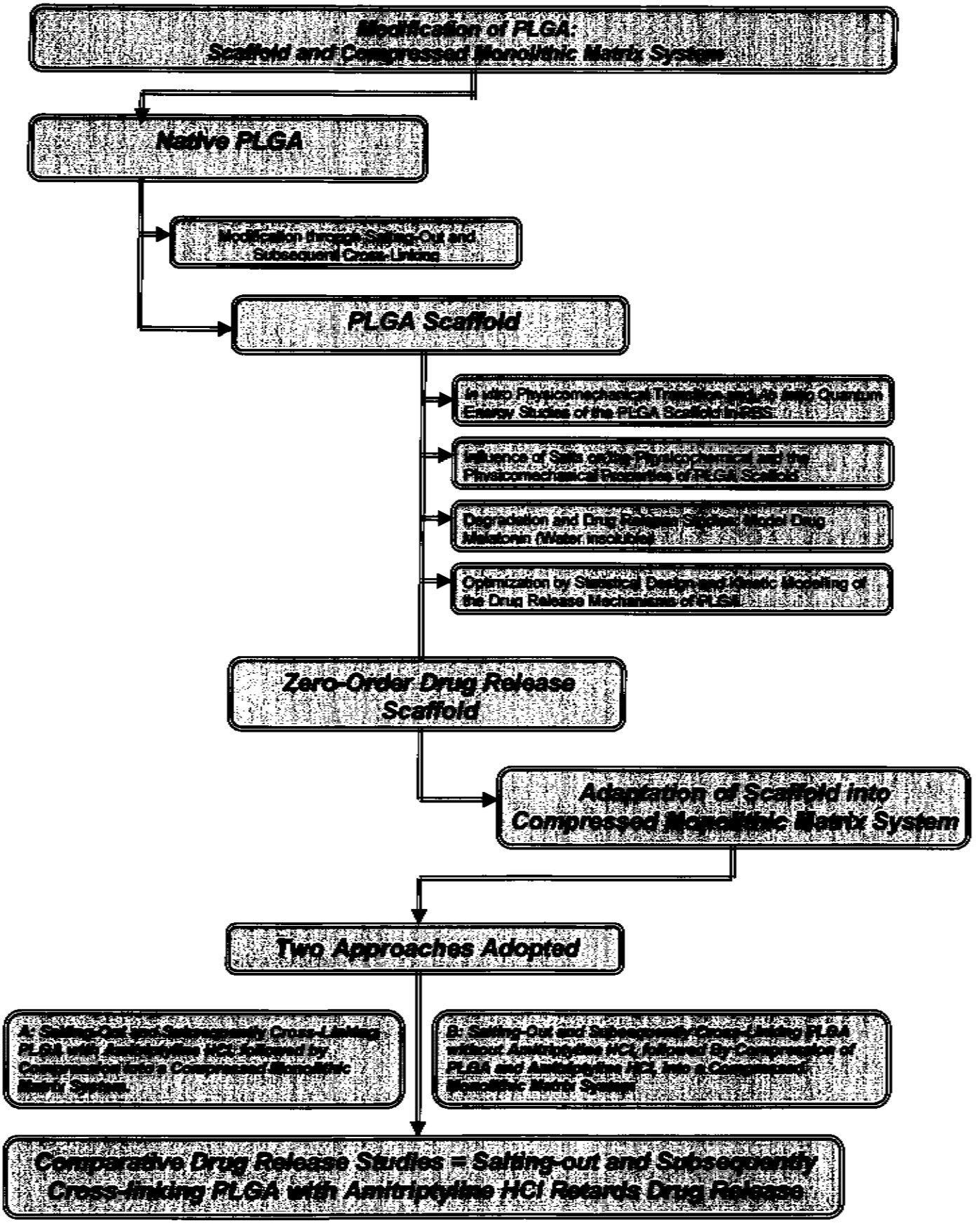
Native PLGA
PLGA Scaffold
Zero-Order Drug Release Scaffold
Two Approaches Adopted

In addition the scaffold and the compressed monolithic matrix system have properties that allow them to act as reservoirs and control the release of both hydrophobic (such as melatonin) and hydrophilic drugs (such as amitriptyline HCl). Other drugs used in the treatment of neurodegenerative disorders, such as, diclofenac an anti inflammatory and drugs for HIV-related neurodegeneration, such as, zidovudine can be incorporated into the scaffold and the compressed monolithic matrix system and delivered to the brain via implantation in the subarachnoid space. Further recommendations also include developing suitable *ex vivo*/*in vivo* models with superior mechanistic approach to further explore:

i. Dissolution and drug release mechanisms inside and outside the body.
ii. Toxicity and safety of the scaffold, such as cell-lined immunogenicity and lack of inflammatory responses when introduced to the body.

## 8. REFERENCES

Abbrent, S., Plestil, J., Hlavata, D., Lindgren, J., Tegenfeldt, J., and Wendsjö, Å., Crystallinity and morphology of PVdF–HFP-based gel electrolytes, *Polymer.*, **42(4)**, (2001), 1407-1416.

Adolfsson, A., and Nyström, C., Tablet strength, porosity, elasticity and solid state structure of tablets compressed at high loads, *Int J Pharm.*, **132(1-2)**, (1996), 95-106.

Ahmed, N., Ahmed, U., Thornalley, P.J., Hager, K., Fleischer, G., and Münch, G., Protein glycation, oxidation and nitration adduct residues and free adducts of cerebrospinal fluid in Alzheimer's disease and link to cognitive impairment, *J Neurochem* ., **92(2)**, (2005), 255-263.

Aslana, E., Camuşcua, N., and Birgörenb, B., Design optimization of cutting parameters when turning hardened AISI 4140 steel (63 HRC) with Al2O3 + TiCN mixed ceramic tool, *Materials & Design.*, **28(5)**, (2007), 1618-1622.

Almeida, S., Almeida, A., Filipe, A., Penedo, C., Rocha, A., Lainesse, A., and Vallee, F., *In vitro* disintegration and dissolution and in vivo bioequivalence of two alendronate once-weekly formulations, *Arzneimittelforschung.*, **56(2)**, (2006), 84-89.

Alvarez-Lorenzo, C., Hiratani, H., Gómez-Amoza, J.L., Martinez-Pacheco, R., Souto, C., and Concheiro, A., Soft contact lenses capable of sustained delivery of timolol, *J Pharm Sci.*, **91**, (2002), 2182–2192.

Amiji, M.A., and Sandmann, B.J., *Applied physical pharmacy*, McGraw-Hill Companies., USA., (2003).

Antikainen, O., and Yliruusi, J., Determining the compression behaviour of pharmaceutical powders from the force-distance compression profile, *Int J Pharm.*, **252**, (2003), 253-261.

Arakawa, T., and Timasheff, S.N., Mechanism of poly(ethylene glycol) interaction with proteins, *Biochemistry.*, **24**, (1985), 6756– 6762.

Arakawa, T., and Timasheff, S.N., Preferential interactions of proteins with solvent components in aqueous amino acid solutions, *Arch Biochem Biophys.*, **224(1)**, (1983), 169-177.

Asthagiri, D., Pratt, L.R., Paulaitis, M.E., and Rempe, S.B., Hydration structure and free energy of biomolecularly specific aqueous dications, including $Zn^{2+}$ and first transition row metals, *J Am Chem Soc.*, **126(4)**, (2004), 1285–1289.

Atta, A.M., Swelling behaviors of polyelectrolyte hydrogels containing sulfonate groups, *Polymers for Advanced Technologies.*, **13**, (2002), 567-576.

Avgoustakis, K., Pegylated poly(lactide) and poly(lactide-co-glycolide) nanoparticles: preparation, properties and possible applications in drug delivery, *Curr Drug Delivery.*, **1(4)**, (2004), 321-333.

Babay, D., Hoffman, A., and Benita, S., Design and release kinetic pattern evaluation of indomethacin microspheres intended for oral administration, *Biomaterials.*, **9(6)**, (1988), 482-8.

Bae Y.H., Smart Polymers in Drug Delivery, *Pharmaceutical News.*, **9(6)**, (2002), 417-424.

Bagchi, B., Chemical reaction dynamics and relaxation phenomena in one component liquids, binary mixtures and electrolyte solutions, *Current 1054 Science.*, **81(8)**, (2001), 1054-1067.

Barakat, N.S., and Radwan, M.A., *In vitro* performance of carbamazepine loaded to various molecular weights of poly (D,L-lactide-co-glycolide), *Drug Deliv.*, **13(1)**, (2006), 9-18.

Barichello, J., Morishita, M., Takayama, K., and Nagai, T., Encapsulation of hydrophilic and lipophilic drugs in PLGA nanoparticles by the nanoprecipitation method, *Drug Dev Ind Pharm.*, **25**, (1999), 471-476.

Barton, J.A. JR., Eick, J.D., and Dickson, G., Comparison of Brinell and Vickers Hardness Tests on Dental Casting Gold Alloys, *J Dent Res.*, **52(1)**, (1973), 163-169.

Bartzatt, R., Synthesis and Alkylation Activity of a Nitrogen Mustard Agent to Penetrate the Blood-Brain Barrier, *Drug Deliv.*, **1(1)**, (2004), 19-26.

Basu, A., Yang, K., Wang, M., Liu, S., Chintala, R., Palm, T., Zhao, H., Peng, P., Wu, D., Zhang, Z., Hua, J., Hsieh, M.C., Zhou, J., Petti, G., Li, X., Janjua, A., Mendez, M., Liu, J., Longley, C., Zhang, Z., Mehlig, M., Borowski, V., Viswanathan, M., and Filpula, D., Structure-function engineering of interferon-beta-1b for improving stability, solubility, potency, immunogenicity, and pharmacokinetic properties by site-selective mono-PEGylation, *Bioconjug Chem.*, **17(3)**, (2006), 618-30.

Benicewicz, B.C., and Hopper P.K., Polymers for absorbable surgical sutures, *J Bioact Compat Polym.*, **6**, (1991) 64-94.

Berthold, J., Rinaudo, M., and Salmén, S., Association of water to polar groups; estimation by an adsorption model for ligno-cellulosic materials, *Colloids and Surfaces: Part A.*, **112**, (1996), 119–131.

Blagoeva, R., and Nedev, A., Monolithic Controlled Delivery Systems: Part II. Basic Mathematical Models, *Bioautomation.*, **5**, (2006), 106 – 117.

Blanco, D., and Alonso, M.J., Protein encapsulation and release from poly (lactide-co-glycolide) microspheres: effect of the protein and polymer properties and of the co-encapsulation of surfactants, *Eur J Pharm Biopharm.*, **45(3)**, (1998), 285-94.

Blomeier, H., Zhang, X., Rives, C., Brissova, M., Hughes, E., Baker, M., Powers, A.C., Kaufman, D.B., Shea, L.D., and Lowe, W.L. Jr., Polymer scaffolds as synthetic microenvironments for extrahepatic islet transplantation, *Transplantation.*, **82(4)**, (2006), 452-459.

Bolen, D.W., and Baskakov, I.V., The osmophobic effect: natural selection of a thermodynamic force in protein folding, *J. Mol. Biol.*, **310**, (2001), 955–963.

Böstman, O., Hirvensalo, E., Makinen, J., and Rokkanen, P., Foreign-body reactions to fracture fixation implants of biodegradable synthetic polymers, *J Bone Joint Surg.*, **72B**, (1977), 592–596, 1977.

Box, G.E.P., Hunter, W.G., and Hunter, J. S., Statistics for experimenters, WileyNew York. (1978).

Broom, W. J., Parton, M. J., Vance, C. A, Russ, C., Andersen, P. M., Hansen, V., Leigh P. N., Powell, J. F., Al-Chalabi, A., and Shaw, C. E., No association of the SOD1 locus and disease susceptibility or phenotype in sporadic ALS, *Neurology.*, **63(12)**, (2004), 2419-22.

Burkoth, A.K., Burdick, J., and Anseth, K.S., Surface and bulk modifications to photocross-linked polyanhydrides to control degradation behaviour, *John Wiley & Sons, Inc.*, (2000).

Cadee, J.A., Brouwer, L.A., den Otter, W., Hennink, W.E., and van Luyn, M.J., A comparative biocompatibility study of microspheres based on crosslinked dextran or poly(lactic-co-glycolic)acid after subcutaneous injection in rats, *J Biomed Mater Res.*, **56(4)**, (2001), 600-9.

Challa, R., Ahuja, K., Ali, J., and Khar R.K., Cyclodextrins in Drug Delivery: An Updated Review, *AAPS PharmSciTech.*, **6(2)(43)**, (2005).

Chandra, A. and Bagchi, B., Chemical Reaction Dynamics of Some Simple Molecules in Solution, *J. Phys. Chem.*, 2000, 9067.

Cheng, A.L., Liu, N., Yue, Y.F., Jiang, Y.W., Gao, E.Q., Yan, C.H., and He, M.Y., Unprecedented 3D entanglement of 1D zigzag coordination polymers leading to a robust microporous framework, *Chem Commun (Camb).*, **4**, (2007), 407-409.

Chen, C., Yu, C.H., Cheng, Y.C., Yu, P.H., and Cheung, M.K., Biodegradable nanoparticles of amphiphilic triblock copolymers based on poly(3-hydroxybutyrate) and poly(ethylene glycol) as drug carriers, *Biomaterials.*, **27(27)**, (2006), 4804-14.

Cheung, R.Y., Ying, Y., Rauth, A.M., Marcon, N., and Yu Wu, X., Biodegradable dextran-based microspheres for delivery of anticancer drug mitomycin C, *Biomaterials.*, **26(26)**, (2005), 5375-85.

Chilamkurti, R.N., Rhodes, C.T., and Schwartz, J.B., Compression properties of formulations containing matrix and drug, *Pharm. Acta Helv*, **58**, (1983), 146-152.

Cho, H.Y., Kang, H.A., and Lee, Y.B., Pharmacokinetics and bioequivalence evaluation of two gabapentin preparations after a single oral dose in healthy Korean volunteers, *Int J Clin Pharmacol Ther.*, **44(8)**, (2006), 386-92.

Chowdhury, E.H., and Akaike, T., Bio-functional inorganic materials: an attractive branch of gene-based nano-medicine delivery for 21st century, *Curr Gene Ther.*, **5(6)**, (2005), 669-676.

Chung, T.W., Tsai, Y.L., Hsieh, J.H., and Tsai, W.J., Different ratios of lactide and glycolide in PLGA affect the surface property and protein delivery characteristics of the PLGA microspheres with hydrophobic additives, *J Microencapsul.*, **23(1)**, (2006), 15-27.

Cilurzo, F., Selmin, F., Minghetti, P., and Montanari, L., The effects of bivalent inorganic salts on the mucoadhesive performance of a polymethylmethacrylate sodium salt, *Int J Pharm.*, **301(1-2)**, (2005), 62-70.

Clesla, M.A., and Roberts, J.E., Meta-analysis of the relationship between HIV infection and risk for depressive disorders, *Am J of Psychiatry.*, **158**, (2001), 725-730.

Cochran, W.G., and Cox, G.M., Experimental designs, 2nd edn., *John Wiley and sons New York*, (1992), 335-375.

Conti, S., Maggi, L., Segale, L., Ochoa Machiste, E., Conte, U., Grenier, P., and Vergnault, G., Matrices containing NaCMC and HPMC 1, Dissolution performance characterization., *Int J Pharm.*, **333(1-2)**, (2007), 136-42.

Coughlan, D.C., and Corrigan, O.I., Drug-polymer interactions and their effect on thermoresponsive poly(N-isopropylacrylamide) drug delivery systems, *Int J Pharm.*, **313(1-2)**, (2006), 163-74.

Czimerova, A., Jankovic, L., and Bujdak, J., Effect of the exchangeable cations on the spectral properties of methylene blue in clay dispersions, *J Colloid Interface Sci.*, **274(1)**, (2004),126-32.

D'Agostino, D.P., Putnam, R.W., and Dean, J.B., Superoxide ({middle dot}O2-) production in CA1 neurons of rat hippocampal slices exposed to graded levels of oxygen, *J Neurophysiol.*, 2007.

Dashevsky, A., Wagner, K., Kolter, K., and Bodmeier, R., Physicochemical and release properties of pellets coated with Kollicoat SR 30 D, a new aqueous polyvinyl acetate dispersion for extended release, *Int J Pharm.*, **16;290(1-2)**, (2005), 15-23.

Dave, B.S., Amin, A.F., and Patel, M.M., Gastroretentive Drug Delivery System of Ranitidine Hydrochloride: Formulation and *In Vitro* Evaluation, *AAPS PharmSciTech.*, **5(2)(34)**, (2004).

Dayal, P., Pillay, V., Babu, R.J., and Singh, M., Box-Behnken experimental design in the development of a nasal drug delivery system of model drug hydroxyurea: characterization of viscosity, *in vitro* drug release, droplet size, and dynamic surface tension, *AAPS PharmSciTech.*, **6(4)**, (2005), E573-E585.

De, K., Aluru, N. R., Johnson, B., Crone, W. C., Beebe, D J., and Moore J., Equilibrium Swelling and Kinetics of pH-Responsive Hydrogels: Models, Experiments, and Simulations, *Journal of MicroelectroMechanical Systems.*, **11(5)**, 2002, 544-555.

De Blaey, C.J., and Polderman, J., Compression of pharmaceuticals: 2: Registration and determination of force-displacement curves, *Pharm. Weekbl.*, **106**, (1971), 57-65.

De Jong, W.H., Bergsma, J.E., Robinson, J.E., and Bos, R.R.M., Tissue response to partially *in vitro* predegraded poly-L-lactide implants, *Biomaterials.*, **26(14)**, (2005), 1781-1791.

Deng, M., and Uhrich, K.E., Effects of *in vitro* degradation on properties of poly (DL-lactide-co-glycolide) pertinent to its biological perfomance, *Journal of Materials Science: Materials in Medicine.*, **13**, (2002),1091-1096.

DeLuca, P.P., Mehta R.C., Hausberger A.G., and Thanoo, B.C., Biodegradable polyesters for drug and polypeptide delivery, In: El-Nokaly, M.A., Piatt, D.M., Charpentier, B.A., eds. Polymeric drug delivery systems. Washington, DC, *American Chemical Society.*, (1993), 53-79.

Dhanikula, A.B., and Panchagnula, R., Development and characterization of biodegradable chitosan films for local delivery of Paclitaxel, AAPS J., **6(3)**, (2004), e27.

Dickers, K.J., Milroy, G.E., Huatan, H., and Cameron, R.E., The use of biodegradable polymers in drug delivery systems to provide pre-programmed release, *The drug delivery companies report autumn/winter, PharmaVentures Ltd.*, (2002), 1-3.

Di Noto, V., and Zago, V., Inorganic-Organic Polymer Electrolytes Based on PEG400 and Al[OCH(CH3)2]3., I. Synthesis and Vibrational Characterizations, *J. Electrochem. Soc.*, **151(2)**, (2004), A216-A223.

Ditchfield, R., Hehre, W. J., and Pople, J. A., Self-consistentmolecular orbital theory IX, An extended Gaussian type basisfor molecular orbital studies of organic molecules, *J. Chem.Phys.*, **54**, (1971)724-772.

Donato, P., Stancanelli, R., Calabrò, M.L., Tommasini, S., Cutroneo, P., Guardo, M., Pagano, B., Chimirri, A., Ficarra, P., and Ficarra, R., Optimization of a LC method for the enantioseparation of a non-competitive glutamate receptor antagonist, by experimental design methodology, *Journal of Pharmaceutical and Biomedical Analysis.*, (2006).

Donohue, J.M., Houck, E.C., and Myers, R.H., Some optimal simulation designs for estimating quadratic response surface functions, *Proceedings of the 1990 Winter Simulation Conference.*, Balci, O., Sadowski, R. P., Nance R.E., (editorss)., (1990).

Dong, W.Y., Körber, M., Esguerra, V.L., and Bodmeier, R., Stability of poly(d,l-lactide-co-glycolide) and leuprolide acetate in in-situ forming drug delivery systems, *Journal of Controlled Release*, **115 (2)**, (2006), 158-167.

Dorta, M.J., Santovena, A., Llabres, M., and Farina, J.B., Potential applications of PLGA film-implants in modulating *in vitro* drugs release, *Int. J. Pharm.*, **28**, (2002), 149-156.

Eerikanen, H., Kauppinen, E.L., and Kansikas, J., Polymeric Drug Nanoparticles Prepared by an Aerosol Flow Reactor Method, *Pharm Res.*, **21**, (2004),136-143.

Efentakis, M., Koutlis, A., and Vlachou, M., Development and evaluation of oral multiple –unit and Single-Unit Hydrophilic Controlled release systems, *AAPS PharmSciTech.*, **1(4)**, 2000.

Ennett, A.B., Kaigler, D., and Mooney, D.J., Temporally regulated delivery of VEGF *in vitro* and *in vivo*, *J Biomed Mater Res A*, **79(1)**, 2006, 176-84.

Fahmy, T.M., Samstein, R.M., Harness, C.C., and Mark, S.W., Surface modification of biodegradable polyesters with fatty acid conjugates for improved drug targeting, *Biomaterial*, **26(28)**, (2005), 5727-36.

Fell, J.T., and Newton, J.M., The tensile strength of lactose tablets, *J. Pharm. Pharmacol.*, **20**, (1968), 657-658.

Feng, S.S., Ruan, G., and Li, Q.T., Fabrication and characterization of a novel drug delivery device liposomes-microspheres, *LIM.*, **25**, (2004), 5181-5189.

Fineberg, N.A., and Craig, K.J., Pharmacological treatment for obsessive–compulsive disorder Psychiatry, **6(6)**, (2007), 234-239.

Franson, N.M., and Peppas, N.A., The Swelling Interface Number as a Criterion for Prediction of Diffusional Solute Release Mechanism in Swelling Polymers, *J Polym Sci Polym, Phys Ed.,* **21**, (1983), 983-987.

Friedman, H.L., Lewis-Randall to McMillan-Mayer conversion for the thermodynamic excess functions of solutions, Part I. Partial free energy coefficients, *Journal of Solution Chemistry.*, **1(5)**, (1972), 387-412.

Fries, W., and Schlapp, M., Modifying the release of gentamicin from microparticles using PLGA blend, *Pharm. Dev. Technol.*, **7**, (2002), 235-248.

Fu, K., Pack, D.W., Klibanov, A.M., and Langer, R., Visual evidence of acidic environment within degrading Poly (lactic-co-glycolic acid) (PLGA) microspheres, *Pharmaceutical Research*, **17(1, 2)**, (2000).

Galinski, E.A., Stein, M., Amendt, B., and Kinder, M., The kosmotropic (structure-forming) effect of compensatory solutes, Comp, *Biochem Physiol.*, **117A**, (1977), 357– 365.

Gao, J., Niklason, N., and Langer, R., Surface hydrolysis of poly(glycolic acid) meshes increases the seeding density of vascular smooth muscle cells, *J Biomed Mater Res.*, **42**, (1998), 417–424.

Gao, H., Jiang, J., Wilson, B., Zhang, W., Hong, J., and Liu, B., Microglial activation-mediated delayed and progressive degeneration of rat nigral dopaminergic neurons: relevance to Parkinson's disease, *J Neurochem.*, **81(6)**, (2002), 1285-97.

Gao, Q., Xue, S., Doneanu, C.E., Shaffer, S.A., Goodlett, D.R., and Nelson, S.D., Pro-cross-link. Software tool for protein cross-linking and mass spectrometry, *Anal Chem.*, **78(7)**, (2006), 2145-2149.

Garg, A., and Kokkoli, E., Characterizing particulate drug-delivery carriers with atomic force microscopy, *Engineering in Medicine and Biology Magazine, IEEE.*, **24(1)**, (2005), 87-95.

Garvin, K., and Feschuk, C., Polylactide-polyglycolide antibiotic implants, *Clin Orthop Relat Res.*, **437**, (2005), 105-110.

Gebrekidan, S., Woo, H.B., and DeLuca, P.P., Formulation and *in vitro* transfection efficiency of poly (D, L-lactide-co-glycolide) microspheres containing plasmid DNA for gene delivery, *AAPS PharmSciTech.*, **1(4)**, (2000), 28.

Georges, P.C., Miller, W.J., Meaney, D.F., Sawyer, E.S., and Janmey, P.A., Matrices with compliance comparable to that of brain tissue select neuronal over glial growth in mixed cortical cultures, *Biophys J.*, **90(8)**, (2006), 3012-3018.

Gnanakaran, S., Lim, M., Volk M., Gooding, E., Kholodenko, Y., and Hochstrasser R.M., Philosophical Transactions: Mathematical, Physical and Engineering Sciences, *Ultrafast Processes in Chemistry and Biology*, **356(1736)**, (1998), 377-388.

Gohel, M.C., Amin, A.F., Patel, K.V., and Panchal, M.K., Studies in release behavior of diltiazem HCl from matrix tablets containing (hydroxypropyl)methyl cellulose and xanthan gum, *Boll Chim Farm.*, **141(1)**, (2002), 21-28.

Gomez-Gaete, C., Tsapis, N., Besnard, M., Bochot, A., and Fattal, E., Encapsulation of dexamethasone into biodegradable polymeric nanoparticles, *Int J Pharm.*, **331(2)**, (2007), 153-159.

Gopferich, A., Polymer degradation and erosion: mechanisms and application, *Eur J Pharm Biopharm.*, **42(1)**, (1996), 1–11.

Göpferich, A., and Langer, R., Modeling monomer release from bioerodible polymers, *J Controlled Release.*, **33**, (1995), 55–69.

Govender, T., Stolnik, S., Garnett, M.C., Illum, L., and Davis, S.S., PLGA nanoparticles prepared by nanoprecipitation: drug loading and release studies of a water soluble drug, *J Control Release.*, **57**, (1999), 171-185.

Grassi, M., and Grassi, G., Mathematical Modeling and Controlled Drug Delivery: Matrix Systems, *Current Drug Delivery.*, **2(1)**, (2005), 97-116.

Gul, B.F., Takac, S.H., and Ozdamar, T., Solvent-catalyst interactions in the decomposition process of 2-isopropylnaphthalenehydroperoxide into 2-naphthol and acetone, *Applied Catalysis A: General.*, **183(2)**, (1999), 377-393(17).

Gulati, K., Ray, A., and Vijayan, V.K., Free radicals and theophylline neurotoxicity: an experimental study, *Cell Mol Biol (Noisy-le-grand).*, **53(5)**, (2007), 42-52.

Guo, Q. Y., Chan, L. W., and Heng, P. W. S., Investigation of the release of aspirin from spray-congealed micro-pellets, *Journal of Microencapsulation.*, **22(3)**, (2005), 245-251(7).

Haddadi, A., Farboud, E.S., Erfan, M., and Aboofazeli, R., Preparation and characterization of biodegradable urea-loaded microparticles as an approach for transdermal delivery, *J Microencapsul.*, **23(6)**, (2006), 698-712.

Harland, R.S., Gazzaniga, A., Sangalli, M.E., Colombo, P., and Peppas, N.A., Drug/polymer matrix swelling and dissolution, *Pharm Res.*, **5**, (1988), 488-494.

Hasirci, V., Berthiaume, F., Bondre, S.P., Gresser, J.D., Trantolo, D.J., Toner M., and Wise, D.L., Expression of liver-specific functions by rat hepatocytes seeded in treated poly(lactic-*co*-glycolic) acid biodegradable foams, *Tissue Eng.*, **7**., (2001), 385–394.

Hayden, M.R., Ehrlich, R., Parker, H., Ferera, S.J., Social perspectives in Huntington's chorea, *S Afr Med J.*, **58(5)** (1980), 201-203.

Heckel, R.W., Density-pressure relationships in powder compaction, Trans. *Metall. Soc. AIME,* **221**, (1961a), 671-675.

Heckel, R.W., An analysis of powder compaction phenomena, *Trans. Metall. Soc. AIME*, **221**, (1961b), 1001-1008.

Heckmann, J.M., Low, W.C., de Villiers, C., Rutherfoord, S., Vorster, A., Rao, H., Morris, C.M., Ramesar, R.S., and Kalaria, R.N., Novel presenilin 1 mutation with profound neurofibrillary pathology in an indigenous Southern African family with early-onset Alzheimer's disease, *Brain.*, **127(Pt 1)**, (2004), 133-142.

Hehre, W.J., Stewart, R.F., and Pople, J.A., Self-consistentmolecular orbital methods. I. Use of Gaussian expansions of Slater-type orbitals, *J. Chem.*, **51**, (1969), 2657-2664.

Helminen, A., Kylmä, J., Tuominen, J., and Seppälä, J. V., Effect of structure modification on rheological properties of biodegradable poly (ester-urethane), *Polym. Eng. Sci.*, **40**, (2000), 1655-1662.

Higuchi, T., Rate of release of medicaments from ointment bases containing drugs in suspension, *J Pharm Sci.*, **50**, (1961), 874-875.

Higuchi, T., Mechanism of sustained-action medication., Theoretical analysis of rates of release of solid drug dispersed in solid matrices, *J. Pharm. Sci.*, **52(12)**, (1963), 1145–1149.

Higuchi, T., Rao, A.N., Busse, L.W., and Swintosky, J.V., The physics of tablet compression: II. The influence of degree of compression on properties of tablets, *J. Am. Pharm. Assoc. Sci. Ed.*, **42**, (1953), 194-200.

Hite, M., Federici C., Turner S., and Fassihi, R., novel design of a self-correcting monolithic controlledrelease delivery system for Tramadol, *Drug Delivery Technology*., (2003), 1-13.

Hoblitzell, J., and Rhodes, C.T., Instrumented tablet press studies on the effect of some formulation and processing variables on the compression process, *Drug Dev. Ind. Pharm.*, **16**, (1990), 469-507.

Hutchinson, F.G., and Furr, B.J.A., Biodegradable polymer systems for the sustained release of polypeptides, *Journal of Controlled Release*, **13(2-3)**, (1990), 279-294.

Horvath, A.L., Handbook of aqueous electrolyte Solutions, *John Wiley and Sons, New York*, (1985).

Hsu, S.H., Chang, S.H., Yen, H.J., Whu, S.W., Tsai, C.L., and Chen, D.C., Evaluation of biodegradable polyesters modified by type II collagen and Arg-Gly-Asp

as tissue engineering scaffolding materials for cartilage regeneration, *Artif Organs.*, **30(1)**, (2006), 42-55.

Huang, R., Chen, G., Sun, M., and Gao, C., A novel composite nanofiltration (NF) membrane prepared from graft copolymer of trimethylallyl ammonium chloride onto chitosan (GCTACC)/poly(acrylonitrile) (PAN) by epichlorohydrin cross-linking, *Carbohydr Res.*, **341(17)**, (2006), 2777-2784.

Huang, S.F., Chen, J.L., Yeh, M.K., and Chiang, C.H., Physicochemical properties and in vivo assessment of timolol-loaded poly (D,L-lactide-co-glycolide) films for long-term intraocular pressure lowering effects, *Ocular Pharmacol Ther.*, **21(6)**, (2005), 445-453.

Huang, Y., Molecular and cellular mechanisms of apolipoprotein E4 neurotoxicity and potential therapeutic strategies, *Curr Opin Drug Discov Devel.*, **9(5)**, (2006), 627-41.

Ishihara, T., Izumo, N., Higaki, M., Shimada, E., Hagi, T., Mine, L., Ogawa, Y., and Mizushima, Y., Role of zinc in formulation of PLGA/PLA nanoparticles encapsulating betamethasone phosphate and its release profile, *J Control Release.*, 105**(1-2)**, (2005), 68-76.

Ivanoiu, A., Adam, S., Van der Linden, M., Salmon, E., Juillerat, A.C., Mulligan, R., and Seron, X., Memory evaluation with a new cued recall test in patients with mild cognitive impairment and Alzheimer's disease, *J Neurol.*, **252(1)**, (2005), 47-55.

Iwatsubo, T., The Gamma-secretase Complex: Machinery for Intramembrane Proteolysis, *Curr Opin Neurobiol.*, **14**, 379-383.

Izaki, M., Miyamoto, N., Nakae, A., Hasegawa, T., Watase, S., Chigane, M., Fujiwara, Y., Ishikawa, M., and Enomoto, H., Martensitic iron-carbon-boron alloy electrodeposit with improved mechanical properties, *J. Electrochem. Soc.*, **149(7)**, (2002), C370-C374.

Izutsu, K. Heller, M.C., Randolph, T.W., and Carpentera J. F., Effect of salts and sugars on phase separation of polyvinylpyrrolidone-dextran solutions induced by freeze-concentration, *J. Chem. Soc., Faraday Trans.*, **94(3)**, (1998), 411È417.

Izutsu, K., and Aoyagi, N., Effect of inorganic salts on crystallization of poly (ethylene glycol) in frozen solutions, *Int J Pharm.*, **288(1)**, (2005), 101-118.

Jackson, J.K., Zhang, X., Liewens, S., Hunter, W.L., and Burt, H.M., The Characterization of Novel Polymeric Paste Formulations for Intratumora Delivery, *Int J Pharm.*, **270**, (2004)185-198.

Jain, R.A., The Manufacturing Techniques of Various Drug Loaded Biodegradable Poly(Lactide-Co-Glycolide) (PLGA) devices, *Biomaterials.*, **21**, (2000), 2475-2490.

Jain, R.A., Rhodes, C.T., Railkar, A.M., Malick, A.W., and Shah, N.H., Controlled delivery of drugs from a novel injectable in-situ formed biodegradable PLGA microsphere system, *J. Microencapsul.*, **17(3)**, (2000), 343–362.

Jadoun, R., Kumar, P., Mishra, B., and Mehta, R., Optimization of process parameters for ultrasonic drilling of advanced engineering ceramics using the Taguchi approach, *Engineering Optimization.*, **38(7)**, (2006), 771-787(17).

Jamzad, S., and Fassihi, R., Development of a controlled release low dose class II drug-Glipizide, *International Journal of Pharmaceutics.*, **312 (1-2)**, (2006), 24-32.

Jayakumar, R., Nwe, N., Tokura, S., and Tamura, H., Sulfated chitin and chitosan as novel biomaterials, *International Journal of Biological Macromolecules.*, **40(3)**, (2007), 175-181.

Jeong, Y.I., Choi, K.C., and Song, C.E., Doxorubicin release from core-shell type nanoparticles of poly(DL-lactide-co-glycolide)-grafted dextran, *Arch Pharm Res.*, **29(8)**, (2006),712-719.

Johansen, P., Men, Y., Merkle H.P., and Gander, B., Revisiting PLA/PLGA microspheres: an analysis of their potential in parenteral vaccination, *Eur J Pharm Biopharm.*, **50(1)**, (2000), 129–146.

Jones, D.S., Andrew, G.P., and Gorman, S.P., Characterization of crosslinking effects on the physicochemical and drug diffusional properties of cationic hydrogels

designed as bioactive urological biomaterials, *J Pharm Pharmacol.*, **57(10)**, (2005), 1251-1259.

Ju, Y.M., Oh, S.H., Lee, K.H., Choi, S.W., Cho C.S., and Lee, J.H., A study on biodegradable polymer scaffolds with uniform 3-dimensional porosity for artificial cartilage, *Biomater Res.*, **4**, (2000), 52–59.

Judas, D., Fradet, A., and Marechal, E., Thickening of polyester resins with MgO: structural study of a model magnesium carboxylate, *Polymer Bulletin.*, **16(1)**, (1986), 13-17.

Julien, C.L., Thompson, J.C., Wild, S., Yardumian, P., Snowden, J.S., and Craufurd, D., Psychiatric disorders in pre-clinical Huntington's disease, *J. of Neurology, Neurosurgery, and Psychiatry.*, (2006), In Press.

Kakinoki, s., Yasuda, C., Kaetsu, I., Uchida, K., Yukutake, K., Nakayama, M., Fujjie, S., Kuroda, D., Kato, M., and Ohyanagi, H., Preparation of poly-lactic acid microspheres containing the angiogenesis inhibitor TNP-470 with medium-chain triglyceride and the *in vitro* evaluation of release profiles, *Eur J Pharm Biopharm.*, **55(2)**, (2003), 155-60.

Kalantzi, L., Reppas, C., Dressman, J.B., Amidon, G.L., Junginger, H.E., Midha, K.K., Shah, V.P., Stavchansky, S.A., and Barends, D.M., Biowaiver monographs for immediate release solid oral dosage forms: acetaminophen (paracetamol), *J Pharm Sci.*, **95(1)**, (2006), 4-4.

Kang, E.T., Neoh, K.G., Shi, J.L., Tan, K.L., and Liaw, D.J., Surface Modification of Polymers for Adhesion Enhancement, *Polymers for Advanced Technologies.*, **10**, (1999), 20-29.

Karatas, A., and Baykara, T., Studies on Indomethacin Inserts Prepared by Water-soluble Polymers-II. The Relation Between Dissolution Rate and Swelling Behaviour II, *Farmaco.*, **56**, (2001), 197-202.

Kato, M., Kinoshita, H., Enokita, M., Hori, Y., Hashimoto, T., Iwatsubo, T., and Toyo'oka, T., Analytical Method for beta-Amyloid Fibrils Using CE-Laser Induced Fluorescence and Its Application to Screening for Inhibitors of beta-Amyloid Protein Aggregation, *Anal Chem.*, **79(13)**, (2007), 4887-4891.

Katz, J., Developments in medical polymers for biomaterials applications, *Biomaterials.*, **122**, (2001).

Khan, M.Z., Rausl, D., Radosevic, S., Filic, D., Danilovski, A., Dumic, M., and Knezevic, Z., Classification of torasemide based on the biopharmaceutics classification system and evaluation of the FDA biowaiver provision for generic products of CLASS I drugs, *J Pharm Pharmacol.*, **58(11)**, (2006), 1475-82.

Kikwai, L., Kanikkannan, N., Babu, R.J., and Singh, M., Effect of vehicles on the transdermal delivery of melatonin across porcine skin *in vitro*, *Journal of Controlled Release.*, **83**, (2002), 307–311.

Killian, D.M., Gharat, L., and Chikhale, P.J., Modulating blood-brain barrier interactions of amino acid-based anticancer agents, *Drug Deliv.*, **7(1)**, (2000), 21-5.

Kim, H., and Fassihi, R., Application of a binary polymer system in drug release rate modulation II. Influence of formulation variables and hydrodynamic conditions on release kinetics, *J Pharm.*, **86**, (1997), 323-328.

Kim, S.S., Park, M.S., Gwak, S.J., Choi, C.Y., and Kim, B.S., Accelerated bonelike apatite growth on porous polymer/ceramic composite scaffolds *in vitro*, *Tissue Eng.*, **12 (10)**, (2006), 2997-3006.

Kimura, K., Sakamoto, H., and Nakamura, T., Application of photoresponsive polymers carrying crown ether and spirobenzopyran side chains to photochemical valve, *J Nanosci Nanotechnol.*, **6(6)**, (2006), 1741-1749.

King, M.E., Can tau filaments be both physiologically beneficial and toxic? *Biochim Biophys Acta.*, **1739(2-3)**, (2005), 260-267.

Kiortsis, S., Kachrimanis, K., Broussali, T., and Malamataris, S., Drug release from tableted wet granulations comprising cellulosic (HPMC or HPC) and hydrophobic component, *Eur J Pharm Biopharm.*, **59(1)**, (2005), 73-83.

Kissel, T., Li, Y., and Unger, F., ABA-triblock copolymers from biodegradable polyester A-blocks and hydrophilic poly(ethylene oxide) B-blocks as a candidate for

in situ forming hydrogel delivery systems for proteins, *Adv Drug Deliv Rev.*, **54(1)**, (2002), 99-134.

Korsemeyer, R., Gurny, R., and Peppas, N., Mechanisms of solute release from porous hydrophilic polymers, *Int J Pharm.*, **15**, (1983), 25-35.

Kranz, H., Ubrich N., Maincent P., and Bodmeier R., Physicomechanical properties of biodegradable Poly(D,L-lactide) and Poly(D,L-lactide-co-glycolide) Films in the Dry and Wet States, *J Pharm Sci.*, **89(12)**, (2000), 1558-1556.

Krycer, I., Pope, D.G., and Hersey, J.A., The interpretation of powder compaction data- a critical review, *Drug Dev. Ind. Pharm.*, **8**, (1982), 307-342.

Kuentz, M., and Leuenberger, H., A new model for the hardness of a compacted particle system, applied to tablets of pharmaceutical polymers, *Powder* Technology., **111**, (2000), 145-153.

Kulbatski, I., Mothe, A.J., Nomura, H., and Tator, C.H., Endogenous and exogenous CNS derived stem/progenitor cell approaches for neurotrauma, *Curr Drug Targets.*, **6(1)**, (2005), 111-26.

Kumar, V.V., Chandrasekar, D., Ramakrishna, S., Kishan, V., Rao, Y.M., and Diwan, P.V., Development and evaluation of nitrendipine loaded solid lipid nanoparticles: influence of wax and glyceride lipids on plasma pharmacokinetics, *Int J Pharm*, **335(1-2)**, (2007), 167-175.

Kushibiki, T., and Tabata, Y., Preparation of poly(ethylene glycol)-introduced cationized gelatin as a non-viral gene carrier, *J Biomater Sci Polym Ed.*, **16(11)**, (2005), 1447-61.

Kuo, Y.C., and Leou, S.N., Effects of composition, solvent, and salt particles on the physicochemical properties of polyglycolide/poly (lactide-co-glycolide) scaffolds, *Biotechnol Prog.*, **22(6)**, (2006), 1664-70.

Kydonieus, A., Treatise on Controlled Drug Delivery: Fundamentals, *Optimization, Applications.*, New York, NY: *CRC Press.*, (1992).

Laeschke, K., Biocompatibility of microparticles into soft tissue fillers, *Semin Cutan Med Surg.*, **23(4)**, (2004), 214-217.

Laks, J., Rocha, M., Capitao, C., Domingues, R.C., Ladeia, G., Lima, M., and Engelhardt, E., Functional and motor response to low dose olanzapine in Huntington's disease: case report, *Arq Neuropsiquiatr.*, **62(4)**, (2004), 1092-1094.

Lallemand, F., Felt-Baeyens, O., Besseghir, K., Behar-Cohen, F., and Gurny, R., Cyclosporine A delivery to the eye: a pharmaceutical challenge, *Eur J Pharm Biopharm.*, **56(3)**, (2003), 307-18.

Langa, K.M., Larson, E.B., Wallace, R.B., Fendrick, A.M., Foster, N.L., Kabeto, M.U., Weir, D.R., Willis, R.J., and Herzog, A.R., Out-of-pocket Health Care Expenditures

Among Older Americans with Dementia, *Alzheimer Dis Assoc Disord.*, **18**, (2004) 90-98.

Langer, R., and Folkman, J., Polymers for the sustained release of proteins and other macromolecules, *Nature.*, **263(5580)**, (1976), 797–800.

Langer, R.S., and Peppas, N.A., Present and future applications of biomaterials in controlled drug delivery systems, *Biomaterials.*, **2**, (1981), 201–214.

Langer, R., and Vacanti, J.P., Tissue engineering, *Science.*, **260**, (1993), 920–926.

Langer R. S., and Wise D. L., Medical Applications of Controlled Release, Applications and Evaluation, I, II, *CRC Press, Boca Raton, Florida.*, **1**, (1984), 41-67.

Lee, S.H., Zhang, Z., and Feng, S.S., Nanoparticles of poly(lactide)-tocopheryl polyethylene glycol succinate (PLA-TPGS) copolymers for protein drug delivery, *Biomaterials.*, 2007.

Lee, V.M., Goedert, M., and Trojanowski, J.Q., Neurodegenerative tauopathies, *Annu. Rev. Neurosci.*, **24**, (2001), 1121-1159.

Lefaucheur, J.P., Motor cortex dysfunction revealed by cortical excitability studies in Parkinson's disease: influence of antiparkinsonian treatment and cortical stimulation, *Clin Neurophysiol .*,**116(2)**, (2005), 244-253.

Lehnig, M., and Kirsch, M., $^{15}$N-CIDNP investigations during tryptophan, N-acetyl-L-tryptophan, and melatonin nitration with reactive nitrogen species, *Free Radical Research*, **41(5)**, (2007), 523–535.

Lewis, G.A., Mathieu D., and Phan-Tan-Luu, R., Pharmaceutical Experimental Design, *Marcel Dekker.*, New York., (1999).

Li, J., Li, X., Ni, X., Wang, X., Li, H., and Leong, K.W., Self-assembled supramolecular hydrogels formed by biodegradable PEO-PHB-PEO triblock copolymers and alpha-cyclodextrin for controlled drug delivery., *Biomaterials.*, **27(22)**, (2006), 4132-4140.

Li, M.Y., Bidez, P., Guterman-Tretter, E., Guo, Y., MacDiarmid, A.G., Lelkes, P.I., Yuan, X.B., Yuan, X.Y., Sheng, J., Li, H., Song, C.X., and Yen, W., Research progresses on electroactive and electrically conductive polymers for tissue engineering scaffolds, *Zhongguo Yi Xue Ke Xue Yuan Xue Bao.*, **28(6)**, (2006), 845-848.

Li, S., Hydrolytic degradation characteristics of aliphatic polyesters derived from lactic and glycolic acids, *J Biomed Mater Res.*, **48(3)**, (1999), 342-53.

Li, S., and Liu, X., Development of polymeric nanoparticles in the targeting of drug carriers, *Sheng Wu Xi Xue Gong Cheng Xue Za Zhi.*, **3**, (2004), 495-497.

Li, S., and Vert, M., Biodegradation of aliphatic polyesters, in: Scott, G., and Gilead, D., *Degradable Polymers.*, *London: Chapman and Hall.*, **Ch 4**, (1995), 43–87.

Limviphuvadh, V., Tanaka, S., Goto, S., Ueda, K., and Kanehisa, M., The commonality of protein interaction networks determined in Neurodegenerative disorders (NDDs), *Bioinformatics.*, **307(1-8)**, (2007).

Liu, L., Won, Y.J., Cooke, P.H., Coffin, D.R., Fishman, M.L., Hicks, K.B., and Ma, P.X., Pectin/poly(lactide-co-glycolide) composite matrices for biomedical applications, *Biomat.*, **25(16)**, (2004), 3201-3210.

Liu, W., Zhu, Y.K., and Ma, L., The oxidative DNA damage of monocytes and its *in vitro* repair by melatonin in patients with tuberculous pleurisy, *Zhonghua Nei Ke Za Zhi.*, **46(3)**, (2007), 213-216.

Lo, J. A., and Lee, W.G., Effect of surfactant film on solubility of hydrophobic organic compounds in fog droplets., *Chemosphere.*, **33(7)**, (1996),1391-1408.

Luchsinger, J.A., and Mayeux, R., Cardiovascular risk factors and alzheimer's disease, *Curr Atheroscler Rep.*, **6**, (2004), 261-266.

Maccarini, M., Steitz, R., Himmelhaus, M., Fick, J., Tatur, S., Wolff, M., Grunze, M., Jane Ccaron Ek, J., and Netz, R.R., Density Depletion at Solid-Liquid Interfaces: a Neutron Reflectivity Study, *Langmuir.*, **23(2)**, (2007), 598-608.

Mani, N., Jun, H. W., Microencapsulation of a hydrophilic drug into a hydrophobic matrix using a salting-out procedure., I: Development and optimization of the process using factorial design, *J Microencapsulation.*, **21(2)**, (2004), 125-135(11).

Manjubala, L., Woesz1, A., Pilz, C., Rumpler, M., Fratzl-zelman, N., Roschger, P., stampfl, J., and Fratzl, P., Biomimetic mineral-organic composite scaffolds with controlled internal architecture, *J mat sci: mat in med.*, **16**, (2005), 1111-1119.

Manzo, R.H., Olivera, M.E., Amidon, G.L., Shah, V.P., Dressman, J.B., and Barends, D.M., Biowaiver monographs for immediate release solid oral dosage forms: Amitriptyline Hydrochloride, *Journal of Pharmaceutical Sciences*, **95(5)**, (2006), 966-973.

Marcus, Y., Ion properties, *Marcel Dekker Inc.*, New York (1997).

Mariette, B., Coudane, J., and Vert, M., Interactions of GRF(1-29)NH2 with plasma proteins and their effects on the release of the peptide from a PLAGA matrix, *J Control Release.*, **106(3)**, (2005), 253-62.

Martinez-Paracheo, R., Vila-Jato, J.L., Souto, C., and Gomez-Amoza, J.L., Prediction of tablet properties by compression force-time profile parameters, *Drug Dev. Ind. Pharm.*, **16**, (1990), 231-241.

Martin-Garcia, E., Darbra, S., and Pallares, M., Involvement of neurosteroids in normal and pathological behaviour, *Rev Neurol.*, **44(11)**, (2007), 661-76.

Masahiko, O., Chemical synthesis of biodegradable polymers, *Progress in polymer science.*, **27(1)**, (2002), 87-133.

Massey, B.L., Wen, X., Rohr, L.R., Tresco, P.A., Dahlstrom, L., and Park, A.H., Resorption rate and biocompatibility characteristics of two polyester ventilation tubes in a guinea pig model, *Otolaryngol Head Neck Surg.*, **131(6)**, (2004), 921-925.

Masterman, D.L., Role of Cholinesterase Inhibitors in Managing Behavioral Problems in Alzheimer's Disease, *Prim Care Companion J Clin Psychiatry.*, **6**, (2004), 126-131.

Matsuo, E.S., Biopsy-derived adult human brain tau is phosphorylated at many of the same sites as Alzheimer's disease paired helical filament tau, *Neuron.*, **13**, (1994), 989-1002.

McCormick, S.E., and Stoessl, A.J., Central administration of the neurotensin receptor antagonist SR48692 attenuates vacuous chewing movements in a rodent model of tardive dyskinesia, Neuroscience., **119(2)**, (2003), 547-55.

Mc Cullagh, S.D., Malcom, R.K., Woolfson, A.D., Gorman, S.P., Jones, D.S., and Cuddy, J., Release kinetics of oleyl alcohol from a self-lubricating silicone biomaterial, *Journal of Material Chemistry.*, **14**, (2004), 1093-1098.

Meese, T.M., Hu, Y., Nowak, R.W., and Marra, K.G., Surface studies of coated polymer microspheres and protein release from tissue-engineered scaffolds, *J Biomater Sci Polym Ed.*, **13(2)**, (2002), 141-51.

Mei, Y., and Ballauff, M., Effect of counterions on the swelling of spherical polyelectrolyte brushes, *Eur Phys J E Soft Matter.*, **16(3)**,(2005), 341-349.

Melander, W., and Horvath, C., Salt effect on hydrophobic interactions in precipitation and chromatography of proteins: an interpretation of the lyotropic series, *Arch Biochem Biophys.*, **183(1)**, (1977), 200-215.

Mehta, R.C., Jeyanthi, R., Calis, S., Thanoo, B.C., Burton, K.W., and DeLuca, P.P., Biodegradable microspheres as depot system for parenteral delivery of peptide drugs, *J. Cont. Rel.*, **29**, (1994), 375-384.

Middleton, J.C., and Tipton, A.J., Synthetic biodegradable polymers as orthopedic devices, *Biomaterials.*, **21**, (2000), 2335-2346.

Moelbert, S., Normand, B., and De Los Rios, P., Kosmotropes and chaotropes: modelling preferential exclusion, binding and aggregate stability, *Biophysical Chemistry.*, **112**, (2004), 45-57.

Mokry, J., Karbanova, J., Lukas, J., Paleckova, V., and Dvorankova, B., Biocompatibility of HEMA copolymers designed for treatment of CNS diseases with polymer-encapsulated cells, *Biotechnol Prog.*, **16(5)**, (2000), 897-904.

Montgomery, D.C., Design and Analysis of Experiments (2nd ed.), *John Wiley*, New York., (1997).

Muhiddinov, Z., Khalikov, D., Speaker, T., and Fassihi, R., Development and characterization of different low methoxy pectin microcapsules by an emulsion-interface reaction technique, *J Microencapsul.*, **(7)**, (2004), 729-41.

Myers, R.H., and Montgomery, D.C., Response Surface Methodology : Process and Product Optimization Using Designed Experiments, *John Wiley & Sons*, New York (*Probability and Statistics Series*)., (1995).

Nadeau, V., Leclair, G., Sant, S., Rabanel, J., Quesnel R., and Hildgen P., Synthesis of new versatile functionalized polyesters for biomedical applications, *Polymer.*, **46(25)**, (2005), 11263-11272.

Nahin, R.L., Identifying and pursuing research priorities at the National Center for Complementary and Alternative Medicine, *FASEB J.*, **19(10)**, 2005, 1209-15.

Nam, Y. S., and Park, T. G., Porous biodegradable polymeric scaffolds prepared by thermally induced phase separation, *Journal of Biomedical Materials Research.*, **47**,(1999), 8-17.

Nam, Y.S., Yoon, J.J., and Park, T.G., A novel fabrication method for macroporous scaffolds using gas foaming salt as porogen additive, *J Biomed Mater Res, Appl Biomater.*, **53**, (2000), 1–7.

Neagu, A., Neagu, M., and Dér, A., Fluctuations and the Hofmeister effect, *Biophysical Journal.*, **81**, (2001), 1285–1294.

Neuzillet, Y., Giraud, S., Lagorce, L., Eugene, M., Debre, P., Richard, F., and Barrou, B., Effects of the molecular weight of peg molecules (8, 20 and 35 KDA) on cell function and allograft survival prolongation in pancreatic islets transplantation, *Transplant Proc.*, **38(7)**, (2006), 2354-5.

Nielsen, C.B., Christiansen, O., Mikkelsen, K.V., and Kongsted, J., Density functional self-consistent quantum mechanics/molecular mechanics theory for linear and nonlinear molecular properties: Applications to solvated water and formaldehyde, *J Chem Phys.*, **126(15)**, (2007), 154112.

Nyström, B., Thuresson, K., and Lindmad, B., Rheological and dynamic light-scattering studies on aqueous solutions of a hydrophobically modified nonionic cellulose ether and its unmodified analogue, *Langmuir.*, **11**, (1995), 1994-2002.

Oesen, O.V., and Linnet, K., Metabolism of the tricyclic antidepressant amitriptyline by cDNA-expressed human cytochrome P450 enzymes, *Pharmacology.*, **55(5)**, (1997), 235-43.

Okamoto, K., and Fukuzumi, S., Hydrogen bonds not only provide a structural scaffold to assemble donor and acceptor moieties of zinc porphyrin-quinone dyads but also control the photoinduced electron transfer to afford the long-lived charge-

separated States, *J Phys Chem B Condens Matter Mater Surf Interfaces Biophys.*, **109(16)**, (2005),7713-23.

Okamoto, K., Mori, Y., Yamada, H., Imahori, H., and Fukuzumi, S., Effects of metal ions on photoinduced electron transfer in zinc porphyrin-naphthalenediimide linked systems, *Chemistry.*, **10(2)**, (2004),474-83.

Oldham, J.B., Lu, L., Zhu, X., Porter, B.D., Hefferan, E., Larson, D.R., Currier, B.L., Mikos, A.G., and Yaszemski, M.J., Biological activity of rhBMP-2 released from PLGA microspheres, *J Biomech Eng.*, **122(3)**, (2000), 289-292.

Olin, J., and Schneider, L., Galantamine for Alzheimer's disease, *Cochrane Database Syst Rev.*, **4**, (2001), CD001747.

Olley, B.O., Seedat, S., Nei, D.G., and Stein, D.J., Predictors of major depression in recently diagnosed patients with HIV/AIDS in South Africa, *AIDS patient care and STDs.*, **18(8)**, (2004), 481-487.

Panchagnula, R., Kumar, Bajpai. A., Agrawal, S., and Ashokraj, Y., Dissolution testing of marketed rifampicin containing fixed dose combination formulations using a new discriminative media: a post marketing retrospective study, *Pharmazie.*, **61(10)**, (2006), 851-854.

Para, G., Jarek, E., and Warszynski, P., The Hofmeister series effect in adsorption of cationic surfactants--theoretical description and experimental results, *Adv Colloid Interface Sci.*, **122(1-3)**, (2006), 39-55.

Paredes, S.D., Terron, M.P., Marchena, A.M., Barriga, C., Pariente, J.A., Reiter, R.J., and Rodriguez, A.B., Effect of exogenous melatonin on viability, ingestion capacity, and free-radical scavenging in heterophils from young and old ringdoves (Streptopelia risoria), *Mol Cell Biochem.*, **101(1)**, (2007), 56-62.

Park K., Ed: Controlled Drug Delivery: Challenges and Strateges, *American Chemical Society.*, Washington., USA., (1997), 1-629.

Park, T.G., Degradation of poly(lactic-co-glycolic acid) microspheres: effect of copolymer composition, *Biomat.*, **16**, (1995),1123–1130.

Park, T.G., Degradation of poly (D,L-lactic acid) microspheres: effect of molecular weight, *J Controlled Release.*, **30**, (1994),161–173.

Parojcic, J., Duric, Z., Jovanovic, M., and Ibric, S., An investigation into the factors influencing drug release from hydrophilic tablets based on novel carbomer polymers, *Drug Deliv.*,**11**, (2004), 59-65.

Paulaitis, M.E., and Pratt, L.R., Hydration Theory for Molecular Biophysics, *Advanced in Protein Chemisrty.*, **62**, (2002), 283.

Pedersen, J., Back, B. B., Bjørnholm, S., Borggreen, J., Diebel, M., and Sletten, G., Population of Triaxial Rotor Levels in $^{182}$Os Phys, *Rev. Lett.*, **54(4)**, (1985), 306 - 308 (1985).

Peltonen, L., Aitta, J., Hyvönen, S., Karjalainen, M., and Hirvonen, J., Improved entrapment efficiency of hydrophilic drug substance during nanoprecipitation of poly(l)lactide nanoparticles, *AAPS PharmSciTech.*, **5(1)(16)**, (2004).

Peppas, N.A., Analysis of Fickian and non-Fickian drug release from polymers, *Pharm Acta Helv.*, **60**, (1985), 110–111.

Peppas, N.A., and Sahlin, J.J., A simple equation for the description of solute release. III. Coupling of diffusion and relaxation, *Int. J. Pharm.*, **57**, (1989), 169–172.

Pillay, V., and Danckwerts, M.P., Textural Profiling and Statistical Optimization of Crosslinked Calcium-Alginate-Pectin-Cellulose Acetophthalate Gelisphere Matrices, *J. Pharml Sci.*, **91**, (2002), 2559-2570.

Pillay, V., and Fassihi, R., Electrolyte-induced compositional heterogeneity: a novel approach for rate-controlled oral drug delivery, *J Pharm Sci.*, **88(11)**, (1999), 1140-1148.

Pillay, V., and Fassihi, R., In situ electrolyte interactions in a disk-compressed configuration system for up-curving and constant drug delivery, *J Control Release.*, **67(1)**, (2000), 55-65.

Pillay, V., and Fassihi, R., Probing the dynamics of matrix in the presence of electrolytes, Drg Deliv., **8(2)**, (2001), 87-92.

Pinzauti, S., Gratteri, P., Furlanetto, S., Mura, P., Dreassi E., and Phan-Tan-Luu, R., Experimental design in the development of voltammetric method for the assay of omeprazole, *J. Pharm. Biomed. Anal.*, **14**, (1996), 881-889.

Piotrowicz, A., and Shoichet, M.S., Nerve guidance channels as drug delivery vehicles, *Biomat.*, **27(9)**, (2006), 2018-2027.

Pople, J. A., A priori geometry predictions. In: Modern Theoretical Chemistry: Applications of Electronic Structure Theory, (H. F. Schaefer, III, Ed.), *Plenum Press, New York.*, **4**, (1977), 1-24.

Porjazoska, A., Yilmaz, O.K., Baysal, K., Cvetkovska, M., Sirvanci, S., Ercan, F., and Baysal, B.M., Synthesis and characterization of poly(ethylene glycol)-poly(D,L-lactide-co-glycolide) poly(ethylene glycol) tri-block co-polymers modified with collagen: a model surface suitable for cell interaction, *J Biomater Sci Polym Ed.*, **17(3)**, (2006), 323-40.

Potonick, F., South African Society of Psychiatrists, Report: *Psychogeriatrichs, Alzheimer's South Africa.,* (2005).

Puoci, F., Iemma, F., Muzzalupo, R., Spizziri, U.G., Trombino, S., Cassano, R., and Picci, N., Spherical Molecularly Imprinted Polymers (SMIPs) Via a Novel

Precipitation Polymerization in the Controlled Delivery of Sulfasalazine, *Macromol Biosci.*, **21**, (2004) 22-26.

Qiu, L., Zhang, Y., Krause, H.J., Braginski, A.I., and Usoskin, A., High-temperature superconducting quantum interference device with cooled LC resonant circuit for measuring alternating magnetic fields with improved signal-to-noise ratio, *Rev Sci Instrum.*, **78(5)**, (2007), 054701.

Raghuvanshi, R.S., Singh, O., and Panda, A.K.,Correlation between *in vitro* release and in vivo immune response from biodegradable polymer particles entrapping tetanus toxoid, *Drug Deliv.*, **9(2)**, (2002), 113-1120.

Ramchandani, M., and Robinson, D., *In vitro* and *in vivo* Release of Ciprofloxacin from PLGA 50:50 Implants., *J Control Release.*, **31**, (1998), 167-175.

Ranucci, E., Ferruti, P., Annunziata, R., Gerges, I., and Spinelli, G., NMR spectroscopy and MALDI-TOF MS characterisation of end-functionalised PVP oligomers prepared with different esters as chain transfer agents, *Macromol Biosci.*, **6(3)**, (2006), 14216-27.

Rapoport, S.I., Osmotic opening of the blood-brain barrier: principles mechanism and therapeutic applications, *Cell Mol Neurobiol.*, **20** (2000), 217–230.

Reimschuessel, H. K., Relationships on the effect of water on glass transition temperature and Young"s modulus of Nylon-6, *Journal of Polymer Science.*, **16**, (1978), 1229–1236.

Renoncourt, A., Vlachy, N., Bauduin, P., Drechsler, M., Touraud, D., Verbavatz, J.M., Dubois, M., Kunz, W., and Ninham, B.W., Specific Alkali Cation Effects in the Transition from Micelles to Vesicles through Salt Addition., *Langmuir.*, 2007.

Repáková, J., Čapková, P., Studenovský, M., and Ilavský, M., Characterization of molecular structures and properties of polyurethanes using molecular dynamics simulations, *Journal of Molecular Modeling.*, **10**,(2004), 240-249.

Reynlods, T.D., Gehrke, S.C., Hussain A.S., and Shenouda, L.S., Polymer Erosion and Drug Release Characterization of Hydroxypropyl Methylcellulose Matrices, *J Pharm Sci.*, **87**, (1998) 1115-1123.

Rinaudo, M., Swelling of polyelectrolyte gels and thermodynamic parameters of solvation, *Charged gels and membranes.*, 1, (1976), 91–120.

Rissman, R.A., Caspase-cleavage of tau is an early event in Alzheimer disease tangle pathology, *J. Clin. Invest.*, **14**, (2004), 121-130.

Ritchie, C.W., Ames, D., Clayton, T., and Lai, R., Metaanalysis of randomized trials of the efficacy and safety of donepezil, galantamine, and rivastigmine for the treatment of Alzheimer disease, *Am J Geriatr Psychiatry.*,**12**, (2004) 358-369.

Ritger, P., and Peppas, N., A simple equation for description of solute release II. Fickian and anomalous release from swellable devices, *J Control Release.*, **5**, (1987), 37–42.

Rosenbaum, T., and Kou, M., Are one or two dangerous? Tricyclic antidepressant exposure in toddlers, *Journal of Emergency Medicine.*, **28(2)**, (2005),169-174.

Rothstein, J.P., and G. H. and McKinley, G.H., Axisymmetric flow-induced birefringence measurements for the flow of a polystyrene boger fluid into an abrupt contraction-expansion, *J. Non-Newtonian Fluid Mech.*, **86**, (1999) 61-88.

Roy, D.S., and Rohera, B.D., Comparative evaluation of rate of hydration and matrix erosion of HEC and HPC and study of drug release from their matrices, *Eur. J. Pharm. Sci.*, **16(3)**, 2002, 193-199.

Rwei, S.P., Chen, T.Y., and Cheng, Y.Y., Sol/gel transition of chitosan solutions., *J Biomater Sci Polym Ed.*, **16(11)**, (2005), 1433-1445.

Salmon, D.P., and Filoteo, J.V., Neuropsychology of cortical versus subcortical dementia syndromes, *Semin Neurol.*, **27(1)**, (2007), 7-21.

Sander, E.A., Alb, A.M., Nauman, E.A., Reed, W.F., and Dee, K.C., Solvent effects on the microstructure and properties of 75/25 poly(D,L-lactide-co-glycolide) tissue scaffolds, *J Biomed Mater Res A.*, **70(3)**, (2004), 506-513.

Sato, H, Miyagawa, Y., Okabe, T., Miyajima, M., and Sunada, H., Dissolution mechanism of diclofenac sodium from wax matrix granules, *Wiley InterScience Journal.*, **86**, (2000), 929-934.

Satturwar, P.M., Fulzele, S.V., Panyam, J., Mandaogade, P.M., Mundhada,D.R., Gogte, B.B., Labhasetwar, V., and Dorle, A.K., Evaluation of new rosin derivatives for pharmaceutical coating, *Int J Pharm.*, **270**, (2004), 27-36.

Savalani, M.M., and Harris, R.A., Layer manufacturing for in vivo devices, *Proc. IMechE., Engineering in Medicine.*, **220(H: J)**, (2006), 505-520.

Schellman, J.A., Selective binding and solvent denaturation, *Biopolymers.*, **26**, (1987), 549–559.

Schugens, C.H., Maquet, V., Grandfils, C., Jerome, R., and Teyssie, PH., Biodegradable and macroporous polylactide implants for cell transplantation: 1. Preparation of macroporous polylactide supports by solid-liquid phase separation, *Polymer.*, **37(6)**, (1996), 1027-1038.

Schutte, D.L., The evolving role of genomics in shaping care for persons with dementia, *Nurs Clin North Am.*, **39(3)**, (2004), 581-592.

Shah, S.S., Cha, Y., and Pitt, C.G., Poly (glycolic acid-co-D,L-lactic acid): diffusion or degradation controlled drug delivery, *J. Control. Release*, **18**, (1992), 261-270.

Shahani, N., and Brandt, R., Functions and malfunctions of the tau proteins, *Cell. Mol. Life Sci.*, **59**, (2002), 1668–1680.

Shi, W., Liu, T., Xie, L., and Wang, S., FK506 in a biodegradable glycolide-co-clatide-co-caprolactone polymer for prolongation of corneal allograft survival, *Curr Eye Res.*, **30(11)**, (2005), 969-976.

Shin, H.J., Lee, C.H., Cho, I.H., Kim, Y.J., Lee, Y.J., Kim, I.A., Park, K.D., Yui, N., and Shin, J.W., Electrospun PLGA nanofiber scaffolds for articular cartilage reconstruction: mechanical stability, degradation and cellular responses under mechanical stimulation *in vitro*, *J Biomater Sci Polym Ed.*, **17(1-2)**, (2006),103-19.

Shive, M.S., and Anderson, J.M., Biodegradation and biocompatibility of PLA and PLGA microspheres, *Adv Drug Deliv Rev.*, **28(1)**, (1997), 5-24.

Sibanda, W., Pillay, V., Danckwerts, M.P., Viljoen, A.M., Van Vuuren, S., and Khan, R.A., Experimental design for the formulation and optimization of novel cross-linked oilispheres developed for *in vitro* site-specific release of mentha piperita oil, *PharmSciTech.*, **5**, (2004), E18.

Siegel, S.J., Kahn, J.B., Metzger, K., Winey, K.I., Werner, K., and Dan, N., Effect of drug type on the degradation rate of PLGA matrices, *European Journal of Pharmaceutics and Biopharmaceutics.*, **64(3)**, 2006, 287-293.

Siepmann, J., Local controlled drug delivery to the brain, *International Journal of Pharmaceutics.*, **314(2)**, (2006), 99-100.

Siepmann, J., and Peppas N. A., Modeling of drug release from delivery systems based on hydroxypropyl methylcellulose (HPMC), *Advanced Drug Delivery Reviews.*, **48**, (2001), 139-157.

Sisay, G., Byung, H.W., and DeLuca, P., Formulation *in vitro* transfection efficiency of poly (D,L lactide-co-glycolide) microspheres containing plasmid DNA for gene delivery, *AAPS Pharm Sci Tech.*, **1(4) (28)**, (2000), 1-9.

Smith, M.J., Silva, M.M., Cerqueira, S., and MacCallum J.R., Preparation and characterization of a lithium ion conducting electrolyte based on poly(trimethylene carbonate), *Solid State Ionics.*, **140(3-4)**, (2001), 345-351.

Sobott, F., Wattenberg, A., Barth, H. D., and Brutschy, B., Ionic clathrates from aqueous solutions detected with laser induced liquid beam ionization/desorption mass spectrometry, *Int. J. Mass Spectr.*, **185-7**, (1999), 271-279.

Souder, E., and Beck, C., Overview of Alzheimer's disease, *Nurs Clin North Am.*, **39**, (2004), 545-559.

Spain, T., Agrawal, C.M., and Athanasiou, K.A., New technique to extend the useful life of a biodegradable cartilage implant, *Tissue Eng.*, **4(4)**, (1998), 343-352.

Squitieri, F., Cannella, M., Piorcellini, A., Brusa, L., Simonelli, M., and Ruggieri, S., Short-term effects of olanzapine in Huntington's disease, *Neuropsychiatry Neuropsychol Behav Neurol.*, **14**, (2001), 69-72.

Stephenson, B.C., Beers, K.J., and Blankschtein, D., Quantifying the hydrophobic effect., 3., A computer simulation-molecular-thermodynamic model for the micellization of ionic and zwitterionic surfactants in aqueous solution, *J Phys Chem B Condens Matter Mater Surf Interfaces Biophys.*,**111(5)**, (2007), 1063-75.

Sudoh, Y., Cahoon, E.E., Gerner P., and Wang G.K., Tricyclic antidepressants as long-acting local anesthetics, *Pain.*, **103(1-2)**, (2003), 49-55.

Sweet, J.L., Optimization of a Cross-linked Multi-Component Intelligent Polyspheric Drug Delivery System: Innovative mechanistic modulation of hydrophilic-hydrophobic polymer composites, *PhD Thesis.*, (2005).

Swenson, J., Smalley, M.V., Hatharasinghe, H.L.M., and Fragneto, G., Interlayer Structure of a Clay-Polymer-Salt-Water System, *Langmuir.*, **17**, (2001), 3813-3818.

Tanaka, M., and Takahashi, K., Determination of the changes of the basic structures of silics species in dependence on the concentration of sodium chloridenby FAB-MS., *Fresenius J Anal Chem.*, **368(8)**, (2000),786-790.

Takatori, T., Yamamoto, K., Yamaguchi, T., Higaki, K., and Kimura, T., Design of controlled-release morphine suppositories containing polyglycerol ester of fatty acid, *Biol Pharm Bull.*, **28(8)**, 2005, 1480-4.

Tapia, C., Escobar, Z., Costa, E., Sapag-Hagar, J., Valenzuela, F., Basualto, C., Nella Gai, M., and Yazdani- Pedram, M., Comparative studies on polyelectrolyte complexes and mixtures of chitosan- alginate and chitosan- carrageenan as prolonged diltiazem clorhydrate release systems, *Science-European Journal of Pharmaceutics and Biopharmaceutics.*, **57**, (2004), 65-75.

Tareste, D., Pincet, F., Lebeau, L., and Perez, E., Hydrophobic forces and hydrogen bonds in the adhesion between retinoid-coated surfaces, *Langmuir.*, **23**, (2007), 3225-3229.

Therin, M., Christel, P., Li, S., Garreau, H., and Vert, M., *In vivo* degradation of massive poly(alpha-hydroxy acids): validation of *in vitro* findings, *Biomaterials.*, **13(9)**, (1992), 594-600.

Tomoda, K., Kojima, S., Kajimoto, M., Watanabe, D., Nakajima, T., and Makino, K., Effects of pulmonary surfactant system on rifampicin release from rifampicin-loaded PLGA microspheres, *Colloids Surf B Biointerfaces.*, **45(1)**, (2005), 1-6.

Uhr, M., Grauer, M.T., Yassouridis, A., and Ebinger, M.J., Blood-brain barrier penetration and pharmacokinetics of amitriptyline and its metabolites in p-

glycoprotein (abcb1ab) knock-out mice and controls, *Psychiatr Res*, **41(1-2)**, (2007), 179-88.

Välimaa, T., and Laaksovirta, S., Degradation behaviour of self-reinforced 80L/20G PLGA devices *in vitro*, *Biomaterials.*, **25(7-8)**, (2004), 1225-1232.

Veldink, J. H., Kalmijn, S., Groeneveld, G. J., Titulaer, M. J., Wokke, J. H.J. and van den Berg L. H., Physical activity and the association with sporadic ALS, *Neurology.*, **64(2)**, (2005), 241-245.

Virto, MR., Elorza, B., Torrado, S., Elorza Mde, L., and Frutos, G., Improvement of gentamicin poly(D,L-lactic-co-glycolic acid) microspheres for treatment of osteomyelitis induced by orthopedic procedures, *Biomaterials.*, 28(5), **(2007)**, 877-885.

Visscher, G.E., Robison, R.L., Maulding, H.V., Fong, J.W., Pearson J.E., and Argentieri, G.J., Biodegradation of and tissue reaction to 50:50 poly(D,L-lactide-co-glycolide) microcapsules, *J Biomed Mater Res.*, **19(3)**, (1985), 349–365.

Vlachy, V., Hribar-Lee, B., Kalyuzhnyi, Y.V., and Dill, K.A., Short-range interactions: from simple ions to polyelectrolyte solutions, *Current Opinion in Colloid and Interface Science.*, **9**, (2004), 128–132.

Vogel, B.M., and Mallapragada, S.K., Synthesis of novel biodegradable polyanhydrides containing aromatic and glycol functionality for tailoring of

hydrophilicity in controlled drug delivery devices, *Biomaterials.*, **26(7)**, (2005), 721-728.

Vogt, F., Stein, A., Rettemeier, G., Krott, N., Hoffmann, R., Vom Dahl, J., Bosserhoff, A.K., Michaeli, W., Hanrath, P., Weber C., and Blindt, R., Long-term assessment of a novel biodegradable Paclitaxel-eluting coronary stent, *Eur Heart J.*, **15**, (2004), 1330-1340.

Voisine, C., Varma, H., Walker. N., Bates, E.A., Stockwell, B.R., and Hart, A.C., Identification of potential therapeutic drugs for Huntington's disease using Caenorhabditis elegans, *PLoS ONE.*, **2**, (2007), e504.

Von Burkrrsroda, F., Schedl, L., and Göpferich, A., Why degradable polymers undero surface erosion or bulk erosion, *Biomaterials.*, **23(21)**, (2002), 4221-4231.

Vostalová, L., Rabisková, M., and Medvecká, G., Release of diltiazem chloride and ibuprofen from hydrophilic matrix tablets, *Ceska Slov Farm.*, **52(6)**, (2003), 295-298.

Vozzi, G., Flaim, C., Ahluwalia, A., and Bhatia, S., Fabrication of PLGA scaffolds using lithography and microsyringe deposition, *Biomaterial.*, **24**, (2003), 2533-2540.

Wang, Y., Ameer, G.A., Sheppard, B.J., and Langer, R., A tough biodegradable elastomer, *Nat Biotechnol.*, **20(6)**, (2002), 602-606.

Wei, H., and Lobenberg, R., Biorelevant dissolution media as a predictive tool for glyburide a class II drug, *Eur J Pharm Sci.*, **29(1)**, (2006), 45-52.

Weihe, S., Schiller, C., Rasche, C., Wehmöller, M., Eufinger, H., and Epple, M., A graded composite material for use in the area of the cranial and facial skull, *Biomed Tech (Berl).*, **47(1)(1)**, (2002), 488-91.

Witt, C., and Kissel, T., Morphological characterization of microspheres, films and implants prepared from poly (lactide-co-glycolide) and ABA triblock copolymers: is the erosion controlled by the degradation, swelling or diffusion? *Eur J Pharm Biopharm.*, **51(3)**, (2001), 171-181.

Wu, X. S., Synthesis, characterization, biodegradation, and drug delivery application of biodegradable lactic/glycolic acid polymers: Part III., Drug delivery application, *Artif Cells Blood Substit Immobil Biotechnol.*, **32(4)**, (2004), 575-591.

Xue, J.M., Tan, C.H., and Lukito, D., Biodegradable polymer-silica xerogel composite microspheres for controlled release of gentamicin, *J Biomed Mater Res B Appl Biomater.*, **78(2)**, (2006), 417-422.

Yasukawa, T., Ogura, Y., Kimura, H., Sakurai, E., and Tabata, Y., Drug delivery from ocular implants, *Expert opin Drug Deliv.*, **3(2)**, (2006), 261-73.

Yamaguchi, K., and Anderson, J.M., *In vivo* biocompatibility studies of medisorb (R) 65/35 d,l-lactide glycolide copolymer microspheres, *J Control Release.*, **24(1–3)**, (1993), 81–93.

Yang, M., Cui, F., You, B., Wang, L., Yue, P., and Kawashima, Y., A novel pH–dependent gradient–release delivery system for nitrendipine II., Investigations of the factors affecting the release of the system, *Int J Pharm.*, **286**, (2004), 99-109.

Yang, A., Yang, L., Liu, W., Li, Z., Xu, H., and Yang, X., Tumor necrosis factor alpha blocking peptide loaded PEG-PLGA nanoparticles: preparation and *in vitro* evaluation, *Int J Pharm.*, **331(1)**, (2007), 123-132.

Yasuo, S., Yoshimura, T., Ebihara, S., and Korf, H.W., Temporal dynamics of type 2 deiodinase expression after melatonin injections in Syrian hamsters, *Endocrinology.*, (2007), 1-35.

Yeht, M.K., Chen, J.L., and Chiang, C.H., Vibrio cholerae-loaded poly(DL lactide-co-glycolide) microparticles, *J Microencapsul.*, **19(2)**, (2002), 203-212.

Ying, W.A., A new hypothesis of neurodegenerative diseases: the deleterious network hypothesis, *Med Hypotheses.*, **47(4)**, (1996), 307-13.

Yoon, J.J., and Park, T.G., Degradation behaviors of biodegradable macroporous scaffolds prepared by gas foaming of effervescent salts, *J Biomed Mater Res.*, **55(3)**, (2001), 401-408.

Young, C.R., Dietzsch, C., Cerea, M., Farrell, T., Fegely, K.A., Rajabi-Siahboomi, A., and McGinity, J.W., Physicochemical characterization and mechanisms of release of theophylline from melt-extruded dosage forms based on a methacrylic acid copolymer, *Int J Pharm.*, **301(1-2)**, (2005), 112-120.

Yu, T.W., Chen, R.R., and Gau, C.S., Production of an extremly low dose procaterol HCl preparation by fluidized-bed coating method: *in vitro* and *in vivo* evaluation, *Drug Dev Ind Pharm.*, **32(6)**, (2006), 651-60.

Yue, I.C., Poff, J., Cortes, M.E., Sinistera, R.D., Faris, C.B., Hildgen, P., Langer,R., and Shastri, V.P., A novel polymeric chlorhexidine delivery device for the treatment of periodontis disease, *Biomaterials.*, **25**, (2004), 5181-5189.

Zainuddin, Z., Hill, D.J., Whittaker, A.K., Lambert, L., and Chirila, T.V., Preferential interactions of calcium ions in poly(2-hydroxyethyl methacrylate) hydrogels, *J Mater Sci Mater Med.*, **18(6)**, (2007),1141-1149.

Zangi, R., and Berne, B.J., Aggregation and dispersion of small hydrophobic particles in aqueous electrolyte solutions, *J Phys Chem B Condens Matter Mater Surf Interfaces Biophys.*, **110(45)**, (2006), 22736-41.

Zhang, X., Goosen, M.F.A., Wyss, P., and Pichora, D., Biodegradable polymers for orthopedic applications, *Rev. Macromol, Chem. Phys.*, **C33 (1)**, (1993), 81-102.

Zhang, X., Wyss, U.P., Pichora, D., and Goosen, M.F.A., An investigation of poly(lactic acid) degradation, *J. Bioact. Compat. Polym.*, **9**, (1992), 80-100.

Zhang, Z., Chisti, Y., and Moo-Young, M., Isolation of a recombinant intracellular beta-galactosidase by ammonium sulfate fractionation of cell homogenates, *Bioseparation.*, **5(6)**, (1995), 329-337.

Zilberman, M., Eberhart, R.C., and Schwade, N.D., *In vitro* study of drug-loaded bioresorbable films and support structures, *J Biomater Sci Polym Ed.*, **13(11)**, (2002), 1221-1240.

Zhu, G., and Schwendeman, S.P., Influence of basic salts on stability and release of proteins in injectable poly(lactide-co-glycolide) delivery devices, *Proceed. Int'l. Symp. Control. Rel. Bioact.Mater.*, **26**, (1999), 1114–1115.